THE UNIVERSITY OF QUEENSLAND

AUSTRALIA

Discovery of Novel, Potent and Selective Glycine Receptor Modulators from Southern Australian Sponges

Walter Balansa, S.IK, M.Sc

A thesis submitted for the degree of Doctor of Philosophy at

The University of Queensland in 2014

Institute for Molecular Bioscience

Abstract

Consisting of five subunits (α1-α4 and β), glycine receptors (GlyRs) orchestrate inhibitory neurotransmission in the central nervous system (CNS). Mutation and/or dysfunction of different GlyR subunits are associated with CNS diseases such as spasticity and movement disorders (GlyRα1), hyperekplexia (GlyR α1, GlyRα2 and GlyRβ), epilepsy (GlyRα2 and GlyRα3) and inflammatory pain (GlyRα1 and GlyRα3). In particular, GlyRα3 has recently emerged as the target of choice for the treatment of chronic inflammatory pain due to its discrete distribution at the lamina II dorsal horn spinal cord, the pain terminal. Unfortunately, while known GlyR modulators lack specificity for GlyRs, that render them undrugable, little is known about GlyR modulators from marine natural products (MNPs), despite the important roles of MNPs in drug discovery programs. Together with the biomedical potential of MNPs and the unmet medical needs in treatment of CNS diseases, recent advances in spectroscopic and ion channel technologies strongly suggest the importance of MNPs in the discovery of novel, potent and specific GlyR modulators.

Consequently, chapter 1 discusses the various potential medical benefits of GlyRs and/or MNPs in the search for a cure for CNS diseases, with emphasis on chronic inflammatory pain. They include:

- Structural diversity and pharmacological aspect of GlyRs;
- Possible uses of GlyR modulators in therapy;
- The importance of advanced technologies in discovering anti-inflammatory pain drugs from marine resource;
- MNPs as a prolific source of bioactive molecules; and
- The role of MNPs in the discovery of new pain relief drugs.

Chapter 2 prioritizes marine extracts as our first step in identifying MNPs as potential GlyR modulators. Taking advantage of the yellow fluorescence protein (YFP) assay, we screened *n*-BuOH extracts of >2,500 Australian and Antarctic marine invertebrates against GlyRα1, GlyRα2 and GlyRα3 and compared the images for control and tested extracts. This screening yielded 27 active extracts (3 strong, 19 moderate and 5 weak antagonist extracts). Along with this screening, liquid chromatography mass spectrometry (LCMS) analysis established 7 priority specimens described in the following three chapters.

Chapter 3 describes 6 new (ircinialactam A (**3.45**), 8-hydroxyircinialactam A (**3.46**), hydroxyircinialactam B (**3.47**), ircinialactam C (**3.48**), *ent*-ircinialactam C (**3.49**) & ircinialactam D (**3.50**) and 3 known (12*E*,20*Z*,18*S*)-8-hydroxyvariabilin (**3.51**), (7*E*,12*E*,20*Z*,18*S*)-variabilin (**3.52**)

and (7*E*,12*Z*,20*Z*,18*S*)-variabilin (**3.53**) compounds from three Irciniidae sponges. The isomers **3.51** and **3.52** were successfully isolated and assigned as a single pure compound without derivatisation. Importantly, by means of liquid chromatography-solid phase extraction nuclear magnetic resonance (LC-SPE-NMR), we managed to isolate and elucidate the structure of minor metabolites (**3.45-3.50**). Ircinialactams (**3.45-3.50**) were unique in that they all featured an unusual functionality, a glycinyl lactam and in case of ircinialactam D, a dihydroxy diacid moiety. Using automated patch clamp electrophysiology (APCE), we evaluated **3.45-3.53** against α1 and α3 GlyRs and identified **3.46** and **3.47** as strong and specific GlyRα1 potentiators with EC_{50} values of 1.0 μM and 0.5 μM respectively and **3.53** as a potent and selective GlyRα3 antagonist (IC_{50} = 7.0 μM).

Chapter 4 discloses 5 novel cyclic sesterterpenes (-)-ircinianinlactam A (**4.11**), (-)-oxo-ircinianin lactam A sulfate (**4.12**), (-)-oxo-ircinianin A (**4.13**), (-)-oxo-ircinianin lactam A (**4.14**), and (-)-ircinianin lactone (**4.15**), two known co-metabolites (-)-ircinianin (**4.1**) & (-)-ircinianin sulfate (**4.2**) and one synthetic derivative, ircinianin acetate (**4.16**). Ircinianins possessed rare functional groups such as the glycinyl lactam in **4.11**, **4.12** and **4.14** and a modified tetronic acid in **4.13** and **4.14** with the latter moiety being hitherto unknown in natural products. Importantly, APCE analysis showed **4.2** as a strong GlyRα3 antagonist (IC_{50} = 3.2 μM), **4.14** as a specific GlyRα1 potentiator and **4.11** as a potent and selective GlyRα3 potentiator (EC_{50} = 8.2 μM). (-)-Ircinianinlactam A (**4.11**) was the first compound to exert such activity against GlyRα3 subunit, the emerging pain target.

Chapter 5 discusses ianthellalactam A (**5.66**) and B (**5.67**) (new), ethyldictyondendrilin (**5.68**) (artefact), aplysinopsin (**5.1**), 8*E*-3′-deimino-oxoaplysinopsin (**5.3**), 8*Z*-3′-deimino-oxoaplysinopsin (**5.4**), dihydroaplysinopsin (**5.10**) and tubastrindole B (**5.34**) (known) from *Ianthella cf. flabelliformis.* Ianthellalactam A and B were the first examples of linear sesquiterpene glycinyl lactams. APCE analysis revealed **5.3** and **5.4** as modest GlyRα3 antagonists (IC_{50} = 67.0 μM) and **5.34** as a strong GlyRα1 potentiator (1.0 μM) but a modest antagonist at high concentration (IC_{50} = 25.9 μM). One pot synthesis produced two strong GlyRα1 antagonists, 8*E*-3′-deimino-4′-demethyl-3′-oxoaplysinopsin (**5.70**) and 8*Z*-3′-deimino-4′-demethyl-3′- oxoaplysinopsin (**5.71**), with IC_{50} values of 8.8 μM.

Finally, chapter 6 describes 30 compounds discovered during this study. Apart from their status (new or known, natural products and/or synthetics), this chapter provides their physicochemical characteristics and bioactivity against GlyRs. Moreover, through a strength-weakness-opportunity-threat (SWOT) analysis, this chapter discusses the possibility of taking the lead compounds (**3.46**, **3.47**, **4.11** & **4.14**) to the pipeline or clinical trials.

Declaration by author

This thesis is composed of my original work, and contains no material previously published or written by another person except where due reference has been made in the text. I have clearly stated the contribution by others to jointly authored works that I have included in my thesis.

I have clearly stated the contribution of others to my thesis as a whole, including statistical assistance, survey design, data analysis, significant technical procedures, professional editorial advice, and any other original research work used or reported in my thesis. The content of my thesis is the result of work I have carried out since the commencement of my research higher degree candidature and does not include a substantial part of work that has been submitted to qualify for the award of any other degree or diploma in any university or other tertiary institution. I have clearly stated which parts of my thesis, if any, have been submitted to qualify for another award.

I acknowledge that an electronic copy of my thesis must be lodged with the University Library and, subject to the General Award Rules of The University of Queensland, immediately made available for research and study in accordance with the *Copyright Act 1968*.

I acknowledge that copyright of all material contained in my thesis resides with the copyright holder(s) of that material. Where appropriate I have obtained copyright permission from the copyright holder to reproduce material in this thesis.

Publications during candidature

Peer-reviewed papers

1. **Balansa**, **W**.; Islam, R.; Fontaine, F.; Piggott, A.M.; Zhang, H.; Webb, T. I.; Gilbert, D.; Lynch, J. W.; Capon, R.J; Sesterterpene glycinyl-lactams: a new class of glycine receptor (GlyR) modulator from Australian marine sponges of the genus *Psammocinia*. *Org. Bomol. Chem***.** 2013, *11*, 4695-4701.
2. **Balansa**, **W**.; Islam, R; Fontaine, F.; Piggott, A.M; Zhang, H; Gilbert, D; Lynch, J.W.; Capon, R.J; Australian marine sponge alkaloids as a new class of glycine-gated chloride channel receptor modulator. *Bioorg. Med. Chem*. 2013, *21*, 4420-4425.
3. **Balansa, W**.; Islam, R.; Fontaine, F.; Piggott, A.M.; Zhang, H.; Webb, T. I.; Gilbert, D.; Lynch, J. W.; Capon, R.J. Ircinialactams: Subunit-Selective Glycine Receptor Modulators from Australian Sponges of the Family Irciniidae. *Bioorg. Med. Chem.* 2010, *18*, 2912-2919.

Conference abstracts

1. **Balansa, W.**; Islam, R.; Piggott, A. M.; Zhang, H.; Vijasarathy, S.; Koo, A.; Xiao, X.; Zulkifli, Z.; Fontaine, F.; Gilbert, D. F.; Lynch, J. W.; Capon, R. J. Targeting Pain Through Marine Biodiscovery. Division of Chemistry and Structural Biology Symposium. Brisbane, Australia November 10, 2011.
2. Islam, R.; **Balansa, W**.; Fontaine, F.; Webb, T. I.; Gilbert, D. L.; Piggott, A. M.; Zhang, H.; Capon, R. J.; Lynch, J. W. Ircinialactams: A New Class of Subunit-Selective Glycine Receptor Modulators. Australian Physiological Society (AuPS/ANS) 2010 Joint Meeting. Sidney, Australia January 28, 2010.
3. **Balansa, W**. Indonesian Marine Bioprospecting: Where Are We Heading?" The World Ocean Conference – Manado, Indonesia May 11-15, 2009.

Publications included in this thesis

1. **Balansa, W**.; Islam, R.; Fontaine F.; Piggott, A.M.; Zhang, H.; Webb, T.I.; Gilbert, D.; Lynch, J.W.; Capon, R.J. Ircinialactams: Subunit-Selective Glycine Receptor Modulators from Australian Sponges of the Family Irciniidae. *Bioorg. Med. Chem.* 2010, *18*, 2912-2919. Incorporated as Chapter 3.

Contributor	**Statement of contribution**
Balansa, Walter	Designed experiment (85%), data analysis (70%), wrote and edited the paper (40%) (Chemistry)
Islam, Robiul	Designed experiment (80%), data analysis (65%), wrote and edited the paper (35%) (Pharmacology)
Fontaine, Frank	Designed experiment (YFP primary screening, 10%), data analysis (YFP primary screening, 10%), wrote and edited the paper (5%) (Pharmacology)
Zhang, Hua	Data analysis (critically analyzed all molecules, 10%), wrote and edited the paper (5%) (Chemistry)
Piggott, Andrew M.	Designed experiment (HPLC-SPE-NMR and HRESIMS, 10%), data analysis (HPLC-SPE-NMR and HRESIMS, 10%), wrote and edited the paper (5%) (Chemistry)
Webb, Timothy.	Designed experiment (YFP primary screening 5%), data analysis (YFP data, 5%), wrote and edited the paper (5%) (Pharmacology)
Gilbert, Daniel	Designed experiment (YFP primary screening 5%), data analysis (YFP data, 5%), wrote and edited the paper (5%) (Pharmacology)
Lynch, Joseph W.	Data analysis (10%), wrote and edited the paper (50%) (Pharmacology)
Capon, Robert J.	Data analysis (10%), wrote an edited the paper (50%) (Chemistry)

2. **Balansa**, **W**.; Islam, R.; Fontaine, F.; Piggott, A.M.; Zhang, H.; Webb, T. I.; Gilbert, D.; Lynch, J. W.; Capon, R.J. Sesterterpene glycinyl-lactams: a new class of glycine receptor (GlyR) modulator from Australian marine sponges of the genus *Psammocinia*. *Org. Bomol. Chem***.** 2013, *11*, 4695- 4701. Incorporated as Chapter 4.

Contributor	**Statement of contribution**
Balansa, Walter	Designed experiment (85%), data analysis (70%), wrote and edited the paper (35%) (Chemistry)
Islam, Robiul	Designed experiment (75%), data analysis (65%), wrote and edited the paper (40%) (Pharmacology)
Gilbert, Daniel F	Designed experiment (YFP primary screening, 10%), data analysis (5%), wrote and edited the paper (YFP data, 10%) (Pharmacology)
Fontaine, Frank	Designed experiment (YFP primary screening, 10%), data analysis (YFP primary screening, 10%), wrote and edited the paper (5%) (Pharmacology)
Webb, Timothy	Designed experiment (YFP primary screening, 5%), data analysis (5%), wrote and edited the paper (YFP data, 5%) (Pharmacology)
Xiao, X	Designed experiment (single ion extraction, Chapter 4, 5%), data analysis (single ion extraction data, Chapter 4, 5%), wrote and edited the paper (5%) (Chemistry)
Zhang, Hua	Data analysis (analysis and interpretation of NMR data for all ircinianins molecules, 10%), wrote and edited the paper (5%) (Chemistry)
Piggott, Andrew M.	Designed experiment (HRESIMS, 5%), data analysis (HRESIMS, 5%), wrote and edited the paper (5%) (Chemistry)
Lynch, Joseph W.	Data analysis (10%), wrote and edited the paper (50%) (Pharmacology)
Capon, Robert J.	Data analysis (10%), wrote an edited the paper (50%) (Chemistry)

3. **Balansa**, **W**.; Islam, R; Fontaine, F.; Piggott, A.M; Zhang, H; Gilbert, D; Lynch, J.W.; Capon, R. J. Australian marine sponge alkaloids as a new class of glycine-gated chloride channel receptor modulator. *Bioorg. Med.Chem*. 2013, *21*, 4420-4425. Incorporated as Chapter 5.

Contributor	**Statement of contribution**
Balansa, Walter	Designed experiments (95%), data analysis (70%), wrote and edited the paper (35%) (Chemistry)
Islam, Robiul	Designed experiment (75%), data analysis (65%), wrote and edited the paper (40%) (Pharmacology)
Fontaine, Frank	Designed experiment (YFP primary screening, 10%), data analysis (YFP primary screening, 10%), wrote and edited the paper (5%) (Pharmacology)
Zhang, Hua	Data analysis (critically analyzed all molecules, 10%), wrote and edited the paper (5%) (Chemistry)
Piggott, Andrew M.	Designed experiment (HRESIMS, 5%), data analysis (HRESIMS, 5%), wrote and edited the paper (5%) (Chemistry)
Xiao, X	Data analysis (synthetic of aplysinopsin, 5%), wrote and edited the paper (5%) (Chemistry)
Webb, Timothy	Designed experiment (YFP primary screening, 5%), data analysis (YFP data, 5%), wrote and edited the paper (5%) (Pharmacology)
Gilbert, Daniel F	Designed experiment (YFP primary screening, 10%), data analysis (5%), wrote and edited the paper (YFP data, 10%) (Pharmacology)
Lynch, Joseph W.	Data analysis (10%), wrote and edited the paper (50%) (Pharmacology)
Capon, Robert J.	Data analysis (10%), wrote an edited the paper (50%) (Chemistry)

Contributions by others to the thesis

The work presented in this thesis was a result of research collaboration between Capon Group of Institute for Molecular Bioscience (IMB) and Lynch Group of the Queensland Brain Institute (QBI), The University of Queensland. In addition to formulating the concept and designing the GlyR project, Professor Robert J. Capon (IMB) and Professor Joseph Lynch (QBI) contributed substantially to drafting, critical analysis and interpretation of the data on the publications. Professor Capon also critically revised this thesis. Dr. Daniel Gilbert, Dr. Timothy I. Webb and Dr. Frank Fontaine conducted preliminary screening while Dr. Robiul Islam performed electrophysiological screening (secondary screening) (as part of his PhD thesis). Dr Andrew Piggott acquired high-resolution mass spectral (HRESIMS) data for all molecules on three publications in this thesis and NMR data for all new compounds isolated by means of HPLC-SPE-NMR in Chapter 3 of this thesis. Dr Xiao Xue obtained all data for single ion extractions at Chapter 4 of this thesis and Dr. Hua Zhang contributed to analysis and interpretation of research data on the publications.

Statement of parts of the thesis submitted to qualify for the award of another degree

"None".

Acknowledgements

All the internal and external battles that I had to fight and mountains that I had to climb to finally complete this thesis would have been in vain without the help of the following exceptional people and institutions. I am truly humbled by your constant support throughout my study at the Institute for Molecular Bioscience (IMB), The University of Queensland (UQ) Australia. You have given me time and opportunities to develop and even when I reached the nadir of my pursuit of a PhD, you never lost faith in my ability to complete it. So, I would like to take this opportunity to acknowledge your extremely useful contributions.

First and foremost, I want to thank my principal supervisor—Professor Robert John Capon—for a thorough grounding in the principle of marine natural product chemistry and the art of scientific writing. I have the privilege of using the state of the art of technologies and research facilities in his laboratory, of getting his encouragements when my research and writing along with its repeated revisions and life felt flat and looked unbearable, of receiving his challenges when I was self-satisfied with my results and of having his wonderful guidance which steers me toward the completion of this thesis.

Thanks are also due to my co-supervisors Dr. Andrew M. Piggott and Dr. Hua Zhang for their precious supervisions (technological and technical assistances, data processing as well as data analysis). Their continuous help and support make this thesis possible. Also, to the members of the Capon research group (Rob, Andrew, Hua, Angela, Frank, Sean, Raju, Fabien, Soumani, Zeinab, Melisa, Victor and Venkat), thanks heaps for lots of birthday cakes and parties, your constant support, friendship and wonderful discussions about marine natural products chemistry, science, life and other things in between at the roof top of the IMB and around UQ's campus.

I am deeply grateful for the assistance of Professor Joseph Lynch, Dr. Robiul Islam and Dr. Daniel Gilbert of Queensland Brain Institute (QBI), The University of Queensland (UQ), Dr. Frank

Fontaine of Institute for Molecular Bioscience (IMB), The University of Queensland for their excellent expertise, insightful discussions and scientific assistances in particular about the GlyR bioassays. Thank you very much for years of fruitful collaboration.

I have benefited greatly from doctoral research funding from Australian Development Scholarship (ADS). I am also indebted to the Institute for Molecular Bioscience, The University of Queensland for financial support during my last three months stay in Australia and all the excellent supports throughout my study at the IMB.

Grateful acknowledgment is made to the Institute for Molecular Bioscience and The University of Queensland for constant support particularly during my 'rough time' at the end of my study. IMB and UQ have been very generous to give me so many chances year after year through UQ's extension scheme program, which has made a difference to my life not only as a student but also as a person. Thank you very for sticking with me when a lot of universities and institutions might have given up!

Further I want to acknowledge Dr. Amanda Carozzi of the Institute for Molecular Bioscience. I am so grateful for all support she has given me from the commencement to the milestones through the long and winding way of my PhD extension program. Thank you very much for bearing with me, for being so patient and generous!

Finally, I want to reach deep into my heart and thank Annie Katiandagho and Kirsten Kirei Hanna Balansa, my best friends, my inspiration and everything. Thank you for always being there for me, helping me to get back into the game of life every time I get knocked down and above all for "dancing" with me "until it rains".

Keywords

Ircinialactam, ianthellalactam, ircinianinlactam, aplysinopsin, tubastrindole, glycine receptor, pain, hyperekplexia, spasticity

Australian and New Zealand Standard Research Classifications (ANZSRC)

1. ANZSRC code: 030401 Biologically Active Molecules 60%
2. ANZSRC code: 110904 Neurology and Neuromuscular Diseases 40%

Fields of Research (FoR) Classification

1. FoR code: 0304, Medicinal and Biomolecular Chemistry 60%
2. FoR code: 1109, Neurosciences 40%

Table of Contents

List of Figures

List of Tables

List of Abbreviation Used in the Thesis

Institutions

IMB	Institute for Molecular Bioscience
QBI	Queensland Brain Institute
UQ	The University of Queensland

Chemicals and Reagents

TFA	Trifluoro Acetic Acid
DCC	Dicyclohexyl Carbodiimide
DMAP	*N,N*-Dimethyl-4- Aminopyridine
MCPBA	*m*-Chloroperbenzoic Acid
$NaBH_3CN$	Sodium Cyano Borohydrate

Pharmacology

GABA	γ-Aminobutyric Acid
$GABA_AR$	γ -Aminobutyric Acid Type-A Receptor
$GABA_CR$	γ -Aminobutyric Acid Type-C Receptor
$5HT_3R$	5-Hydroxytryptamine Type-3 Receptor
EC_{50}	Equivalent Agonist Concentration required to activate 50% of maximum available current
IC_{50}	Equivalent Antagonist Concentration required to inhibit 50% of activated current
Cys-loop	Cysteine Loop
nAChR	Nicotinic Acetylcholine Receptor
PGE_2	Prostaglandin E2
PKA	c-AMP Dependent Protein Kinase
PKC	Protein Kinase C
YFP	Yellow Fluorescence Protein
EC	Extracellular
TM	Transmembrane
GlyRs	Glycine Receptors

GlyRα1/α1GlyR	Glycine Receptor Subunit α Type 1
GlyRα2/α2GlyR	Glycine Receptor Subunit α Type 2
GlyRα3/α3GlyR	Glycine Receptor Subunit α Type 3
GlyRα4/α4GlyR	Glycine Receptor Subunit α Type 4
GlyRβ/	Glycine Receptor Subunit β Type
TFT	Tail Flicking Test
HPT	Hot Plate Test

Chromatography/Spectroscopy

[α]D	Optical Rotation (room temperature)
DAD	Diode Array Detector
ELSD	Evaporative Light Scattering Detector
HRESIMS	High Resolution Electrospray Ionization Mass Spectrometry
LRESIMS	High Resolution Electrospray Ionization Mass Spectrometry
HPLC	High Performance Liquid Chromatography
MS	Mass Spectrometry
NMR	Nuclear Magnetic Resonance
SPE	Solid Phase Extraction
UV-vis	Ultraviolet Visible
LCMS	Liquid Chromatography Mass Spectrometry
LC-SPE-NMR	Liquid Chromatography Solid Phase Extraction Nuclear Magnetic Resonance

Nuclear Magnetic Resonance (NMR)

COSY	Correlation Spectroscopy Gradient Correlation Spectroscopy Gradient
HSQC	Heteronuclear Single Quantum Coherence Gradient
HMBC	Heteronuclear Multiple Bond Correlation Coupling Constant (in Hertz)
NOE	Nuclear Overhauser Effect
d	Doublet
t	Triplet
q	Quartet
m	Multiplet

Other

DBE	Double Bond Equivalents
MW	Molecular Weight
rt	Room Temperature
t_R	Retention Time

Appendices

CHAPTER 1
GENERAL INTRODUCTION

1. 1. Cys-loop ligand gated ion channels

Cys-loop receptors that mediate fast excitatory and inhibitory synaptic neurotransmissions belong to ligand gated ion channels (LGICs)[1-3], which was the third most targeted of the recent 324 approved drug targets[4]. Typically, the cys-loop receptors form a pentameric structure with a family of four ionotropic receptors—all of which are crucial targets for the treatments of neurological disorders—including serotonin type-3 receptors (5-HT_3Rs), the nicotinic acetylcholine receptors (nAChRs), γ-amino butyric acid type-A ($GABA_AR$) and type-C ($GABA_CR$) and glycine receptors (GlyRs)[1]. 5-HT_3Rs, and nAChRs that form cation (Ca^{2+} and K^+) pentameric sensitive pore facilitate excitatory neurotransmission leading to depolarization in the cells[2,3]. In contrast, GABARs and GlyRs that construct anion (Cl^- and HCO_3^-) permeable pore mediate rapid inhibitory neurotransmission resulting in hyper-polarization in the cells[3,5]. Both stimulatory and inhibitory synaptic transmissions have well-established roles in maintaining various neurological functions and whose disruptions are inflicted with neurological disorders and/or diseases[5-7].

5-HT_3Rs and nAChRs, for example, sculpt excitatory neurotransmission in the brain, peripheral and central nervous system (CNS) and are targets for many neurological diseases[6,7]. nAChRs reside in both the CNS (highly expressed in the hippocampus) and peripheral nervous system (PNS) particularly at the skeletal neuromuscular junction and in the autonomic nervous system[6]. At these locations, nAChRs play a variety of crucial physiological functions ranging from learning memory to improving cognition through memory formation[6]. Dysfunctions of nAChRs are implicated with various neurological disorders (Alzheimer's diseases, schizophrenia, depression, attention deficit, hyperactivity disorder and tobacco addiction)[6]. The serotonin type-3 receptors (5-HT_3Rs) are also important excitatory neurotransmitters in the brain mainly expressed in the area postrema, the caudate nucleus, hippocampus and the amygdala[8]. These receptors are relevant targets for the treatments of CNS diseases such as depression[9] and psychotic disorders[10].

In contrast, the chloride channel receptors $GABA_A$Rs and GlyRs are the major inhibitory neurotransmitters in the brain and CNS[5]. Specifically, $GABA_A$Rs signalling orchestrates synaptic inhibition in the brain with these receptors being clinically relevant targets for anti-convulsant, anxiolytic, sedative-hypnotic, epileptic[11], cognitive deficit, schizophrenic, antidepressant and substance abuse agents[12]. GlyRs are the major neurotransmitters in the CNS but with more restricted distribution than $GABA_A$Rs[13]. GlyRs are expressed specifically in the spinal cord, brain stem and in particular part of the brain such as cerebellum, the retina and hippocampus[5]. At these sites, GlyRs play key roles in respiratory rhythms, motor control, muscle tone, temporal tone and epilepsy as well as sensory and pain processing[13]. The discrete distribution of GlyRs is beneficial as it provides fewer side effects as a pain target compared to cannabinoid receptors[14] and a more localized enhancement of glycinergic inhibition[13].

1.2. GlyRs as A Drug Target

Like other members of cys-loop LGICs, GlyRs feature pentameric structures (Figure 1.1) drawn from their homology with nAChRs, the prototypical cys-loop LGICs[15]. In total, five genes (GlyRα1-4 and GlyRβ) of GlyRs have been identified in mammalian tissues with different distribution in the spinal cord, brain stem and other parts of the brain[2]. These discrete expression and distribution dictate the pharmacological profiles, with dysfunctions of GlyRs linked with a range of neurological diseases/disorders such as hyperekplexia[16], muscle tension[14], spasticity[17], epilepsy[18] and inflammatory pain[1,19].

1.2.1 GlyRs Structure

Each subunit of the pentameric GlyRs contains an amino-terminal extracellular domain with a loop connected by disulphide bonds acting as the ligand binding site, four transmembrane domains (M1-M4) assembled together with the second transmembrane (M2) forming the pentameric chloride sensitive pore, a large intracellular loop (IL) between M3 and M4 as the intracellular modulation sites (Figure 1.1)[2]. M3 and M4 are linked by a large, poorly conserved, intracellular domain that contain phosphorylation sites and other sites mediated by cytoplasmic factors[2]. Several GlyR modulators including gingkolides, bilobalide and picrotoxins are known to modulate the second and the third transmembrane domain (M2-M3)[20] (discussed in section 1.4.2, page 9). A very recent

discovery also stressed the importance of a group of polar amino acids in these two transmembranes and the vicinity of transmembrane domains in facilitating a hydrogen interaction between tetrahydrocannabinoids (THC) and modulation of GlyRs by THC respectively[21].

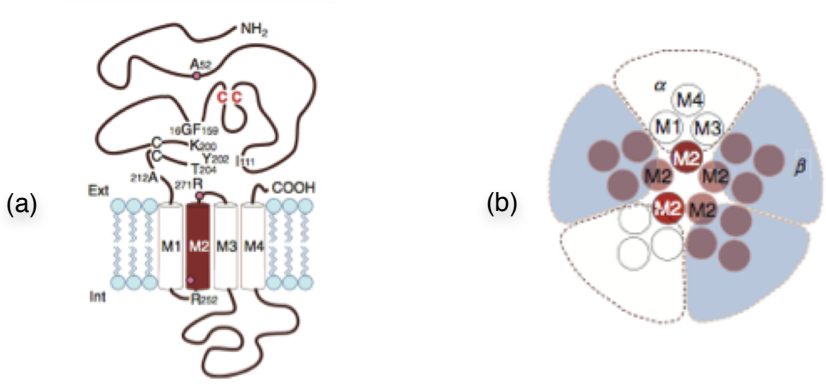

Figure 1.1. The structure of GlyRs. (a) The topology of α subunit featuring the disulphide bridge that forms the Cys-loop signature of LGIC (red). (b) The mature α2β3 receptor with two copies of α subunits (transparent), three of β subunits (light blue), four transmembrane (M1-M4) regions (cylinders) and pore-forming domain M2 (dark brown) modified from Vannier and Triller 2009[22].

The five GlyRs subunits (α1-α4) and β have distinct expressions and distributions depending on the period of embryonic development. In the early developmental stage, GlyRα2 and GlyRα4 are highly expressed in most CNS areas, but are totally replaced by α1β heteromer in the postnatal period[2,23] with both subunits retained until adulthood in specific area such as retinal cells[24,25]. In the mature neurons, however, GlyRs comprise GlyRα1 and GlyRβ subunits with GlyRs being expressed at high level in the spinal cord and brain stem, but at lower level in the thalamus and hypothalamus[2]. Following low levels of expression during embryonic phase, GlyRα1 and GlyRβ accumulate and maintain high levels of expression in mature neurons with both subunits contributing to the ligand binding domain[26]. GlyRα3 mirrors expressional pattern of GlyRα1 but with limited spatial expression and lower concentrations than GlyRα1, except for retinal cells where GlyRα3 dominate all other subunits[24].

The pentameric GlyRs also feature distinct subunit compositions and binding sites. They can exist either as α homomers or αβ heteromers assembled in 2α/3β stoichiometry (Figure 1.1b)[22] with the glycine-binding site of α/β heteromeric GlyRs is jointly formed by α and β subunits[26]. Although β subunits can form functional GlyRs, these subunits interact with gephyrin and thereby mediate synaptic clustering of GlyRs[27]. GlyRα1 has been proposed to have at least two binding sites while GlyRα1β has at least three binding sites at which allosteric ligands such as ivermectins exerted different effects as both antagonists and potentiators of GlyRα1[1].

Together, the above different subunit compositions, expressions and arrangements and binding sites determine pharmacological characteristics of different subunits of GlyRs.

1.2.2. GlyRs Pharmacology

Many research groups recently reported important roles of GlyRs both in non-neuronal[28] and neuronal cells[1,2,20,23]. However, due to their major functions as neurotransmitter receptors, the following focuses exclusively on the role of GlyRs in the CNS and part of the brain where they control excitatory neurotransmissions. Dysfunctions and defects of GlyRs subunits are known to underlie many intractable CNS related diseases such as muscular tension[17], epilepsy[18], spasticity[17], inflammatory pain[19] and hyperekplexia[29].

1.2.2.1 Hyperekplexia

The glycinergic defects due to mutations of and/or dysfunction of GlyRα1 are associated with spasticity[17,29] and inflammatory pain[19] with the human hereditary disorder (startle diseases)[30] as the most predominant case[1,30]. Hyperekplexia is a neurological disorder typified by an exaggerated response to unexpected stimuli[31]. For instance, hyperekplexia patients can suddenly jump, yell or raise their hands in response to unexpected touch or sound[32] and in a severe case, they can even convulsively jerk in responding to light stimulus, a similar response to strychnine poisoning[33]. At least, seven points of GlyRs mutation have been related to hyperekplexia[34] with mutations at R271L and R271Q in the extracellular M2-M3 linker of GlyRα1 being the major cause of the disorder (Figure 1.2)[16,35].

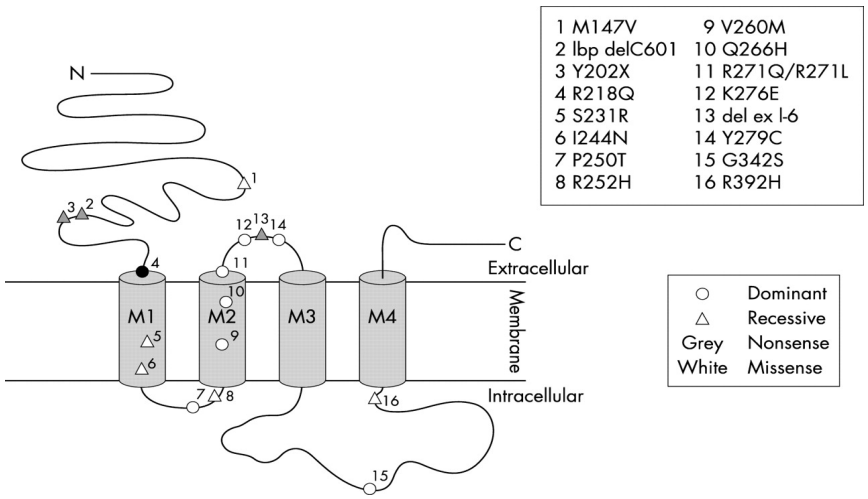

Figure 1.2. Mutations of GlyRα1 related to hyperekplexia[35]

1.2.2.2 Spasticity

A similar hypertonic motor disorder, spasticity, has also been identified in GlyRα1 mutated mice and rats[17,36]. Spasticity is characterized by an increase in motor neuron excitability and synaptic inputs owing to muscle stretch triggered by hyper excitability of spinal reflexes and reduced glycinergic inhibition.[17] Similar to hyperekplexia, spasticity can cause excessive startle reaction in addition to increasing muscle tone. In mice, spasmodic mutation (GlyRα1 ^{spd}) was caused by amino acid substitution (A52S) within the *N*-terminal domain of GlyRα1, a process known to affect agonist activity of the subunit[37]. This progressively disabling disease normally starts to appear one year after patients experience spinal cord injury (SPI). Spasticity is triggered by a down-regulation of potassium chloride co-transporter (KCC2), in the motor neurons resulting in depolarization of the chloride equilibrium potential thereby reducing postsynaptic glycinergic inhibition[17]. Since the GlyRα1 glycinergic inhibition is known to dampen motor neurons, these facts suggest that GlyRα1 is a promising target for treating spasticity[38].

GlyRα1 also mediates glycinergic inhibition in the retina[39,40] and the pain pathway[19]. Together with the other GlyR subtypes, GlyRα1 has been identified in the mouse retina with 30% of this subtype co-localizing with GlyRα3 in amacrine cells. In addition, it is known that GlyRα1 also colocalizes with GlyRα3 in the lamina II of the dorsal horn CNS where pain neurons terminate.[19] These facts suggest the importance of GlyRα1 in vision and

treatment of inflammatory pain although the absence of phosphorylation site in GlyRα1 was believed to indicate bigger risks of side effect than the GlyRα3[1,19].

The relative abundances of GlyRα2 and GlyRα4 in the retinal cells suggest the potential of these subunits in vision[39-41]. Due to the presence of a premature stop codon, GlyRα4 is considered as a pseudo-human gene[12], while GlyRα2 is also known to play a pivotal role in neuronal cell development switching the immature to mature neuron cells[20], in addition to delaying the onset of hyperekplexia disease[42].

1.2.2.3. Epilepsy

Another important pharmacological role of GlyRs relates to α2 and α3 GlyR splicing. Two variants of GlyRα3 namely α3KGlyR and α3LGlyR have been discovered in highly damaged human hippocampus of intractable temporal epilepsy (TLE) patients, strongly suggesting the importance of α3 GlyR splicing in pathophysiology of the temporal lobe epilepsy[18].

1.2.2.4 Inflammatory Pain

Perhaps the most interesting finding in GlyRs is the discovery of GlyRα3 in superficial layers of the spinal cord dorsal horn, the pain terminal[19]. This discovery has attracted much attention because α3 GlyRs mediates inhibitory neurotransmission onto spinal nociceptive neurons controlling inflammatory pain[1,43,44]. It has been proposed that injured or damaged tissues induce expression of two enzymes, COX-2 and PGE synthase, which in turn trigger the production of prostaglandin E_2 type in the spinal cord. Because PKA phosphorylation was present at GlyRα3, but not GlyRα1, PGE_2 via PKA-dependent phosphorylation only inhibited GlyRα3 (Figure 1.3)[19,43]. This inhibition reduces the inhibitory drive onto nociceptive projection neurons and increases the transmission of pain stimuli to the brain, strongly suggesting GlyRα3 subunit as an ideal target for pain treatment[1,19,43,44]. This discovery offers an interesting opportunity for scientists to discover safe and effective pain relief drugs[1,19,44].

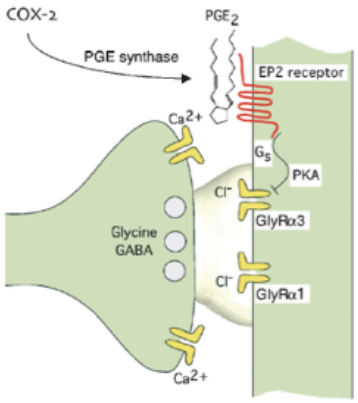

Figure 1.3. Model for glycinergic inhibition of GlyRα3 on dorsal horn lamina II of the central nervous system, reproduced from Zeilhofer 2005[43].

1.3. GlyR and Chronic Inflammatory Pain

In fact, the recent ineffectiveness of and safety issues associated with pain relief drugs have stirred serious concerns among medical professionals[45]. It has been estimated that patients received only 25% pain relief even after proper treatment with approved analgesics such as non-narcotic analgesics, non-steroidal anti-inflammatory drugs (NSAIDs) antidepressants, anticonvulsants and selective cyclooxygenase-2 (COX_2) inhibitors[45]. In addition, medication with opioids can have adverse side effects (euphoric effects leading to addiction and reduced efficacy among them) on patients. Based on 2010 figures, these analgesics retain a high market share (from 5% to 29% of US$27 billion) in 7 major pharmaceutical markets (US, Japan, France, Germany, Italy, Spain and UK)[45].

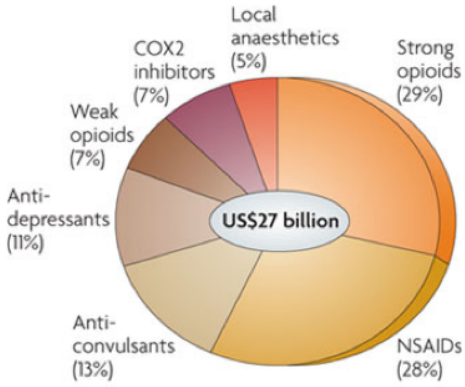

Figure 1.4. The percentage for market sharing of approved pain relief drugs adopted Melnikova 2010[45]

The above situation is not ideal and demands an ongoing improvement in the search for pain relief drugs, in particular the opportunity is offered by new and improved modes of action[45]. The marine cone snail derived pain drug ziconotide is an excellent example exerting its anti-inflammatory effect by modulating *N*-type calcium channels located on the primary nociceptive afferent nerves in the superficial layers of the dorsal horn of the spinal cord[46,47]. Because GlyRα3 is discretely distributed and mediates inhibitory neurotransmission in exactly the same area[19], it is believed that GlyRα3 subunit modulators offer the prospect of being safer pain drugs than opioids[14]. We endorse the hypothesis that treatment of pain is ideally targeted at this subunit[1], and that GlyRs represent a novel therapeutic strategy in treating pain and other CNS related diseases[13].

1.4. GlyR Modulators

Today, several molecules are known to modulate GlyRs mainly through allosteric and antagonistic modulations. Of the allosteric modulators, tropisetron (**1.5**), zatosetron (**1.7**) and bemesetron (**1.8**) are considered the best because of their potent modulating activity, displacing GlyRs with nanomolar potency[48,49], and high bioavailability against GlyRs[1]. Similarly, strychnine represents the best example of GlyR antagonist[1] as this alkaloid is the prototypic competitive antagonist of GlyRs showing nanomolar *K*i values at recombinant and native receptors in binding and functional assays[2]. Despite their promising activities, the pharmacological potentials of known GlyRs modulators are hampered by a lack of GlyR isoform specificity[1,38]. As a result, strychnine is known as non-specific pharmacological probe for GlyRs and no GlyR modulators (antagonists, agonists or potentiators) have advanced to the clinic[1,44].

1.4.1. GlyR Allosteric Modulators

Ivermectins (**1.1-1.2**), picrotoxins (**1.3-1.4**) and tropeins (**1.5**-**1.10)** are positive allosteric modulators of GlyRs, showing bifunctional activities either as potentiators or antagonists of GlyRs depending on concentration[1,48,49]. Ivermectin, a mixture of 22,23-dihydroivermectins B_{1a} (**1.1, ~**85%) and 22,23-dihydroivermectins B_{1b} (**1.2**, ~15%)—potentiated α1 GlyR at low concentration (0.01 μM) but activated the heteromer 1αβ GlyR at higher concentration (0.03 μM)[50]. These macrocyclic lactones were also capable of activating desensitized GlyR[50] and

modulating $GABA_A$, glutamate and acetylcholine receptors[1,49]. Picrotoxin, a mixture of picrotin (**1.3**) and picrotoxinin (**1.4**), acted as an allosteric GlyR with an inhibitory potency that decreased as the glycine concentration increased[1]. Howtrone and Lynch showed that picrotoxin strongly antagonized several mutan GlyRs with IC_{50} value of 0.64 to 10.3 μM by allosterically eliciting specific effects on the M2-M3 loop[51]. For decades, however, picrotoxin has been known as a potent inhibitor of both GlyRs and GABARs[52]. Tropeines such as tropisetron (**1.5**), LY-278,584 (**1.6**), zatosetron (**1.7**), bemesetron (**1.8**), granisetron (**1.9**) and atropine (**1.10**) also allosterically modulated GlyRs with **1.5**-**1.8** and **1.9**-**1.10** known as positive and negative GlyR agents respectively[48]. In the presence of glycine, **1.5**-**1.8** strongly (nanomolar) and **1.9**-**1.10** moderately (micromolar) displaced GlyRs[48]. In particular, **1.5** and **1.8** potently potentiated GlyRs with EC_{50} value of 10-1000 nM but inhibited the receptors at IC_{50} = 1-24 μM[53]. However, lack of specificity with cross modulation of other members of cys-loop LGIC (i.e. 5-HT_3 and α7 of nAChRs receptors) rendered them undruggable[54].

1.4.2. Antagonists

GlyR antagonists also show the same specificity issue. Gingkolides A-C and J (**1.11-1.14**) strongly antagonized GlyRs (α1, α2 and α1β) with IC_{50} value of 0.69-12 μM[55] and gingkolides B (**1.12**) and C (**1.13**) potently antagonized native GlyRs in native hippocampal neurons with IC_{50} values around 273 and 269 nM respectively[56]. Unfortunately, in addition to showing other neuromodulatory properties[57], the active constituents of *Gingko biloba* also activated $GABA_AR$ α1β2γ2L with IC_{50} value of 10 μM[58] and platelet activating factor (PAF) receptor with *K*i values of 0.07 to 0.9 μM[57,59]. Similarly, although several cannabinoid agonists such as HU-308 (**1.15**), HU-210 (**1.16**), WIN-212-2 (**1.17**), *N*-arachidonyl-ethanolamine (**1.18**) and *N*-arachidonyl-glycine (**1.19**) exerted strong antagonist activity against the GlyRs (10-15 μM), they strongly antagonised CB_1 and CB_2 receptor[38]. Finally, the plant alkaloid strychnine (**1.20**) is known as the classical antagonist of GlyRα1 inhibiting the subunit at IC_{50} =196.6 nM[60]. In addition to strychnine, protostrychnine (**1.21**), brucine 3 (**1.22**) and brucine 4 (**1.23**) exerted similar modulating activity against GlyRα1 although with weaker antagonistic activity (IC_{50} > 1 μM)[60]. However, like other known GlyR modulators, strychnine and derivatives were non specific GlyR modulators as they modulated $GABA_A$, nAChR and other members of LGIC[61].

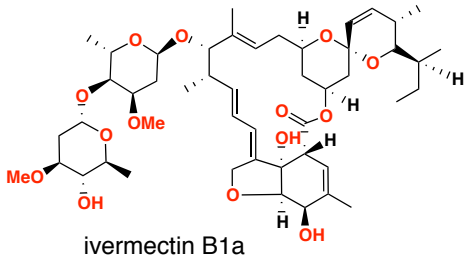

ivermectin B1a
(1.1)

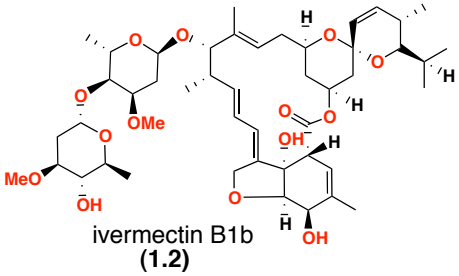

ivermectin B1b
(1.2)

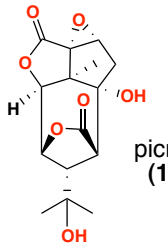

picrotin
(1.3)

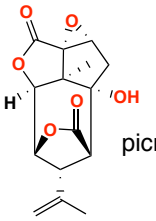

picrotoxinin
(1.4)

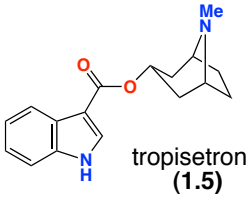

tropisetron
(1.5)

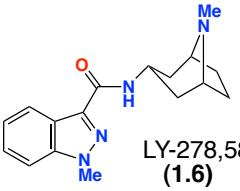

LY-278,584
(1.6)

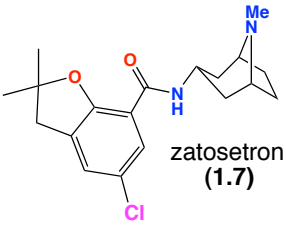

zatosetron
(1.7)

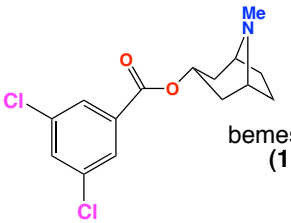

bemesetron
(1.8)

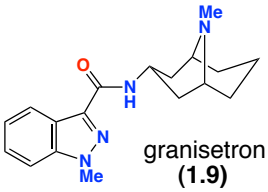

granisetron
(1.9)

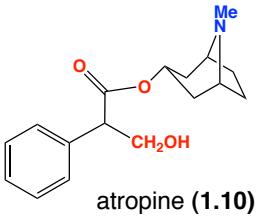

atropine **(1.10)**

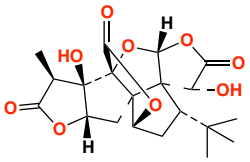

ginkgolide A **(1.11)**

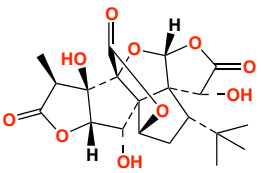

glnkgolide B **(1.12)**

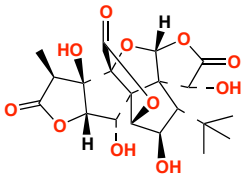

ginkgolide C **(1.13)**

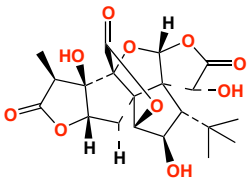

ginkgolide J **(1.14)**

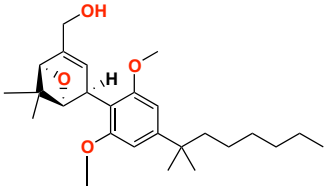

HU-308
(1.15)

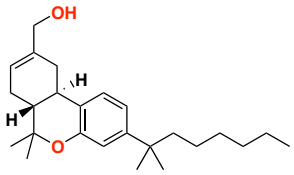

HU-210
(1.16)

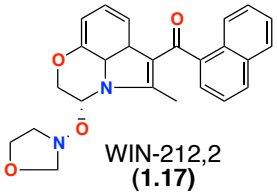

WIN-212,2
(1.17)

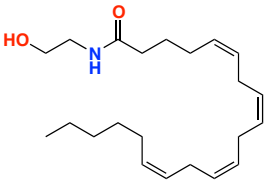

N-arachydonoyl
ethanolamine **(1.18)**

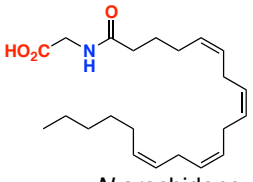

N-arachidonoyl
glycine **(1.19)**

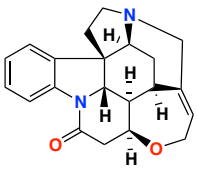

strychnine **(1.20)**

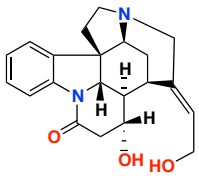

protostrychnine **(1.21)**

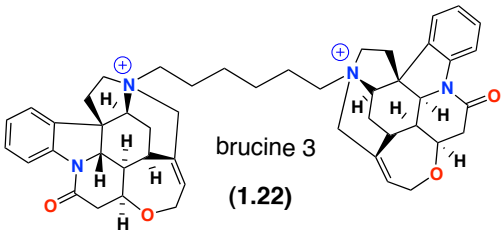

brucine 3

(1.22)

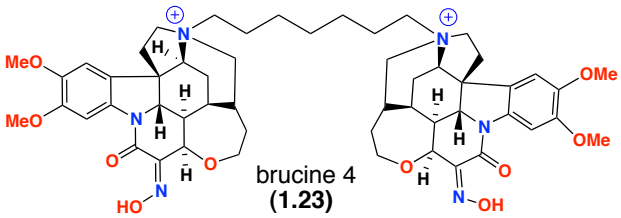

brucine 4
(1.23)

1.4.3. Possible Uses

Both GlyR antagonists and positive allosteric modulators have potential to be pharmacological probes and drugs. It has been demonstrated that potent and selective GlyR antagonists can have potential in treating convulsion and anxiety[62]. Likewise, evidence has been presented that upregulation of RNA edited GlyRα2 and GlyRα3 is a causal factor associated with temporal lobe epilepsy (TLE), suggesting that GlyR inhibitors could treat this debilitating disease[18,63]. However, because GlyR-mediated diseases such as inflammatory pain[19], spasticity[17], hyprekplexia[16,64] are identical with diminished GlyRs activity, positive GlyR modulators are presumably preferable[13]. Unfortunately, all known GlyR modulators have been hampered by their promiscuous modulating activities against receptors other than GlyRs. Although several synthetic cannabinoids and anandamide effected a strong pharmacological discrimination between α1 and GlyRα3, these ligands were considered unsuitable for physiological or behavioural studies due to non-specific actions at cannabinoid receptors CB1 and CB2[38]. Similarly, all GlyR positive allosteric modulators lacked receptor specificity, making them unsuitable for a therapeutics targeting specifically towards GlyRs[1,13]. The lack of specificity is even shown by strychnine, which remains the only known pharmacological probe for GlyRs[1]. These facts show the urgent need and value in discovering specific GlyR modulators that can serve as either pharmacological probes and/or drugs for treating various CNS diseases mediated by GlyRs.

Although many GlyR modulators have been discovered through recent discovery programs, receptor specificity remains a serious issue, arguably due to a heavy focus on the discovery of GlyR modulators from known non-specific modulators[48,65]. While strategically quick to deliver GlyR modulators, the approach seems predestined to fail on delivering the requisite selectivity[48,54]. This situation and the current high demand for novel, potent and specific GlyR modulators[1] clearly warrant a new approach to discover GlyR modulators. One of the ways to achieve this is by screening GlyR modulators from a potential source of bioactive molecules including marine invertebrates[66-68].

Curiosuly, most marine invertebrates have soft body, are sessile and therefore are prone to predation. Yet, they thrive in a competive marine environment such as coral reef presumably because they have developed chemical defense enabling them to establish a particular niche[68]. Although early discovery of bioactive molecules from these marine invertebrates was an aferthought, recently there has been a realisation that these active compounds

would ultimately be useful for treatments of human diseases[68]. Over the years, sponge, tunicate, bryozoan and coral have inspired researchers to identify and discover both new pharmacological tools and marine drugs from these marine invertebrates[66-68]. In fact, these invertebrates have proven to be a very rich source of potent bioactive compounds many of which have advanced to Phase II/III chlinical trials in anticancer, analgesic, allergic and cognitive diseases, discussed in detail below[68].

1.5. Marine Natural Products (MNPs) as a Source of Bioactive Molecules

The last five decades have witnessed the emergence of marine natural products as an important source of bioactive molecules with pharmacological potential[66]. Four marine derived drugs have made their way to the market, with thirteen MNPs being in the different stages of clinical trials and many others in pre-clinical trials[66]. With the recent technological improvements[5,67,69], it is anticipated that MNPs will continue to make a significant contribution to the discovery of new pharmacological tools and drugs for treating many human diseases[70], including diseases related to the dysfunction of ion channels. In addition to ziconotide, there are a number of MNP derived modulators of voltage gated ion channel (VGIC)[71]. Up to now, however, little is known about MNPs as LGIC modulators[72].

1.5.1. Marine Natural Product in Medical Clinic

Ara-A (**1.24**), Ara-C (**1.25**), ziconotide (**1.26**), and trabectedin (**1.27**) (Figure 1.5) represent four MNP derived drugs known today. Cytosine arabinosine or Ara-C, cytarabine or Ara-A were synthetic purine and pyrimidine nucleosides respectively inspired by two nucleosides isolated from the Caribbean sponge *Tethya crypta*. Ara-C and Ara-A received FDA approval in 1969 and 1976 as anticancer and antibiotic agents respectively[66]. Both MNP derived drugs have given significant impacts on antibiotic and cancer pharmacology generating 13,008 and 3640 peer review publications respectively[66]. The pain relief drug, ziconotide or Prialt (**1.26**), successfully made to the market in 2004, almost three decades after the approval of Ara-A. This synthetic peptide developed from the peptide of a fish hunting cone snail *Conus magnus*[73] exerts its anti-inflammatory by blocking the sodium voltage gated ion channel[47]. Three years after the approval of ziconotide, trabectedin also known as Yondelis (ET-743)

discovered from the Caribbean tunicate, *Ecteinascidia turbinata*[74] received European Union's approval as an anticancer drug for the treatments of soft tissue sarcoma[75] and platinum sensitive ovarian cancer[76]. As 2011, trabectedin was also in the phase III of clinical trials in the US[66].

Thirteen MNPs have advanced to various levels of clinical trials (Figure 1.5). The tetrahydorisoquinoline alkaloid, trabectedin (**1.27**), peptide soblidotin (**1.28**) and polyether macrolide eribulin mesylate (E7389) (**1.29**) are now in the phase III clinical trials[66]. These molecules were originally isolated from tunicates *Ecteinascidia turbinaria*[77] and *Symploca* sp[78] and a sponge *Halicondria okadai* [79] respectively as anticancer agents targeting tubulin[80]. Seven marine metabolites are also now in the phase II clinical trial[66]. They include the peptide tasidotin (**1.30**) from a tunicate *Symloca sp*., cyclic peptide elisidepsin (**1.31**) from *Elysia refuscens*[81], depsipeptide plitidepsin (**1.32**) from *Aplidium ablicans*, alkaloid PM1004 from tunicate *Jeruna funerbis* (**1.33**), diketopiperazine plinabulin (**1.34**) from marine bacteria *Aspergillus* sp., and alkaloid DMXBA (**1.35**) from a marine worm *Ampiphorus angulatatus* and diterpene glycoside pseudopterosin (**1.36**) from *Pseudopterogorgia elisabethae* (Figure 1.5)[66]. Of these, **1.30-1.34** are anticancer agents targeting tubulin, solid tumour, and DNA triplets, while the alkaloid DMXBA (**1.35**) peptide pseudopterosin (**1.36**) target cognition/schizophrenia and wound healing respectively[66,82]. Finally, three MNPs have entered phase I clinical trial as anticancer including protein inhibitor bryostatin (**1.37**) from bryozoans *Bugula*, proteasome binding salinosporamide A (**1.38**) from a marine bacterium *Salinospora tropica*[83] and tubulin inhibitor hemiasterlin (**1.39**) from a sponge *Hemiasterella minor*[84].

Although the number of marine drugs and the drug discovery in the pipeline are low compared to terrestrial natural products, this is not a measure of relative potential but rather reflects the invaluable marine biodiscovery. From 1998 to 2006, hundreds of MNPs advanced to preclinical trials, including 592 molecules with anti tumour and cytotoxic activities and 666 compounds with antibacterial, anticoagulant, anti-inflammatory, antifungal, anthelmintic, antiplatelet, antiprotozoal and antiviral activities, actions on the cardiovascular, endocrine, immune and nervous systems as well as other miscellaneous mechanisms of actions[66]. By 2009, there were already 705 Pub Med references for marine pharmacology[70]. As pointed out by William Fenical of the Scripps Institute of Oceanography "*Since the field of marine natural products chemistry began in the mid 1960s, it has been clear that the oceans and their diverse biota represent a significant resource, perhaps the greatest resource on Earth (34 of the 36 phyla of life), for the discovery of new drugs. During the first decade of this science (ca. 1970–*

1980), researchers explored the oceans to discover the specific biological taxa that would yield bioactive molecules. Hundreds of structurally novel, bioactive molecules were discovered proving that marine organisms had the potential to be developed into drugs in many areas of human therapy"[70].

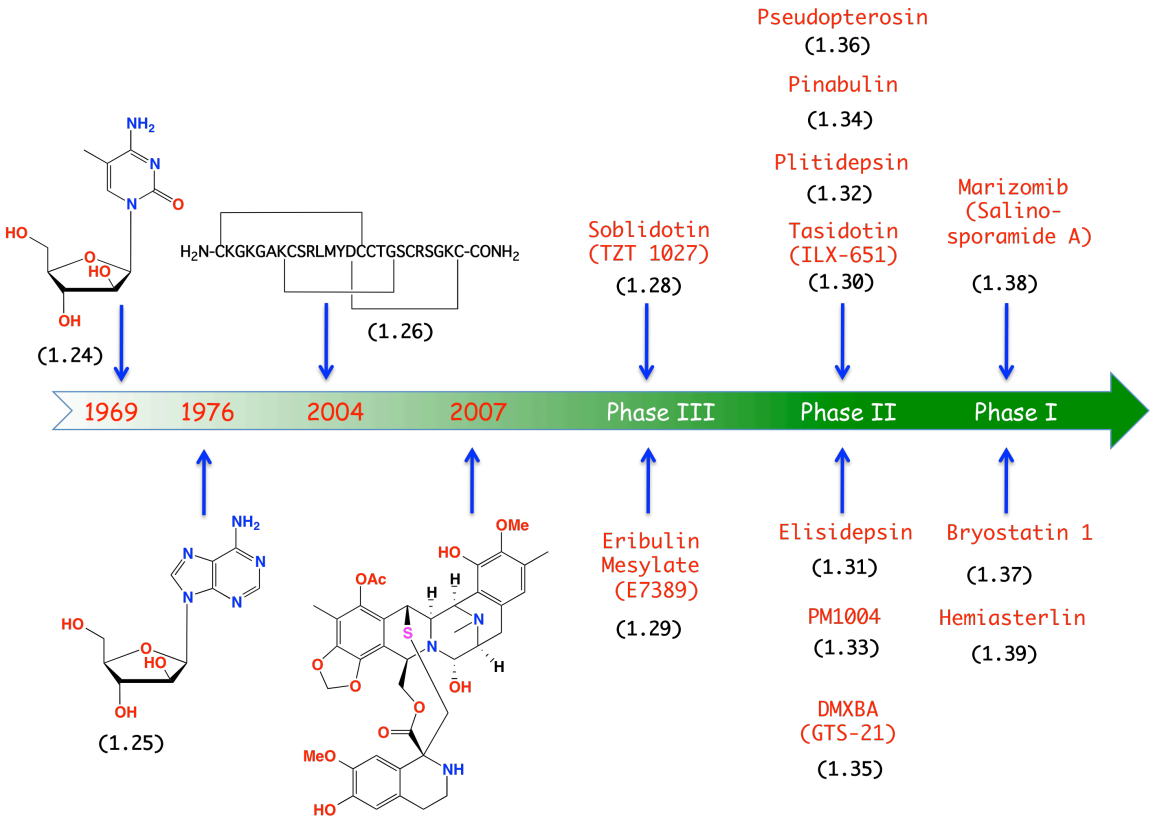

Figure 1.5. Examples of MNPs that have been approved as drugs and advanced to different stages of clinical trials modified from Mayer *et al* 2010 [66]

Early MNP researchers emphasized the discovery of novel chemical entities, while latter researchers have shifted the emphasis to bioactivity[66]. Traditionally, the discovery of bioactive MNPs were guided by phenotype-oriented bioassays such as cytotoxicity and/or antimicrobial tests[85]. Mechanism of actions targeted approach to drug discovery was not introduced to MNPs until recently[85]. An important challenge to developing MNP drugs is supply[66-68,86,87]. For example, to supply 2.0 gram of trabectedin[68] or 18.0 gram bryostatin required the harvest of 1 ton tunicate *Ecteinascidia turbinata* and 13 tons of bryozoans *Bugula nerita* respectively[86]. In the words of David Newman of the National Cancer Institute (NCI) "*In retrospect, this is one of the major reasons that the field evolved slowly. Discovery of a given compound was easy in relative terms, but development, which required large amounts, was, and still is, not simple*"[68].

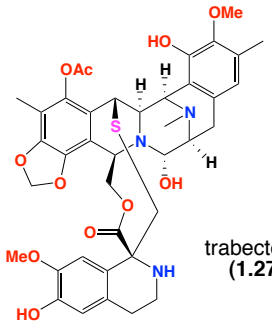

trabectedin (**1.27**)

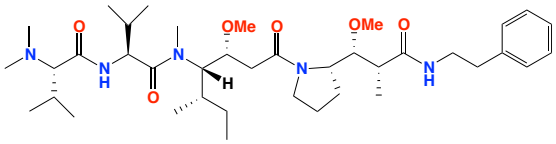

soblidotin (**1.28**)

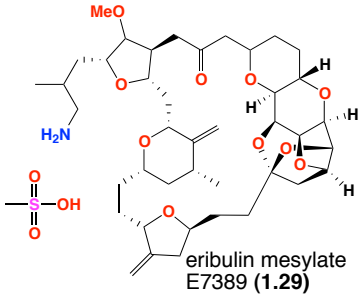

eribulin mesylate E7389 (**1.29**)

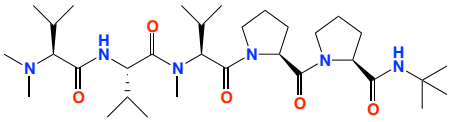

tasidotin (**1.30**)

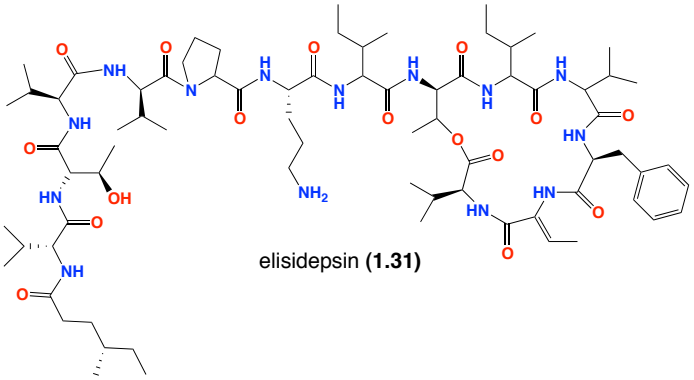

elisidepsin (**1.31**)

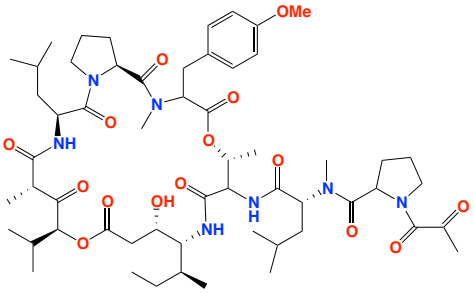

plitidepsin (**1.32**)

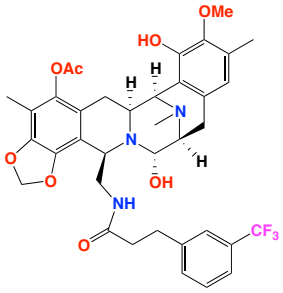

PM1004 (**1.33**)

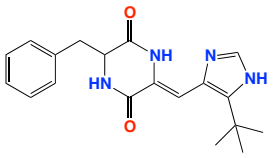

pinabulin (**1.34**)

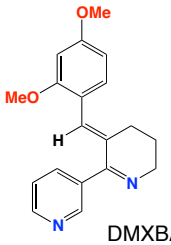

DMXBA (**1.35**)

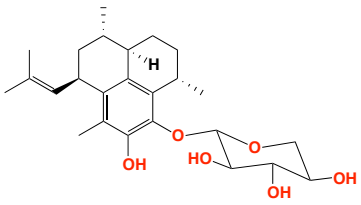

pseudopterosin (**1.36**)

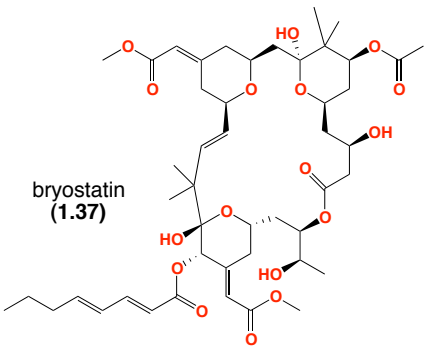

bryostatin (**1.37**)

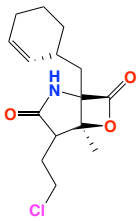

salinosporamide A (**1.38**)

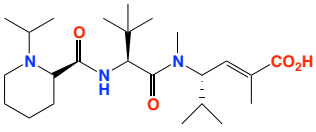

hemiasterlin (**1.39**)

1.5.2. The role of technology

Despite the challenge faced by MNP chemistry, recent technological improvements have significantly propelled the development of MNPs[66,67,70,87]. In the case of trabectedin, the supply issue has been successfully overcome by synthesis of trabectedin from its intermediate safracin B obtained from *Pseudomonas fluoresens*[68]. Although it is still work in progress, similar approaches also seem promising for bryostatins[66]. Structure elucidations of very limited MNPs (nanomole scale)[88] have been assisted by high temperature superconducting Nuclear Magnetic Resonance (NMR) cryoprobe[88] and limited, unstable as well as lacking UV-vis MNPs by LC-SPE-NMR[89,90,91]. Several molecules having complex structures have also been successfully synthesized[69] with (+)-discordemolide featuring 13 stereogenic centres and high degree of chemical sensitive functionality as an excellent example[92]. Moreover, MNPs profit from the recent developments in mass spectrometry technique simplifying the lengthy and complicated processes in identifying bioactive molecules through combination with other techniques such as multitarget affinity/specificity screening (MASS) and frontal affinity chromatography (FAC)[69]. Similarly, MNPs benefits from the discovery of myriad novel drug targets including ion channel receptors (Figure 1.6)[67], which were ranked third (LGIC) and fourth (VGIC) out of the 324 most approved drug targets[4]. Coupled with currently introduced automated patch clamp technology[93] and interdisciplinary collaboration[66], ion channel drug can be advanced by MNPs.

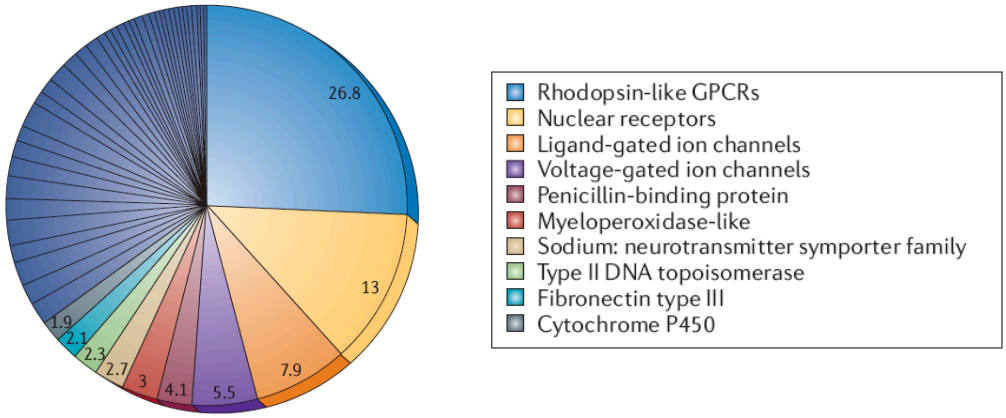

Figure 1.6. Top ten approved drug target revealing ligand gated ion channel (LGIC) as the third more popular approved drug target adopted from Overington 2006[4].

1.5.3. Ion Channel Modulators

Many scientists have explored the potential of MNPs as modulators of receptors belonged to voltage gated ion channel (VGICs). In addition to the peptide ziconotide[66] and many other marine toxins[72], several small molecules were capable of modulating VGIC receptors including 2β,3α-epitaondiol (**1.40**), flabellinol (**1.41**) and flabellinone (**1.42**), jamaicamide A (**1.43**), jamaicamide B (**1.44**), jamaicamide C (**1.45**), kalkitoxin (**1.46**), clathrodin A (**1.47**) and dibromosceptrin (**1.48**). The meroditepeneoids (**1.40-1.42**) isolated from brown algae *Stypopodium flabelliforme* act on sodium channel with the IC_{50} values of 0.7, 2.0 and 7.0 μM respectively[94,95]. The dinoflagellate *Lyngbya majuscula* produce three polyketide-peptide neurotoxins (**1.43-1.45**) that antagonize sodium channel with IC_{50} value of 5 μM[96]. The thiazole containing lipopeptide (**1.46**) from the Caribbean *L. majuscula* potently block sodium channel with an IC_{50} of 1.0 μM[97]. Two metabolites of genus *Agelas*, clathrodin A (**1.47**) and dibromosceptrin (**1.48**), also modulate Na_V channels by different mechanism with the monomer (**1.47**) activating and the dimer (**1.48**) inhibiting the sodium channel[98,99].

Up to now, however, little is known about the modulators for receptors members of LGIC superfamily other than anabaseine, an alkaloid isolated from a marine worm *Amphiporus lactifloreus*[100]. Anabaseine has been reported to activate the acetylcholine receptors in various animal species especially the neuromuscular $\alpha1_2\beta1\gamma\delta$ (embryonic) or $\alpha1_2\beta1\gamma\varepsilon$ (adult) and α7 nAChRs[100]. Inspired by this activity, 200 analogues were synthesized resulting in the discovery of 2,4-dimethoxy-benzylidine anabaseine (DMXBA) (**1.35**, Figure 1.4). This anabaseine derivative improved memory in animal models and is now in clinical trial for cognitive problems related with schizophrenia[100]. Today, however, almost nothing is known about GlyR modulator from MNPs notwithstanding the potentials of GlyRs as an emerging drug target for treatments of CNS diseases[5,21].

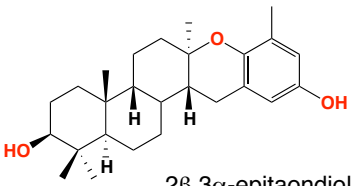

2β,3α-epitaondiol
(1.40)

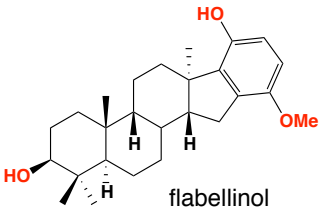

flabellinol
(1.41)

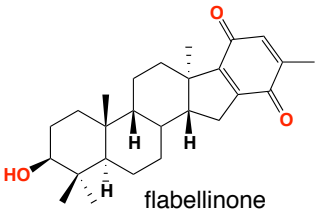

flabellinone
(1.42)

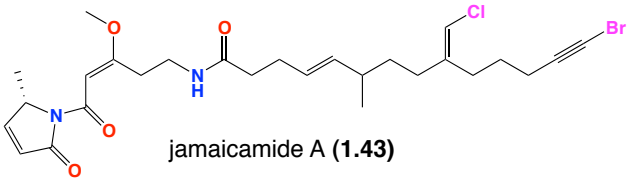

jamaicamide A **(1.43)**

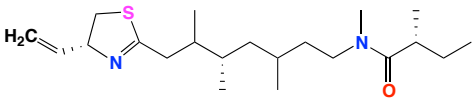

kalkotoxin **(1.46)**

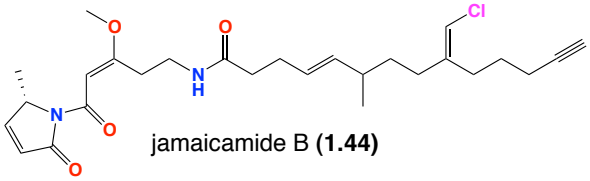

jamaicamide B **(1.44)**

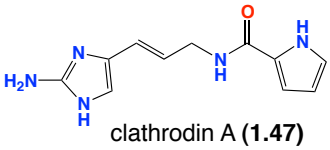

clathrodin A **(1.47)**

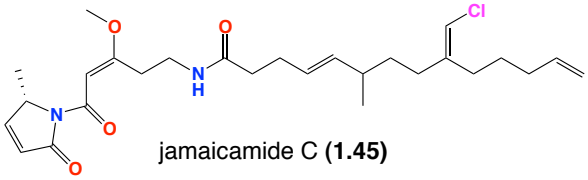

jamaicamide C **(1.45)**

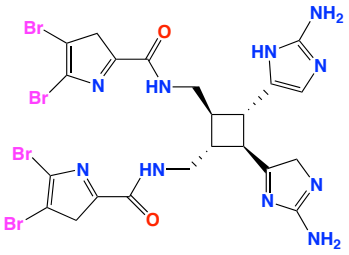

dibromosceptrin **(1.48)**

The emergence of GlyRs as a new drug target for treating CNS diseases[5], the lack of receptor specificity among existing GlyR modulators[1,44,101], the absence of GlyR modulators from MNPs despite being important source of bioactive molecules and the current high demand for high affinity and specificity GlyR modulators[1,20,44] encouraged us to explore the potential of MNPs as a new source of novel, potent and specific GlyR modulators.

CHAPTER 2

MARINE EXTRACT SCREENING

In order to discover MNP GlyR modulators, we screened >2,500 southern Australian and Antarctic marine invertebrate extracts using two assays, the yellow fluorescence protein (YFP) assay and automated patch clamp electrophysiology (APCE). While the YFP was used to screen crude marine extracts in order to detect priority samples, the APCE was employed to evaluate bioactivity of pure compounds of corresponding extracts previously observed in YFP analysis.

2.1. Yellow Fluorescence Protein (YFP)

The YFP assay takes advantage of yellow fluorescence protein sensitivity towards anion quenching. This assay is capable of reporting anionic influx into HEK293 cells[102]. In practice, an extract/compound is considered as an agonist when it opens (agonises) GlyRs allowing the influx of iodide ions and quenching YFP (Figure 2.1, (A1). Control (Figure 2.1, (A2) left) and test (Figure 2.1, (A2) right) images were taken and compared with quenching (changed in tested images) suggesting a GlyR agonist. In the same way, a potentiator opens (agonises) the GlyR. Unlike an antagonist, which can activate the receptor both in the presence and in the absence of glycine, a potentiator agonises the receptor only in the presence of low dose of glycine (Figure 2.1 (B1) but not in the absence of glycine. The control image (Figure 2.1 (B2) left) and the test image (Figure 2.1(B2) right) were taken and compared with the absence of quenching (no change in test image) suggesting potentiator of GlyRs. In contrast, an extract or a molecule is considered as an antagonist when it blocks the receptor, preventing the anion from quenching the YFP (Figure 2.1 (C1). The control images (Figure 2.1 (C2) left) and test image (Figure 2.1(C2) right) were also taken and compared with no difference between control and test images indicating the absence of YFP quenching or an antagonist activity. This activity was later confirmed by screening pure compound(s) isolated from corresponding active extract(s) against different GlyR subunits using an automated patch clamp electrophysiology.

(A1)

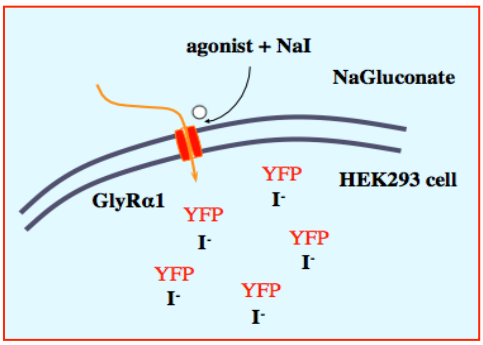

(A2)

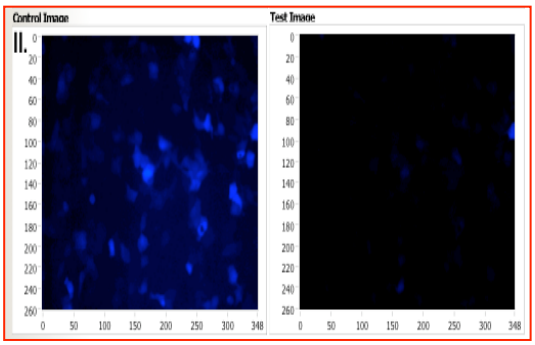

(B1)

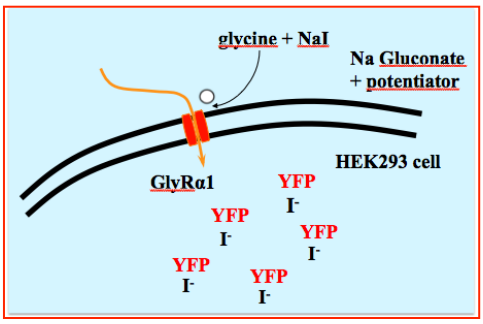

(B2)

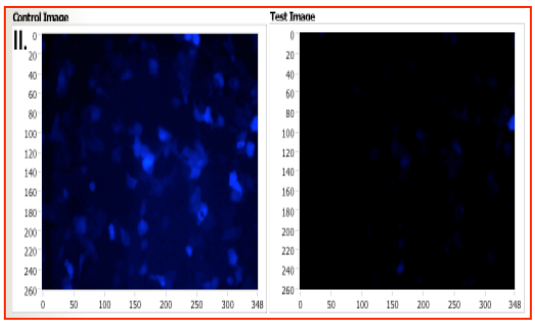

(C1)

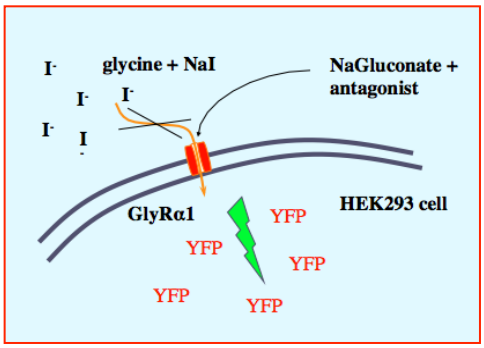

(C2)

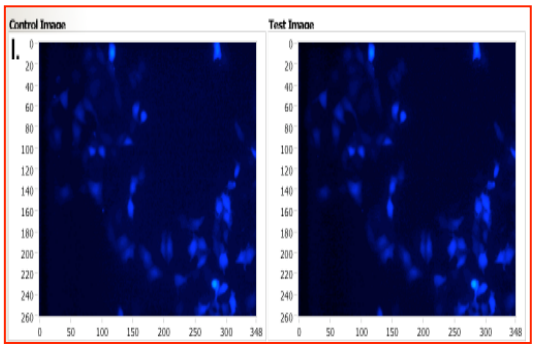

Figure 2.1. Illustration of agonist (A1), potentiator (B1) and antagonist (C1) with corresponding control images (A2), (B2) and (C2) respectively.

2.2. Electrophysiology (Automated patch clamp)

Patch clamp technique is one of the choices for secondary screening or lead optimization and is considered the gold standard in validating ion channel modulators[93,103]. In particular, the automated patch clamp has recently revolutionized the discovery of ion channel modulators through its capacity in performing high-throughput high sensitivity screening[103]. This automated technique has bridged the longstanding gap between the primary screening and secondary screening[93], a quality that may benefit MNPs whose active compounds are frequently only available in a very low yield[69].

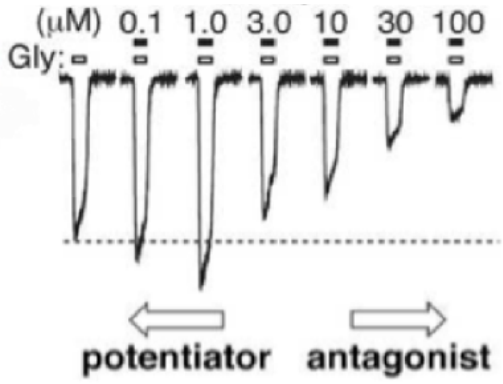

Figure 2.2. Illustration of agonist, potentiator and antagonist of GlyR (Electrophysiology). Doted line is the transition of conductance for glycine. Spikes above the transition conductance (3.0-100 μM) represent antagonist activity while spikes below the doted line (0.1-1.0 μM) suggests an agonist or a potentiator activity with the previous occurring both in the presence and in the absence of glycine while the latter taking place only in the presence of low dose of glycine.

Hence, this technique was used in our secondary screening to evaluate the biological activity of all pure compounds successfully obtained from the fractionation and purification of all priority extracts. Figure 2.2 illustrates patch clamp recording with doted line representing the transition of conductance for glycine, spikes below the transition of conductance (e.g. 0.1 and 1.0 μM) suggesting an antagonist activity and those above the transition conductance (e.g. 3.0-100 μM) suggesting either an antagonist or a potentiator activity. As previously described for YFP test, agonist activity occurs both in the presence and in the absence of glycine while potentiator takes place only in the presence of low dose glycine (Figure 2.2).

2.3. Marine Diversity Library

The above ion channel technologies were employed to screen a library of >2500 marine invertebrate and alga samples, collected from intertidal, coastal and deep-sea locations across southern Australia and Antarctica. The specimens were processed to generate an extract library suitably formatted for medium to high throughput bioassay. A portion (7.0 mL) of the archived EtOH extract of each marine sample was decanted, concentrated *in vacuo,* weighed and partitioned into *n*-BuOH (2.0 mL) and H_2O (2 mL). This pre-processing achieves a >10 fold concentration of "drug-like" small molecules, while simultaneously desalting and simplifying the solubility characteristics of, the *n*-BuOH soluble. Aliquots (1.0 mL) of both *n*-BuOH and H_2O phases were transferred to deep 96-well plates, to generate a set of extract library plates. These plates were subsequently used to prepare 10- and 100-fold dilution plates.

2.4. Biological Profiling

Primary screening was performed in two steps. In the first round screening, the EtOC extracts of >2,500 specimens were screened for antagonist activity against GlyRα1, leading to the identification of 27 hits (Table 2.1). As previously described for antagonist activity in YFP test (pages 19-20) and shown in Figure 2.3 (page 23), the hits were defined by comparing control and test images of corresponding extracts. For example, both test and control images for CMB-03344 extract were identical, indicating the absence of quenching during the test. As a result, this extract was assigned as having a strong antagonist activity (Figure 2.3, red). In contrast, there was a considerable difference between the control and test images of CMB-03322 with slightly lesser cells observed in the test image compared to the control, indicative of a modest quenching or a moderate antagonist activity (Figure 2.3, orange). Furthermore, a sharp contrast was observed between control and test images of CMB-02718 with much lesser cells observed in the test image, suggesting a strong quenching or a weak antagonist activity (Figure 2.3, yellow). In similar manner, we assigned in total 27 hits consisting of 3 strong, 19 moderate and 5 weak hits (Table 2.1) in the first round screening of 2,500 Australian and Antarctic marine invertebrates.

Following partition of the EtOH extract into *n*-BuOH and water-soluble extracts, we screened *n*-BuOH and water soluble against GlyRα1-GlyRα3. This screening resulted in 10, 5 and 7 GlyRα1, GlyRα2 and GlyRα3 antagonists for *n*-BuOH part as well as 3 and 1 GlyRα1 and GlyRα3 antagonists for water-soluble part. In order to determine priority extracts, the10 extracts were further subjected to chemical profiling (described in Table 2.2).

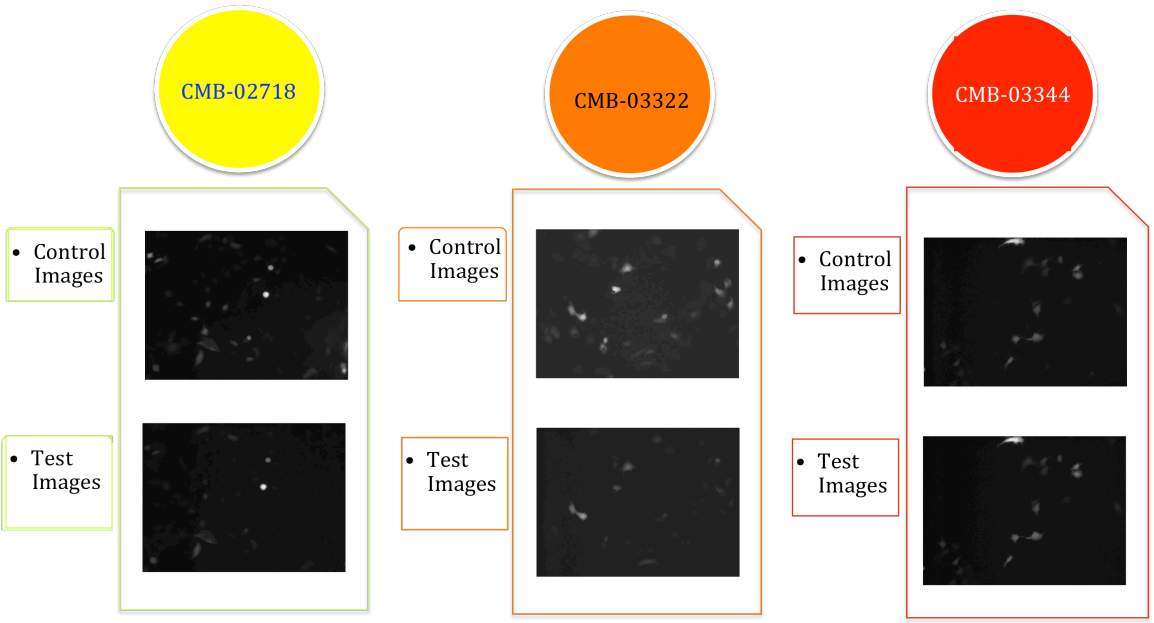

Figure 2.3. Control and test images of weak (yellow), moderate (orange) and strong (red) hits. Comparison of control image of CMB-02718

Table 2.1. Hits resulted from highthroughput screening of more than 2,500 specimens

CMB Marine GlyR Screening	Primary Screening (EtOH) extracts)	HITS					
		Butanol Extracts			Water Extracts		
		α1	α2	α3	α1	α2	α3
	CMB-01008						
	CMB-01064						
	CMB-01457						
	CMB-01510						
	CMB-01940						
	CMB-02433						
	CMB-02694						
	CMB-02709						
	CMB-02718						
	CMB-02816						
	CMB-02830						
	CMB-02858						
	CMB-03023						
	CMB-03102						
	CMB-03105						
	CMB-03174						
	CMB-03199						
	CMB-03200						
	CMB-03020						
	CMB-03022						
	CMB-03023						
	CMB-03231						
	CMB-03322						
	CMB-03344						
	CMB-03363						
	CMB-03590						
	CMB-03608						

Note: red, orange and yellow mean strong, moderate and weak activities while α1, α2 and α3 indicated (GlyRα1–α3) respectively.

2.5. Chemical Profiling

The *n*-BuOH soluble fractions were sequentially triturated into hexane, dichloromethane (DCM), methanol (MeOH) and water (H_2O). Likewise, water-soluble fractions were sequentially triturated into MeOH and H_2O soluble (Scheme 2.1). Further purification of active fraction was achieved by various combination of chromatography with an emphasis on HPLC.

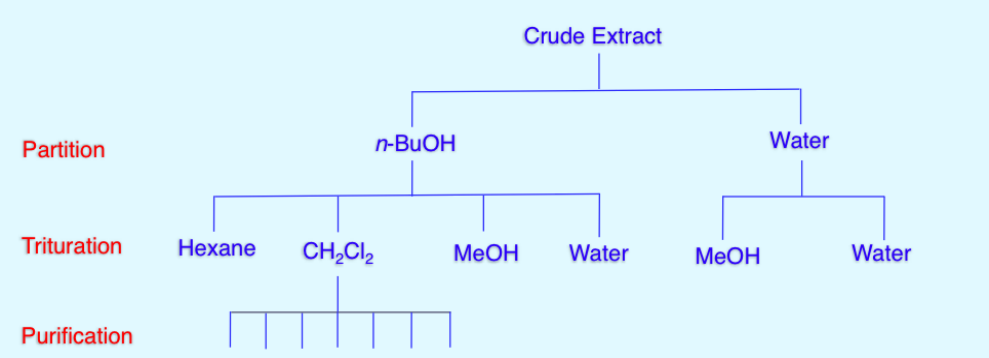

Scheme 2.1. Extract fractionation through solvent partition and trituration followed by chromatography.

Chemical profiling identified four-structure classes of extracts common to nine priority extracts. Online database (Marinelit) searching against spectroscopic data (*m/z*) coupled with ^{1}H NMR data analysis indicated the likelihood of at least four different structure classes as suggested by molecular weights (Table 2.2).

Table 2.2. Chemical and biological profiling on prioritized extracts and associated fractions.

		LRESIMS and Bioassay Guided Fractionation on Nine Potential Specimens							
		n-BuOH **Fraction mass (mg)/bioactivity**				**LRESIMS**			
	CMB-01064	**Petrol**	**DCM**	**MeOH**	**H_2O**	**tR (min)**	**ESI(+)MS**	**ESI(-)MS**	*MW*
		5.6	590.7	109.3	5.3				
			✔	✔		9.50	490 (M+ H)	488 (M-H)	489
			✔	✔		9.80	472 (M+ H)	470 (M-H)	471
			✔	✔		10.50	490 (M+ H)	488 (M-H)	489
			✔	✔		10.70	406 (M+H)	404 (M-H)	405
			✔	✔		14.50	413 (M+H)	468 (M-H)	416
			✔	✔		17.00	429 (M+H)	427 (M-H)	398
	CMB-03231	**Petrol**	**DCM**	**MeOH**	**H_2O**	**tR (min)**	**ESI(+)MS**	**ESI(-)MS**	*MW*
		1.4	75.3	43.4	-				
			✔	✔		11.50	406 (M+H)	404 (M-H)	405
			✔	✔		12.20	552 (M+H)	550 (M-H)	551
	CMB-03363	**Petrol**	**DCM**	**MeOH**	**H_2O**	**tR (min)**	**ESI(+)MS**	**ESI(-)MS**	*MW*
		8.4	267.8	208.1	41.4				
			✔	✔		6.75	472 (M+ H)	470 (M-H)	471
			✔	✔		7.25	490 (M+ H)	488 (M-H)	489
			✔	✔		7.50	406 (M+H)	404 (M-H)	405
			✔	✔		7.75	452 (M+H)	550 (M-H)	551
			✔	✔		9.80	413 (M+H)	468 (M-H)	416
			✔	✔		13.90	429 (M+H)	427 (M-H)	398
	CMB-01008	**Petrol**	**DCM**	**MeOH**	**H_2O**	**tR (min)**	**ESI(+)MS**	**ESI(-)MS**	*MW*
		5.6	590.7	109.3	5.3				
			✔	✔		9.25		547 (M-H)	547
			✔	✔		10.67	470 (M+H)	468 (M-H)	469
			✔	✔		11.76		475 (M-H)	475
			✔	✔		12.78	413 (M+H)	411 (M-H)	412
			✔	✔		14.84	397 (M+H)	395 (M-H)	396
	CMB-02858	**Petrol**	**DCM**	**MeOH**	**H_2O**	**tR (min)**	**ESI(+)MS**	**ESI(-)MS**	*MW*
		3.0	75.9	20.9	-				
			✔	✔		6.5		485 (M-H)	485
			✔	✔		10.52	429 (M+H)	427 (M-H)	428
			✔	✔		13.10	457 (M+H)	455 (M-H)	456
			✔	✔		14.12	413 (M+H)	411 (M-H)	412
	CMB-03344	**Petrol**	**DCM**	**MeOH**	**H_2O**	**tR (min)**	**ESI(+)MS**	**ESI(-)MS**	*MW*
		0.6	**255.0**	**74.6**	**3.3**				
			✔	✔		10.34	470 (M+H)	468 (M-H)	469
			✔	✔		11.16		475 (M-H)	475
			✔	✔		12.28	413 (M+H)	411 (M-H)	412
			✔	✔		14.38	397 (M+H)	395 (M-H)	396
	CMB-03322	**Petrol**	**DCM**	**MeOH**	**H_2O**	**tR (min)**	**ESI(+)MS**	**ESI(-)MS**	*MW*
		52.7	283.0	74.6	3.3				
			✔	✔		5.60	509 (M+H)	507 (M-H)	508
			✔	✔		5.67	257 (M+ H)	255 (M-H)	256
			✔	✔		9.13	254 (M+H)	253 (M-H)	254
			✔	✔		9.49	256 (M+ H)	254 (M-H)	255
			✔	✔		10.73	292 (M+H)	290 (M-H)	291
			✔	✔		11.21	292 (M+H)	290 (M-H)	291
			✔	✔		14.18	251 (M+H)	249 (M-H)	250
	CMB-01457	**Petrol**	**DCM**	**MeOH**	**H_2O**	**tR (min)**	**ESI(+)MS**	**ESI(-)MS**	*MW*
		8.2	24.8	92.5	9.8				
			✔	✔		9.06	380 (M+H)	378 (M-H)	379
			✔	✔		9.30	394 (M+H)	392 (M-H)	393
	CMB-01510	**Petrol**	**DCM**	**MeOH**	**H_2O**	**tR (min)**	**ESI(+)MS**	**ESI(-)MS**	*MW*
		19.6	74.2	115.1	9.7				
			✔	✔		9.23	394 (M+H)	392 (M-H)	393
			✔	✔		9.55	394 (M+H)	392 (M-H)	393
			✔	✔		15.00	329 (M+H)	327 (M-H)	328
			✔	✔		16.00	283 (M+H)	222 (M-H)	281

Note: red, orange and yellow for fractions mean strong, moderate and weak activities while on the molecular weight (MW) blue and red indicated known and unknown molecular weights. LCMS condition: Zorbax $C_3/C_8/C_{18}$ analytical columns (150 x 4.6 mm) eluted with 90% H_2O/MeCN to MeCN with 0.5% HCO_2H modifier.
LRESIMS = low resolution electrospray ionisation mass spectrometry

Chemical profiling on extracts from three sponges coded CMB-01064, CMB-03231 and CMB-03363 showed very similar profiles (Table 2.2) with both known and likely new molecular features. The three specimens were collected in the Great Australian Bight, off The Pinnacles Reef and off Port Phillip Heads, Victoria, Australia and identified as *Psammocinia* sp., and *Ircinia* spp. respectively, two of the three main members of Irciniidae family[104]. Apart from *Sarcotragus*[105-107], these two genera are also known for furanoterpene tetronic acids[108-112]. LRESIMS analysis showed that CMB-01064 and CMB-03363 contained virtually the same molecular weights (398, 416, 405, 471, 489, Table 2.2), two of which (398 and 416) were consistent with the known furenosesterterpene tetronic acid variabilins. This assumption was supported by ^{1}H NMR and HRESIMS analysis, comparison to our authentic sample of variabilin[113] and online search on the Marinelit focusing on known members of variabilin structure class and metabolites of *Ircinia* spp. and *Psammocinia* sp. These profiling efforts confirmed the presence of known variabilin type compounds and several unreported co-metabolites with molecular weights of 405, 471, 489 and 551 in CMB-01064 and CMB-03363 (Table 2.2). Of these, 405 and 521 were also observed in CMB-03231 (Table 2.2), which upon ^{1}H NMR and HRESIMS analysis proved to be similar molecules to those in CMB-01064 and CMB-03363. These structural resemblances placed these three priority extracts (CMB-03363, CMB-01064 and CMB-03231) in the first group. Also, as the fractions for the unknown metabolites showed strong modulation activity against GlyRα1 and GlyRα3, they strongly encouraged more detail chemical analysis.

In the same way, chemical and biological profiling allowed CMB-01008, CMB-02858 and CMB-03344 to be assembled into a second group. These three specimens were collected off Durras New South Wales, off Port Phillip Heads, Victoria and off Barwon Heads, Victoria respectively and were all identified as *Psammocinia* spp. LRESIMS revealed similar molecular weights for DCM and MeOH fractions. Again, the close similarity of molecular weights and ^{1}H NMR in these three specimens (CMB-01008, CMB-02858 and CMB-03344) suggested their structural similarity, which was further confirmed by a single ion extraction shown in detailed in Supporting Information in Chapter 4 of this thesis. Of interest, a minor fraction at t_R = 10.34 min from CMB-03344 showed selective potentiating activity against GlyRα3 with little or no such effect on GlyRα1.

Unlike the other groups, there is only one specimen in the third group (CMB-03322) collected from Lonsdale Port Phillip Heads, Victoria Australia and identified as *Ianthella cf. flabelliformis*. This specimen contained two-distinctive structure classes distributed in DCM and MeOH fractions (Table 2.2) as shown by their different molecular weights (Table 2.2). Although the DCM fraction was inactive against GlyRs, this fraction contained two unreported identical molecular weights 291 suggesting the presence of new compounds. Although MeOH fraction contained known pseudomolecular ions, bioassay confirmed that there was GlyR modulators (Table 2.2) while known pseudomolecular corresponded to monomer (t_R = 5.67-9.49 min.) and dimer aplysinopsins (tR = 5.60 min., Table 2.2). Our GlyR bioassay revealed indole alkaloid fractions as the active component of the Australian *Ianthella cf. flabelliformis*. In particular, a fraction (t_R = 5.60 and 9.13 min., Table 2.2) corresponding to molecular weights of 508 and 254 (dimer and monomer aplysinopsins) showed potent potentiating activity against GlyRα1. These data have encouraged us to study the metabolites of *Ianthella cf. flabelliformis* as new source of novel, potent and selective GlyR modulators. The following paper details our discovery of new terpenes and novel GlyR modulators from Australian marine sponge, *Ianthella cf. flabelliformis*.

The final group consists of two specimens (CMB-01045 and CMB-01510) whose pseudomolecular ions also were very similar (in particular the peaks corresponding to *m/z* 393) with online database search showed very few hits. Unfortunately, the limited amount of material made further chemical analysis impractical (at this time).

Following on from the analysis of the 27 extracts detected in the primary screening of >2,500 Australian and Antarctic marine invertebrates and algae against the GlyRs, only 7 specimens were prioritized for chemical analysis including CMB-01064, CMB-01008, CMB-02858, CMB-03231, CMB-03322, CMB-03344 and CMB-03363, clustered into three groups: Group 1 (CMB-01064, CMB-03231 and CMB-03363) (**Chapter 3**); Group 2 (CMB-01008, CMB-02858 and CMB-03344) (**Chapter 4**); and Group 3 (CMB-03322) (**Chapter 5**).

CHAPTER 3

IRCINIALACTAMS

3.1. Declaration

This chapter describes three known sesterterpene tetronic acids from the variabilin structure class and new co-metabolites named ircinialactams discovered from three Australian sponges of the family Ircinidae, three of the seven previously described priority specimens. Of these, three metabolites showed promising bioactivity potently and specifically modulating GlyRα1 and GlyRα3 with a paper describing the discovery published in **Bioorganic & Medicinal Chemistry** in **2010**[101]. This was the first of three papers published between the Capon Group of the Institute for Molecular Bioscience (IMB) and the Lynch Group of Brain Institute (QBI) of The University of Queensland Australia.

The two-research groups contributed equally to the publication of the ircinialactam paper. I was responsible for chemical investigation (isolation, purification and structure elucidation) of all metabolites discovered from three Australian Ircinidae sponges (CMB-01064, CMB-03231 and CMB-03363). During my lab work at the IMB, I received technical assistance (lab work and data analysis) from Dr. Hua Zhang and Dr. Andrew M. Piggott and was supervised by Professor Robert J. Capon as the head of chemistry lab. Similarly, the other co-authors have contributed to the work on ircinialactams paper. Dr. Robiul Islam performed bioassays (Yellow Fluorescence Protein and Patch Clamp assays) at the QBI. He received technical assistance from Dr. Daniel F. Gilbert, Dr. Frank Fontaine and Dr. Timothy I. Webb and was under the supervision of Professor Joseph W. Lynch as the head of pharmacology lab. The contributions of all co-authors to the publication of ircinialactams paper are listed in the table given below.

Balansa, W.; Islam, R.; Fontaine F.; Piggott, A. M.; Zhang, H.; Webb, T. I.; Gilbert, D.; Lynch, J. W.; Capon, R. J. Ircinialactams: Subunit-Selective Glycine Receptor Modulators from Australian Sponges of the Family Irciniidae. *Bioorg. Med. Chem.* **2010**, *18*, 2912–2919.

Contributor	Statement of contribution
Balansa, Walter	Responsible for chemistry (100% working)
Islam, Robiul	Responsible for bioassay (100% working)
Fontaine, Frank	Assisted with lab work and data analysis
Zhang, Hua	Assisted with lab work and data analysis
Piggott, Andrew M.	Assisted with lab work and data analysis
Webb, Timothy.	Assisted with lab work and data analysis
Gilbert, Daniel	Assisted with lab work and data analysis
Lynch, Joseph W.	Head of pharmacology lab.
Capon, Robert J.	Head of chemistry lab.

3.2. Introduction

3.2.1 Variabilin Structure and Diversity

Members of Irciniidae family represent the most prolific source of sesterterpene tetronic acids such as variabilin (**3.1**)[105,109,112,114,115]. First reported by Faulkner from *Ircinia variabilis*, the antimicrobial variabilin was typified by a β-substituted furan δ_H (6.25, 7.18 and 7.31) and a conjugated tetronic acid δ_H (1.81 and 5.41) moieties attached to the opposite end of a linear polyisoprenoid that features $\Delta^{7,12}$ double bond configuration[109]. Structure of this type but with $\Delta^{8,13}$ configuration named strobilinin (**3.2**) was also reported by Rothberg and Subiak from a sponge *I. strobilina* in 1975 as an antibiotic agent against *Staphylococcus aureus* and *Bacillus subtilis*[116]. None of these original reports, however, addressed the geometry of trisubstituted or conjugated double bonds or the stereochemistry (C-18).

Subsequently, in 1983 Gonzales *et al* assigned the stereochemistry of the trisubstituted double bonds of variabilin with upfield chemical shifts ^{1}H (<1.5 ppm) and ^{13}C (<20.0 ppm) of the olefinic methyls being consistent with an *E* geometry while downfield chemical shifts ^{1}H (>1.5 ppm) and ^{13}C (>20.0 ppm) were consistent with *Z* geometry[110]. When studying the metabolites of a New Zealander *Sarcotragus* sp. in 1989, Barrow *et al* assigned the stereochemistry of conjugated double bond (C-20) with a shielded chemical shift (< 120.0 ppm) consistent with *E* geometry and a deshielded chemical shift (>120.0 ppm) being consistent with a *Z* configuration[105]. Following these empirical NMR rules, in 1994 Davis and Capon reassigned the reported single pure compound strobilinin (**3.2**) as a mixture of two geometric isomers 8*E*-13*E*-20*Z*-strobilinin (**3.3**) and 8*E*-13*Z*-20*Z*-strobilinin (**3.4**)[117]. The authors used molecular rotation to assign 18*S* and 18*R* configurations to variabilin and strobilinins respectively and went on to apply this same approach to assign 18*S* configurations to ircinin-1 (**3.5**) and ircinin 2 (**3.6**)[113].

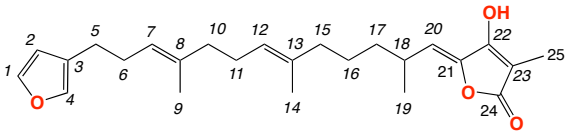

variabilin (**3.1**)

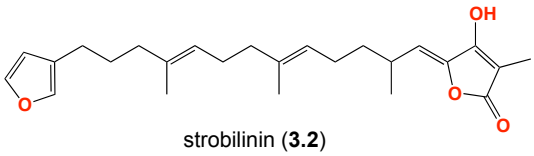

strobilinin (**3.2**)

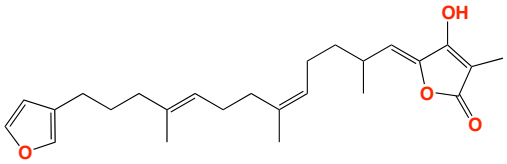

(8*E*,13*Z*,20*Z*)-strobilinin (**3.3**)

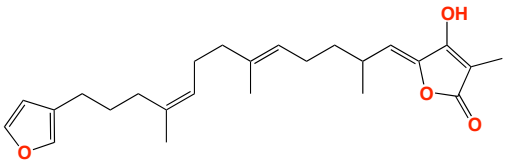

(8*Z*,13*E*,20*Z*)-strobilinin (**3.4**)

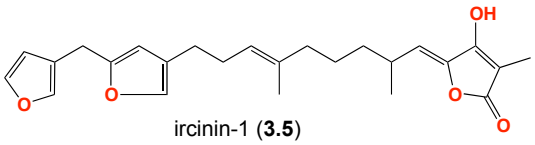

ircinin-1 (**3.5**)

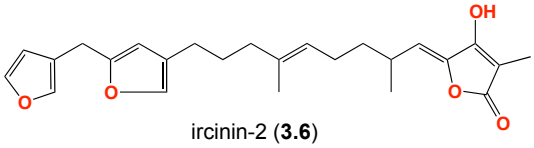

ircinin-2 (**3.6**)

Ever since, these above approaches have been widely applied in assigning the stereochemistry of variabilin and its related metabolites. These include the stereochemical assignments of variabilin and its geometric isomers isolated from a Maltese *I. oros* by Conig *et al* in 1997[111], from three *Ircinia* spp. by Martinez *et al* in 1997[112], from a South African nudibranch *Hypselorides capensis* by Coetzee *et al* in 1998[118], from a *Smenonspongia* in 1998[119] by Shin *et al* and from several *Sarcotragus* spp. by Jung *et al* and Shin *et al* in eight years period from 2001 to 2009[107,108,114,115].

Of note, variabilin type compounds and their geometric isomers were known to resist purification in HPLC (high performance liquid chromatography) arguably due to their overlapping peaks[112]. In most cases, these furanosesterterpene geometric isomers were assigned as a mixture or purified as acetylated analogues as noted in reports of variabilin related metabolites from a number of Korean sponges of the genera *Smenospongia* and *Sarcotragus*, from an Australia *I. strobilina*[117] and a Maltese *I. oros*[111]. By contrast, this derivatization approach was not effective in assisting purification of a mixture of variabilins, strobilinins and flexinins from three Colombian *I. felix*, *I. strobilina* and *I. campana*[112].

In addition to geometric isomers, variations on variabilin structure class also arise from the modifications to the furan and tetronic acid termini. Examples include a series of metabolites isolated from Korean *Sarcotragus* spp. reported during last decade featuring unconjugated or truncated tetronic acids in place of conjugated tetronic acid

and hydroxybutenolide, dimethoxy or amino acid derivatives including leucine, isoleucine, glycine or phenylalanine in exchange of furan.

For example in 2001, Shin *et al* reported sarcotragin A and B from a Korean *Sarcotragus* sp. consisting of trinorsesterterpene and phenylethilamine lactam moiety[120]. Apart from the unusual α,β-unsaturated lactam, sarcotragins (**3.7**, **3.8**) were also unique in that the tetronic acids functional group has been replaced by an α-hydroxy methyl ester. In 2002 and 2003, Liu *et al* reported a series of closely related structures named sarcotrines A-F (**3.9**-**3.18**) featuring coupling between terpene and amino acid derivatives such as leucine, isoleucine, glycine or phenylalanine from another two *Sarcotragus* spp.[114,115]. While sarcotines A-E (**3.9**-**3.17**) contain unconjugated tetronic acid, this moiety is replaced by α,β-hydroxymethoxybutanone and α,β-dihydroxybutenone moieties in sarcotragins A-B (**3.7** and **3.8**) and sarcotines F (**3.18**-**3.19**) respectively. Variations among sarcotines also derive from epimerism such as in sarcotines A-C (**3.9**-**3.14**), isomerism such as in sarcotines E-F (**3.16-3.19**) and lactam regiochemistry such as in sarcotines E-F. Of interest, the chemical shifts of an olefin and a quaternary carbon at lactam moiety could be used to differentiate lactam regiochemistry with downfield resonances (~6.74 (H-2), ~137.6 (C-2) and ~140.2 (C-3) ppm attributed to an α-substituted lactam and less shielded resonances (~5.7 (H-2), ~ 121.0 (C-2) and 136.0 (C-3)) ppm attributed to a β-substituted lactam[114,115]. In 2004, Choi *et al* reported psammocinins A_1-B (**3.20-3.22**) from another Korean *Sarcotragus* sp. lacking a methyl substituent in the conjugated tetronic acid of psammocinin A_1 and A_2 (**3.20-3.21**) as well as the replacement of the furan with an oxidized dimethylacetal moiety in psammocinin B (**3.22**)[108].

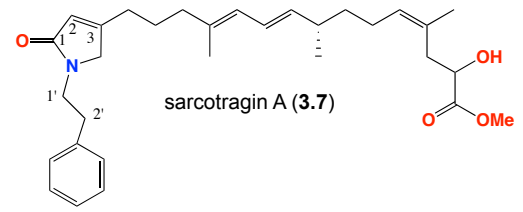
sarcotragin A (**3.7**)

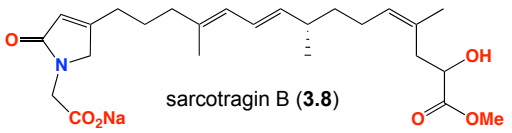
sarcotragin B (**3.8**)

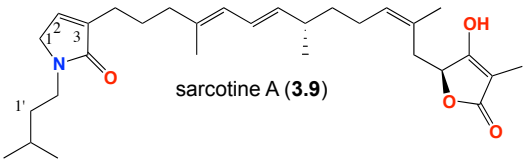
sarcotine A (**3.9**)

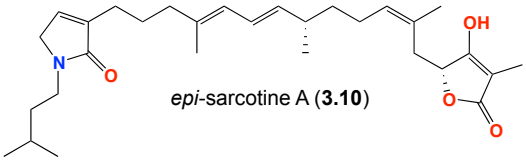
epi-sarcotine A (**3.10**)

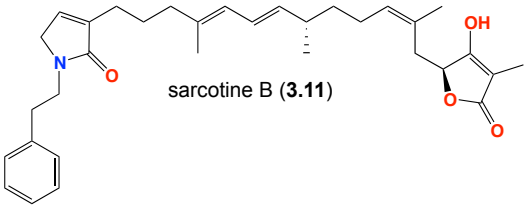
sarcotine B (**3.11**)

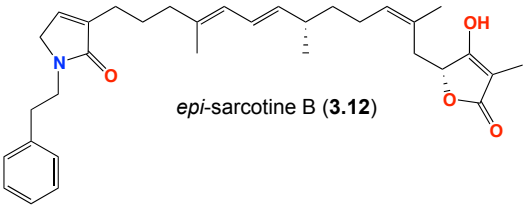
epi-sarcotine B (**3.12**)

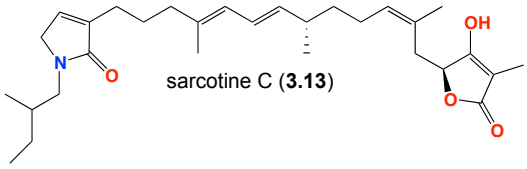
sarcotine C (**3.13**)

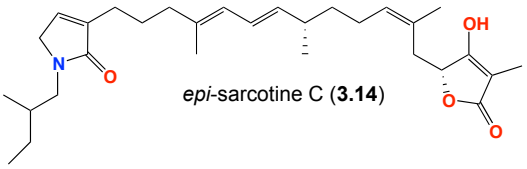
epi-sarcotine C (**3.14**)

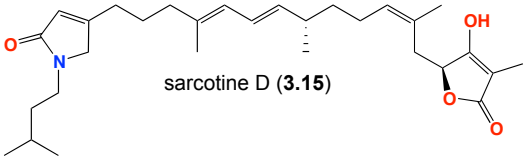
sarcotine D (**3.15**)

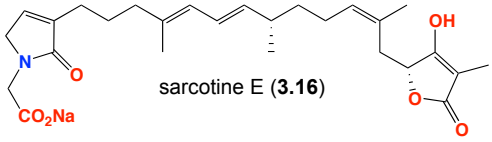
sarcotine E (**3.16**)

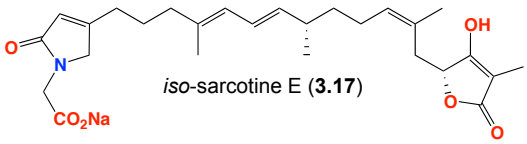
iso-sarcotine E (**3.17**)

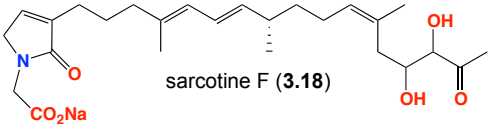
sarcotine F (**3.18**)

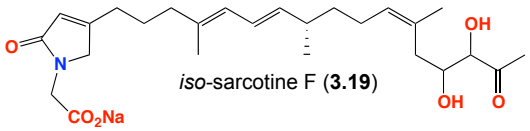
iso-sarcotine F (**3.19**)

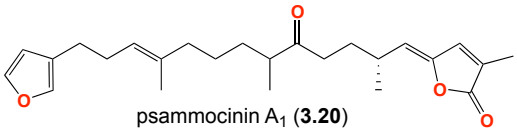
psammocinin A_1 (**3.20**)

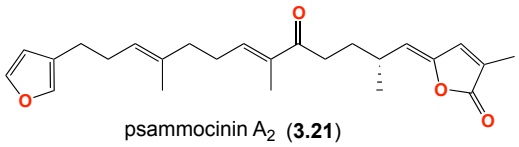
psammocinin A_2 (**3.21**)

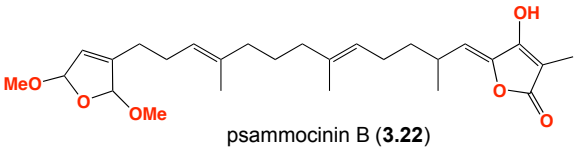
psammocinin B (**3.22**)

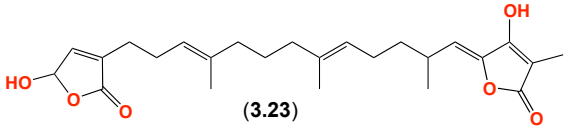
(**3.23**)

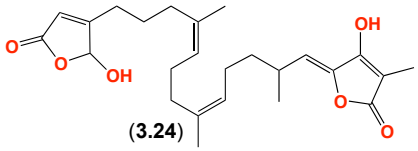
(**3.24**)

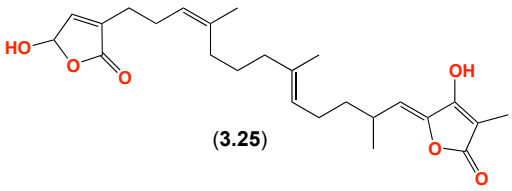
(**3.25**)

In 2008, Wang *et al* discovered a series of sesterterpenes containing furan, γ-lactone, γ-lactam or methyl acetal at one termini and tetronic acids, carboxylic acid or dimethyl diester moieties at the other termini of a linear terpene from a Korean *Sarcotragus* sp (**3.23**-**3.41**)[107].

Three of the metabolites (**3.23-3.25**) share a very close structure with variabilin except that furan moiety in the **3.23**-**3.25** has been replaced by α,β-substituted regioisomeric hydroxy γ-lactones. Although γ-hydroxybutenolide has been commonly reported to co-occur with furan in marine terpenes such as the luffarins[121] and spongiabutenolides[122], to date **3.23**-**3.25** represent the only hydroxybutenolides known for variabilin structure class[107]. Faulkner and co-workers reported regioisomeric hydroxybutenolides through a singlet oxidation of 3 or 3,4[122] substituted furans and Barrow *et al* obtained hydroxybutenolide as one of the major products in an autoxidation study of variabilin[123].

Four of these linear terpenes (compounds **3.26**-**3.29**) feature furan and carboxylic acid at the opposite end of a linear terpene. The C_{21} linear terpene was previously reported by Barrow *et al* from a New Zealand *Sarcotragus* sp[105]. Biogenetically, it was proposed by Faulkner that hydrolysis of a tetronic acid gave rise to an α-diketone which in turn underwent oxidation, losing four-carbon fragment to deliver the carboxylic acid (Scheme 3.1)[124]. Compounds **3.30**-**3.37** contain furan and dimethyl diester moieties connected by a linear terpene. The latter functionality was previously reported as a product of acid treatment and has never been reported as natural product until the 2009 report by Shin *et al*[107]. It was proposed that the dimethyl diester functionality also underwent hydrolysis to yield an α-diketone which upon a rearrangement resulted in dimethyl diester moiety (Scheme 3.2)[124]. Interestingly, from the same sponge, the authors isolated different isomers of the dimethyl diesters distinguishable from their differing optical rotation properties. Together with compounds **3.26-3.30**, they represent the only known molecules bearing dimethyl diester functional group.

In addition to being dimethyl diesters, compounds **3.38**-**3.41** also contain the glycinyl lactam functional group, a functional group reported only from haumanamide isolated from a Hawaiian sponge[125] and spongolactams C isolated from a Japanese Sponge *Spongia* sp[126] and several nitrogenous terpenes from Korean *Sarcotragus* spp[107,114,115,120]. It has been previously proposed that the formation of the lactam from a furan moiety was enzyme catalyzed. In a nucleophilic attack of ethanolamine to an electron deficient, ring fission and formation of an aldehyde took place, which through concomitant cyclisation and oxidation could deliver the target lactam (Scheme 3.2 (A)[127]. However, a few synthetic studies have reported that instead of cyclisation such lactamization

required intermediate lactones and amino acids[128]. These data along with the fact that hydroxybutenolides are known to be produced by singlet oxidation[122] and as auto oxidation of variabilin[123] suggest an alternative plausible transformation of furan to lactam proceeding via oxidation of the furan to regioisomeric hydroxybutenolides, which undergo conjugation with glycine to yield the target glycinyl lactam (Scheme 3.2 (B).

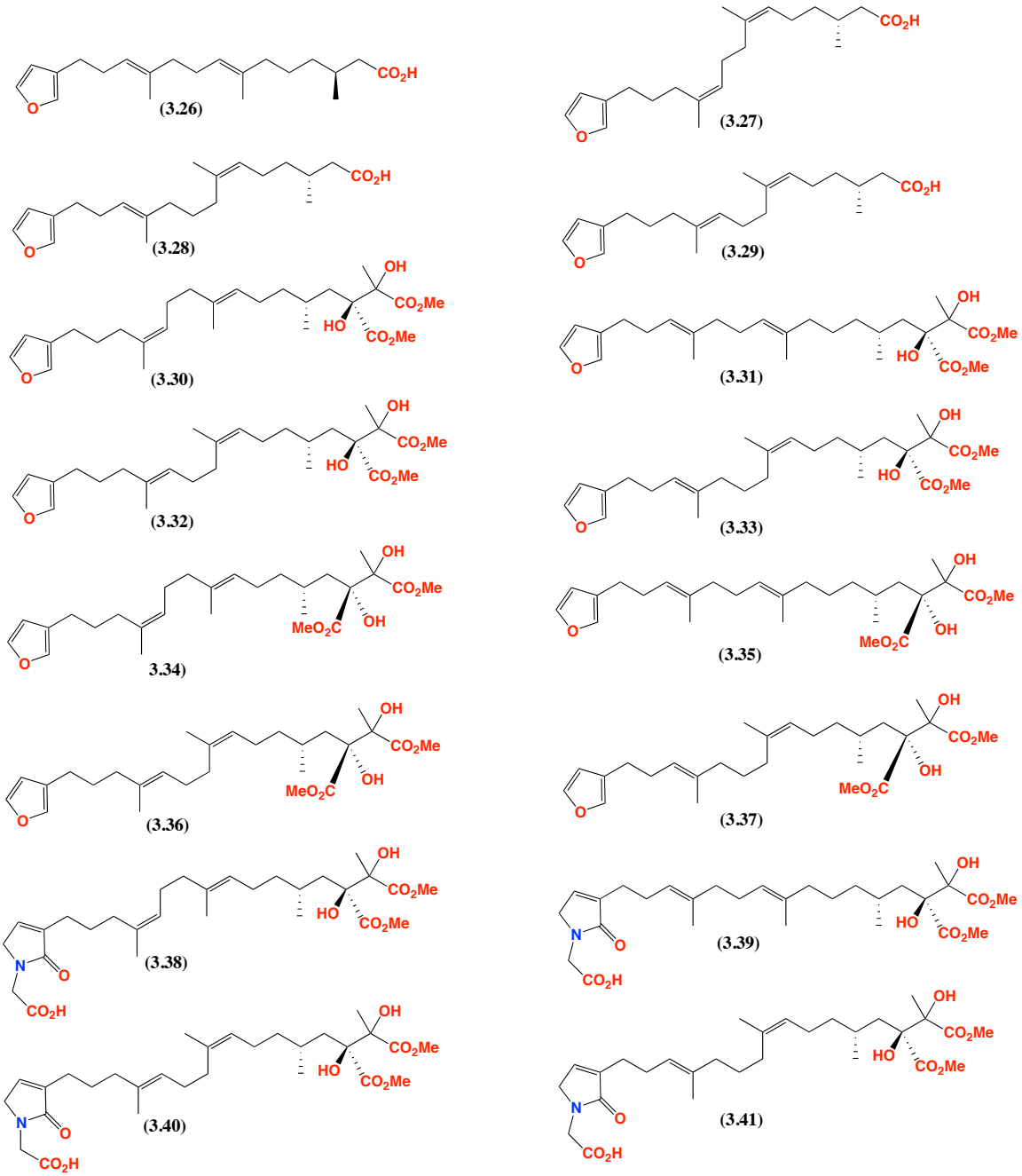

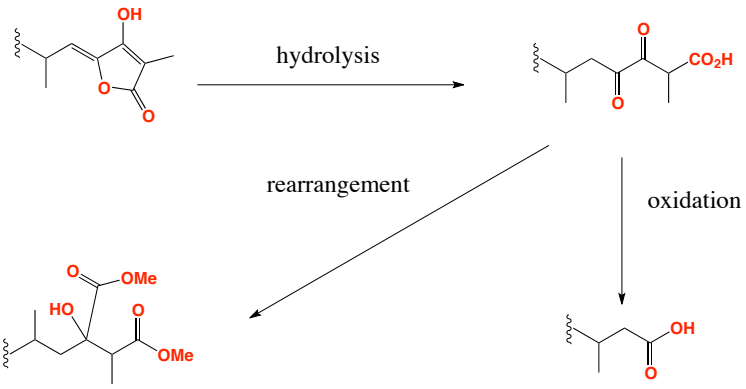

Scheme 3.1. The formation of carboxylic acid and dimethyl diester from tetronic acid adopted from Gonzales *et al* 1983[97]

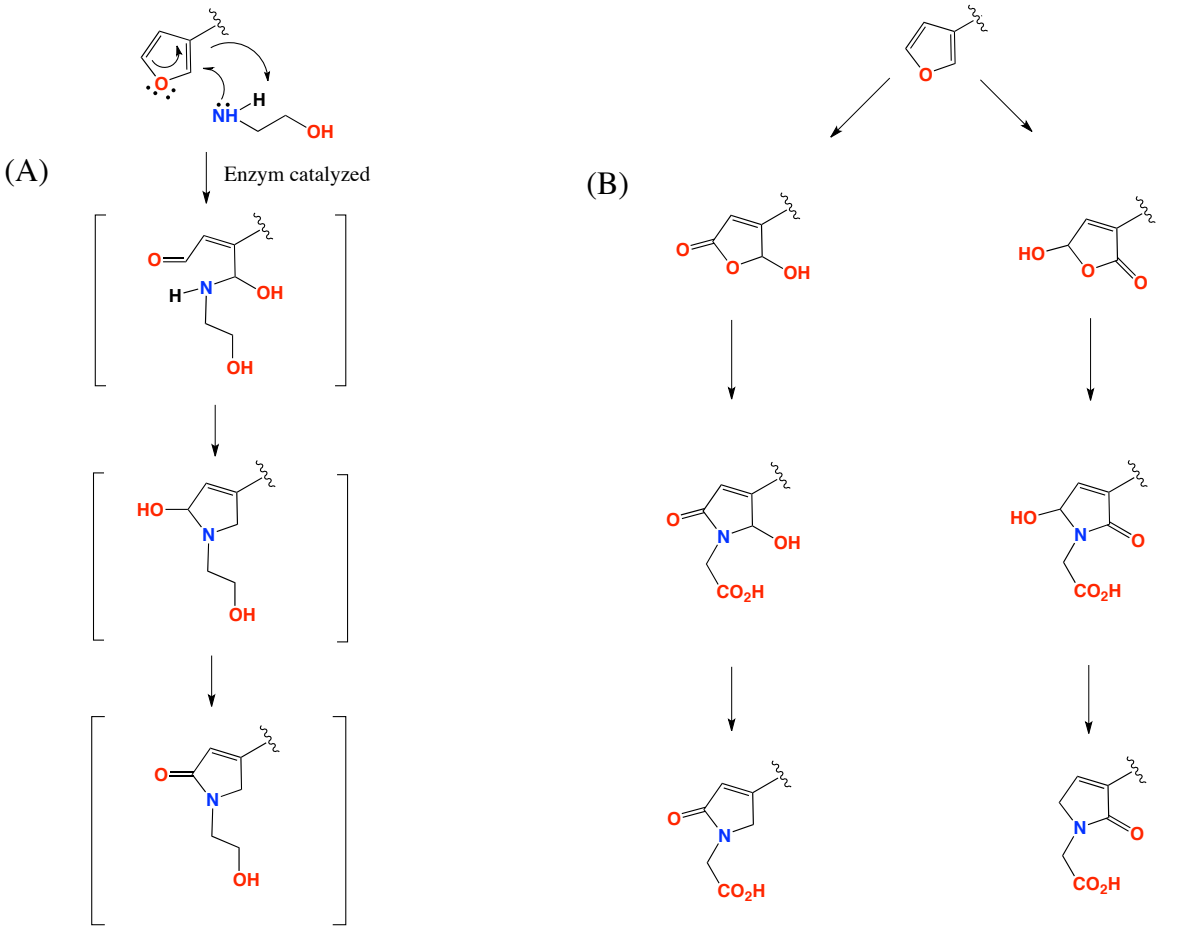

Scheme 3.2. Plausible formation of glycinyl lactam from furan proposed earlier by Hamman *et al* 1999[127] (A) and our plausible formation of furan to butenolide to lactam (B).

3.2.2. Synthesis of Variabilin and Glycinyl Lactam

Indeed, the same process has been shown in synthesis of spongolactams and derivatives from their corresponding furan by Mori *et al* in 2009[126]. The authors obtained regioisomeric hydroxybutenolides from their respective furan and conjugated them with a range of amino acids including histamine, glycine and phenylalanine followed by reduction of the hydroxy group to produce a range of α and β γ-lactam containing metabolites. The synthesis of variabilin was also reported by Takabe *el al* by means of asymmetric synthesis employing enzymatic desymmetrization[129].

3.2.3. Ecological Consideration

In addition to structural variations and synthesis efforts, a few papers have addressed the ecological role of variabilin. Pawlik *et al* have reported that variabilin isolated from Caribbean sponges of the genus *Ircinia* was capable of deterring the wrasse *Thalassoma bifasciatum* at concentration of 0.5 mg/ml in aquarium fish feeding assay[130]. Similarly, Epifanio *et al* have also found that variabilin and derivatives isolated from the Western Atlantic sponge *Ircinia strobilina* produced fish predation deterrent[131].

3.2.4 Biological Activity

Variabilin and its oxidative derivatives were also known to be active in many bioassays. As mentioned before, variabilin was first reported as an antimicrobial agent[109]. Subsequently, variabilin derivatives have been reported to exert a range of biological activities including antiviral and antibacterial[105,106], antitumor, cytotoxic against K562 cell line[107] and SK-MEL-2 (human tumor cell line) inhibitors of isocitrate lyase and DNA replication[108] and a dual inhibitor of human secretory and cytosolic Phospholipase A2[132]. Unlike variabilin and its oxidative derivatives, to date known linear sesterterpene glycinyl lactams have proved to be inactive both in antibacterial[107] and cytotoxic[107,114] assays.

In contrast, chemical and biological profiling suggested that the active components for three Australian Irciniidae concentrated in two fractions at t_R = 9.50-10.70 (CMB-01064); t_R = 11.50-12.20 (CMB-03231) and t_R = 6.5-7.5 (CMB-03363) which HPLC-MS analysis confirmed to contain likely new nitrogenous molecules (Table 2.2). These results encouraged us to investigate the metabolites of these three Australian Irciniidae sponges as a source of potentially new GlyR modulators.

Described in the following paper is the discovery of six novel linear glycinyl lactams including ircinialactam A (**3.45**), 8-hydroxyircinialactam A (**3.46**), 8-hydroxyircinialactam B (**3.47**), ircinialactam C (**3.48**), *ent*-ircinialactam C (**3.49**) and ircinialactam D (**3.50**) as well as three known compounds such as 7*E*,12*E*,18*R*,variabiln (**3.51**), 7*E*,12*Z*,18*R*-variabilin (**3.52**) and 12*E*,20*Z*-18*S*-8-hydroxyvariablin (**3.53**). While geometrically isomeric variabilins were normally reported as a mixture or acetylated derivatives[107,112,114,115], compounds **3.50** and **3.51** were isolated by HPLC without derivatisation. Importantly, all glycinyl lactams except **3.47** and **3.49** were successfully isolated by SPE-LC-NMR. Together with 7,8-dihydroisopalinurin (**3.52**) and cometin A (**3.53**), **3.45-3.51** were evaluated against GlyRs in a structure activity relationship (SAR) study. Of these, **3.46, 3.47** and **3.53** were active against GlyRα1 and GlyRα3 with **3.53** strongly modulating both GlyRα1 and GlyRα3 while **3.46** and **3.47** only potently potentiang GlyRα1 suggesting **3.46** and **3.47** specific GlyRα1 potentiators.

*Note that the numbering system for ircinialactams and variabilins in this introduction and conclusion of this thesis is different from those used in the ircinialactam paper and its supporting information.

Bioorganic & Medicinal Chemistry 18 (2010) 2912–2919

Contents lists available at ScienceDirect

Bioorganic & Medicinal Chemistry

journal homepage: www.elsevier.com/locate/bmc

Ircinialactams: Subunit-selective glycine receptor modulators from Australian sponges of the family Ircinidae

Walter Balansa [a], Robiul Islam [b], Frank Fontaine [a], Andrew M. Piggott [a], Hua Zhang [a], Timothy I. Webb [b], Daniel F. Gilbert [b], Joseph W. Lynch [b], Robert J. Capon [a,*]

[a] Institute for Molecular Bioscience, The University of Queensland, St. Lucia, QLD 4072, Australia
[b] Queensland Brain Institute and School of Biomedical Sciences, The University of Queensland, St. Lucia, QLD 4072, Australia

ARTICLE INFO

Article history:
Received 8 February 2010
Revised 2 March 2010
Accepted 3 March 2010
Available online 6 March 2010

Keywords:
Glycine receptor (GlyR) chloride channels
Glycinyl lactam sesterterpenes
Marine natural products
Ircinidae

ABSTRACT

Screening an extract library of >2500 southern Australian and Antarctic marine invertebrates and algae for modulators of glycine receptor (GlyR) chloride channels identified three Ircinidae sponges that yielded new examples of a rare class of glycinyl lactam sesterterpene, ircinialactam A, 8-hydroxyircinialactam A, 8-hydroxyircinialactam B, ircinialactam C, *ent*-ircinialactam C and ircinialactam D. Structure–activity relationship (SAR) investigations revealed a new pharmacophore with potent and subunit selective modulatory properties against α1 and α3 GlyR isoforms. Such GlyR modulators have potential application as pharmacological tools, and as leads for the development of GlyR targeting therapeutics to treat chronic inflammatory pain, epilepsy, spasticity and hyperekplexia.

1. Introduction

Glycine-gated chloride channel receptors (GlyRs) play a pivotal role in orchestrating inhibitory neurotransmission in the central nervous system.[1] Although they are generally known to be concentrated at the post-synaptic densities of neurons in the spinal cord, brainstem and retina, GlyRs are also located pre-synaptically at several synapses.[2–4] GlyRs are members of the Cys-loop ion channel receptor family and comprise a family of five subunits, α1–α4 and β. Functional GlyRs can be formed either as pentameric α subunit homomers or as αβ subunit heteromers.[1,5] The α1–α4 subunits exhibit differential central nervous system distribution patterns that are particularly evident in the superficial dorsal horn of the spinal cord,[6] and the retina.[7–9] On the other hand, the β subunit is broadly distributed throughout the brain. The physiological consequences of the differential α subunit distribution patterns are difficult to establish, as there are currently few pharmacological probes that can selectively inhibit specific GlyR isoforms.[10,11] Although several synthetic cannabinoid agonists (e.g., HU-210, HU-308 and WIN-55,212-2) effect a strong pharmacological discrimination between α1-containing and α3-containing GlyRs,[12] these ligands are generally unsuitable for physiological or behavioural studies due to non-specific actions at cannabinoid receptors CB1 and CB2. As such, small molecule subunit selective modulators of GlyRs would have significant value as pharmacological tools.

A further reason for identifying novel GlyR subunit-specific ligands is to identify therapeutic lead compounds for muscle relaxation, inflammatory pain, immunomodulation and epilepsy. As α1β GlyRs mediate inhibitory neurotransmission onto spinal motor neurons,[1] increasing α1β GlyR activity dampens motor neuron activity and hence reduces muscle contractility. Although generally sparsely distributed, the α3 subunit is strongly expressed in glycinergic synapses on nociceptive sensory neurons in the superficial layers of the spinal cord dorsal horn.[6] A variety of evidence[13] indicates that inflammatory pain sensitisation is caused by a prostaglandin E2-mediated down-regulation of α3-mediated glycinergic inhibitory currents in nociceptive neurons. This could produce 'disinhibition' of nociceptive projection neurons, resulting in the increased transmission of pain impulses to the brain, thereby explaining inflammatory pain sensitisation. Agents that restore (i.e., potentiate) glycinergic currents could therefore have potential as analgesics for chronic inflammatory pain. Although α1 is also expressed in nociceptive neurons, the α3 GlyR is considered a more promising therapeutic target as its sparse distribution outside the dorsal horn implies a reduced risk of side-effects.[11,13,14]

Functional GlyRs are also present in a variety of immune cells, including macrophages and leucocytes, where they are thought to mediate the anti-inflammatory effects of glycine.[15,16] Thus, the systemic administration of enhancing agents specific for α1- or α2-containing GlyRs could limit the damage inflicted by the inflammatory immune response on essential biological molecules, cells and organs. Finally, RNA-edited high-affinity transcripts of α2 and α3 GlyRs are upregulated in human temporal lobe epilepsy

* Corresponding author. Tel.: +61 7 3346 2979; fax: +61 7 3346 2090.
E-mail address: r.capon@imb.uq.edu.au (R.J. Capon).

0968-0896/$ - see front matter © 2010 Elsevier Ltd. All rights reserved.
doi:10.1016/j.bmc.2010.03.002

and there is evidence for a causative relationship between this upregulation and the condition.[17,18] Thus, antagonists selective for high-affinity α2- or α3-containing GlyRs may be useful for treating this chronic and debilitating neurological disorder. Considering all this information, it would be potentially useful to identify novel compounds with potent and specific potentiating or inhibitory effects on any individual GlyR isoform.

The aim of this study was to identify novel GlyR subunit-specific modulators from marine natural products with potential either as therapeutic leads or as pharmacological probes for unravelling glycinergic mechanisms in the central nervous system and immune system.

2. Results

2.1. Fluorescence-based screening

A collection of >2500 southern Australian and Antarctic marine invertebrates and algae were initially screened against recombinantly expressed α1 and α3 GlyRs using a yellow fluorescent protein (YFP)-based anion influx assay as described in Section 5. While the fluorescence assay employed was robust, some problems associated with autofluorescence of the extracts were encountered. These problems were largely overcome by using cell selection masks during quantitative microscopy to only measure fluorescence specifically associated with cell cytoplasms. In addition, some extracts resulted in false positives due to disruption of cellular membranes and leakage of YFP. Consequently, the cellular morphology in all active wells had to be assessed to ensure membrane integrity had been maintained. Finally, all active fractions were subjected to a second round of screening, yielding 27 marine extracts with confirmed antagonistic activity.

2.2. Isolation and structure elucidation

Chemical investigation of active extracts derived from three sponges of the Family Ircinidae yielded the known sponge metabolites (7*E*,12*E*,20*Z*,18*S*)-variabilin (**1**), (7*E*,12*Z*,20*Z*,18*S*)-variabilin (**2**) and (12*E*,20*Z*,18*S*)-8-hydroxyvariabilin (**3**), along with new examples of a rare class of glycinyl lactam sesterterpenes, ircinialactam A (**4**), 8-hydroxyircinialactam A (**5**), 8-hydroxyircinialactam B (**6**), ircinialactam C (**7**), *ent*-ircinialactam C (**8**) and ircinialactam D (**9**) (Scheme 1). All these metabolites belong to a common biosynthetic family, collectively known as sesterterpene tetronic acids, with the archetypal example being **1**. It is noteworthy that the ircinialactams were present at 10–100-fold lower concentrations in the sponge extracts than the corresponding variabilins, necessitating the use of HPLC–SPE–NMR for structure elucidation.

(7*E*,12*E*,20*Z*,18*S*)-Variabilin (**1**) was first reported from the marine sponge *Ircinia variabilis* in 1973,[19] and its full stereostructure described in 1994.[20] Over the last 25+ years several dozen variabilins have been reported, featuring differing levels of oxidation, stereochemistry and double bond regiochemistry. These include **2** from a Maltese *Ircinia oros*[21] and **3** from a New Zealand *Sarcotragus* sp.[22] Samples of **1**–**3** recovered during this current investigation were identified by spectroscopic analysis, with configurations

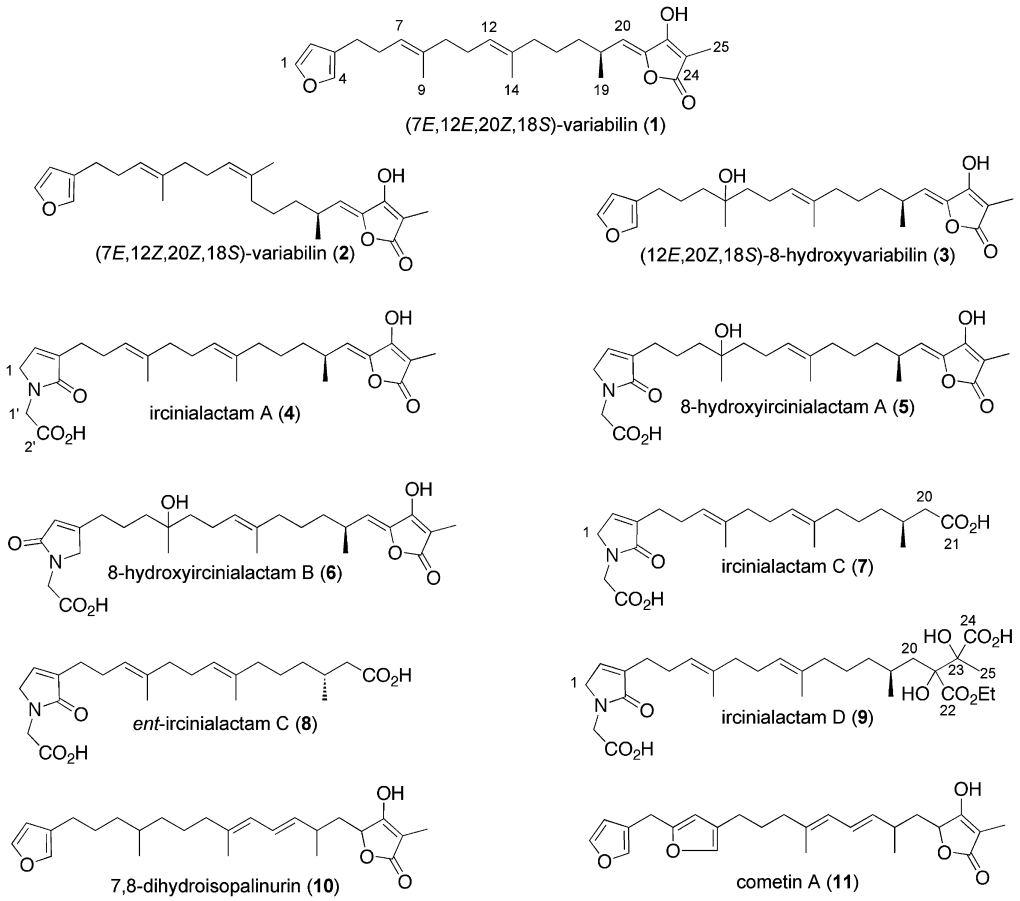

Scheme 1. Marine natural products investigated for GlyR modulating properties.

about $\Delta^{7,8}$ and $\Delta^{12,13}$ defined by the ^{13}C NMR chemical shifts for the corresponding olefinic methyls (E ~16 ppm, Z ~23 ppm), and configuration about $\Delta^{20,21}$ defined by the ^{13}C NMR chemical shift for C-20 (E ~121 ppm, Z ~117 ppm).[22] Double bond regiochemistry was determined from 2D NMR correlations, and absolute configuration by $[\alpha]_D$ measurements[20,22–24] and biogenetic considerations. Full 1D and 2D NMR (methanol-d_4) data for **1**–**3** are presented in the Supplementary data.

The remaining metabolites **4**–**9** are noteworthy in that the precursor furan moiety has undergone modification to the rare glycinyl lactam functionality. Such sesterterpene glycinyl lactams are a relatively recent addition to the scientific literature, having been described from Korean *Sarcotragus* spp.[25–27] Diagnostic NMR resonances consistent with conversion of a furanyl to a glycinyl lactam include replacement of α-furan methines (H-1 and H-4) with resonances for glycinyl (1′-H_2, δ_H ~4.2) and lactam (1-H_2 or 4-H_2 δ_H ~4.0) methylenes, and the appearance of a lactam carbonyl (C-4 or C-1, δ_C ~174).[26] The ^1H NMR chemical shift for H-2 is also diagnostic of lactam regiochemistry, (1-H_2, δ_H ~6.8; 4-H_2, δ_H ~5.8).[26] Metabolites **7**–**8** are glycinyl lactams further modified by biosynthetic truncation of the carbon skeleton (C_{25}–C_{21}) with concomitant transformation of the tetronic acid to a carboxylic acid. Such C_{21} furanoterpenes have been reported as co-metabolites with sesterterpene tetronic acids from a Spanish *Ircinia* sp.,[28] as well as both New Zealand[22] and Korean[27] *Sarcotragus* spp. Metabolite **9** is a glycinyl lactam further modified by ring opening and rearrangement of the tetronic acid functionality, to return a distinctive dihydroxy diacid (ester) terminus. The first reported examples of such a dihydroxy diacid (as the dimethyl ester) appeared as recently as 2008, as co-metabolites with sesterterpene tetronic acids from a Korean *Sarcotragus* sp.[27] A more detailed account of the structure proofs of **4**–**9** is presented below.

(+)HRESIMS analysis of ircinialactam A (**4**) returned a pseudomolecular ion $[M+Na]^+$ consistent with a molecular formula ($C_{27}H_{37}NO_6$, Δmmu 0.5) requiring ten double bond equivalents (DBE) and indicative of a glycinyl lactam analog of **1**. Analysis of the NMR data (Table 1) revealed diagnostic resonances for configurations about $\Delta^{7,8}$ (C-9, δ_C 16.0, E), $\Delta^{12,13}$ (C-14, δ_C 15.9, E) and $\Delta^{20,21}$ (C-20, δ_C 115.9, Z), and the glycinyl lactam regiochemistry (H-2, δ_H 6.88). Excellent correlations between the ^{13}C NMR data for **4** with that of **1**, particularly across the C-12 to C-25 structure fragment, together with analysis of the complete 1D and 2D NMR data and a −ve $[\alpha]_D$, supported the assigned structure.

(+)HRESIMS analysis of 8-hydroxyircinialactam A (**5**) returned a pseudomolecular ion $[M+Na]^+$ consistent with a molecular formula ($C_{27}H_{39}NO_7$, Δmmu 0.6) requiring nine DBE and indicative of a glycinyl lactam analog of **3**. Analysis of the NMR data (Table 2) revealed diagnostic resonances for configurations about $\Delta^{12,13}$ (C-14, δ_C 15.7, E) and $\Delta^{20,21}$ (C-20, δ_C 115.7, Z), and the glycinyl lactam regiochemistry (H-2, δ_H 6.93). Excellent correlations between the ^{13}C NMR (methanol-d_4) data for **5** with that of **3**, particularly across the C-12 to C-25 structure fragment, together with analysis of the complete 1D and 2D NMR data and a −ve $[\alpha]_D$, supported the assigned structure. The configuration about C-8 remains unassigned. The isomeric co-metabolite 8-hydroxyircinialactam B (**6**) displayed excellent NMR comparisons to **5**, with resonances diagnostic for configurations about $\Delta^{12,13}$ (C-14, δ_C 15.7, E) and $\Delta^{20,21}$ (C-20, δ_C 115.8, Z), and for the alternative glycinyl lactam regiochemistry (H-2, δ_H 5.88). Analysis of the complete 1D and 2D NMR data (Table S4, Supplementary data) and a −ve $[\alpha]_D$, supported the assigned structure.

(+)HRESIMS analysis of ircinialactam C (**7**) returned a pseudomolecular ion $[M+Na]^+$ consistent with a molecular formula ($C_{23}H_{35}NO_5$, Δmmu 0.6) requiring seven DBE, suggestive of the glycinyl lactam of C_{21} furanoterpene analogue of **1**. Analysis of the NMR data (Table 3) revealed diagnostic resonances for configurations about $\Delta^{7,8}$ (C-9, δ_C 16.1, E) and $\Delta^{12,13}$ (C-14, δ_C 15.9, E), and the glycinyl lactam regiochemistry (H-2, δ_H 6.89). Excellent correlations between ^{13}C NMR data for **7** and **4**, particularly across the C-1 to C-19 structure fragment, together with analysis of the complete 1D and 2D NMR data and a −ve $[\alpha]_D$, supported the assigned

Table 1
NMR data (600 MHz, methanol-d_4) for ircinialactam A (**4**)

#	δ_H (mult, J Hz)	δ_C[a]	COSY	HMBC (^1H–^{13}C)
1	4.05 (br s)	52.9	2	2, 3
2	6.88 (br s)	138.7	1	1, 4
3		139.2		
4		174.2		
5	2.28[b]	26.8		3, 6
6	2.26[b]	27.0	7	3, 5, 7, 8
7	5.14 (br t, 6.5)	124.5	6	5, 9, 10
8		137.2		
9	1.59 (br s)	16.0		7, 8, 10
10	1.99 (t, 7.3)	40.7	11	8, 9, 11, 12
11	2.08 (m)	27.4	10, 12	10, 12, 13
12	5.10 (br t, 6.5)	125.6	11	11, 14, 15
13		135.9		
14	1.56 (br s)	15.9		12, 13, 15
15	1.96 (m)	40.4	16	12, 13, 14, 16
16	1.39[c]	26.8	15	17
17a	1.39[c]	37.5	16, 18	16
17b	1.31 (m)			16
18	2.75 (m)	31.8	19, 20	
19	1.06 (d, 7.0)	21.6	18	17, 18, 20
20	5.28 (d, 10.1)	115.9	18	17, 19, 21, 22
21		144.9		
22		164.2		
23		99.2		
24		173.3		
25	1.75 (s)	6.1		22, 23, 24
1′	4.22 (s)	44.3		1, 4, 2′
2′		172.3		

[a] ^{13}C assignments supported by HSQC experiment.
[b,c] Overlapping signals.

Table 2
NMR data (600 MHz, methanol-d_4) for 8-hydroxyircinialactam A (**5**)

#	δ_H (mult, J Hz)	δ_C[a]	COSY	HMBC (^1H–^{13}C)
1	4.06 (br s)	52.9	2, 5	2, 3
2	6.93 (br s)	138.6	1	1, 3, 4, 5
3		139.4		
4		174.3		
5	2.27 (br t, 7.3)	27.2	1, 6	2, 4, 6
6	1.62 (m)	23.1	5, 7	5
7	1.50 (m)	42.2	6	6
8		73.2		
9	1.14 (s)	26.7		7, 8, 10
10	1.45 (m)	42.7	11	8, 11
11	2.01 (m)	23.5	10, 12	10, 12, 13
12	5.13 (br t, 7.1)	126.0	11, 14	11, 14, 15
13		135.9		
14	1.58 (br s)	15.7		12, 13, 15
15	1.96 (br t, 7.0)	40.4	16	16
16	1.39[b]	26.7	15	17
17a	1.39[b]	37.5	17b	16
17b	1.31 (m)		17a	
18	2.75 (m)	31.8	19, 20	
19	1.06 (d, 6.7)	21.0	18	17, 18, 20
20	5.28 (d, 10.2)	115.7	18	17, 19, 21, 22
21		145.0		
22		164.6		
23		98.9		
24		173.5		
25	1.75 (s)	6.1		22, 23, 24
1′	4.22 (s)	44.3		1, 4, 2′
2′		172.6		

[a] ^{13}C assignments supported by HSQC experiment.
[b] Overlapping signals.

Table 3
NMR data (600 MHz, methanol-d_4) for ircinialactam C (**7**)

#	δ_H (mult, *J* Hz)	δ_C[a]	COSY	HMBC (^1H–^{13}C)
1	4.05 (s)	52.9	2	2
2	6.89 (br s)	138.7	1	1, 4, 5
3		[d]		
4		174.2		
5	2.30[b]	26.9		2, 6
6	2.27[b]	27.0	7	5, 7, 8
7	5.16 (br t, 6.6)	124.5	6	5, 9, 10
8		137.1		
9	1.61 (br s)	16.1		7, 8, 10
10	2.01 (br t, 7.9)	40.8	11	7, 8, 9, 11
11	2.09[c] (m)	27.6	10, 12	10, 12, 13
12	5.11 (br t, 6.6)	125.5	11	14, 15
13		136.0		
14	1.59 (br s)	15.9		12, 13, 15
15	1.97 (br t, 8.0)	40.7	16	12, 13, 14, 16, 17
16	1.44 (m)	26.3	15	
17a	1.31 (m)	37.5		
17b	1.17 (m)			
18	1.92 (m)	31.4	19, 20a	
19	0.94 (d, 5.7)	20.1	18	17, 18, 20
20a	2.27[b]	42.6	18, 20b	17, 18, 19, 21
20b	2.07[c]		20a	17, 18, 19, 21
21		177.0		
1′	4.22 (s)	44.3		1, 2′, 4
2′		172.9		

[a] ^{13}C assignments supported by HSQC experiment.
[b,c] Overlapping signals.
[d] Not observed.

structure. The isomeric metabolite *ent*-ircinialactam C (**8**) displayed identical NMR data (Table S5, Supplementary data) to **7**, with resonances diagnostic for configurations about $\Delta^{7,8}$ (C-9, δ_C 16.3, *E*) and $\Delta^{12,13}$ (C-14, δ_C 16.1, *E*), and for the glycinyl lactam regiochemistry (H-2, δ_H 6.88). Analysis of the complete 1D and 2D NMR data, and more significantly a +ve $[\alpha]_D$, supported the assigned structure.

(+)HRESIMS analysis of ircinialactam D (**9**) returned a pseudomolecular ion $[M+Na]^+$ consistent with a molecular formula ($C_{29}H_{45}NO_9$, Δmmu 0.3) requiring eight DBE, suggestive of a glycinyl lactam of **1** in which the tetronic acid moiety had undergone ring opening and rearrangement. Analysis of the NMR data (Table S6, Supplementary data) revealed diagnostic resonances for configurations about $\Delta^{7,8}$ (C-9, δ_C 16.1, *E*) and $\Delta^{12,13}$ (C-14, δ_C 16.0, *E*), and the glycinyl lactam regiochemistry (H-2, δ_H 6.89), as well as resonances for an ethyl ester (δ_H 4.19/4.22, m, $CO_2CH_2CH_3$; δ_H 1.29, t, $CO_2CH_2CH_3$; δ_C 176.6, $CO_2CH_2CH_3$) and a carboxylic acid (δ_C 175.2, CO_2H). Excellent correlations between NMR data for **9** and **7**, particularly across the C-1 to C-19 structure fragment, as well as **9** and published data for a known dimethyl ester analogue,[27] together with analysis of the complete 1D and 2D NMR data, supported the structure as shown. While the relative configurations at C-21 and C-23 were not resolved, an 18*S* configuration was assigned on the basis of the known co-metabolites (**1**–**3**) and biogenic considerations.

2.3. Bioassay

The metabolites **1**–**9** represent known and new examples of the 'variabilin' family of marine sponge sesterterpenes. To further broaden our structure–activity relationship (SAR) investigations we also had access to authentic samples of the marine sponge metabolites 7,8-dihydroisopalinurin (**10**)[23] from a *Psammocinia* sp. and cometin A (**11**)[29] from a *Spongia* sp. All compounds were screened against recombinant α1 and α3 GlyRs using whole cell patch-clamp electrophysiology. The standard electrophysiological protocol involved voltage-clamping α1 or α3 GlyR-expressing HEK293 cells at −40 mV and inducing an inward current flux by applying an EC_{20} glycine concentration (i.e., a concentration that activates 20% of the saturating glycine-gated current). For α1 and α3 GlyRs, this corresponded to glycine concentrations of 15 and 100 μM, respectively. Unless otherwise indicated, GlyRs were first activated with a 2 s pulse of glycine alone and then with the same concentration of glycine plus a defined concentration of test compound. Usually a 1 min period elapsed between successive glycine plus compound applications. Under these experimental conditions, the known sesterterpene tetronic acids **1** and **2** had no significant effect on either α1 or α3 GlyRs at concentrations up to 100 μM (Table 4). However, the 8-hydroxy analogue **3** produced potent potentiation of α1 GlyRs. Examples of the effects of increasing concentrations of **3** at the α1 GlyR are shown in Figure 1A, with an averaged dose–response presented in Figure 1B. As summarised in Table 4, this compound exhibited a mean EC_{50} of 1.2 ± 0.2 μM and a maximum potentiation magnitude of 215 ± 39% (both $n = 3$ cells). It is apparent that a slowly-developing inhibition can also be observed at concentrations >30 μM, although this was not quantified. In contrast, **3** potently inhibited α3 GlyRs with a mean IC_{50} of 7.0 ± 1.5 μM ($n = 3$). Given this subunit-specific activity, we also tested the effects of **3** on transiently expressed α2 GlyRs using conventional whole cell patch-clamp recording, as described previously.[12] Receptors were activated with an EC_{20} (50 μM) glycine concentration and **3** applied at a concentration of 10 μM. Averaged from six cells, we found that this resulted in weak inhibition, to 87 ± 2% of control current magnitude.

As summarised in Table 4, the glycinyl lactam analogue **4** was a moderate potentiator of α1 GlyRs, producing an enhancement of 140 ± 12% ($n = 7$) at a concentration of 100 μM. Analogue **4** was also a modest inhibitor of α3 GlyRs (Table 4). Combining structural features of **3** and **4**, the 8-hydroxy glycinyl lactam **5** had no significant effect on α3 GlyRs at concentrations up to 100 μM, but was an effective potentiator of α1 GlyRs, with potentiation being significant at 1 μM and reaching 217 ± 15% ($n = 6$) at 100 μM, the highest concentration tested. However, as the potentation did not saturate by 100 μM, an EC_{50} could not be measured. By contrast, the isomer **6** was an exceptionally strong potentiator of α1 GlyRs. Examples of the effects of increasing concentrations of **6** at the α1 GlyR are shown in Figure 2A, with an averaged dose–response presented

Table 4
Summary of the potentiation (EC_{50}) and antagonism (IC_{50}) of GlyRs

Compound	Potentiation		Antagonism	
	α1 GlyR EC_{50} (μM) MP (%)	α3 GlyR EC_{50} (μM) MP (%)	α1 GlyR IC_{50} (μM)	α3 GlyR IC_{50} (μM)
1	–	–	–	–
2	–	–	–	–
3	1.2 ± 0.2 215 ± 39	–	–	7.0 ± 1.5[a]
4	No saturation 140 ± 12	–	–	30–100
5	No saturation 217 ± 15	–	–	–
6	0.5 ± 0.3[b] 330 ± 28	No saturation 183 ± 19	–	–
7	–	–	–	30–100
8	–	–	–	30–100
9	–	–	–	30–100
10	–	–	–	–
11	–	–	–	–

MP = maximum potentiation expressed as a percentage of EC_{20} glycine current. A dash (–) indicates no activity was observed. No saturation = no current saturation was observed at drug concentrations up to 100 μM and hence EC_{50} values could not be calculated. All mean data were averaged from 3–7 cells.
[a] Hill coefficient (n_H) = 0.9 ± 0.15 μM.
[b] Hill coefficient (n_H) = 0.5 ± 0.3 μM.

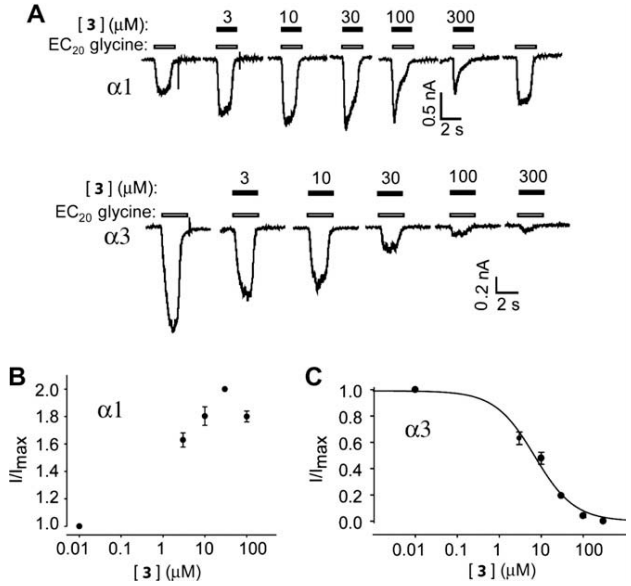

Figure 1. Effects of **3** on α1 and α3 GlyRs. (A) Effects of indicated concentrations of **3** on currents activated by EC_{20} glycine concentrations α1 and α3 GlyRs (upper and lower panels, respectively). Unfilled bars denote glycine applications and filled bars denote compound applications. (B) Averaged dose–response of **3** at α1 GlyRs ($n = 3$ cells). (C) Averaged dose–response of **3** at α3 GlyRs ($n = 3$ cells). Mean parameters of best fit to dose–response curves are given in the text.

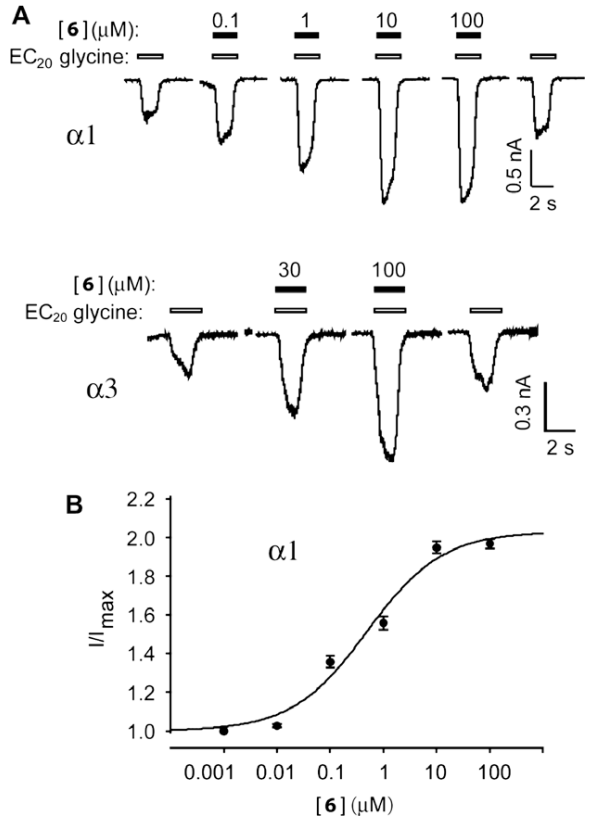

Figure 2. Effects of **6** on α1 and α3 GlyRs. (A) Effects of indicated concentrations of **6** on currents activated by EC_{20} glycine concentrations α1 and α3 GlyRs (upper and lower panels, respectively). Unfilled bars denote glycine applications and filled bars denote compound applications. (B) Averaged dose–response of **6** at α1 GlyRs ($n = 5$ cells). Mean parameters of best fit to dose–response curves are given in the text.

in Figure 2B. As summarised in Table 4, the dose–response was fitted with a mean EC_{50} of 0.5 ± 0.3 μM and a maximum potentiation magnitude of 330 ± 28% (both $n = 5$ cells). Compound **6** also potentiated α3 GlyRs with much weaker potency. The mean potentiation elicited by 100 μM of **6** was 183 ± 19% ($n = 6$). These data support the proposition that the 8-hydroxy and glycinyl lactam functionalities are key elements of the GlyR potentiating pharmacophore.

Negligible to at best modest antagonist activity (30–100 μM) associated with **7**–**9** highlights the significance of the conjugated tetronic acid moiety (Table 4). These observations on the pharmacophore are further confirmed by the absence of significant activity associated with **10**–**11**.

3. Discussion

Analogs **3**, **5** and **6** all modulated GlyRs in the sub-micromolar to low-micromolar range and exhibited differential effects on α1 and α3 GlyRs. Analog **3** exhibited the strongest subunit-specificity. At a 10 μM concentration, **3** strongly potentiated α1 GlyRs, had little effect on α2 GlyRs and potently inhibited α3. This is the first α3 specific inhibitor yet identified. Until now, the only compounds known to exhibit strong subunit-specific inhibition of GlyRs were the synthetic cannabinoids (HU-210, HU-308 and WIN-55,212-2). These compounds all inhibited both α2 and α3 GlyRs with affinities ranging from 50 nM to 1 μM, while having little or no inhibitory effect on α1 GlyRs up to 30 μM.[12] HU-210 did, however, produce strong potentiation of α1 GlyRs. Of course, the synthetic cannabinoids have numerous off-target actions that render them unsuitable as pharmacological probes or GlyR-targeted therapeutics. Provided **3** does not exhibit off-target actions, it may be useful as a pharmacological probe for identifying the presence of α3-containing GlyRs and for investigating their contribution to glycinergic signalling on spinal nociceptive sensory neurons. Due to its ability to selectively inhibit α3 GlyRs, **3** may also be a promising starting point for the development of lead compounds to treat temporal lobe epilepsy.[17,18]

Analogs **3**, **5** and **6** selectively and dramatically potentiated α1 GlyR currents at sub- to low-micromolar concentrations. As **5** and **6** had little effect on α3 GlyRs in this concentration range, they can thus be considered as α1 GlyR-specific potentiators. To date only a few α1 GlyR-specific potentiators have been identified. NV-31, a gingkolide derivative, exhibits an α1 GlyR-specific potentiating action at 1–10 μM, although the magnitude of its effect (135%) is small.[30] While some dihydropyridine and tropeine derivatives selectively potentiate α1 GlyRs over other GlyR subtypes,[31–35] both compound classes have well-known, clinically important effects on other ion channels. Finally, pregnenolone, an endogenous steroid, potentiates α1 but not α2 GlyRs in the 2–20 μM range,[36] although it has much higher potencies at GABA-A receptors.[37] Thus, all previously identified GlyR α1-specific potentiators have either weak activity or potent off-target actions. If **5** and **6** prove to be highly specific as α1 GlyR enhancers, they could be useful as therapeutic leads for movement disorders such as spasticity and hyperekplexia.[38]

Literature reports of novel natural products can prompt total syntheses targeting both the natural products themselves, and the structure class in general. In addition to developing valuable new methodology, synthetic studies are typically justified by the claim that an effective synthesis can be essential for supplying the material needed for pharmacological investigation. This claim is particularly accurate in the case of marine sponge metabolites, where recollection and resupply is often problematic or impossible, isolated yields are low, and poor stability can limit the duration of access to a particular metabolite, often precluding or at least curtailing biological assessment. The value of successful total

syntheses notwithstanding, choice of target is frequently driven by factors other than pharmacological imperative. In the absence of knowledge of its unique effect on GlyRs, it is hardly surprising that, despite being known for two decades, the sesterterpene tetronic acid **3** failed to attract the attention of synthetic chemists. Our findings reveal that sesterterpene tetronic acids, such as **3**, **5** and **6**, embody an exciting new pharmacophore worthy of synthetic attention. Future synthetic studies could provide a library of natural products and analogues for both in vitro and in vivo evaluation, defining the importance of the glycinyl lactam, 8-hydroxy and conjugated tetronic acid moieties to the pharmacophore, characterising requirements for subunit selectivity, and differentiating the molecular basis behind antagonism versus potentiation.

4. Conclusion

In this investigation, we successfully challenged a library of >2500 marine extracts to focus attention on three geographically distinct sponges of the Family Ircinidae that in turn yielded an array of sesterterpene tetronic acids, examples of which were shown to be potent subunit-selective GlyR modulators. The glycinyl lactam pharmacophore identified during this investigation may inspire the development of new pharmacological tools capable of probing the distribution and function of GlyR isoforms, potentially advancing the development of GlyR targeting therapeutics to treat chronic inflammatory pain, epilepsy, spasticity and/or hyperekplexia.

5. Experimental

5.1. Equipment

Chiroptical measurements ($[\alpha]_D$) were obtained on a JASCO P-1010 polarimeter in a 100 × 2 mm cell. UV spectra were acquired from a Cary 50 UV–vis spectrophotometer. NMR spectra were obtained on a Bruker Avance DRX600 spectrometer equipped with a 3 mm HPLC–SEI ^{1}H–^{13}C/D Z-GRD flow probe in the solvents indicated and referenced to residual ^{1}H signals in the deuterated solvents. HPLC–DAD–SPE was performed using an Agilent 1100 Series Separations Module equipped with a Bruker Diode Array Detector coupled to a Spark Prospekt2 SPE unit. All NMR data was acquired in methanol-d_4 unless otherwise specified. Electrospray ionisation mass spectra (ESIMS) were acquired using an Agilent 1100 Series separations module equipped with an Agilent 1100 Series LC/MSD mass detector in both positive and negative ion modes. High-resolution ESIMS measurements were obtained on a Bruker micrOTOF mass spectrometer by direct infusion in MeCN at 3 μL/min using sodium formate clusters as an internal calibrant. HPLC was performed using an Agilent 1100 Series separations module equipped with Agilent 1100 Series diode array and/or multiple wavelength detectors and Agilent 1100 Series fraction collector, controlled using ChemStation Rev.9.03A and Purify version A.1.2 software.

Fluorescence experiments were performed using an automated imaging system with a robot-controlled liquid handling system constructed in the laboratory. The 384-well plates were placed onto a motorised stage (Prior ProScan II, GT Vision, Hagerstown, MD, USA) of an Olympus IX51 inverted microscope and cells were imaged with an Olympus 10× objective (UPlanFLN, N.A. 0.30). Illumination to excite YFP fluorescence was provided by an Osram 100 W mercury short arc lamp (HBO 103/2), passing through an Olympus YFP dichroic mirror (86002V2 JP4 C76444). Emitted fluorescence passed through a magnifier lens (diopter 8, mineral glass), and was then imaged by a Photometrics CoolSNAP CF monochrome camera (Roper Scientific GmbH, Ottobrun, Germany) and digitised onto a personal computer. The final resolution of the images was 696 × 520 pixels. The maximum image acquisition rate used in these experiments was 1.25 Hz. Liquid-handling was performed with an LC PAL autosampler (CTC Analytics, Zwingen, Switzerland) using a 100-μL syringe. A suite of LabView 8.2.1 software (National Instruments Corp, Austin, Texas, USA) routines purpose-written in the laboratory were used for hardware control, image acquisition, storage, image analysis and data quantification. Whole cell patch-clamp recordings were performed using an automated planar patch-clamp device (Patchliner, Nanion Technologies GmbH, Munich, Germany).

5.2. Marine extracts library

A library of >2500 marine invertebrate and alga samples, collected from locations across southern Australia and Antarctica, including intertidal, coastal and deep sea locations, were acquired (Capon) over a period of 25+ years. Individual samples were documented, diced and steeped in EtOH at −30 °C for prolonged storage. A portion (7 mL) of each EtOH extract was decanted into a labelled, tared screw cap vial (8 mL) and the solvent evaporated in vacuo. The residue was weighed (25–50 mg) and partitioned in situ by addition of *n*-BuOH (2 mL) and H_2O (2 mL). Typically, the biomass partitioned 10–20% into *n*-BuOH and 80–90% into H_2O. Aliquots (1 mL) of both *n*-BuOH and H_2O phases were transferred to deep 96-well plates, to generate a set of extract library plates. These plates were subsequently used to prepare 10- and 100-fold dilution plates. The full set of extract and dilution plates represented a resource to support screening programs against a diverse array of bioassays.

For the initial screening, an aliquot (90 μL) of each 100-fold diluted *n*-BuOH partition was transferred into 384-well plates and each well was dried under a stream of nitrogen. The plates were stored at −30 °C, protected from light, until required. On the day of the assay, Ringer buffer (30 μL) was added to each well of the plates and an aliquot (10 μL) of each solution was transferred onto cells pre-incubated in Ringer buffer (15 μL). Assays were performed in horizontal duplicate. For the hit confirmation, an aliquot (24 μL) of each 10-fold diluted *n*-BuOH partition was transferred into 384-well plates, which were dried and stored as described previously. On the day of the assay, extracts were resuspended in Ringer buffer (80 μL) and aliquots (17 or 10 μL) were then transferred in horizontal duplicate onto cells pre-incubated in Ringer buffer (15 μL). The concentration dependence assisted in ranking extract potency for later prioritisation. Isolated pure compounds were prepared as 100 mM DMSO stock solution (10 μL), and were tested with patch-clamp at concentrations ranging from 10–300 μM final.

5.3. Extraction and isolation

A portion of the aqueous EtOH extract of specimen CMB-01064 (genus *Ircinia*; Museum Victoria Registry Number MVF 166265) was decanted and concentrated in vacuo, and the residue (2.25 g) partitioned between H_2O and *n*-BuOH. The *n*-BuOH soluble fraction was concentrated in vacuo (876.0 mg) and the residue was further triturated with light petroleum (19.9 mg), DCM (473.7 mg), MeOH (343.4 mg) and water (25.5 mg). A portion of the DCM soluble fraction (60.0 mg) was subjected to HPLC fractionation (Zorbax C_{18}, 5 μm 250 × 9.4 mm column, 4 mL/min gradient elution, 10–100% MeCN/H_2O with isocratic 0.01% TFA modifier) over 25 min to yield a mixture of **1** and **2** (6.5 mg, 5.9%), **3** (2.1 mg, 1.9%), **4** (4.0 mg, 3.6%), **5** (3.2 mg, 2.9%) and **6** (1.3 mg, 1.2%) (Scheme S1, Supplementary data). Yields calculated as a percentage of *n*-BuOH soluble fraction.

A portion of the aqueous EtOH extract of specimen CMB-03363 (genus *Ircinia*; Museum Victoria Registry Number MVF 166224) was decanted and concentrated in vacuo, and the residue (1.68 g) was partitioned between H_2O and *n*-BuOH. The *n*-BuOH soluble fraction was concentrated in vacuo (526.9 mg) and the residue further triturated with light petroleum (8.4 mg), DCM (267.8 mg), MeOH (208.1 mg) and water (41.4 mg) soluble. The DCM soluble fraction was subjected to HPLC (Zorbax C_8, 5 μm, 250 × 9.4 mm column, 4 mL/min gradient elution, 10–100% MeCN/H_2O with isocratic 0.01% TFA modifier over 25 min) to yield three fractions (I–III). Fraction II was essentially pure and was identified as **3** (10.0 mg, 1.9%). HPLC separation of a portion (3.2 mg) of fraction III (Zorbax C_3, 5 μm, 150 × 4.6 mm column, 1 mL/min gradient elution 50–100% MeCN/H_2O with isocratic 0.01% TFA modifier over 25 min) yielded **1** (1.2 mg, 3.7%) and **2** (1.4 mg, 4.4%). HPLC separation of fraction I (Zorbax C_8, 5 μm, 150 × 4.6 mm column, 1 mL/min gradient elution 10–100% MeCN/H_2O with isocratic 0.01% TFA modifier over 25 min) yielded **4** (0.3 mg 0.057%), **5** (0.2 mg, 0.037%), **7** (0.3 mg, 0.057%) and **9** (0.3 mg, 0.057%) (Scheme S2, Supplementary data). Yields calculated as a percentage of *n*-BuOH soluble fraction.

A portion of the EtOH extract of the third specimen, CMB-03231 (genus *Psammocinia*; Museum Victoria Registry Number MVF 166220), was also decanted and concentrated in vacuo and the residue (238.1 mg) was partitioned between H_2O and *n*-BuOH. The *n*-BuOH soluble fraction was concentrated in vacuo and the residue (124.8 mg) triturated with petroleum (1.4 mg), DCM (75.3 mg) and MeOH (43.4 mg). The DCM soluble fraction was subjected to HPLC fractionation (Zorbax C_8, 5 μm, 250 × 9.4 mm column, 4 mL/min gradient elution, 10–100% MeCN/H_2O with isocratic 0.01% TFA modifier over 25 min) yielded **8** (0.7 mg, 0.6%) (Scheme S3, Supplementary data). Yields calculated as a percentage of *n*-BuOH soluble fraction.

5.4. Characterisation of compounds

5.4.1. (7*E*,12*E*,20*Z*,18*S*)-Variabilin (1)

Colourless oil. $[\alpha]_D$ −24.8 (*c* 0.06, MeOH); UV–vis (MeOH) λ_{max} (log ϵ) 203 (4.27), 257 (3.93) nm; NMR data see Supplementary data Table S1; (+)HRESIMS *m/z* 421.2356 (calcd for $C_{25}H_{34}O_4Na$ 421.2349).

5.4.2. (7*E*,12*Z*,20*Z*,18*S*)-Variabilin (2)

Colourless oil. $[\alpha]_D$ −27.1 (*c* 0.05, MeOH); UV–vis (MeOH) λ_{max} (log ϵ) 202 (4.19), 249 (3.98), 308 (3.74) nm; NMR data see Supplementary data Table S2; (+)HRESIMS *m/z* 421.2356 (calcd for $C_{25}H_{34}O_4Na$ 421.2349).

5.4.3. (12*E*,20*Z*,18*S*)-8-Hydroxyvariabilin (3)

Colourless oil. $[\alpha]_D$ −37.4 (*c* 0.34, MeOH); UV–vis (MeOH) λ_{max} (log ϵ) 203 (4.33), 253 (4.27) nm; NMR data see Supplementary data Table S3; (+)HRESIMS *m/z* 439.2462 (calcd for $C_{25}H_{36}O_5Na$ 439.2455).

5.4.4. Ircinialactam A (4)

Colourless oil. $[\alpha]_D$ −20.5 (*c* 0.03, MeOH); UV–vis (MeOH) λ_{max} (log ϵ) 203 (4.40), 250 (4.14) nm; NMR data see Table 1; (+)HRESIMS *m/z* 494.2508 (calcd for $C_{27}H_{37}NO_6Na$ 494.2513).

5.4.5. 8-Hydroxyircinialactam A (5)

Colourless oil. $[\alpha]_D$ −19.5 (*c* 0.02, MeOH); UV–vis (MeOH) λ_{max} (log ϵ) 203 (4.33) nm; NMR data see Table 2; (+)HRESIMS *m/z* 512.2626 (calcd for $C_{27}H_{39}NO_7Na$ 512.2632).

5.4.6. 8-Hydroxyircinialactam B (6)

Colourless oil. $[\alpha]_D$ −12.0 (*c* 0.02, MeOH); UV–vis (MeOH) λ_{max} (log ϵ) 202 (4.40) nm; NMR data see Supplementary data Table S4; (+)HRESIMS *m/z* 512.2630 (calcd for $C_{27}H_{39}NO_7Na$ 512.2632).

5.4.7. Ircinialactam C (7)

Colourless oil. $[\alpha]_D$ −30.8 (*c* 0.03, MeOH); UV–vis (MeOH) λ_{max} (log ϵ) 203 (4.27) nm; NMR data see Table 3; (+)HRESIMS *m/z* 428.2413 (calcd for $C_{23}H_{35}NO_5Na$ 428.2407).

5.4.8. *ent*-Ircinialactam C (8)

Colourless oil. $[\alpha]_D$ +28.3 (*c* 0.03, MeOH); UV–vis (MeOH) λ_{max} (log ϵ) 201 (4.33) nm; NMR data see Supplementary data Table S5; (+)HRESIMS *m/z* 428.2404 (calcd for $C_{23}H_{35}NO_5Na$ 428.2407).

5.4.9. Ircinialactam D (9)

Colourless oil. $[\alpha]_D$ −19.9 (*c* 0.03, MeOH); UV–vis (MeOH) λ_{max} (log ϵ) 203 (4.48) nm; NMR data see Supplementary data Table S6; (+)HRESIMS *m/z* 574.2990 (calcd for $C_{29}H_{45}NO_9Na$ 574.2987).

5.4.10. 7,8-Dihydroisopalinurin (10)

Colourless oil. $[\alpha]_D$ +9.9 (*c* 0.09, MeOH); UV–vis (MeOH) λ_{max} (log ϵ) 204 (4.20) nm; NMR data see Supplementary data Table S7; (+)HRESIMS *m/z* 423.2507 (calcd for $C_{25}H_{36}O_4Na$ 423.2506).

5.4.11. Cometin A (11)

Colourless oil. $[\alpha]_D$ −11.5 (*c* 0.05, $CHCl_3$); UV–vis (EtOH) λ_{max} (log ϵ) 240 (3.85) nm; (+)HRESIMS *m/z* 433.1988 (calcd for $C_{25}H_{30}O_5Na$ 433.1985). NMR data consistent with published data.[29]

5.5. GlyR Bioassay

The first round of screening of marine extracts was performed using a YFP-based anion flux assay as described in detail previously.[39] Briefly, the cDNAs for YFP-I152L[40] and the human α1, α2 and α3L GlyR were subcloned separately into the pcDNA3.1 plasmid vector. HEK293 cells were transfected with the cDNAs for YFP-I152L plus one of the GlyR cDNAs using a calcium phosphate precipitation method. After termination of this procedure, cells were plated into wells of a 384-well plate at a density of around 3000 cells per well. Experiments were performed 24–48 h later. Around an hour before experiments, the culture medium in each well was replaced by 15 μL of Na gluconate solution containing (in mM): Na gluconate 140, KCl 5, $CaCl_2$ 2, $MgCl_2$ 1, HEPES 10, glucose 10, pH 7.3/NaOH. An aliquot (10 μL) of each fraction (containing 300 μg/mL dried material) was added to each well 30–45 min before experiments were commenced. Individual fractions were tested in duplicate. The experiments were performed using an automated imaging system with a robot-controlled liquid handling system constructed in the laboratory. The experimental protocol involved adding 50 μL of NaI solution (containing (in mM): NaI 140, KCl 5, $CaCl_2$ 2, $MgCl_2$ 1, HEPES 10, glucose 10, pH 7.3/NaOH) + 1 mM glycine to cells in each well to yield a final glycine concentration of ~670 μM. The chloride-induced fluorescence change was monitored 5–10 s later. Typically, 100–200 fluorescent GlyR-expressing cells were imaged per well. Fractions producing significant changes to either the resting or glycine-stimulated fluorescence levels were re-tested to confirm activity.

5.6. Generation of stably-expressing HEK293 cell lines

The human α1 and α3L GlyR subunit cDNAs in the pcDNA3.1 plasmid vector were linearized using ScaI and transfected into HEK293 cells using a calcium phosphate method and then maintained for 10–14 days in selection medium containing 1 mg/mL

G-418 and 10 μM strychnine for α1 GlyR and 500 μg/mL G-418 for α3 GlyR cell lines. From thenceforth, the two respective cell lines were always cultured in these selective media. Surviving transfected colonies were isolated and grown in the same media in 96-well plate for two weeks. Any large monoclonal colonies were screened for functional response to 10 mM glycine using the YFP-based chloride flux assay described above. In these experiments, several clones of either α1 or α3 GlyRs that exhibited a significant fluorescence quench to glycine exposure were identified and one clonal cell line of each subunit was selected for further characterisation using both patch-clamp and YFP assays.

5.7. Electrophysiology

We employed a Nanion Patchliner automated planar chip patch-clamp device (NPC-16A, Nanion Technologies GmbH, Munich, Germany) to perform whole cell recordings on up to 8 cells simultaneously. In addition to increasing throughput, this device permits complete exchange of the solution bathing the cells with 25 μL of new solution. For Patchliner experiments, the stable α1 and α3 GlyR-HEK293 cells were suspended in the standard external solution containing (in mM): 140 NaCl, 4 KCl, 2 $CaCl_2$, 1 $MgCl_2$, 10 HEPES/NaOH and 5 glucose (pH 7.4) at a density of 1×10^6–5×10^7 cells/mL. The cell suspension, the pre-prepared internal solution [(in mM) 50 KCl, 10 NaCl, 60 KF, 2 $MgCl_2$, 10 HEPES/KOH (pH 7.2), and 20 EGTA], the external solution and the compound-containing solutions are all placed at pre-defined positions on the workstation and were applied to cells via robotic control. For dose–response experiments, cells were voltage-clamped at −40 mV at room temperature (20–24 °C). Compounds to be tested were dissolved in DMSO and kept at −20 °C, with solutions for experiments prepared from these stocks on the day of recording.

Results are expressed as mean ± SEM of three or more independent experiments. The Hill equation was used to calculate the half-maximal concentration (EC_{50}) and Hill coefficient (n_H) values for activation. A similar equation was also used to calculate the half-maximal concentrations for inhibition (IC_{50}) and n_H values for inhibition. All curves were fitted using a non-linear least squares algorithm (Sigmaplot 9.0, Jandel Scientific). Statistical significance was determined by unpaired Student's *t*-test with $P<0.05$ representing significance.

Acknowledgements

We thank L. Goudie (Museum Victoria) for taxonomic analysis and S. Nevin for help with the Patchliner. W.B. was supported by an Australian Development Scholarship and J.W.L. was supported by a fellowship from the National Health and Medical Research Council of Australia. We also acknowledge the support of the Australian Research Council Special Research Centre for Functional and Applied Genomics, the Institute for Molecular Bioscience and The University of Queensland.

Supplementary data

Supplementary data associated with this article can be found, in the online version, at doi:10.1016/j.bmc.2010.03.002.

References and notes

1. Lynch, J. W. *Physiol. Rev.* **2004**, *84*, 1051.
2. Jeong, H. J.; Jang, I. S.; Moorhouse, A. J.; Akaike, N. *J. Physiol.* **2003**, *550*, 373.
3. Turecek, R.; Trussell, L. O. *Nature* **2001**, *411*, 587.
4. Ye, J. H.; Wang, F.; Krnjevic, K.; Wang, W.; Xiong, Z. G.; Zhang, J. *J. Neurosci.* **2004**, *24*, 8961.
5. Betz, H.; Laube, B. *J. Neurochem.* **2006**, *97*, 1600.
6. Harvey, R. J.; Depner, U. B.; Wassle, H.; Ahmadi, S.; Heindl, C.; Reinold, H.; Smart, T. G.; Harvey, K.; Schutz, B.; Abo-Salem, O. M.; Zimmer, A.; Poisbeau, P.; Welzl, H.; Wolfer, D. P.; Betz, H.; Zeilhofer, H. U.; Muller, U. *Science* **2004**, *304*, 884.
7. Haverkamp, S.; Muller, U.; Harvey, K.; Harvey, R. J.; Betz, H.; Wassle, H. *J. Comp. Neurol.* **2003**, *465*, 524.
8. Haverkamp, S.; Muller, U.; Zeilhofer, H. U.; Harvey, R. J.; Wassle, H. *J. Comp. Neurol.* **2004**, *477*, 399.
9. Heinze, L.; Harvey, R. J.; Haverkamp, S.; Wassle, H. *J. Comp. Neurol.* **2007**, *500*, 693.
10. Webb, T. I.; Lynch, J. W. *Curr. Pharm. Des.* **2007**, *13*, 2350.
11. Lynch, J. W. *Neuropharmacology* **2009**, *56*, 303.
12. Yang, Z.; Aubrey, K. R.; Alroy, I.; Harvey, R. J.; Vandenberg, R. J.; Lynch, J. W. *Biochem. Pharmacol.* **2008**, *76*, 1014.
13. Zeilhofer, H. U. *Rev. Physiol. Biochem. Pharmacol.* **2005**, *154*, 73.
14. Zeilhofer, H. U. *Cell. Mol. Life Sci.* **2005**, *62*, 2027.
15. Froh, M.; Thurman, R. G.; Wheeler, M. D. *Am. J. Physiol. Gastrointest. Liver. Physiol.* **2002**, *283*, G856.
16. Gundersen, R. Y.; Vaagenes, P.; Breivik, T.; Fonnum, F.; Opstad, P. K. *Acta Anaesthesiol. Scand.* **2005**, *50*, 1108.
17. Eichler, S. A.; Kirischuk, S.; Jüttner, R.; Schafermeier, P. K.; Legendre, P.; Lehmann, T. N.; Gloveli, T.; Grantyn, R.; Meier, J. C. *J. Cell Mol. Med.* **2008**, *12*, 2848.
18. Eichler, S. A.; Förstera, B.; Smolinsky, B.; Jüttner, R.; Lehmann, T. N.; Fähling, M.; Schwarz, G.; Legendre, P.; Meier, J. C. *Eur. J. Neurosci.* **2009**, *30*, 1077.
19. Faulkner, D. J. *Tetrahedron Lett.* **1973**, *39*, 3821.
20. Capon, R. J.; Dargaville, T. R.; Davis, R. *Nat. Prod. Lett.* **1994**, *41*, 51.
21. Holler, U.; Konig, G. M.; Wright, A. D. *J. Nat. Prod.* **1997**, *60*, 832.
22. Barrow, C. J.; Blunt, J. W.; Munro, M. H. G.; Perry, N. B. *J. Nat. Prod.* **1988**, *51*, 275.
23. Murray, L.; Hamit, H.; Hooper, J. N. A.; Hobbs, L.; Capon, R. J. *Aust. J. Chem.* **1995**, *48*, 1899.
24. Martinez, A.; Duque, C.; Sato, N.; Tanaka, R.; Fujimoto, Y. *Nat. Prod. Lett.* **1995**, *6*, 1.
25. Shin, J.; Rho, J.-R.; Seo, Y.; Lee, H.-S.; Cho, K. W.; Sim, C. J. *Tetrahedron Lett.* **2001**, *42*, 3005.
26. Liu, Y. H.; Mansoor, T. A.; Hong, J. K.; Lee, C. O.; Sim, C. J.; Im, K. S.; Kim, N. D.; Jung, J. H. *J. Nat. Prod.* **2003**, *66*, 1451.
27. Wang, N.; Song, J.; Jang, K. H.; Lee, H. S.; Li, X.; Oh, K. B.; Shin, J. *J. Nat. Prod.* **2008**, *71*, 551.
28. Gonzalez, A. G.; Rodriguez, M. L.; Barrientos, A. S. *J. Nat. Prod.* **1983**, *46*, 256.
29. Urban, S.; Capon, R. J. *Aust. J. Chem.* **1992**, *45*, 1255.
30. Lynch, J. W.; Chen, X. *Neurosci. Lett.* **2008**, *435*, 147.
31. Supplisson, S.; Chesnoy-Marchais, D. *Mol. Pharmacol.* **2000**, *58*, 763.
32. Yang, Z.; Ney, A.; Cromer, B. A.; Ng, H. L.; Parker, M. W.; Lynch, J. W. *J. Neurochem.* **2007**, *100*, 758.
33. Chesnoy-Marchais, D.; Cathala, L. *Eur. J. Neurosci.* **2001**, *13*, 2195.
34. Chen, X.; Cromer, B.; Webb, T. I.; Yang, Z.; Hantke, J.; Harvey, R. J.; Parker, M. W.; Lynch, J. W. *Neuropharmacology* **2009**, *56*, 318.
35. Maksay, G.; Laube, B.; Schemm, R.; Grudzinska, J.; Drwal, M.; Betz, H. *J. Neurochem.* **2009**, *109*, 1725.
36. Maksay, G.; Laube, B.; Betz, H. *Neuropharmacology* **2001**, *41*, 369.
37. Lambert, J. J.; Cooper, M. A.; Simmons, R. D.; Weir, C. J.; Belelli, D. *Psychoneuroendocrinology* **2009**, *34*, S48.
38. Laube, B.; Maksay, G.; Schemm, R.; Betz, H. *Trends Pharmacol. Sci.* **2002**, *23*, 519.
39. Kruger, W.; Gilbert, D.; Hawthorne, R.; Hryciw, D. H.; Frings, S.; Poronnik, P.; Lynch, J. W. *Neurosci. Lett.* **2005**, *380*, 340.
40. Galietta, L. J.; Haggie, P. M.; Verkman, A. S. *FEBS Lett.* **2001**, *499*, 220.

Supporting Information

Ircinialactams: Subunit-Selective Glycine Receptor Modulators from Australian Sponges of the Family Irciniidae

Walter Balansa,[a] Robiul Islam,[b] Frank Fontaine,[a] Andrew M. Piggott,[a] Hua Zhang,[a] Timothy I. Webb[b] Daniel Gilbert,[b] Joseph W. Lynch[b] and Robert J. Capon [a] *

a *Institute for Molecular Bioscience, The University of Queensland, St. Lucia, QLD, 4072, Australia*

b *Queensland Brain Institute, The University of Queensland, St. Lucia, QLD, 4072, Australia*

The ethanolic extract from three priority specimens (CMB-03363, CMB-03231 and CMB-01064) were concentrated *in vacuo* and subjected to trituration into *n*-hexane, dichloromethane, methanol and water. Aliquots of 25–50 μg/mL were prepared from respective CMB-03363, CMB-03231 and CMB-01064 partitions and were tested against the glycine gated chloride channel receptors (GlyRs) using a yellow fluorescence assay. Observed inhibitory effects were attributed in part to metabolite(s) in the CH_2Cl_2 and MeOH partitions where several HPLC fractionations were performed. In the case of CMB-03231, CMB-01064 and CMB-03363, HPLC fractionations led to the discovery of 9 linear sesterterpene tetronic acids consisting of 3 known and 6 new variabilin type compounds shown in detailed at Figure 3S1, 3S2 and 3S3 and whose detailed discovery process is as follows.

Collection and Taxonomy of Sponge CMB-03363

An *Ircinia* sp. (CMB-03363) (Class Demospongiae, Order Dictyoceratida, Family Ircinidae) was collected in 2001 during scientific SCUBA operations off the Nepean Wall, in The Rip, Port Phillip Heads, Victoria (Latitude 38° 18.13' Longitude 144° 38.12'). Growth form irregular lamellate-lobate; colour in EtOH grey; texture compressible but very tough to tear; oscules discrete; surface opaque, glossy, conulose; spicules none; ectosome collagenous; choanosome a reticulation of spongin fibres forming fascicles and cored with detritus. Collagen a mass of tangled fibrils with ampules clearly visible, some detritus scattered (Museum Victoria Registry Number MVF 166224).

Isolation and purification of the metabolites of CMB-03363 were focused on three fractions: (1) eluted at 6 to 8 min (red), (2) at 9 to min 10 (blue) and (3) at 13.5 to 14.5 min (pink). At the first purification stage, only fraction t_R = 9 min (blue) was pure identified as the known 12E,20Z,18S-hydroxyvariabilin (**3**), while the less polar fraction t_R = 6 min (red) and the more polar fraction t_R = 13.5 to 14.5 min (pink) existed as mixtures, posing a challenge in isolation and purification of these two fractions.

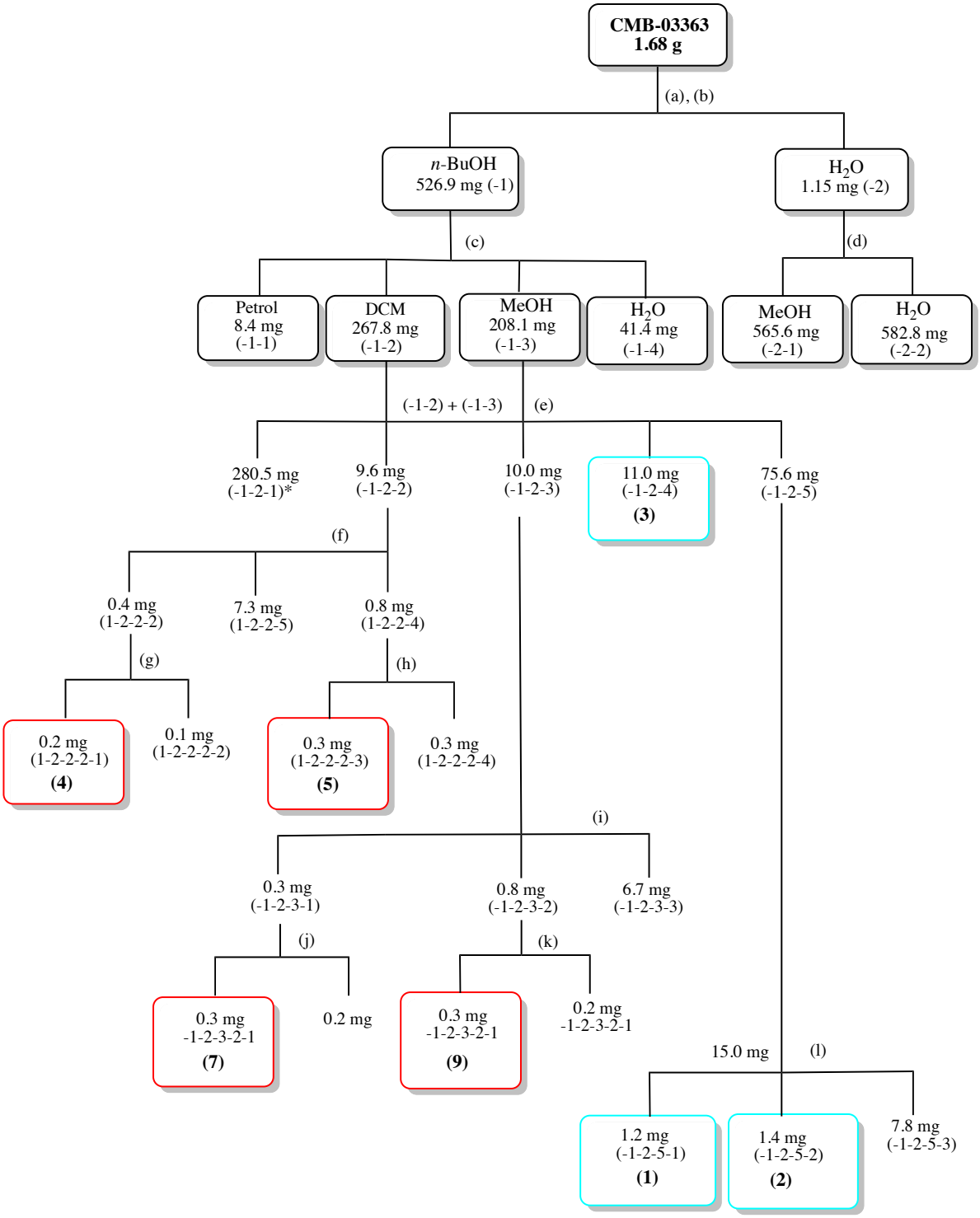

Scheme 3S1. Extraction and Purification of CMB-03363

(a). Partition [*n*-BuOH (-1) and H_2O (-2)];
(b). Trituration on *n*-BuOH soluble (Petrol (-1-1), DCM (-1-2), MeOH (-1-3) and H_2O (-1-4)]
(c). Trituration on water soluble [MeOH (-2-1) and H_2O (-2-2)];
(d-f, h). HPLC Zorbax C_8 (250 × 9.4 mm) 4.0 mL/min 10-100% MeCN/H_2O with isocratic 0.01% TFA modifier over 25 minutes;
(i, j). LC-SPE-NMR Zorbax C_8 (150 × 4.6 mm) 1.0 mL/min 0-100% MeCN/H_2O over 15 minutes);
(l). HPLC Zorbax (C3, 150 × 4.6 mm) 1.0 mL/min 50% MeCN/H_2O over 15 minutes.

Although the less-polar HPLC fraction collected at 13.5 to 14.0 minutes appeared to be a single pure compound (Figure 3S1), ^{1}H NMR analysis revealed this fraction as comprising two isomers, 7*E*,12*E*,20*E*,18*R*-variabilin (**1**) and 7*E*,12*Z*,20*E*,18*R*-variabilin (**2**). As mentioned before in the introduction of this chapter, such isomers have previously been reported as inseparable mixture and characterized on the mixture[107,115]. Even after derivatisation, Fujimoto *et al* only managed to purify one of five mixture of 7*E*,12*E*,20*E*,18*R*-variabilin, 8*Z*,13*Z*,20*Z*-strobilinin, 8*E*,13*Z*,20*Z*-strobilinin and 7*E*,13*Z*,20*Z*-felexinin, 7*E*,13*E*,20*Z*-felixinin[112]. In our hands, the mixture of 7*E*,12*E*,20*E*,18*R*-variabilin (**1**) and 7*E*,12*Z*,20*E*,18*R*-variabilin (**2**) isomers were successfully resolved (Zorbax C_3, 5 μm, 150 × 4.6 mm column, 1 mL/min gradient elution 50-100% MeCN/H_2O with isocratic 0.01% TFA modifier over 25 min) and characterized.

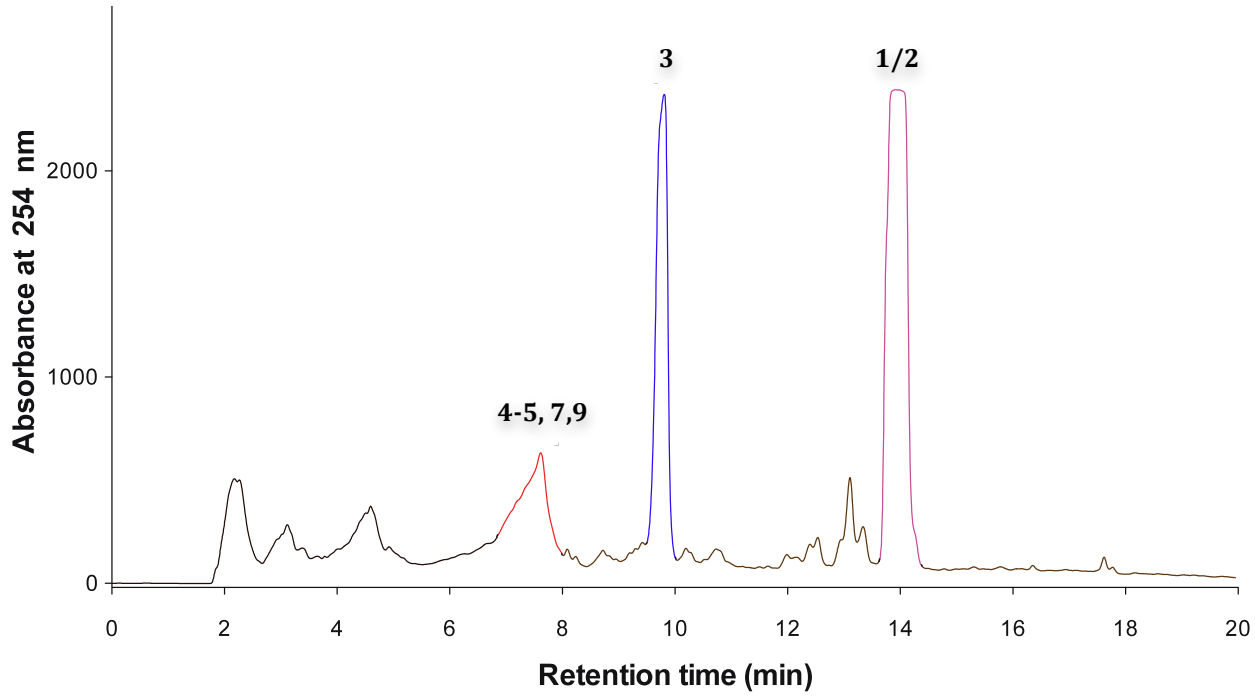

Figure 3S1. HPLC chromatogram of CMB-03363-1-2 (Zorbax C_{18} (250 x 9.4 mm) 4.0 mL/min 10-100% MeOH/H_2O with isocratic 0.01% TFA modifier over 15 minutes.

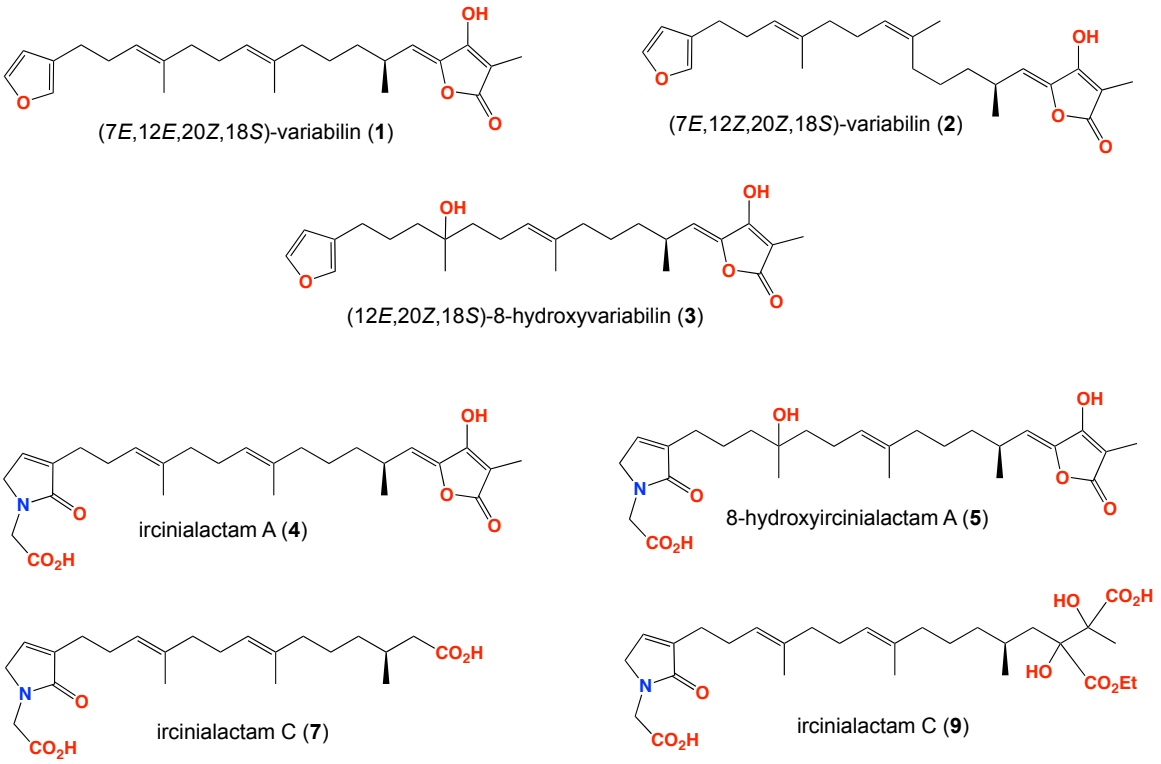

Purification of trace metabolites yielded four compounds (Figure 3S1 and Scheme 3S1). In order to obtain enough of the metabolites, the combined DCM and MeOH fractions were purified to yield fractions -1-2-2 and -1-2-3 (~20 mg), which were further purified to obtain individual semi-pure compounds (-1-2-2-2), (-1-2-2-4), (-1-2-3-1) and (-1-2-3-2) (Scheme 3S1). Due to the close retention time of the metabolites in this fraction, we employed LC-SPE-NMR. Figure 3S2 displays an overlay chromatogram of four metabolites after separation with LC-SPE-CMR (Zorbax C_8, 5 µm, 150 × 4.6 mm column, 1 mL/min gradient elution 10-100% MeCN/H_2O with isocratic 0.01% TFA modifier over 25 min). The metabolites isolated through this process included ircinialactam A (**4**), hydroxyircinialactam **(5),** ircinialactam C (**7**) and ircinialactam D (**9**).

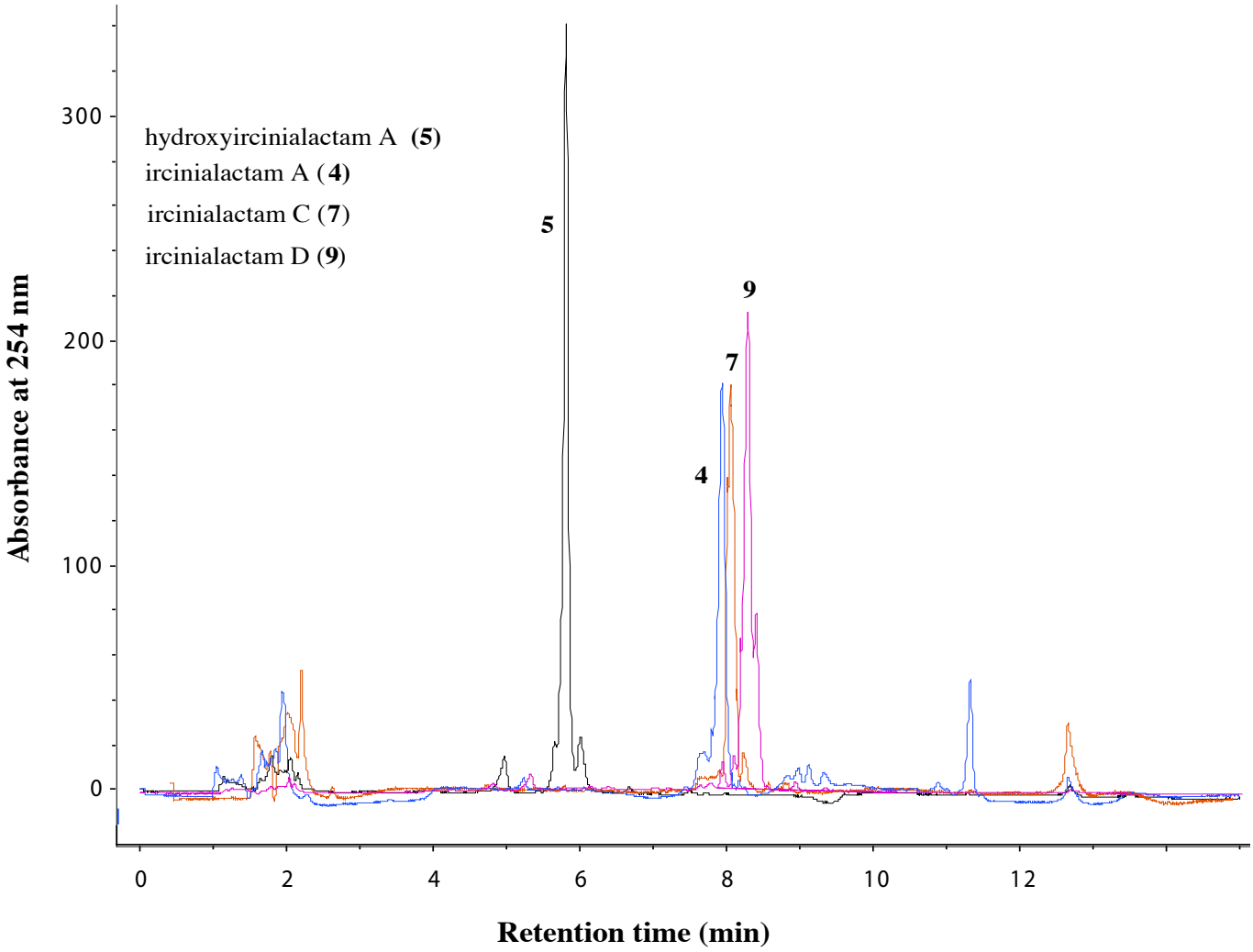

Figure 3S2. Overlay of HPLC chromatogram of pure compounds **4-5, 7 and 9** [Zorbax C_8 (150 x 4.6 mm) 1.0 mL/min 50-100% MeCN/H_2O with isocratic 0.01% TFA modifier] over 15 minutes, resolved by LC-SPE-NMR with careful peak shriving.

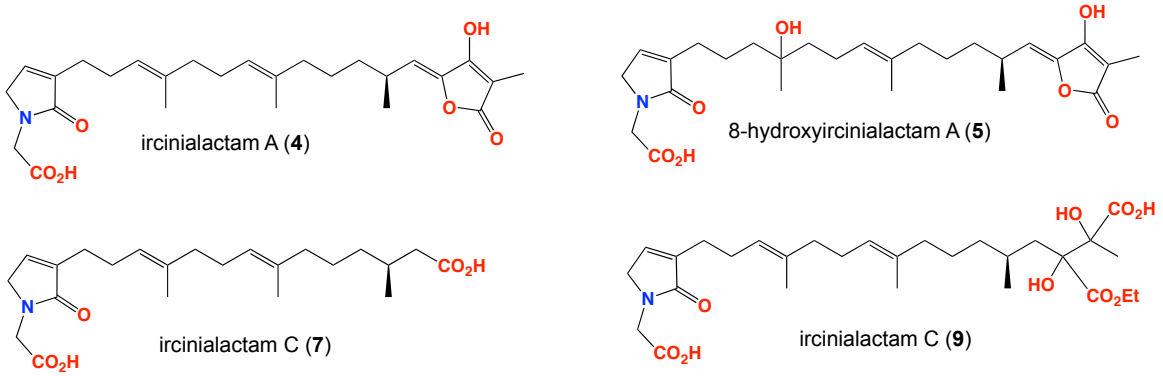

Collection and Taxonomy of Sponge CMB-01064

An *Ircinia* sp. (CMB-01064) (Class Demospongiae, Order Dictyoceratida, Family Irciniidae) was collected in the Great Australian Bight, during commercial trawling operations aboard the FV Comet, in May 1990. Growth form massive-irregular; colour on deck not seen, colour in EtOH is grey; texture compressible but arenaceous and tough to tear; oscules not seen; surface opaque; conulose; spicules none; ectosome indistinct, collagenous; choanosome a mass of collagen fibrils with terminal ampules and detritus obscuring fiber reticulation (Museum Victoria Registry Number MVF 166265).

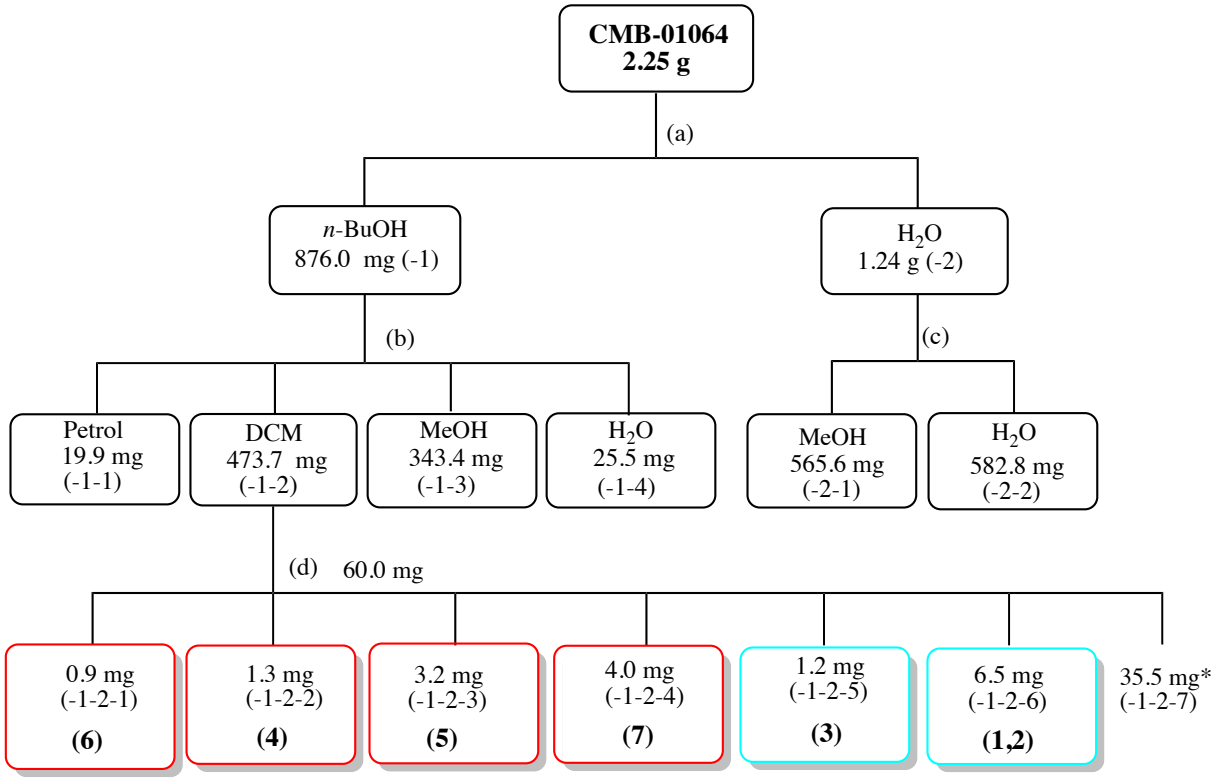

(a). Partition [n-BuOH (-1) and H_2O (-2);
(b). Trituration on *n*-BuOH soluble (Petrol (-1-1), DCM (-1-2), MeOH (-1-3) and H_2O (-1-4)]
(c). Trituratin on water soluble [MeOH (-2-1) and H_2O (-2-2)];
(d). HPLC [Zorbax $C1_8$ (250 x 9.4 mm) 4.0 mL/min 90% H_2O/MeCN to MeCN + 0.01 TFA over 25 minutes
* Uninvetistigated

Scheme 3S2. Extraction and Purification of sponge CMB-01064

The isolation and characterization of the metabolites of CMB-01064 were focused on six fractions including 4 (green), 5 (yellow), 5 (pink), 7 (black), 3 (blue), 1 and 2 (red), five of which (**4**, **5**-**7** and **9**) were already pure. Apart from **6**, other compounds have been isolated from CMB-03363 (Figure 3S3) as shown by spectroscopic data analysis and comparison with the metabolites isolated from CMB-03363. Chemical profiles (NMR and HRESIMS data) of metabolites isolated from CMB-01064 showed close similarity to those obtained from CMB-03363. The only exception was that CMB-01064 did not produce **9** but instead this specimen contained a new metabolite, 8-hydroxyircinialactam A (**6**) (Scheme 3S2).

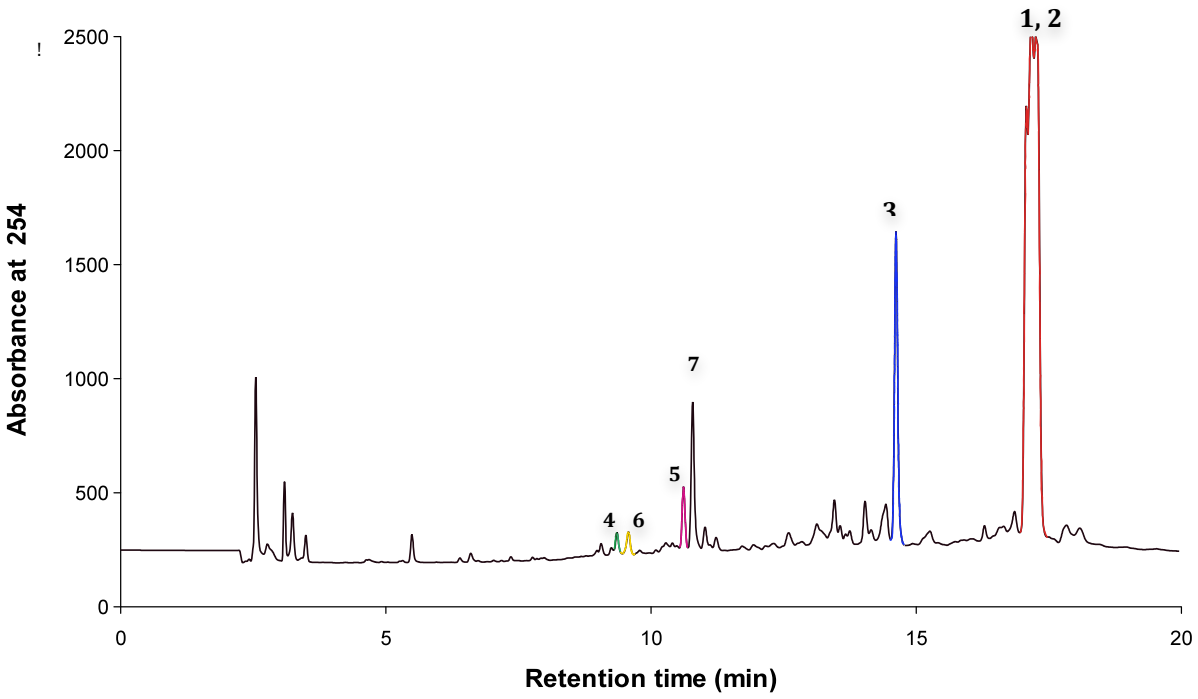

Figure 3S3. HPLC chromatogram of CMB-01064-1-2 (Zorbax C_{18} (250 x 9.4 mm) 4.0 mL/min 10-100% MeOH/H_2O with isocratic 0.01% TFA modifier over 15 minutes.

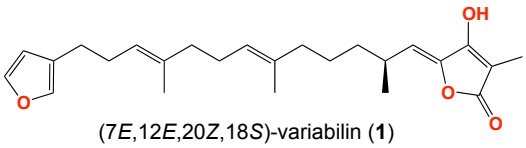

(7*E*,12*E*,20*Z*,18*S*)-variabilin (**1**)

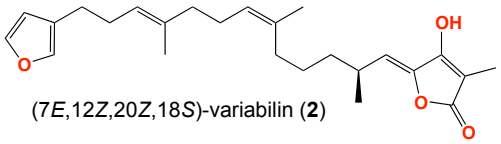

(7*E*,12*Z*,20*Z*,18*S*)-variabilin (**2**)

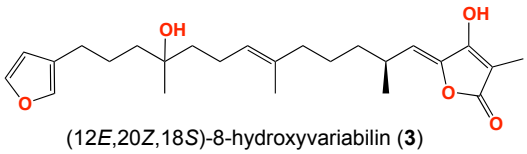

(12*E*,20*Z*,18*S*)-8-hydroxyvariabilin (**3**)

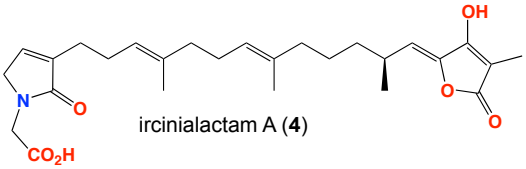

ircinialactam A (**4**)

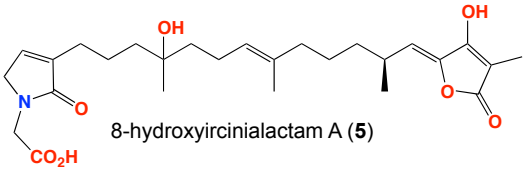

8-hydroxyircinialactam A (**5**)

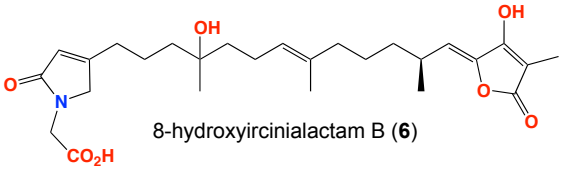

8-hydroxyircinialactam B (**6**)

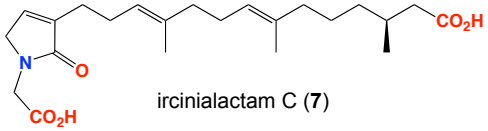

ircinialactam C (**7**)

Collection and Taxonomy of Sponge CMB-03231

A *Psammocinia* sp. (CMB-03231) (Class Demospongiae, Order Dictyoceratida, Family Ircinidae) was collected off The Pinnacles Reef, offshore Point Lonsdale, Victoria (Latitude 38° 17.50' Longitude 144° 35.20'. Growth form massive-irregular; colour in EtOH sandy; texture spongy but tough to tear; oscules scattered with membranous lip; surface translucent, wrinkled; spicules none; ectosome a distinct layer of detritus 300-400 μm thick; choanosome-spongin bound tracts of detritus in dense mass of collagen fibrils (Museum Victoria Registry Number MVF 166220).

Although the last specimen (CMB-03231) yielded only low levels of sesterterpenes, we managed to isolate one new molecule *ent*-ircinialactam (**8**) from this specimen (Figure 3S4 and Scheme 3S3), the enantiomer of ircinialactam C (**7**) recovered from CMB-03363 and CMB-01064. Identification of this molecule and all metabolites isolated from CMB-01064 and CMB-03363 are described in detail in the following pages.

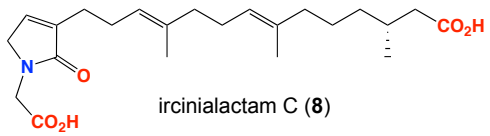

ircinialactam C (**8**)

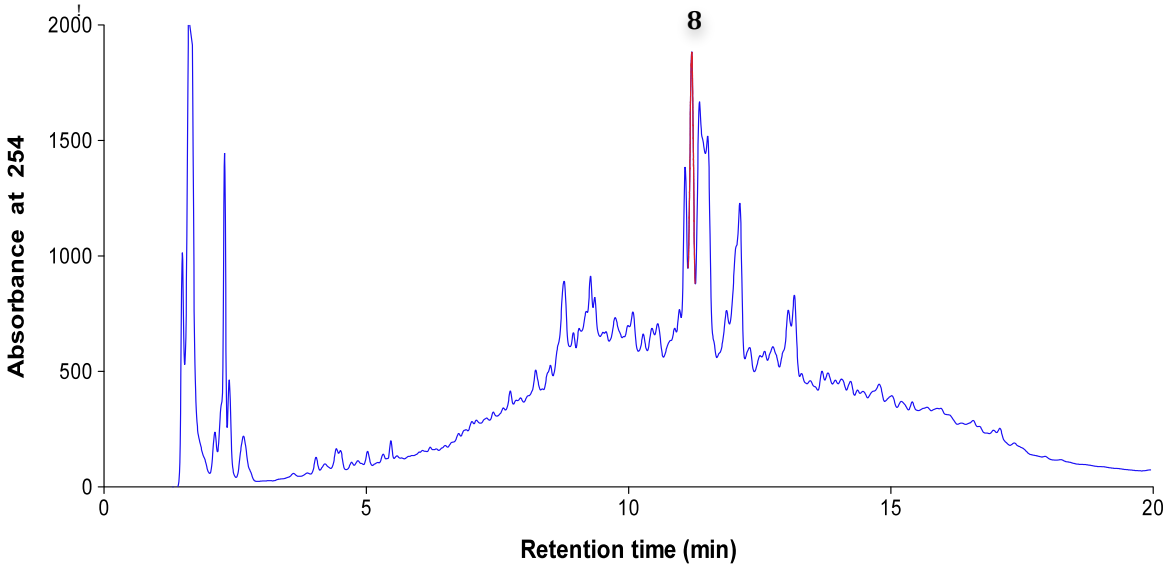

Figure 3S4. HPLC chromatogram of CMB-03231-1-2 (Zorbax C_{18} (250 x 9.4 mm) 4.0 mL/min 10-100% MeOH/H_2O

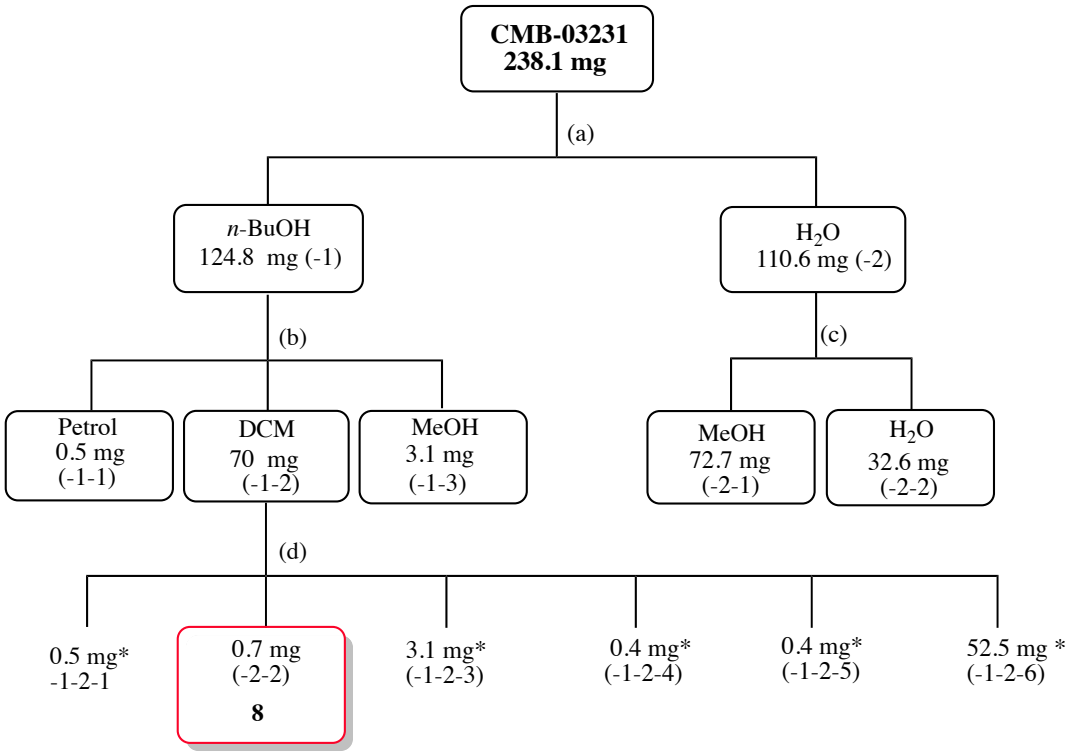

(a). Partition [*n*-BuOH (-1) and H_2O (-2);
(b). Trituration on *n*-BuOH soluble (Petrol (-1-1), DCM (-1-2), MeOH (-1-3) and H_2O (-1-4)];
(c). Trituratin on water soluble [MeOH (-2-1) and H_2O (-2-2)];
(d). HPLC [Zorbax C_{18} (250 x 9.4 mm) 4.0 mL/min 90% H_2O/MeCN to MeCN + 0.01 TFA over 25 minutes;
Red indicates new compound while * means univestigated.

Scheme 3S3. Extraction and Purification of sponge CMB-03231

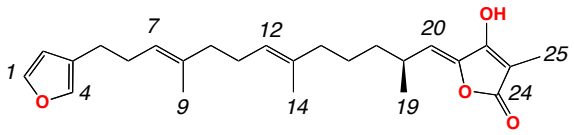

(7*E*,12*E*,20*Z*,18*S*)-variabilin (**1**)

Table 3S1: NMR (600 MHz, CD_3OD) data for (7*E*,12*E*,20*Z*,18*S*)-variabilin (**1**)

#	δ_H (mult., *J* (Hz))	δ_C[A]	COSY	HMBC (^1H-^{13}C)
1	7.36 (t, 1.7)	143.9	2	2, 3, 4
2	6.29 (br s)	112.2	1	1, 3, 4
3		125.7		
4	7.24 (br s)	140.2	5	1, 2, 3
5	2.43 (t, 7.5)	26.1	4, 6	2, 3, 4, 6
6	2.23 (dt, 7.5, 7.5)	29.8	5, 7	5, 7, 8
7	5.16 (br t, 7.5)	125.4	6	5, 6, 9, 10
8		136.7		
9	1.57 (br s)	16.3		7, 8, 10
10	1.98[B]	40.9	11	7, 8, 9, 11
11	2.08 (dt, 7.3, 7.3)	27.6	10, 12	12, 13, 15
12	5.09 (br t, 7.2)	125.4	11	10, 11, 14
13		136.0		
14	1.56 (br s)	16.0		12, 13, 15
15	1.95[B]	40.6	16	12, 13, 14, 16, 17
16	1.38[C]	27.0	15, 17a	17
17a	1.39[C]	37.8	16	16
17b	1.31 (m)			16
18	2.74 (m)	32.0	19, 20	
19	1.05 (d, 8.5)	21.3	18	17, 18, 20
20	5.26 (d, 10.5)	115.3	18	17, 19, 21, 22
21		145.7		
22		166.8		
23		97.5		
24		174.2		
25	1.72 (s)	6.2		21, 22, 23, 24

[A] ^{13}C NMR assignments supported by HSQC experiment. [B,C] overlapping signals within the column.

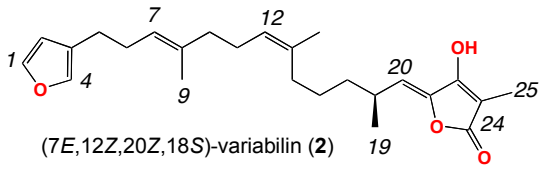

(7*E*,12*Z*,20*Z*,18*S*)-variabilin (**2**)

Table 3S2. NMR (600 MHz, CD_3OD) data for (7*E*,12*Z*,20*Z*,18*S*)-variabilin (**2**)

#	δ_H (mult., *J* (Hz))	δ_C[A]	COSY	HMBC (^1H-^{13}C)
1	7.36 (t, 1.7)	143.9	2	2, 3, 4
2	6.29 (br s)	112.2	1	1, 3, 4
3		126.4		
4	7.24 (br s)	140.3	5	1, 2, 3
5	2.44 (br t, 7.4)	26.2	4, 6	2, 3, 4, 6, 7
6	2.24 (dt, 7.2, 7.2)	29.8	5, 7	5, 7, 8
7	5.15 (br t, 7.5)	125.5	6	5, 6, 9, 10
8		136.7		
9	1.55 (br s)	16.1		7, 8, 10
10	1.95[B]	40.8	11	7, 8, 11, 12
11	1.97[B]	27.2	10, 12	12, 13
12	5.11 (br t, 7.5)	126.0	11	11, 14, 15
13		137.0		
14	1.65 (br s)	23.8		12, 13, 15
15	1.93[B]	32.4	16	16, 17
16	1.43 (m)	27.5	15	13
17	a 1.47 (m)	38.9		16, 18, 19, 20
	b 1.35 (m)			16, 18, 19, 20
18	2.74 (m)	32.0	19, 20	
19	1.06 (d, 6.8)	21.4	18	17, 18, 20
20	5.28 (d, 10.1)	115.4	18	17, 19, 21, 22
21		145.4		
22		165.8		
23		98.1		
24		173.8		
25	1.73 (s)	6.3		21, 22, 23, 24

[A] ^{13}C NMR assignments supported by HSQC experiment. [B] overlapping signals within the column.

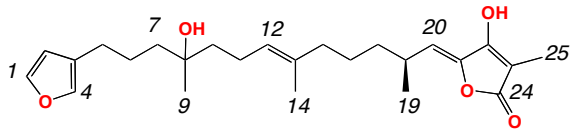

(12*E*,20*Z*,18*S*)-8-hydroxyvariabilin (**3**)

Table 3S3. NMR (600 MHz, CD_3OD) data for (12*E*,20*Z*,18*S*)-8-hydroxyvariabilin (**3**)

#	δ_H (mult., *J* (Hz))	δ_C[A]	COSY	HMBC (^1H-^{13}C)
1	7.38 (t, 1.6)	144.1	2	2, 3, 4
2	6.30 (br s)	112.0	1	1, 3, 4
3		126.5		
4	7.26 (br s)	140.2	5	1, 2, 3
5	2.41 (br t, 7.3)	26.3	4, 6	2, 3, 4, 6, 7
6	1.60 (m)	25.8	5, 7	7
7	1.47[B]	42.3	6	
8		73.4		
9	1.13 (s)	27.0		7, 8, 10
10	1.45[B]	42.8	11	8, 9
11	2.00[C]	23.7	10, 12	10, 12, 13
12	5.12 (br t, 7.0)	126.2	11	11, 14, 15
13		135.9		
14	1.57 (br s)	15.9		12, 13, 15
15	1.97[C]	40.6	16	12, 13, 14, 16, 17
16	1.39[D]	26.9	15	17
17	a 1.39[D]	37.7	17b	
	b 1.32 (m)		17a	16
18	2.75 (m)	32.0	19, 20	
19	1.06 (d, 6.8)	21.2	18	17, 18, 20
20	5.28 (d, 10.1)	116.0	18	17, 19, 21, 22
21		144.1		
22		164.7		
23		99.2		
24		173.6		
25	1.75 (s)	6.3		22, 23, 24

[A] ^{13}C NMR assignments supported by HSQC experiment. [B-D] overlapping signals within the column.

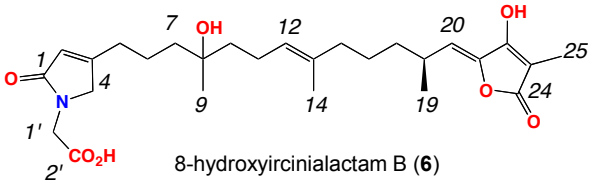

8-hydroxyircinialactam B (**6**)

Table 3S4. NMR (600 MHz, CD_3OD) data for 8-hydroxyircinialactam B (**6**)

#	δ_H (mult., *J* (Hz))	δ_C [A]	COSY	HMBC (^1H-^{13}C)
1		174.7		
2	5.88 (br s)	121.1	4	1, 3, 4, 5
3		164.7		
4	4.13 (br s)	56.4	2	2, 3
5	2.45 (br t, 7.4)	30.9	6	2, 3, 4, 6, 7
6	1.66 (m)	23.0	5, 7	
7	1.50 (m)	42.1	6	
8		73.2		
9	1.16 (s)	26.4		7, 8, 10
10	1.46 (m)	42.7	11	11
11	2.03 (m)	23.4	10, 12	10, 12, 13
12	5.14 (br t, 7.1)	126.0	11	11, 14, 15
13		135.8		
14	1.58 (br s)	15.7		12, 13, 15
15	1.97 (br t, 7.1)	40.4	16	14, 16
16	1.39[B]	26.6	15	17
17	a 1.40[B] b 1.32 (m)	37.5	18	
18	2.75 (m)	31.8	17a, 19, 20	
19	1.06 (d, 6.7)	20.9	18	17, 18, 20
20	5.28 (d, 10.1)	115.8	18	19, 21, 22
21		144.9		
22		164.1		
23		99.1		
24		173.2		
25	1.75 (s)	6.0		22, 23, 24
1′	4.19 (s)	43.9		1, 4, 2′
2′		172.3		

[A] ^{13}C NMR assignments supported by HSQC experiment. [B] overlapping signals

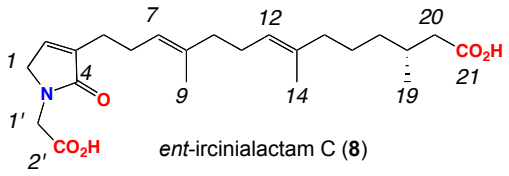

ent-ircinialactam C (**8**)

Table 3S5. NMR (600 MHz, CD_3OD) data for *ent*-ircinialactam C (**8**)

#	δ_H (mult., *J* (Hz))	δ_C[A]	COSY	HMBC (^1H-^{13}C)
1	4.05 (br s)	53.1	2	2
2	6.88 (br s)	138.8	1	1, 4, 5
3		*		
4		174.4		
5	2.30[B]	27.1		2, 6
6	2.28[B]	27.2	7	5, 7, 8
7	5.16 (br t, 6.7)	124.8	6	5, 9, 10
8		137.3		
9	1.61 (br s)	16.3		7, 8, 10
10	2.01 (br t, 7.7)	41.0	11	7, 8, 9, 11
11	2.09[C]	27.7	10, 12	10, 12, 13
12	5.11 (br t, 7.1)	125.7	11	11, 14, 15
13		136.1		
14	1.59 (br s)	16.1		12, 13, 15
15	1.97 (br t, 8.1)	41.0	16	12, 13, 14, 16, 17
16	1.44 (m)	26.5	15	
17	a 1.32 (m) b 1.18 (m)	37.5		
18	1.92 (m)	31.6	19, 20a	
19	0.95 (d, 6.7)	20.3	18	17, 18, 20
20	a 2.26[B] b 2.07[C]	42.8	18, 20b 20a	17, 18, 19, 21 17, 18, 19, 21
21		177.2		
1′	4.20 (s)	45.0		1, 2′, 4
2′		173.1		

[A] ^{13}C NMR assignments supported by HSQC experiment. [B,C] overlapping signals within the column. * Not observed

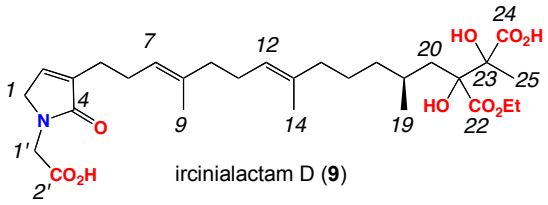

ircinialactam D (**9**)

Table 3S6. NMR (600 MHz, CD_3OD) data for ircinialactam D (**9**)

#	δ_H (mult., *J* (Hz))	δ_C [A]	COSY	HMBC (^1H-^{13}C)
1	4.05 (br s)	52.9	2	3
2	6.89 (br s)	138.8	1	1, 4
3		139.6		
4		174.2		
5	2.29[B]	26.9		3, 6
6	2.27[B]	27.0	7	3, 5, 7, 8
7	5.16 (br t, 6.6)	124.5	6	5, 9, 10
8		137.2		
9	1.61 (br s)	16.1		7, 8, 10
10	2.00[C]	40.9	11	7, 8, 9, 11
11	2.09 (m)	27.5	10, 12	10, 12, 13
12	5.10 (br t, 6.9)	125.4	11	14, 15
13		136.2		
14	1.58 (br s)	16.0		12, 13, 15
15	1.93 (br t, 7.2)	40.8	16	12, 13, 14, 16, 17
16	1.37 (m)	26.3	15	
17	a 1.24 (m)	38.9	17, 18	
	b 1.11 (m)			
18	1.47 (m)	30.9	19, 20a, 20b	
19	0.96 (d, 6.5)	22.1	18	17, 18, 20
20	a 1.97[C]	40.6	18	
	b 1.84 (dd, 14.2, 7.7)		18	18, 19, 21, 22
21		83.6		
23		81.3		
25	1.49 (s)	21.1		21, 23, 24
22		176.6		
24		175.2		
$CO_2\underline{CH_2}CH_3$	a 4.22 (m)	62.5	$CO_2CH_2\underline{CH_3}$	
	b 4.19 (m)			
$CO_2CH_2\underline{CH_3}$	1.29 (t, 7.2)	14.4	$CO_2\underline{CH_2}CH_3$	26
1′	4.23 (s)	44.3		1, 2′, 4
2′		172.4		

[A] ^{13}C NMR assignments supported by HSQC experiment. [B,C] overlapping signals within the column.

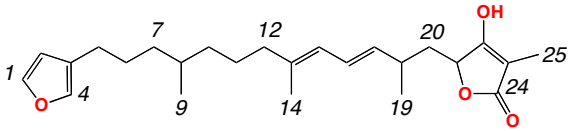

7,8-dihydroisopalinurin (**11**)

Table 3S7. NMR (600 MHz, CD_3OD) data for 7,8-dihydroisopalinurin (**10**)

#	δ_H (mult., *J* (Hz))	δ_C[A]	COSY	HMBC (^1H-^{13}C)
1	7.37 (t, 1.7)	144.0	2	2, 3, 4
2	6.27 (m)	112.1	1	1, 3, 4
3		126.5		
4	7.23 (m)	140.1	5	1, 2, 3
5	2.39 (td, 7.3, 3.4)	25.8	4, 6	2, 3, 4, 6
6	1.52[B]	29.2	5, 7a	5
7	a 1.44[C] b 1.14 (m)	36.9	6, 7b 7a, 8	
8	1.75 (m)	31.0	7b, 9, 10a	
9	0.97 (d, 6.7)	21.0	8	7, 8, 10
10	a 1.87 (ddd, 14.4, 7.5, 3.0) b 1.31[D]	41.0	8, 10b 8, 10a, 11a	7, 8, 9 7, 8
11	a 1.52[B] b 1.43[C]	26.1	10b, 11b, 12 11a, 12	10, 13
12	2.04 (m)	41.0	11a, 11b	11, 13, 15
13		137.0		
14	1.72 (d, 1.1)	16.6	15	12, 13, 15
15	5.78 (br d, 10.7)	126.6	14, 16	12, 14, 16, 17
16	6.20 (ddd, 15.0, 10.7, 0.8)	126.5	15, 17	13, 15, 18
17	5.38 (dd, 15.0, 8.2)	139.2	16, 18	15, 16, 18, 19
18	2.17 (m)	38.4	17, 19	16, 17, 19, 20
19	0.99 (d, 6.7)	21.6	18	17, 18, 20
20	a 1.34[D] b 1.29[D]	38.0	21 21	17, 18, 21 17, 18, 21
21	4.63 (brd, 9.5)	79.3	20a, 20b	24
22		179.4		
23		94.8		
24		181.1		
25	1.63 (d, 0.9)	6.1		22, 23, 24

[A] ^{13}C NMR assignments supported by HSQC experiment. [B-D] overlapping signals within the column.

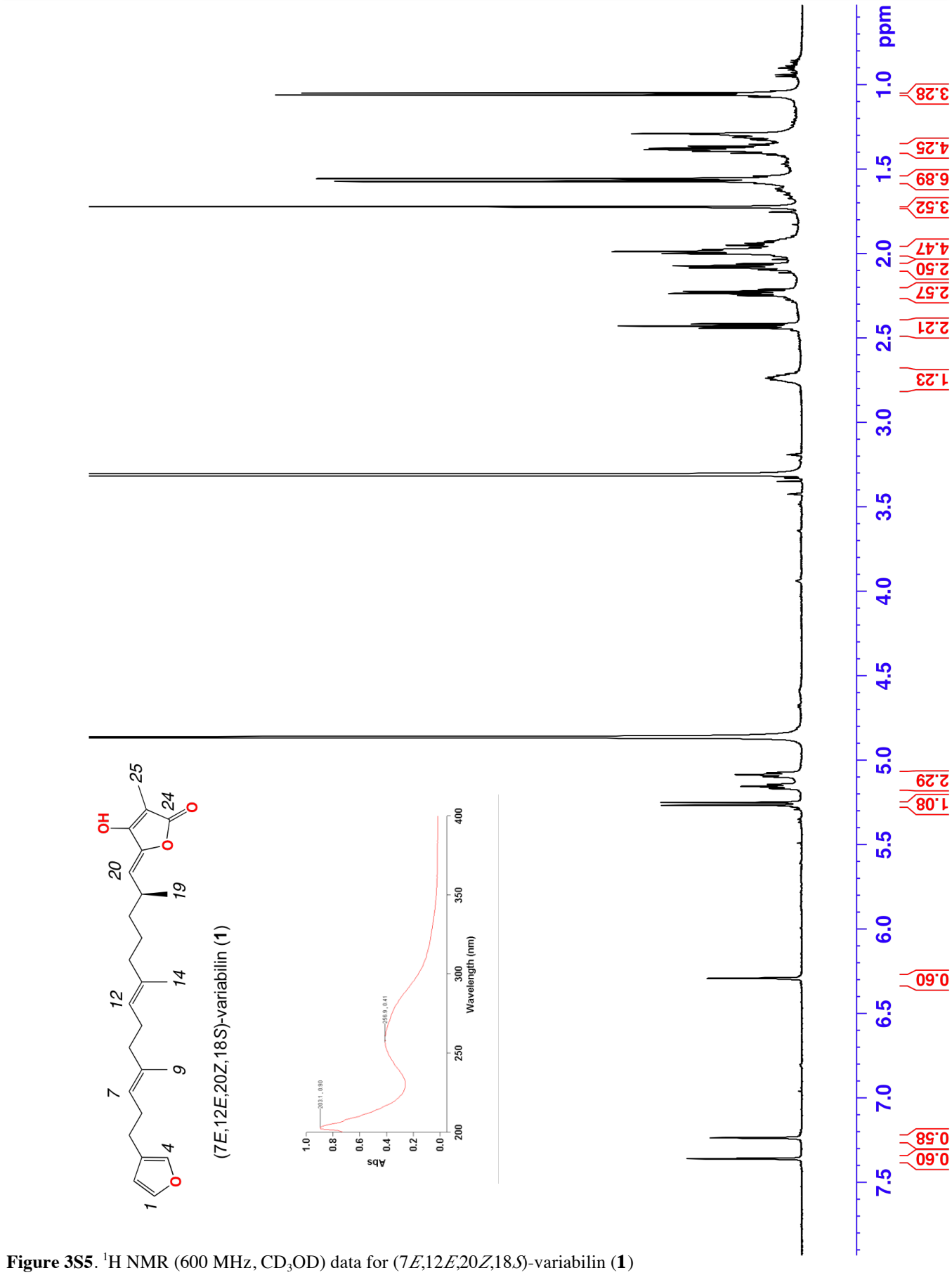

Figure 3S5. ^{1}H NMR (600 MHz, CD_3OD) data for (7*E*,12*E*,20*Z*,18*S*)-variabilin (**1**)

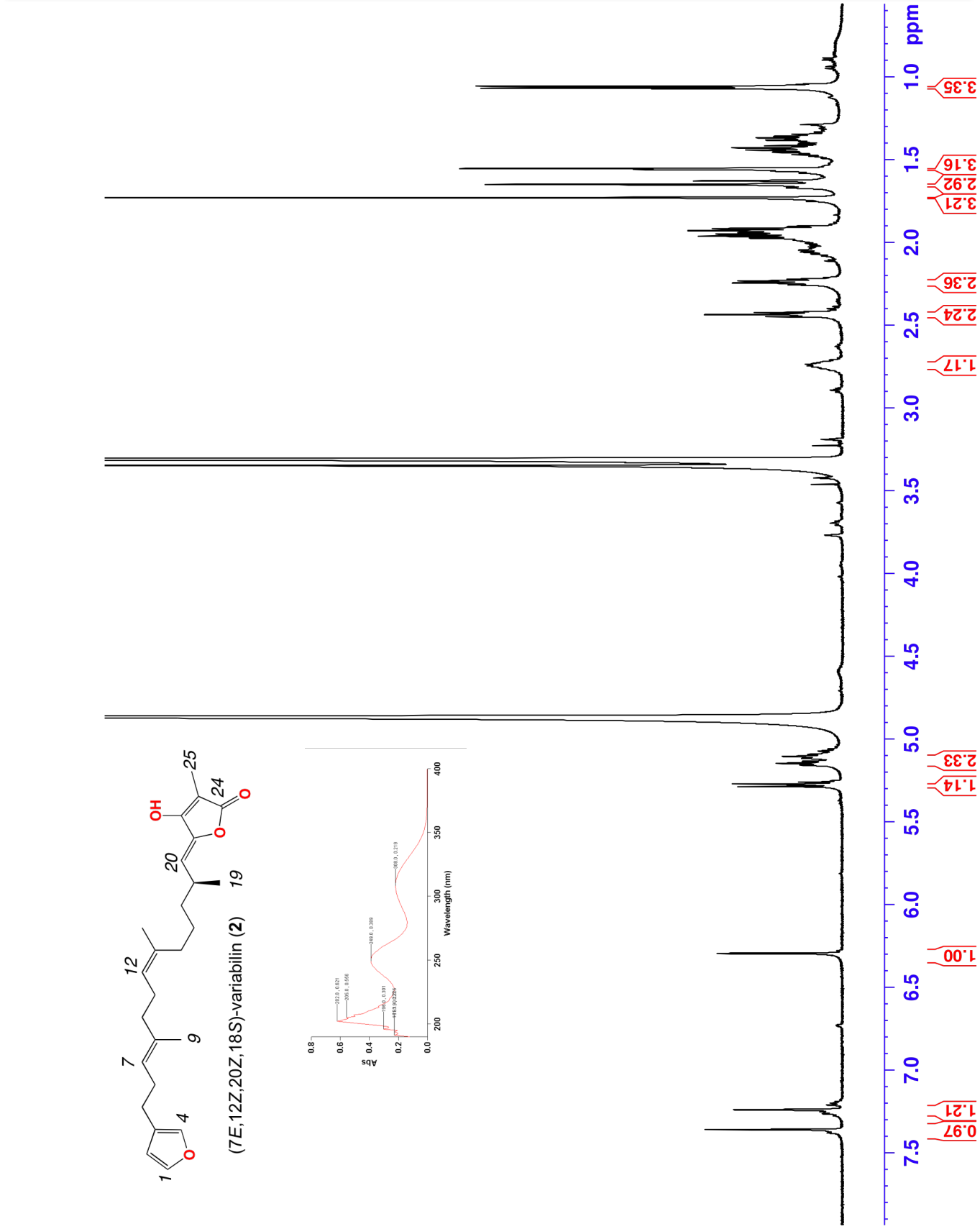

Figure 3S6. ^{1}H NMR (600 MHz, CD_3OD) data for (7*E*,12*Z*,20*Z*,18*S*)-variabilin (**2**)

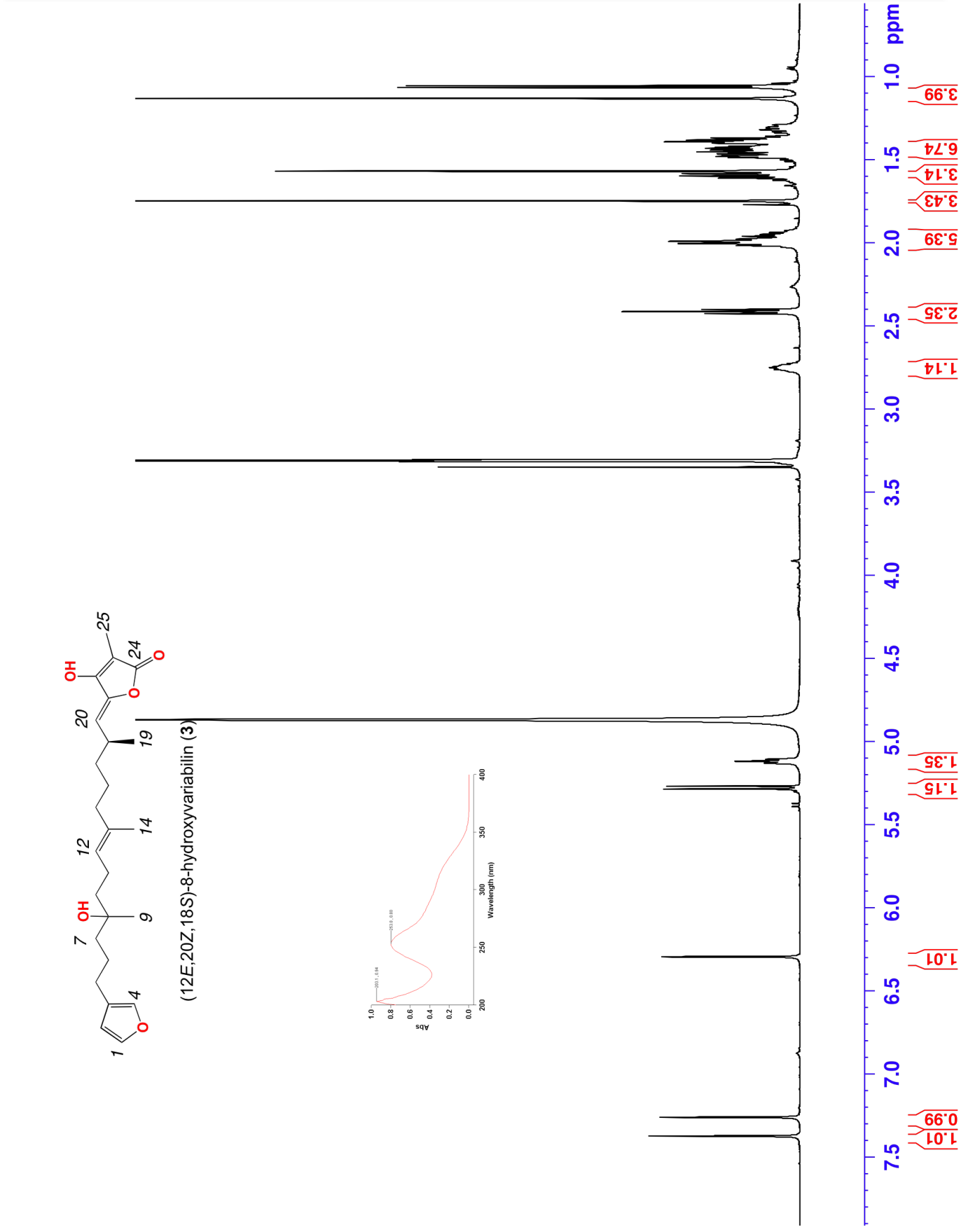

Figure 3S7. ^{1}H NMR (600 MHz, CD_3OD) data for (12*E*,20*Z*,18*S*)-8-hydroxyvariabilin (**3**)

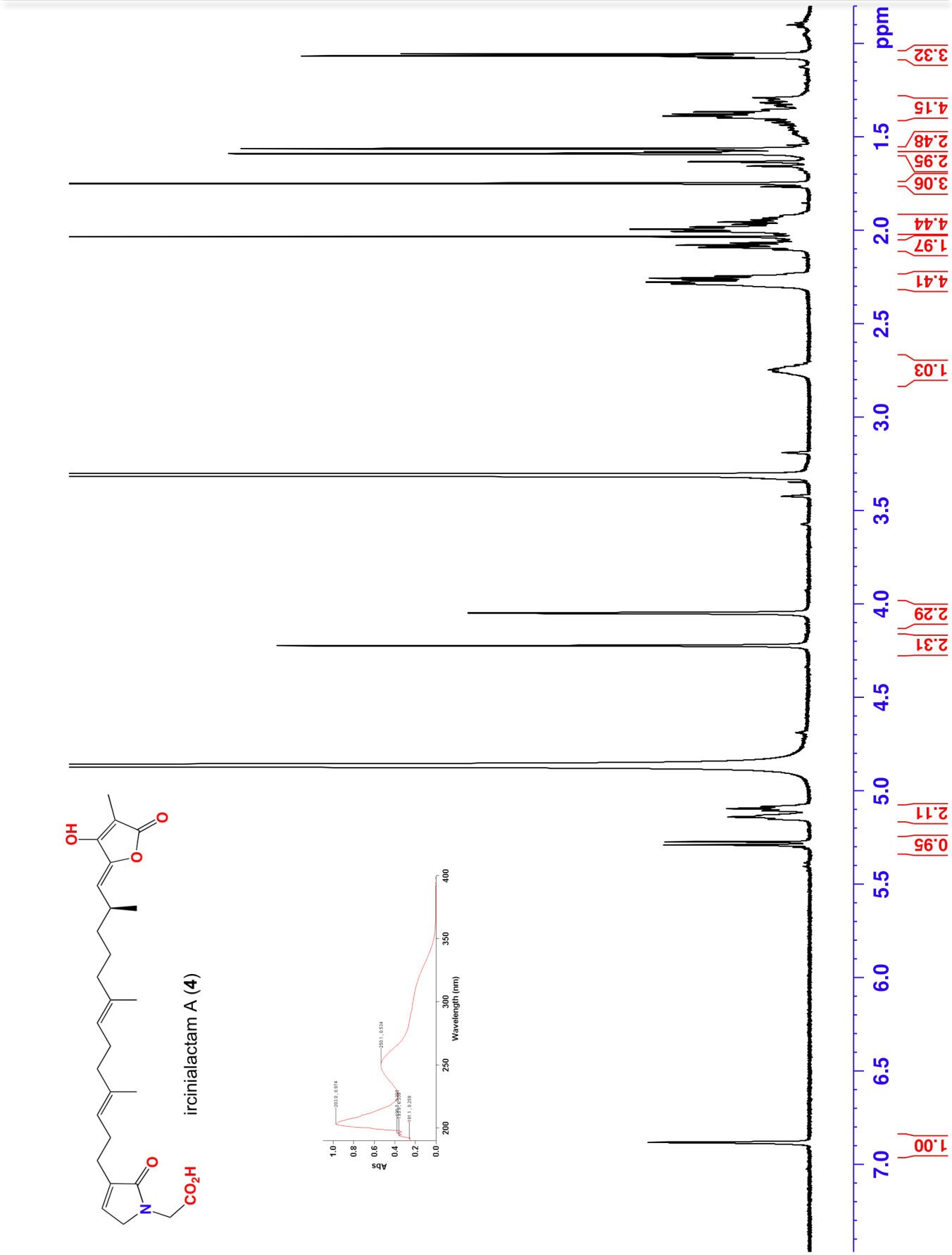

Figure 3S8. ^{1}H NMR (600 MHz, CD_3OD) data for ircinialactam A (**4**)

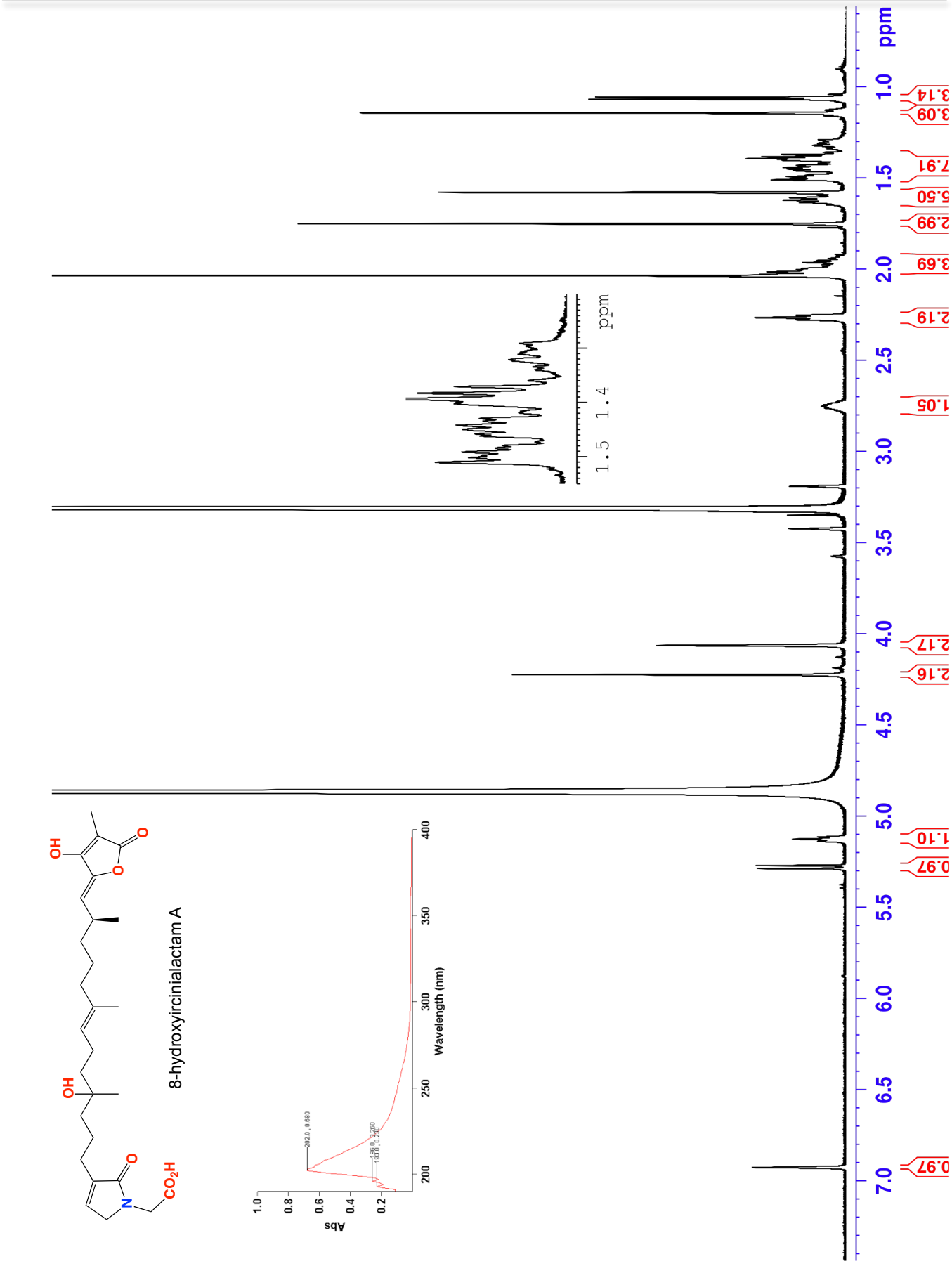

Figure 3S9. ^{1}H NMR (600 MHz, CD_3OD) data for 8-hydroxyircinialactam A (**5**)

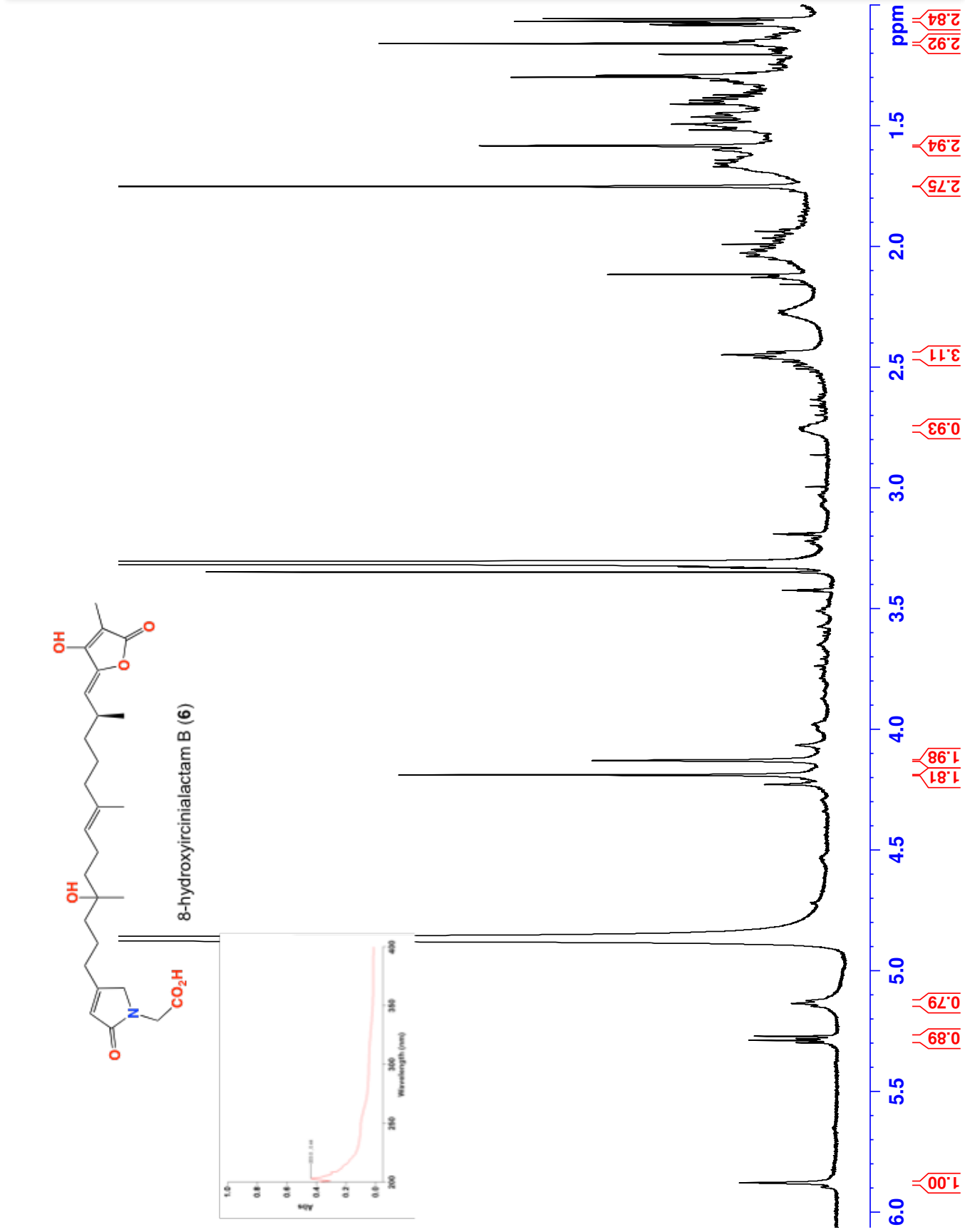

Figure 3S10. ^{1}H NMR (600 MHz, CD_3OD) data for 8-hydroxyircinialactam B (**6**)

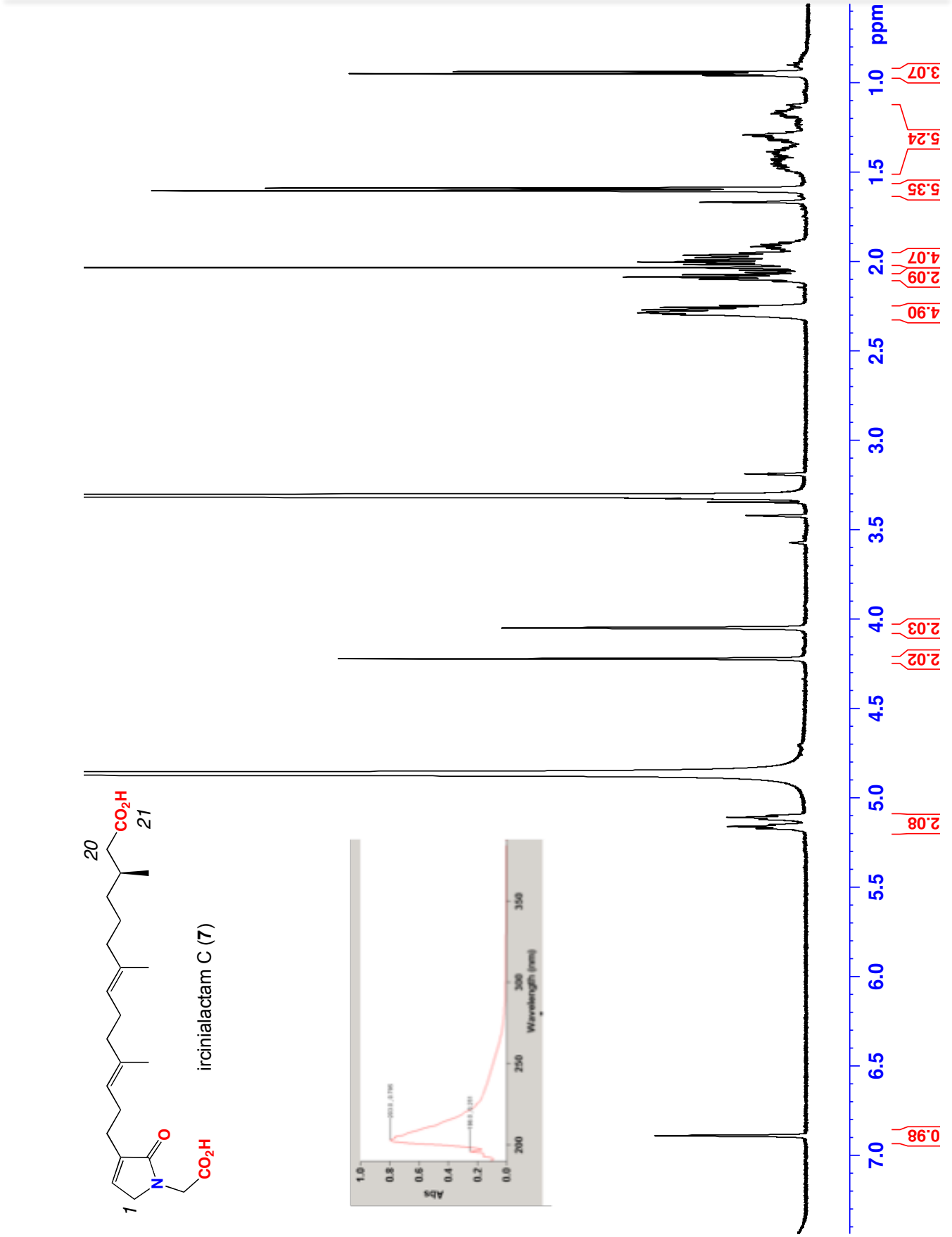

Figure 3S11. ^{1}H NMR (600 MHz, CD_3OD) data for ircinialactam C (**7**)

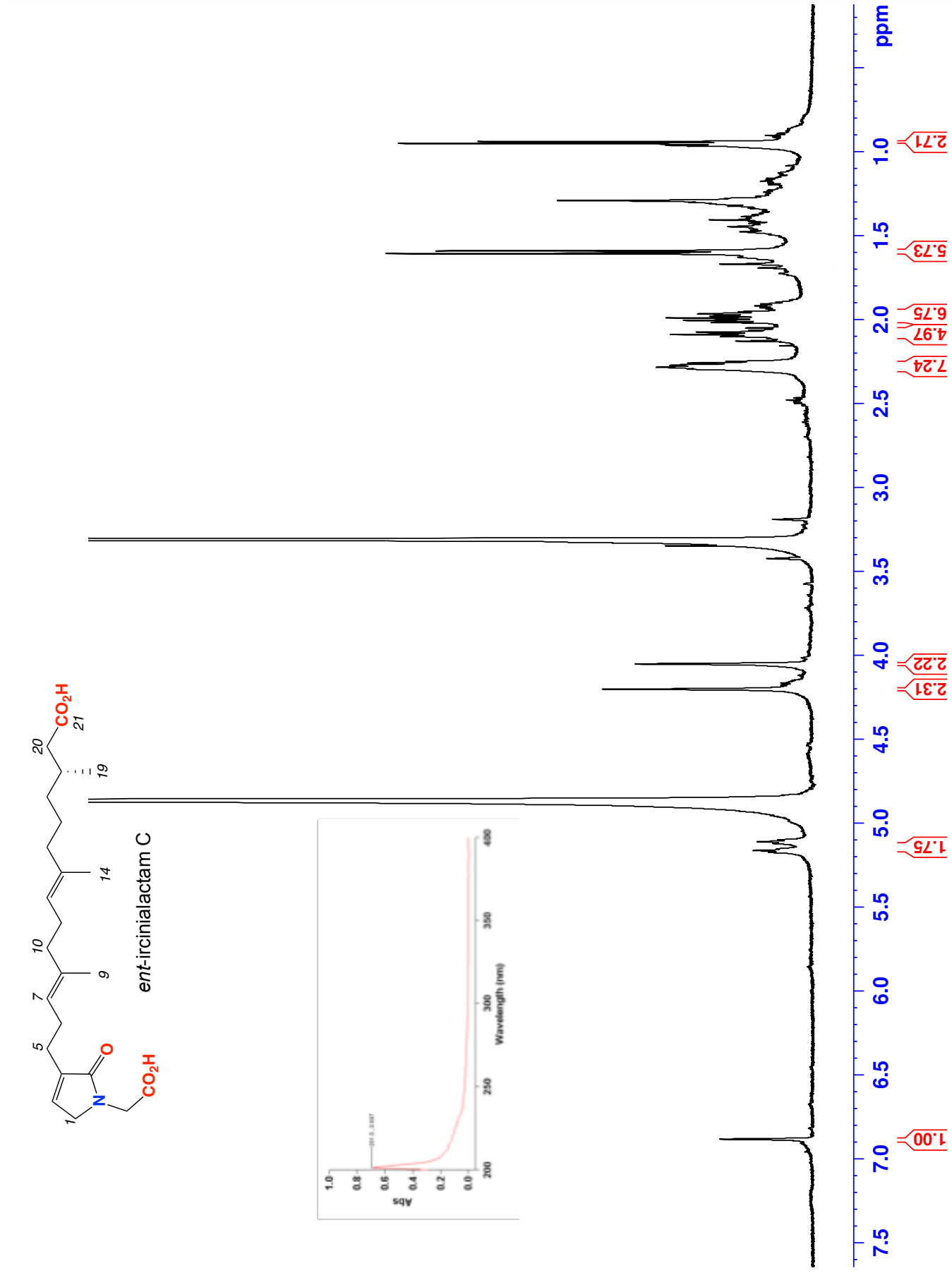

Figure 3S12. ^{1}H NMR (600 MHz, CD_3OD) data for *ent*-ircinialactam C (**8**)

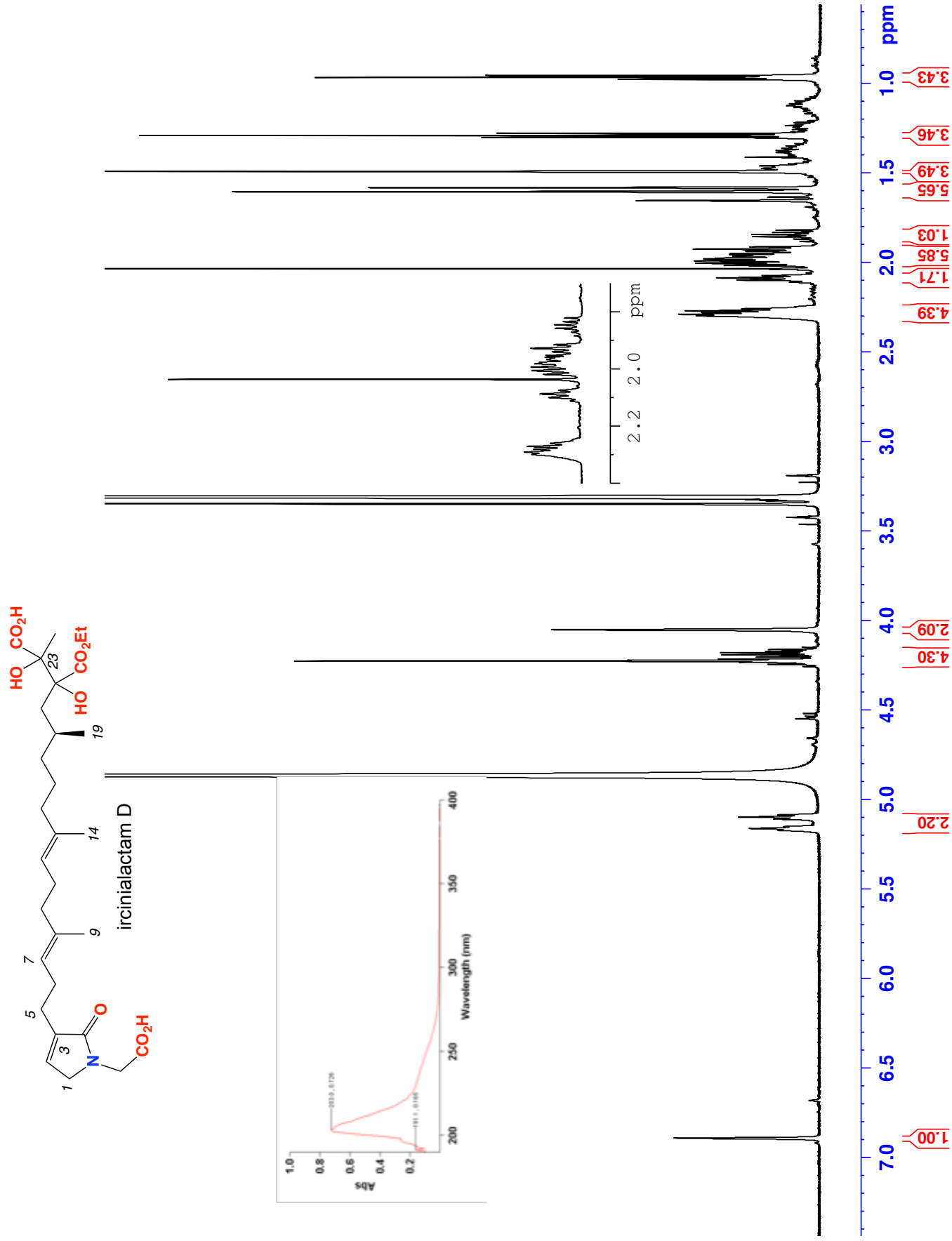

Figure 3S13. ^{1}H NMR (600 MHz, CD_3OD) data for ircinialactam D (**9**)

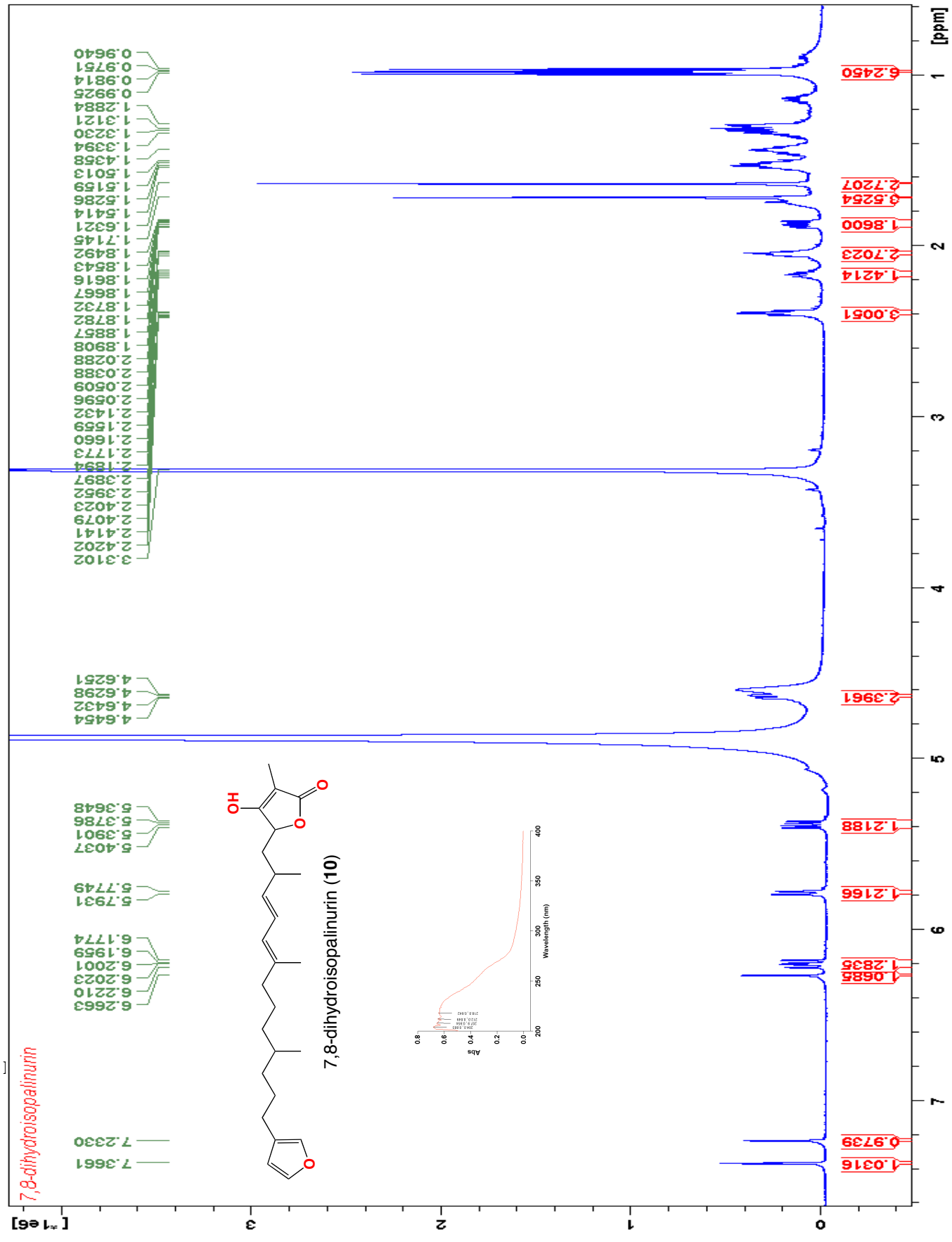

Figure 3S14. ^{1}H NMR (600 MHz, CD_3OD) data for 7,8-dihyroisopalinurin (**10**)

CHAPTER 4

IRCINIANINS

4.1. Declaration

This chapter describes a series of rare cyclic sesterterpene tetronic acids ircinianins discovered from three priority Australian *Psammocinia* spp. Our collaborative study identified two rare cyclic sesterterpene tetronic acids and new co-metabolites from three Australian sponges of the genus *Psammocinia*, two of which potently modulated GlyRα1 and GlyRα3. A paper describing the discovery of this new structure class of GlyR modulators was recently published in **Organic and Biomolecular Chemistry**[133]. This was the second paper published so far from research collaboration on **GlyR modulators from Australian Marine Resource** between the Capon Group of the Institute for Molecular Bioscience (IMB) and the Lynch Group of the Queensland Brain Institute (QBI) of The University of Queensland Australia.

The two-research groups contributed equally to the publication of the ircinianins paper. As in the first paper I was responsible for chemical investigation (isolation, purification and structure elucidation) of all metabolites discovered from three Australian *Psammocinia* spp (CMB-01008, CMB-02858 and CMB-03344). During my lab work at the IMB, I received technical assistance (lab work and data analysis) from Dr. Hua Zhang, Dr. Andrew M. Piggott and Dr. Xiao Xue and was supervised by Professor Robert J. Capon as the head of chemistry lab. Similarly, other co-authors have contributed to the work. Dr. Robiul Islam performed bioassays (Yellow fluorescence Protein and Patch Clamp assays) at the QBI The University of Queensland. He received technical assistance from Dr. Daniel F. Gilbert, Dr. Frank Fontaine and Dr. Timothy I. Webb and was under the supervision of Professor Joseph W. Lynch as the head of pharmacology lab. The contributions of all co-authors to the publication of ircinialactams paper were listed in the table given below.

Balansa, W.; Islam, R.; Fontaine, F.; Piggott, A. M.; Zhang, H.; Xue, X.; Timothy, I. Webb.; Gilbert, D.F.; Lynch, J. W.; Capon, R. J. Sesterterpene glycinyl-lactams: a new class of glycine receptor modulator from Australian marine sponges of the genus Psammocinia. *Org. Biomol. Chem.* **2013**, 11, 4695-4072.

Contributor	Statement of contribution
Balansa, Walter	Responsible for chemistry (100% working)
Islam, Robiul	Responsible for bioassay (100% working)
Fontaine, Frank	Assisted with lab work and data analysis
Zhang, Hua	Assisted with lab work and data analysis
Piggott, Andrew M.	Assisted with lab work and data analysis
Xiao Xua	Assisted with lab work and data analysis
Webb, Timothy.	Assisted with lab work and data analysis
Gilbert, Daniel	Assisted with lab work and data analysis
Lynch, Joseph W.	Head of pharmacology lab.
Capon, Robert J.	Head of chemistry lab.

4.2. Introduction

4.2.1. Structure and Diversity

Sponges of the genus *Ircinia* are known to produce a range of furanosesterterpene tetronic acids[101,107,114,115,134]. These include linear furanosesterterpene tetronic acids such as variabilin and its unusual cyclic counterparts including the tetracyclic (+)-ircinianin[135] and pentacyclic (+)-wistarin[133,134,136,137]. While structural variations are well known in linear furanosesterterpene tetronic acids (described in detail in Chapter 3), little is known about such molecular features in cyclic sesterterpene tetronic acids. So far, only four members of this structure class are known in the literature including (–)-ircinianin (**4.1**)[135], (–)-ircinianin sulfate (**4.2**)[134], (+)-wistarin (**4.3**)[137] and (–)-wistarin (**4.4**)[138], all of which, except (–)-wistarin (**4.4**), were reported from Australian *Ircinia* spp. indicative of the rarity of the ircinianin structure class[133,134].

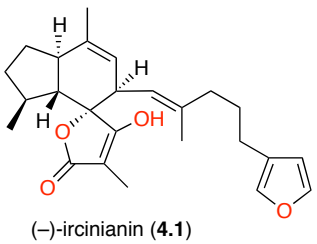

(–)-ircinianin (**4.1**)

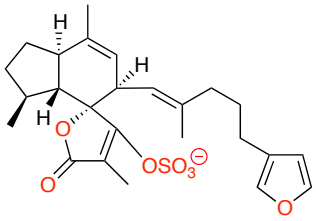

(–)-ircinianin sulfate (**4.2**)

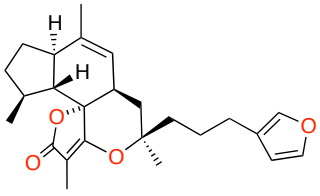

(+)-wistarin (**4.3**)

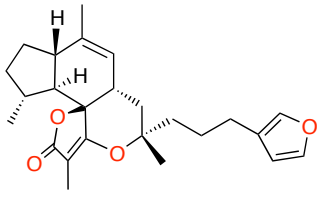

(–)-wistarin (**4.4**)

Structurally, members of ircinianin structure class can be classified into two groups. The first group features a tetracyclic structure with a bicyclo[4.3.0]nonane ring attached to a tetronic acid or sulfate ester through a spiro junction ring and connected to a furan moiety through an isoprene unit such as in (–)-ircinianin (**4.1**) or ircinianin sulfate (**4.2**). The second group displays a pentacylic structure with a tetrahydropyran attached to hexahydroindan ring and γ-lactone and connected to furan such as in (+)-wistarin (**4.3**) and (–)-wistarin (**4.4**).

(–)-Ircinianin (**4.1**) was first reported by Hofheinz and Schonholzer in 1977 from an Australian *Ircinia wistarii* collected from Wistarii Reef with structure determined by X-ray analysis[135]. Subsequently, the tetracylic furanosesterterpene was re-isolated from *I. wistarii* from several locations around Australia including Heron Island, Swain Reef on the Great Barrier Reef, Lamont Reef the Great Barrier Reef and the Great Australian Bight[134]. The pentacylic (+)–wistarin (**4.3**)[137] was first reported by Gregson and Ouvrier from a Gladstone Queensland *I. wistarii* in 1982 co-existing with (–)-ircinianin sulfate (**4.2**) as a major unstable metabolite in $CDCl_3$. In addition to discovering **4.2**, Coll *et al* also reported the occurrence of wistarin and ircinianin from an Australian *Ircinia*/*Psammocinia* sp. in 1997[134]. Two years later, Fontana *et al* discovered (–)-wistarin (**4.4**) from a Red Sea *Ircinia* sp, representing the first case of enantiomeric sesterterpene[138].

The recurrent co-occurrence of wistarin and ircinianin in Australian *I. wistarii* has raised contradictive speculations regarding the formation of wistarin and biosynthetic relationship between linear and cyclic furanosesterterpene tetronic acids. In the original report, Gregson and Ouvrier proposed that (–)-ircinianin underwent *in vivo* cyclisation to form (+)-wistarin based on a molecular model[137]. Even though in that report the treatment of (–)-ircinianin with acid, Lewis acid or bases did not result in cyclisation of (–)-ircinianin to (+)-wistarin[137], Coll *et al* successfully recovered 18% (+)-wistarin from treating (–)-ircinianin sulfate with $CDCl_3$ leading to a claim that cyclisation of (+)-wistarin was pH catalized[134], a claim further supported by Uenishi *et al* through a base catalysed reaction[136]. Following this approach, both the racemate (–)-wistarin have been synthesized in the manner that suggests they are biosynthetically derived from putative linear precursor via Diels Alder cycloaddition[136]. It was assumed that ircinianin was biogenetically derived by the action of a Diels Alderase acting on an acyclic precursor 8,11,13,20-tetraene (**4.5**) (Scheme 4.1)[138]. Supportive of this proposal was the thermal transformation of ircinianin from its acyclic precursor 8,11,13,20-tetraene (**4.5**) shown by Uenishi and co-workers[136].

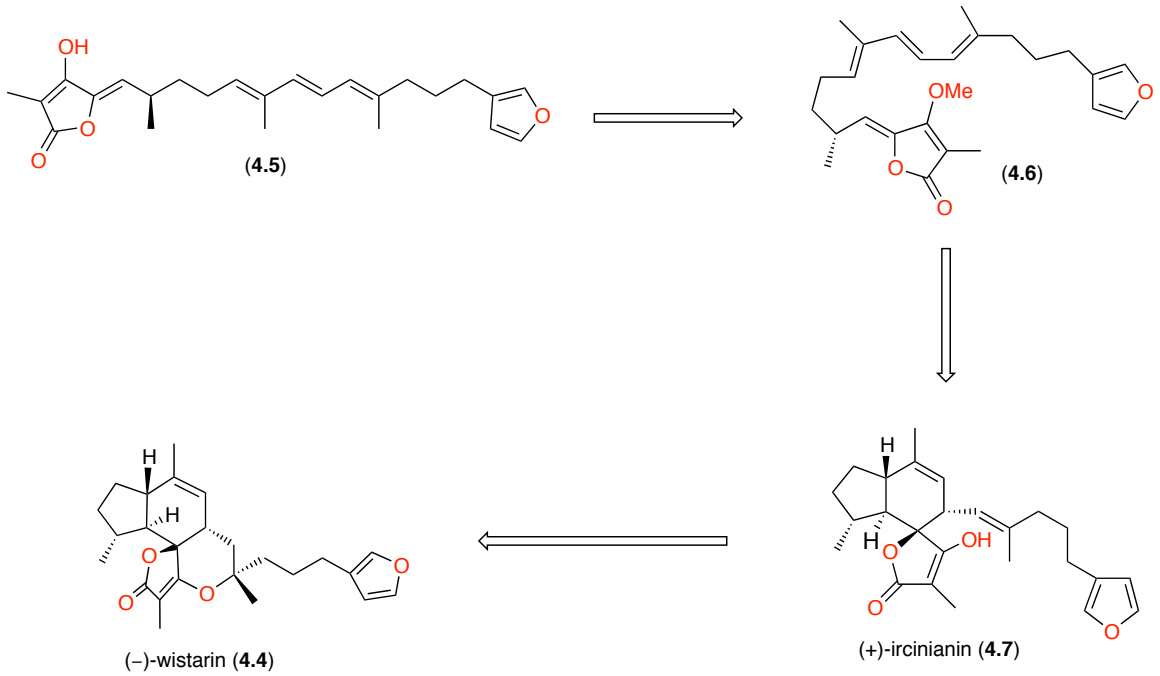

Scheme 4.1. Plausible biosynthetic relationship between linear and cyclic furanosesterterpene tetronic acids adopted from Cimino *et al*[138].

4.2.2. Synthesis and Bioactivity

Although the ircinianin structure class has been known for more than three decades, and members are synthetically accessible, little is known of their biological activity. In 1997, Uenishi *et al* successfully synthesized (+)–wistarin and (-)–ircinianin in a 17-step total synthesis providing the access to biological studies and allowing the assignment of the absolute stereochemistry of ircinianin type compounds[136]. This stereochemical assignment revised previously proposed stereochemistry for (+)-wistarin[136,138] but confirmed the relative stereochemistry for (–)-ircinianin assigned earlier by an X-ray analysis[135,136]. Of interest, both results consistently showed (–)-ircinianin as having negative molecular rotation values $[\alpha]_D$ = –232 obtained from X-ray[134] and $[\alpha]_D$ = –235 from synthetic analysis[135,136]. Also, in the same report Uenishi *et al* obtained three isomeric ircinianin methyl eters (**4.7**-**4.9**). Two of these isomers had positive optical rotation values $[\alpha]_D$ = +124 and $[\alpha]_D$ = +45 and were assigned as (+)-ircinianin methyl ether (**4.8**) and (**4.9**) while the remaining isomer (**4.7**) with $[\alpha]_D$ = -167 was assigned as (–)-ircinianin methyl eter (**4.7**). This assignment was consistent with the assignment of absolute stereochemistry for (–)-ircinianin (**3.1**) by X-ray ($[\alpha]_D$ = –232)[135] and synthetic ($[\alpha]_D$ = –235) methods[136]. Surprisingly, 16 years after the synthetic triumph, no biological activity has been described for ircinianin structure class, standing in stark

contrast to the linear counterpart variabilins whose members have been intensively studied over the years (discussed in detail in Chapter 3).

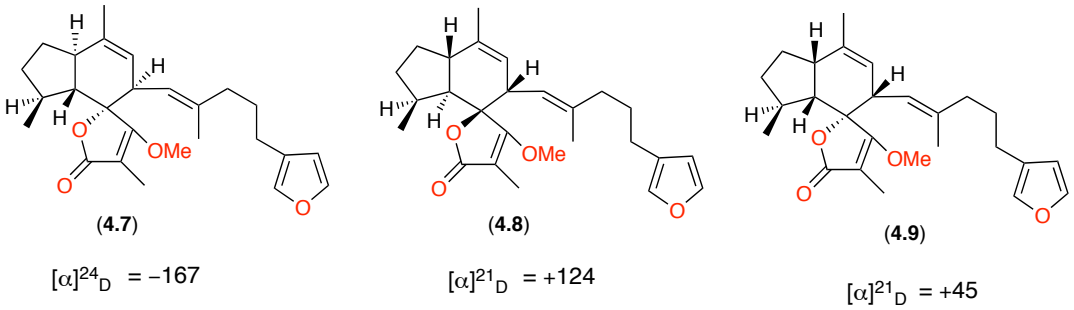

Figure 4.1. Three Ircinianin methyl eter isomers with different molecular rotation values synthesized by Uenishi *et al* 1999[136].

Chemical profiling on the extracts of two Australian *Psammocinia* spp. (CMB-01008, CMB-02858 and CMB-03344) revealed molecular weights consistent with the known ircinianin and ircinianin sulfate as well as a series of new compounds (Table 2.2). Mass spectrometry analysis and online study (Marinlit) and ^{1}H NMR comparison to authentic sample for ircinianin (CMB-library) confirmed the presence of both known and new cyclic sesterterpene tetronic acids. Importantly, in YFP assay, minor metabolites of two extracts (CMB-02858 and CMB-03344) strongly modulated either GlyRα1 or GlyRα3. These observations encouraged further study of the metabolites of three Australian sponges of the genus *Psammocinia* leading to the discovery of six new cyclic sesterterpenes including (−)-ircinianin lactam A (**4.11**), (−)-ircinianinlactam A sulfate (**4.12**), (−)-oxoircinianin (**4.13**), (−)-oxoircinianin lactam A (**4.14**), ircinianin lactone (**4.15**), one semisynthetic derivative ircinianin acetate (**4.16**), and two known molecules, ircinianin (**4.1**) and ircinianin sulfate (**4.2**). Of these **4.11** and **4.14** potently and specifically modulated GlyRα1 and GlyRα3 respectively whose details are described in the following paper.

*Note that the numbering system in this introduction and conclusion of this thesis is different from the ones in the paper and supporting information.

Organic & Biomolecular Chemistry

RSC Publishing

PAPER

View Article Online
View Journal | View Issue

Cite this: Org. Biomol. Chem., 2013, 11, 4695

Sesterterpene glycinyl-lactams: a new class of glycine receptor modulator from Australian marine sponges of the genus *Psammocinia*†

Walter Balansa,[a] Robiul Islam,[b] Frank Fontaine,[a] Andrew M. Piggott,[a] Hua Zhang,[a] Xue Xiao,[a] Timothy I. Webb,[b] Daniel F. Gilbert,[b,c] Joseph W. Lynch*[b,d] and Robert J. Capon*[a]

Received 26th April 2013,
Accepted 23rd May 2013

DOI: 10.1039/c3ob40861b

www.rsc.org/obc

Bioassay guided fractionation of three southern Australian marine sponges of the genus *Psammocinia*, selected for their ability to modulate glycine-gated chloride channel receptors (GlyRs), yielded the rare marine sesterterpenes (–)-ircinianin (**1**) and (–)-ircinianin sulfate (**2**), along with the new biosynthetically related metabolites (–)-ircinianin lactam A (**3**), (–)-ircinianin lactam A sulfate (**4**), (–)-oxoircinianin (**5**), (–)-oxoircinianin lactam A (**6**) and (–)-ircinianin lactone A (**7**). Acetylation of **1** returned (–)-ircinianin acetate (**8**). Whole cell patch-clamp electrophysiology on **1–8** established **3** as an exceptionally potent and selective α3 GlyR potentiator, and **6** as a selective α1 GlyR potentiator. The discovery and characterization of sesterterpenes **1–8**, and in particular the glycinyl-lactams **3** and **6**, provide valuable new insights into GlyR pharmacology. These insights have the potential to inform and inspire the development of new molecular tools to probe GlyR distribution and function, and therapeutics to treat a wide array of GlyR mediated diseases and disorders.

Introduction

As members of the Cys-loop ion channel receptor family, glycine-gated chloride channel receptors (GlyRs) play a pivotal role in orchestrating inhibitory neurotransmission in the spinal cord, brainstem and retina.[1] The α1–α4 and β-GlyR subunits exhibit differential central nervous system distributions that are particularly evident in the superficial dorsal horn of the spinal cord[2] and the retina.[3] Notwithstanding the biological importance of GlyRs, the physiological consequences of differential distribution are difficult to establish as there are currently few pharmacological probes that can selectively inhibit GlyR isoforms.[4] As a consequence, small-molecule isoform-selective GlyR modulators would have great value both as pharmacological tools, and as drug lead candidates for inflammatory pain,[2,5] opioid-induced breathing disorders,[6] epilepsy[7] and movement disorders.[8]

In an attempt to address this need, we screened a library of >2500 southern Australian and Antarctic marine invertebrates and algae to detect extracts and metabolites displaying GlyR-modulating properties. In a preliminary report, we described the ircinialactams from three southern Australian sponges of the Family Ircinidae, as exemplars of a rare and promising new class of GlyR modulator.[9] More recently we reported on the GlyR modulating properties of indolo-alkaloids from a southern Australian sponge, *Ianthella cf. flabelliformis*.[10] This current report extends earlier findings, describing our analysis of three southern Australian sponges of the genus *Psammocinia*, leading to the discovery of the ircinianin glycinyl-lactams (**3** and **6**) as the most promising new class of tunable isoform-selective GlyR potentiators we have discovered to date.

(–)-Ircinianin (**1**) was first isolated in 1977 from a Great Barrier Reef marine sponge *Ircinia wistarii*, and its structure (with relative configuration) assigned by X-ray analysis.[11] A 1982 re-isolation of **1** from another Australian *I. wistarii* specimen reported the isomeric "co-metabolite" (+)-wistarin,[12] while a subsequent 1997 re-isolation of **1** from a Great Barrier Reef *Ircinia* (*Psammocinia*) *wistarii* described the new co-metabolite (–)-ircinianin sulfate (**2**).[13] This latter study also

[a]Institute for Molecular Bioscience, The University of Queensland, St. Lucia, QLD 4072, Australia. E-mail: r.capon@uq.edu.au; Fax: +61-7-3346-2090; Tel: +61-7-3346-2979
[b]Queensland Brain Institute, The University of Queensland, St. Lucia, QLD 4072, Australia. E-mail: j.lynch@uq.edu.au; Fax: +61-7-3346-6301; Tel: +61-7-3346-6375
[c]Institute of Medical Biotechnology, Department of Chemical and Biological Engineering, Friedrich-Alexander University Nuremberg-Erlangen, Germany
[d]School of Biomedical Sciences, The University of Queensland, St. Lucia, QLD 4072, Australia

†Electronic supplementary information (ESI) available: ^{1}H NMR spectra and tabulated 2D NMR data for all compounds, sponge taxonomy, chemical profiling, fractionation schemes and electrophysiology results. See DOI: 10.1039/c3ob40861b

View Article Online

Paper Organic & Biomolecular Chemistry

confirmed that (+)-wistarin was an acid-catalyzed handling artifact of **2**. In 1997, the structure and absolute configuration of **1** was confirmed by total synthesis,[14] while a 1999 account of (−)-wistarin from a Red Sea *Ircinia* sp. raised the prospect that ircinianins may exist in nature in both enantiomeric forms.[15] Although the ircinianin sesterterpene scaffold has been known for >35 years, structure diversity and access remains remarkably limited. Significantly, in the absence of a practical natural or synthetic source, this enigmatic class of marine sponge metabolite has eluded any biological evaluation – existing merely as molecular curios in the virtual chemical space that is the scientific literature. Our investigations reveal for the first time that new natural product analogues of the ircinianin scaffold exhibit very significant and valuable GlyR pharmacology.

Results and discussion

Bioassay-guided fractionation of three southern Australian *Psammocinia* spp. yielded the known sesterterpenes (−)-ircinianin (**1**) and (−)-ircinianin sulfate (**2**), with structure assignments confirmed by detailed spectroscopic analysis and comparisons to literature data (Tables 1 and 2 and ESI Tables S1 and S2†). Further fractionation of *Psammocinia* sp. (CMB-03344), collected in 2001 off Port Phillip Heads, Victoria, yielded (−)-ircinianin lactam A (**3**) and (−)-oxoircinianin (**5**). *Psammocinia* sp. (CMB-01008), collected in 1986 off Durras on the mid-south coast of New South Wales, yielded (−)-ircinianin sulfate lactam A (**4**), while *Psammocinia* sp. (CMB-02858), collected in 1999 off Barwon Heads, Victoria, yielded (−)-oxoircinianin lactam A (**6**) and trace amounts of (−)-ircinianin lactone A (**7**). Structures for the new ircinianin analogues **3–7** (Fig. 1) were assigned by detailed spectroscopic analysis.

HRESI(+)MS analysis of **3** established a molecular formula ($C_{27}H_{35}NO_6$) which, based on our earlier characterization of ircinialactams[9] and ianthellalactams,[10] was consistent with a glycinyl-lactam analogue of **1**. Comparison of the NMR (methanol-d_4) data for **1** with **3** (Tables 1 and 2 and ESI Tables S1 and S3†) attributed the only significant difference to replacement of the furanyl in **1** with a glycinyl-lactam moiety in **3**. A deshielded ^{1}H NMR chemical shift for H-2 (δ_H 6.89),[9] supported by diagnostic 2D NMR correlations, permitted identification of (−)-ircinianin lactam A (**3**) as shown.

Table 1 ^{13}C NMR data (150 MHz, methanol-d_4) for **1–7**

	δ_C						
Pos.	**1**	**2**	**3**	**4**	**5**	**6**	**7**
1	144.0	143.8	53.0	54.4	144.0	53.1	72.2
2	112.1	112.3	138.0	137.8	112.1	139.0	148.0
3	126.5	126.8	139.0	139.3	126.6	140.1	134.6
4	140.3	140.2	173.2	173.4	140.4	174.5	177.2
5	25.3	25.7	25.8	26.6	25.0	26.3	25.8
6	29.5	29.2	26.9	26.8	29.3	26.9[B]	26.9
7	40.5	40.7	40.4	40.5	40.3	40.4	40.4
8	136.5	137.1	135.1	137.1	137.9	137.8	136.1
9	16.3	16.5	16.2	16.4	16.5	16.5	16.2
10	125.1	124.3	125.5	124.2	121.6	124.1	125.5
11	48.7	49.0	48.6	49.3	48.2	48.2	48.6
12	123.6	124.1	123.5	123.8	123.9	121.6	123.5
13	137.1	137.2	137.2	137.1	137.2	137.2	137.2
14	20.8	20.5	20.74[A]	20.4	21.3	21.3	20.74[C]
15	46.2	46.5	46.2	46.4	45.7	45.6	46.2
16	27.3	27.3	27.3	27.0	26.9	26.8[B]	27.3
17	33.6	33.8	33.6	33.6	34.1	34.1	33.6
18	33.2	33.4	33.2	33.0	33.0	33.0	33.2
19	20.7	21.0	20.66[A]	21.0	20.8	20.8	20.66[C]
20	52.0	52.3	51.9	52.0	52.0	52.0	51.9
21	86.9	87.5	[ND]	87.5	[ND]	92.9	86.9
22	179.5[A]	177.7	179.5	177.7	208.1	208.1	179.5[D]
23	97.2	102.6	97.4	102.7	70.2	70.2	97.4
24	177.7[A]	171.1	[ND]	171.0	175.8	175.7	177.7[D]
25	6.1	9.4	6.1	9.7	19.8	19.8	6.1
1′			47.1	46.8		44.5	
2′			[ND]	173.0		172.5	

[ND] Not detected; [A–D] assignments interchangeable.

HRESI(−)MS analysis of **4** established a molecular formula ($C_{27}H_{34}NO_9S$) consistent with a sulfate analogue of **3**. Comparison of the NMR (methanol-d_4) data for **3** with **4** (Tables 1 and 2 and ESI Tables S3 and S4†) revealed the only significant differences being a deshielding/shielding of ^{13}C NMR resonances for C-22 ($\Delta\delta_C$ −1.8), C-23 ($\Delta\delta_C$ +5.3) and C-25 ($\Delta\delta_C$ +3.6), comparable with differences observed between the tetronic acid **1** and its sulfate **2** [C-22 ($\Delta\delta_C$ −1.8), C-24 ($\Delta\delta_C$ −6.6) and C-25 ($\Delta\delta_C$ +3.3)]. A deshielded ^{1}H NMR chemical shift for H-2 (δ_H 6.92),[9] supported by diagnostic 2D NMR correlations, permitted identification of (−)-ircinianin sulfate lactam A (**4**) as shown.

Table 2 Selected ^{1}H NMR data (600 MHz, methanol-d_4) for **1–7**

	δ_H (mult, J (Hz))						
Pos.	**1**	**2**	**3**	**4**	**5**	**6**	**7**
1	7.38 (dd, 1.7, 1.7)	7.35 (dd, 1.6, 1.6)	4.07 (br s)	4.05 (s)	7.38 (dd, 1.6, 1.6)	4.07 (td, 1.7, 1.7)	4.83 (td, 1.8, 1.6)
2	6.30 (m)	6.32 (br s)	6.89 (br s)	6.92 (s)	6.32 (m)	6.96 (tt, 1.7, 1.7)	7.37 (tt, 1.6, 1.6)
4	7.26 (m)	7.26 (br s)			7.29 (m)		
5	2.41 (br t, 7.6)	2.37 (m)	2.26 (m)	2.23 (m)	2.42 (br t, 7.4)	2.26 (br t, 7.7)	2.26 (m)
6	1.68 (m)	1.73 (m)	1.71 (m)	1.80 (m)	1.67 (m)	1.67 (m)	1.71 (m)
9	1.57 (d, 1.3)	1.57 (br s)	1.58 (d, 1.4)	1.59 (s)	1.57 (d, 1.3)	1.58 (d, 1.3)	1.58 (d, 1.4)
14	1.71 (dd, 2.8, 1.4)	1.71 (br s)	1.71 (dd, 2.9, 1.4)	1.71 (s)	1.73 (dd, 2.7, 1.4)	1.73 (dd, 2.8, 1.4)	1.71 (dd, 2.9, 1.4)
19	0.92 (d, 6.3)	1.00 (d, 6.4)	0.92 (d, 6.3)	1.01 (d, 6.6)	0.84 (d, 6.3)	0.83 (d, 6.2)	0.92 (d, 6.3)
25	1.64 (s)	2.00 (s)	1.64 (s)	2.01 (s)	1.39 (s)	1.38 (s)	1.64 (s)
1′			4.07 (br s)	4.03 (s)		4.23 (s)	

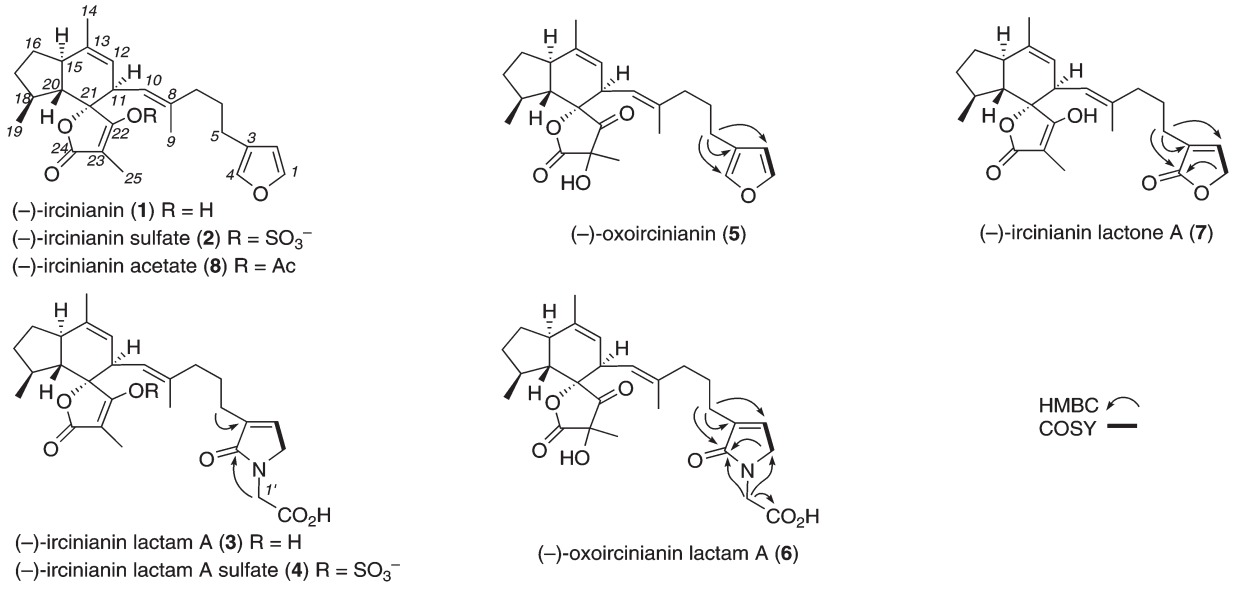

Fig. 1 Structures for **1–8** with selected 2D NMR correlations.

HRESI(+)MS analysis of **5** established a molecular formula ($C_{25}H_{32}O_5$) consistent with an oxidized analogue of **1**. Comparison of the NMR (methanol-d_4) data for **1** with **5** (Tables 1 and 2 and ESI Tables S1 and S5†) revealed the only significant differences as being centered on the tetronic acid moiety, with C-22 (δ_C 208.1) being indicative of a ketone carbonyl, and C-23 (δ_C 70.2) and C-25 (δ_H 1.39; δ_C 19.8) a tertiary alcohol moiety. Collectively these observations supported identification of (–)-oxoircinianin (**5**) as the oxidized analogue of **1**, as shown – incorporating an unprecedented C-21 to C-25 oxidized tetronic acid motif.

HRESI(+)MS analysis of **6** established a molecular formula ($C_{27}H_{35}NO_7$) consistent with a glycinyl-lactam analogue of **5**. Comparison of the NMR (methanol-d_4) data for **5** with **6** (Tables 1 and 2 and ESI Tables S5 and S6†) supported this hypothesis, with differences being comparable to those observed between **1** and **3** (discussed above). A deshielded ^{1}H NMR chemical shift for H-2 (δ_H 6.96),[9] supported by diagnostic 2D NMR correlations, permitted identification of (–)-oxoircinianin lactam A (**6**) as shown.

HRESI(+)MS analysis of **7** established a molecular formula ($C_{27}H_{32}O_5$) isomeric with **5**, consistent with an oxidized analogue of **1**. Comparison of the NMR (methanol-d_4) data for **1** with **7** (Tables 1 and 2 and ESI Tables S1 and S7†) attributed the only significant difference to replacement of the furanyl in **1** with a 2-alkyl-γ-butenolide (lactone) moiety in **5**. A deshielded ^{1}H NMR chemical shift for H-2 (δ_H 7.37),[9] supported by diagnostic 2D NMR correlations, permitted identification of (–)-ircinianin lactone A (**3**) as shown.

The fact that the new sesterterpenes **3–7** were co-metabolites with the known metabolites **1** and **2** (whose relative and absolute configurations had been fully assigned by a combination of X-ray analysis,[11] total synthesis[14] and chemical interconversion[13]), permitted assignment of a common absolute configuration. An exception to this assignment is the configuration about C-23 in **5** and **6**, which remains unassigned. In proposing a plausible biosynthetic relationship between **1–7**, we suggest that (–)-ircinianin (**1**) is the progenitor of this structure class, undergoing sulfation and oxidation of the tetronic acid to deliver **2** and **5**, and oxidation of the furan to yield **7**. Conjugation of the lactone **7** with glycine would yield the glycinyl-lactam **3**, which in turn undergoes sulfation and oxidation to deliver **4** and **6** (Fig. 2). Although we could only isolate subsets of **1–7** from each of the three *Psammocinia* specimens, careful analysis of the HPLC-DAD-MS data sets using a single

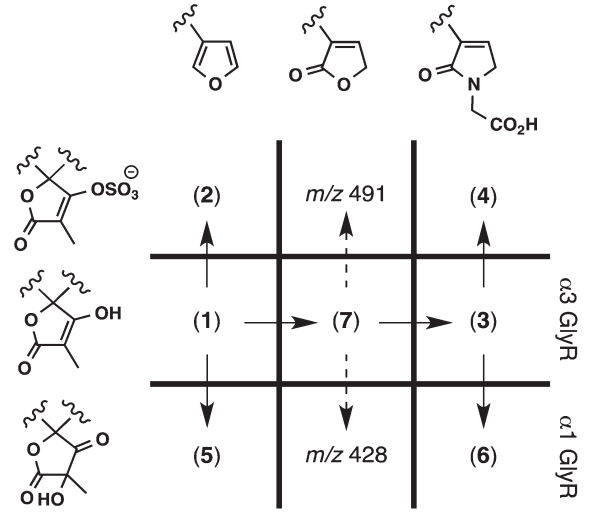

Fig. 2 Plausible biosynthetic relationship between **1–7**.

ion extraction approach succeeded in detecting **1–7** in all three extracts (see ESI†). Consistent with this biosynthetic proposal, HPLC-DAD-MS (single ion extraction) analysis of all three sponge extracts also successfully detected trace metabolites consistent with putative intermediates (−)-ircinianin lactone A sulfate (*m/z* 491) and (−)-oxoircinianin lactone A (*m/z* 428). To assist in GlyR structure activity relationship (SAR) investigations, a sample of **1** was acetylated to yield (−)-ircinianin acetate (**8**), which was subjected to detailed spectroscopic analysis (ESI Table S8†).

The sesterterpenes **1–8** were screened against human α1 and α3 GlyRs stably expressed in HEK293 cells *via* automated planar chip whole cell patch-clamp recording. The effects of compounds were quantified at −40 mV by inducing an inward current flux by applying an EC_{20} glycine concentration (α1 GlyR EC_{20} = 15 μM; α3 GlyR EC_{20} = 100 μM). GlyRs were first activated with a 2 s pulse of glycine, and then with a 2 s pulse of the same concentration of glycine plus a defined concentration of **1** to **8**, with a 1 min pause between successive applications. Full electrophysiology results are documented in the ESI (Fig. S9 and S10 and Table S9†), and are summarized in Fig. 3. Analysis of the α1 GlyR data confirmed the glycinyl-lactam **6** as a selective potentiator of α1 GlyRs (110 ± 8% at 100 μM), while **2** was a modest antagonist (IC_{50} 38.4 ± 2.8 μM, Hill slope n_H 0.76 ± 0.6), **1** and **4** were modest potentiators (80 ± 10% and 70 ± 7%, at 100 μM), and **3**, **5**, **7** and **8** exerted no significant effect (Fig. 3). Analysis of the α3 GlyR data confirmed the glycinyl-lactam **3** as an exceptionally potent and selective α3 GlyR potentiator (260 ± 15% at 100 μM, EC_{50} 8.5 ± 2.1 μM, n_H 1.3 ± 0.3), while **2** was an antagonist (IC_{50} 3.2 ± 1.3 μM, Hill slope n_H 0.48 ± 0.12), and **1**, **4**, **5**, **7** and **8** exerted no significant effect (Fig. 3). An SAR analysis of all these data established that the glycinyl-lactam moiety is optimal for a potentiating effect, with the level of tetronic acid oxidation dictating α1 *versus* α3 GlyR selectivity.

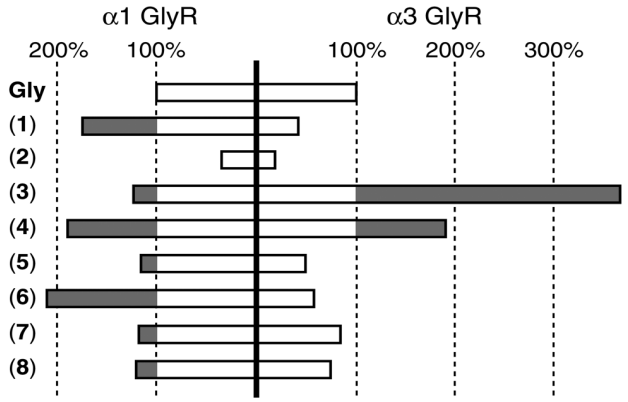

Fig. 3 Maximal effects of **1–8** at α1 and α3 GlyRs as determined by whole-cell electrophysiological recording. Compounds were tested on currents activated by an EC_{20} glycine concentration and the effect of each drug is shown as a percentage of this current magnitude. The degree of potentiation is highlighted by grey shading.

Experimental

General experimental details

Optical rotations were measured on a JASCO P-1010 polarimeter with a 10 cm length cell. UV spectra were obtained on a Cary 50 UV-visible spectrophotometer with 1 cm pathway cell. NMR experiments were performed on a Bruker Avance DRX600 spectrometer and referenced to residual non-deuterated signals in the deuterated solvents. ESI-MS analyses were carried out on an Agilent 1100 series LC/MSD instrument. HR-ESI-MS data were acquired on a Bruker micrOTOF mass spectrometer by direct infusion in MeCN at 3 μL min^{-1} flow using sodium formate clusters as an internal calibrant. All HPLC analyses and separations were performed on Agilent 1100 series LC instruments with corresponding detectors, collectors and software inclusive. All chemicals were purchased from Merck, Sigma-Aldrich or Fluka. Solvents used for general purposes were of at least analytical grade, and solvents used for HPLC were of HPLC grade.

Marine extracts library

A library of >2500 marine invertebrate and alga samples, collected from intertidal, coastal and deep sea locations across southern Australia and Antarctica, were processed to generate an extract library suitably formatted for medium to high throughput bioassay. A portion (7 mL) of the archived EtOH extract of each marine sample was decanted, concentrated *in vacuo*, weighed and partitioned into *n*-BuOH (2 mL) and H_2O (2 mL). This pre-processing achieves a >10 fold concentration of "drug-like" small molecules, while simultaneously desalting and simplifying the solubility characteristics of, the *n*-BuOH solubles. Aliquots (1 mL) of both *n*-BuOH and H_2O phases were transferred to deep 96-well plates, to generate a set of extract library plates. These plates were subsequently used to prepare 10- and 100-fold dilution plates.

Extraction and fractionation

***Psammocinia* sp. (CMB-01008).** A portion (~500 mL) of the EtOH extract of *Psammocinia* sp. (CMB-01008) was decanted and concentrated *in vacuo* to return a black solid (2.31 g), which was subsequently partitioned between *n*-BuOH (3 × 50 mL) and H_2O (50 mL). GlyR bioassays established that all activity was concentrated in the *n*-BuOH solubles (730.3 mg), which were sequentially triturated with aliquots (2 × 15 mL) of hexanes, CH_2Cl_2 and MeOH, and concentrated *in vacuo* to return 5.6, 590.7 and 109.3 mg respectively. A portion (298.0 mg) of the CH_2Cl_2 solubles was subjected to HPLC fractionation (Zorbax SB-C_{18} 250 × 9.4 mm, 5 μm column, 4 mL min^{-1} gradient elution from 10–100% MeCN–H_2O over 25 min, with isocratic 0.01% TFA modifier) to yield (−)-ircinianin (**1**) (t_R = 14.8 min; 46.6 mg, 12.0%), (−)-ircinianin sulfate (**2**) (t_R = 10.8 min; 99.2 mg, 13.6%) and a third fraction (t_R = 8.2 min; 9.8 mg), which was subjected to further HPLC fractionation (Zorbax SB-C_{18} 150 × 4.6 mm, 5 μm column, 1 mL min^{-1} gradient elution from 10–100% MeCN–H_2O over 25 min, with isocratic 0.01% TFA modifier) to yield (−)-ircinianin lactam A sulfate (**4**) (t_R = 8.4 min; 1.1 mg, 0.14%).

***Psammocinia* sp. (CMB-03344).** A portion (~250 mL) of the EtOH extract from *Psammocinia* sp. (CMB-03344) was decanted and concentrated *in vacuo* to return brown solid (1.74 g), which was subsequently partitioned between *n*-BuOH (3 × 50 mL) and H_2O (50 mL), with GlyR bioassays confirming that all activity was concentrated in the *n*-BuOH solubles (246 mg). The *n*-BuOH soluble material was sequentially triturated with aliquots (2 × 15 mL) of hexanes, CH_2Cl_2 and MeOH, and concentrated *in vacuo* to yield 0.6, 155.0 and 54.6 mg fractions respectively. Following spectroscopic and chemical analysis the combined CH_2Cl_2 and MeOH solubles were fractionated by HPLC (Zorbax SB-C_{18} 250 × 9.4 mm, 5 μm column, 4 mL min^{-1} gradient elution from 10–100% MeCN–H_2O over 25 min, with isocratic 0.01% TFA modifier) to yield (−)-ircinianin (**1**) (t_R = 15.5 min; 28.7 mg, 11.6%), (−)-ircinianin sulfate (**2**) (t_R = 11.8 min; 17.3 mg, 7.03%), (−)-oxoircinianin (**5**) (t_R = 16.2 min; 1.2 mg, 0.48%) and a fourth fraction (t_R = 9.5 min; 1.5 mg), which was further purified by HPLC (Zorbax SB-C_{18} 150 × 4.6 mm, 5 μm column, 1 mL min^{-1} gradient elution from 10–100% MeCN–H_2O over 25 min, with isocratic 0.01% TFA modifier) to yield (−)-ircinianin lactam A (**3**) (t_R = 9.5 min; 0.3 mg, 0.12%).

***Psammocinia* sp. (CMB-02858).** A portion (~250 mL) of the EtOH extract from *Psammocinia* sp. (CMB-02858) was decanted and concentrated *in vacuo* to return a brown solid (315.0 mg), which was subsequently partitioned between *n*-BuOH (3 × 15 mL) and H_2O (20 mL), with GlyR bioassays confirming that all activity was concentrated in the *n*-BuOH solubles (103.4 mg). The *n*-BuOH soluble material was sequentially triturated with aliquots (2 × 15 mL) of hexanes, CH_2Cl_2 and MeOH, and concentrated *in vacuo* to yield 3.0, 75.9 and 20.9 mg fractions respectively. The CH_2Cl_2 and MeOH fractions were combined and fractionated by HPLC (Zorbax SB-C_{18} 250 × 9.4 mm, 5 μm column, 4 mL min^{-1} gradient elution from 10–100% MeCN–H_2O over 25 min, with isocratic 0.01% TFA modifier) to yield two subfractions (t_R = 9.5 min; 18.5 mg and t_R = 12.5 min; 2.5 mg). The first subfraction was subjected to HPLC (Zorbax SB-C_{18} 250 × 9.4 mm, 5 μm column, 4 mL min^{-1} gradient elution from 10–100% MeCN–H_2O over 25 min, with isocratic 0.01% TFA modifier) to yield (−)-oxoircinianin lactam A (**6**) (t_R = 10.2 min; 1.7 mg, 1.6%). The second subfraction was subjected to HPLC (Zorbax SB-C_{18} 150 × 4.6 mm, 5 μm column, 1 mL min^{-1} gradient elution from 10–100% MeCN–H_2O over 25 min, with isocratic 0.01% TFA modifier) to yield a third subfraction (t_R = 12.8 min; 0.4 mg), which was further purified by HPLC (Zorbax SB-C_{18} 150 × 4.6 mm, 5 μm column, 1 mL min^{-1} gradient elution from 50–100% MeCN–H_2O over 15 min, with isocratic 0.01% TFA modifier) to yield (−)-ircinianin lactone A (**7**) (t_R = 13.0; 0.2 mg, 0.19%).

Characterization of natural products

(−)-Ircinianin (1).[11] White solid; $[\alpha]_D$ −206 (*c* = 0.5, MeOH); UV-vis (MeOH) λ_{max} (log ε) 208 nm (4.54); NMR (600 MHz, methanol-d_4) see Tables 1 and 2 and ESI Table S1 and Fig. S1;† HRESI(+)MS *m*/*z* 419.2185 (calcd for $C_{25}H_{32}O_4Na^+$ 419.2193).

(−)-Ircinianin sulfate (2).[13] Pale yellow solid; $[\alpha]_D$ −108 (*c* = 0.5, MeOH); UV-vis (MeOH) λ_{max} (log ε) nm 203 (4.28), 210 (4.22), 217 (4.12), 226 (3.96); NMR (600 MHz, methanol-d_4) see Tables 1 and 2 and ESI Table S2 and Fig. S2;† HRESI(−)MS *m*/*z* 475.1799 (calcd for $C_{25}H_{31}O_7S^-$ 475.1796).

(−)-Ircinianin lactam A (3). Colorless oil; $[\alpha]_D$ −17 (*c* = 0.1, MeOH); UV-vis (MeOH) λ_{max} (log ε) 205 nm (4.38) nm; NMR (600 MHz, methanol-d_4) see Tables 1 and 2 and ESI Table S3 and Fig. S3;† HRESI(+)MS *m*/*z* 492.2357 (calcd for $C_{27}H_{35}NO_6Na^+$ 492.2357).

(−)-Ircinianin lactam A sulfate (4). Colorless oil; $[\alpha]_D$ −33 (*c* = 0.1, MeOH); UV-vis (MeOH) λ_{max} (log ε) 208 nm (4.06) nm; NMR (600 MHz, methanol-d_4) see Tables 1 and 2 and ESI Table S4 and Fig. S4;† HRESI(−)MS *m*/*z* 548.1970 (calcd for $C_{27}H_{34}NO_9S^-$ 548.1973).

(−)-Oxoircinianin (5). Pale yellow oil; $[\alpha]_D$ −62 (*c* = 0.07, MeOH); UV-vis (MeOH) λ_{max} (log ε) 205.0 (4.55), 261 nm (3.09); NMR (600 MHz, methanol-d_4) see Tables 1 and 2 and ESI Table S5 and Fig. S5;† HRESI(+)MS *m*/*z* 435.2144 (calcd for $C_{25}H_{32}O_5Na^+$ 435.2142).

(−)-Oxoircinianin lactam A (6). Pale yellow oil; $[\alpha]_D$ −17 (*c* = 0.1, MeOH); UV-vis (MeOH) λ_{max} (log ε) 205 nm (4.38), 196 nm (3.74); NMR (600 MHz, methanol-d_4) see Tables 1 and 2 and ESI Table S6 and Fig. S6;† HRESI(+)MS *m*/*z* 508.2306 (calcd for $C_{27}H_{35}NO_7Na^+$ 508.2306).

(−)-Ircinianin lactone A (7). Pale yellow oil; $[\alpha]_D$ −74 (*c* = 0.1, MeOH); UV-vis (MeOH) λ_{max} (log ε) 204 nm (4.30); NMR (600 MHz, methanol-d_4) see Tables 1 and 2 and ESI Table S7 and Fig. S7;† HRESI(+)MS *m*/*z* 435.2142 (calcd for $C_{25}H_{32}O_5Na^+$ 435.2142).

Synthetic transformations

(−)-Ircinianin acetate (8). A solution of (−)-ircinianin (**1**) (2.0 mg) and acetic anhydride (0.2 mL) in pyridine (0.5 mL) was stirred at room temperature overnight, after which it was concentrated *in vacuo* and the residue subjected to HPLC fractionation (Zorbax C_{18} 5 μm, 150 × 4.6 mm column, 25 min gradient elution at 1 mL min^{-1} from 90% H_2O–MeOH to 100% MeOH with isocratic 0.01% TFA–MeOH modifier) to yield (−)-ircinianin acetate (**8**) (0.9 mg, 45%) as a colorless oil; $[\alpha]_D$ −87 (*c* = 0.1, MeOH); UV-vis (MeOH) λ_{max} (log ε) 208 nm (4.32); NMR (600 MHz, methanol-d_4) see ESI Table S8 and Fig. S8;† HRESI(+)MS *m*/*z* 461.2294 (calcd for $C_{27}H_{34}O_5Na^+$ 461.2298).

Primary GlyR screening of marine extracts

The initial screen of >2500 marine extracts against recombinantly expressed α1 and α3 GlyRs was performed using a yellow fluorescent protein-based anion flux assay as previously described.[9,16] In this bioassay, 90 μL of each 100-fold diluted *n*-BuOH partition was transferred into one well of a 384-well plate, and was dried under nitrogen. The plates containing dried *n*-BuOH partitions were protected from light and stored at −30 °C until required. On the day of the experiment an aliquot (30 μL) of extracellular solution [NaCl (140 mM), KCl (5 mM), $CaCl_2$ (2 mM), $MgCl_2$ (1 mM), HEPES (10 mM), and glucose (10 mM) (pH 7.4 using NaOH)] was added to each well and mixed/

dissolved using a multi-channel pipette. Subsequently, an aliquot (10 μL) of this solution was transferred into the corresponding well of a 384-well plate containing approx. 5000 cells and 15 μL of extracellular solution per well, and incubated at room temperature for 30 min. The 384-well plates were then placed onto the motorized stage of an in-house imaging system[16] and cells were imaged twice: once in 25 μL of extracellular solution containing the *n*-BuOH partition and once 10 s after the injection of 50 μL NaI solution supplemented with 500 μM glycine. The NaI solution was similar in composition to NaCl control solution except the NaCl was replaced by equimolar NaI.

Images of fluorescent cells were segmented and quantitatively analyzed using a modified version of DetecTIFF software.[17] In brief, images were segmented using an iterative size and intensity-based thresholding algorithm and the fluorescence signal of identified cells was calculated as the mean of all pixel values within the area of a cell. GlyR activation response was used as a measure of extract potency and was defined as $(F_{init} - F_{final}) \times 100/F_{init}$, where F_{init} and F_{final} were the initial and final values of fluorescence, respectively. All experiments were performed twice in neighboring wells. Hits were selected by visual inspection of color maps generated by analysis software. For hit confirmation, 24 μL of the corresponding 10-fold diluted *n*-BuOH partition was transferred into a well of a 384-well plate, and was dried and stored as described above. On the day of the experiment the dried 10-fold diluted *n*-BuOH partitions were resuspended in 80 μL extracellular solution as described above and two aliquots each of 17 and 10 μL respectively were then transferred in neighboring wells containing ~5000 cells and 15 μL extracellular solution per well. Imaging and image analysis were conducted as described above. The concentration dependence of the drug effects was used as measure for extract potency and level of prioritization.

Automated electrophysiology

Electrophysiological screening was performed using an automated planar patch-clamp device (Patchliner, Nanion Technologies GmbH, Munich, Germany). Stable α1 and α3 GlyR-expressing HEK293 cell lines, produced as previously described,[9,17] were maintained in minimal essential medium. After 2–3 days in culture, cells were trypsinized and suspended in extracellular solution [NaCl (140 mM), KCl (4 mM), $CaCl_2$ (2 mM), $MgCl_2$ (1 mM), HEPES–NaOH (10 mM) and glucose (5 mM) (pH 7.4 adjusted with NaOH)] at a density of 1×10^6 cells per mL before injecting into the Patchliner chip. This standard extracellular solution was employed in all Patchliner experiments. The internal solution contained KCl (50 mM), NaCl (10 mM), KF (60 mM), $MgCl_2$ (2 mM), EGTA (20 mM), HEPES–KOH (10 mM) (pH 7.2). All experiments were performed at room temperature (19–22 °C). 1 M glycine (Ajax Finechem, Seven Hills, NSW, Australia) stocks were prepared in water and stored at −20 °C. All test compounds were dissolved in DMSO (Sigma-Aldrich) and stored at −20 °C. From these stocks, solutions for experiments were prepared on the day of recording.

Data analysis

Results are expressed as mean ± standard error of the mean of three or more independent experiments. The Hill equation was used to calculate the half inhibitory concentration (IC_{50}) and Hill coefficient (n_H) values of individual concentration–response relationships. All curves were fitted using a nonlinear least squares algorithm (Sigmaplot 11.0; Jandel Scientific, San Rafael, CA, USA). Statistical significance was determined by unpaired Student's *t*-test, with $p < 0.05$ representing significance.

Conclusions

In summary, this study successfully demonstrated a high-throughput marine biodiscovery approach capable of discovering and evaluating potent new isoform selective small molecule GlyR potentiators. The discovery and characterization of **1–8**, and in particular the glycinyl-lactams **3** and **6**, provides valuable new insights into GlyR pharmacology. These insights have the potential to inform and inspire the development of new molecular tools to probe GlyR distribution and function, and new therapeutics to treat chronic inflammatory pain and a range of other neurological disorders.

Acknowledgements

We thank L. Goudie for taxonomic identification of marine sponges and acknowledge the generous support of an Australian Development Scholarship (W.B.) and a University of Queensland Scholarship (R.I.). This research was funded in part by the Institute for Molecular Bioscience, the Queensland Brain Institute, The University of Queensland, the National Health and Medical Research Council (project grant #613448) and the Australian Research Council (LP120100088).

Notes and references

1 J. W. Lynch, *Physiol. Rev.*, 2004, **84**, 1051.
2 R. J. Harvey, U. B. Depner, H. Wassle, S. Ahmadi, C. Heindl, H. Reinold, T. G. Smart, K. Harvey, B. Schutz, O. M. Abo-Salem, A. Zimmer, P. Poisbeau, H. Welzl, D. P. Wolfer, H. Betz, H. U. Zeilhofer and U. Muller, *Science*, 2004, **304**, 884.
3 (*a*) S. Haverkamp, U. Muller, K. Harvey, R. J. Harvey, H. Betz and H. Wassle, *J. Comp. Neurol.*, 2003, **465**, 524; (*b*) S. Haverkamp, U. Muller, H. U. Zeilhofer, R. J. Harvey and H. Wassle, *J. Comp. Neurol.*, 2004, **477**, 399; (*c*) L. Heinze, R. J. Harvey, S. Haverkamp and H. Wassle, *J. Comp. Neurol.*, 2007, **500**, 693; (*d*) F. Weltzien, C. Puller, G. A. O'Sullivan, I. Paarmann and H. Betz, *J. Comp. Neurol.*, 2012, **520**, 3962.
4 T. I. Webb and J. W. Lynch, *Curr. Pharm. Des.*, 2007, **13**, 2350.

5 W. Xiong, T. Cui, K. Cheng, F. Yang, S. R. Chen, D. Willenbring, Y. Guan, H. L. Pan, K. Ren, Y. Xu and L. Zhang, *J. Exp. Med.*, 2012, **209**, 1121.

6 T. Manzke, M. Niebert, U. R. Koch, A. Caley, S. Vogelgesang, S. Hulsmann, E. Ponimaskin, U. Muller, T. G. Smart, R. J. Harvey and D. W. Richter, *J. Clin. Invest.*, 2010, **120**, 4118.

7 S. A. Eichler, S. Kirischuk, R. Juttner, P. K. Schaefermeier, P. Legendre, T. N. Lehmann, T. Gloveli, R. Grantyn and J. C. Meier, *J. Cell Mol. Med.*, 2008, **12**, 2848.

8 S. K. Chung, J. F. Vanbellinghen, J. G. Mullins, A. Robinson, J. Hantke, C. L. Hammond, D. F. Gilbert, M. Freilinger, M. Ryan, M. C. Kruer, A. Masri, C. Gurses, C. Ferrie, K. Harvey, R. Shiang, J. Christodoulou, F. Andermann, E. Andermann, R. H. Thomas, R. J. Harvey, J. W. Lynch and M. I. Rees, *J. Neurosci.*, 2010, **30**, 9612.

9 W. Balansa, R. Islam, F. Fontaine, A. M. Piggott, H. Zhang, T. I. Webb, D. F. Gilbert, J. W. Lynch and R. J. Capon, *Bioorg. Med. Chem.*, 2010, **18**, 2912.

10 W. Balansa, R. Islam, D. F. Gilbert, F. Fontaine, X. Xiao, H. Zhang, A. M. Piggott, J. W. Lynch and R. J. Capon, *Bioorg. Med. Chem.*, 2013, DOI: 10.1016/j.bmc.2013.04.061, in press.

11 W. Hofheinz and P. Schönholzer, *Helv. Chim. Acta*, 1977, **60**, 1367.

12 R. P. Gregson and D. Ouvrier, *J. Nat. Prod.*, 1982, **45**, 412.

13 J. C. Coll, P. S. Kearns, J. A. Rideout and J. Hooper, *J. Nat. Prod.*, 1997, **60**, 1178.

14 J. Uenishi, R. Kawahama and O. Yonemitsu, *J. Org. Chem.*, 1997, **62**, 1691.

15 A. Fontana, I. Fakhr, E. Mollo and G. Cimino, *Tetrahedron: Asymmetry*, 1999, **10**, 3869.

16 W. Kruger, D. Gilbert, R. Hawthorne, D. H. Hryciw, S. Frings, P. Poronnik and J. W. Lynch, *Neurosci. Lett.*, 2005, **380**, 340.

17 D. F. Gilbert, T. Meinhof, R. Pepperkok and H. Runz, *J. Biomol. Screen.*, 2009, **14**, 944.

SUPPORTING INFORMATION

Sesterterpene Glycinyl-Lactams: A New Class of Glycine Receptor Modulator from Australian Marine Sponges of the Genus *Psammocinia*

Walter Balansa,[a] Robiul Islam,[b] Frank Fontaine,[a] Andrew M. Piggott,[a] Hua Zhang,[a] Xue Xiao,[a] Timothy I. Webb,[b] Daniel F. Gilbert,[b,c] Joseph W. Lynch[b,d]* and Robert J. Capon [a]*

[a] *Institute for Molecular Bioscience, The University of Queensland, St. Lucia, QLD, 4072, Australia.*
[b] *Queensland Brain Institute, The University of Queensland, St. Lucia, QLD, 4072, Australia.*
[c] *Institute of Medical Biotechnology, Department of Chemical and Biological Engineering, Friedrich-Alexander University Nuremberg-Erlangen, Germany.*
[d] *School of Biomedical Sciences, The University of Queensland, St. Lucia, QLD, 4072, Australia.*

TABLE OF CONTENT

NMR Spectra

Pharmacology

Collection and Taxonomy

CMB-01008 was collected in 1986 by R. J Capon (SCUBA) off Durras, New South Wales, Australia. A description of the specimen is as follows: Growth form massive-irregular; color in EtOH sandy; texture spongy but tough to tear; oscules scattered with membranous lip; surface translucent, wrinkled; spicules none; ectosome a distinct layer of detritus 300–400 μm thick; choanosome rectangular reticulation of spongin fibres 50–100 μm thick cored by tracts of sand grains, mesohyl a dense mass of collagen fibrils. The sponge was identified as *Psammocinia* sp. (Order Dictyoceratida, Family Ircinidae) and a type specimen registered with the Museum of Victoria (Registry No. MVF166222).

CMB-03344 was collected in 1990 by R. J Capon (SCUBA) off The Rip, Nepean Wall, Port Phillip Heads, Victoria, Australia (latitude 38° 18.13′, longitude 144° 38.12′). A description of the specimen is as follows: Growth form lamellate; color in EtOH sandy; texture hard, stony, arenaceous; oscules not seen; surface opaque, regular, sandy; spicules none; ectosome sand grains bound by spongin; choanosome a mass of sand grains bound by spongin with collagen fibrils evident between tracts. The sponge was identified as *Psammocinia* sp. (Order Dictyoceratida, Family Ircinidae) and a type specimen registered with the Museum of Victoria (Registry No. MVF166223).

CMB-02858 was collected in 1999 by R. J Capon (SCUBA) off 12 Pound Reef, Barwon Heads, Victoria, Australia (latitude 38° 17.0′, longitude 144° 38.37′). A description of the specimen is as follows: Growth form lamellate; color in EtOH sandy; texture firm, barely compressible, arenaceous; oscules scattered; surface opaque, sandy, evenly pitted on one surface, porous on the other; spicules none; ectosome distinct fine layer of sand and foreign spicule fragments; choanosome a reticulation of fibres evenly cored by sand and detritus, primary fibres indistinct from secondary fibres, spongin evident connecting adjacent fibres with the appearance of stretched plastic. Collagen fibrils were evident throughout. The sponge was identified as *Psammocinia* sp. (Order Dictyoceratida, Family Ircinidae) and a type specimen registered with the Museum of Victoria (Registry No. MVF166216).

Chemical Profiling

***Psammocinia* sp. (CMB-01008):** An HPLC-DAD (210 nm) analysis (Zorbax C_8 150 × 4.6 mm, 1.0 mL/min 20 min gradient elution from 10–100% MeCN/H_2O with isocratic 0.01% TFA/MeCN modifier) of the crude *n*-BuOH soluble revealed an extract rich in chemical diversity. Chemical fractionation yielded (–)-ircinianin (**1**), (–)-ircinianin sulfate (**2**) and (–)-ircinianin lactam A sulfate (**4**).

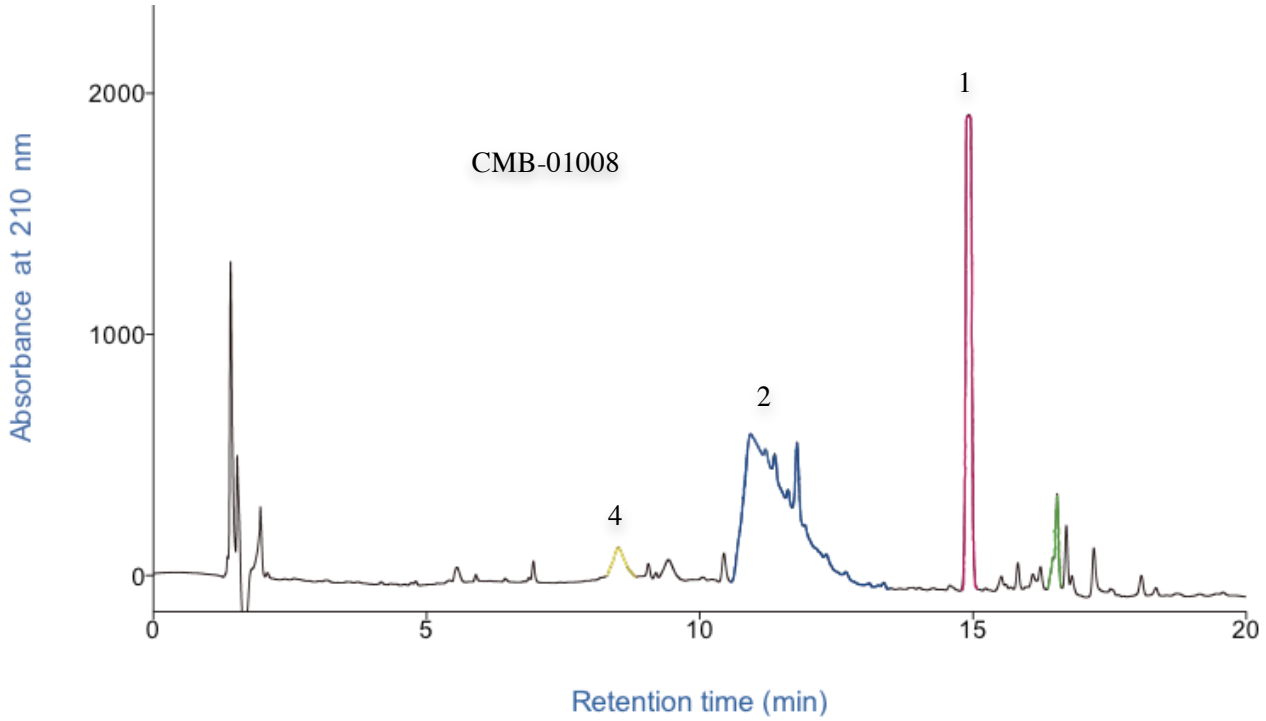

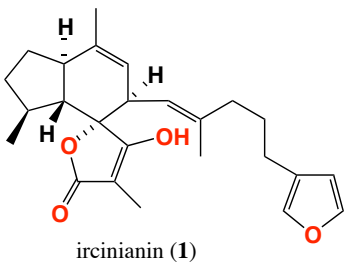

ircinianin (**1**)

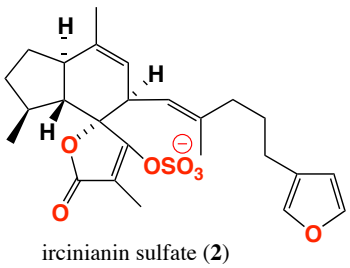

ircinianin sulfate (**2**)

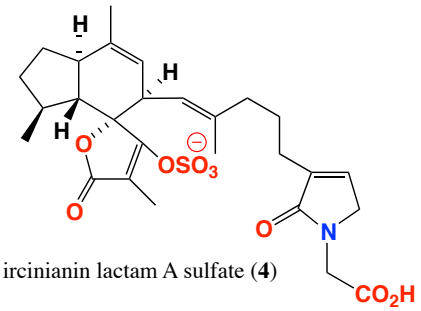

ircinianin lactam A sulfate (**4**)

***Psammocinia* sp. (CMB-03344)**: An HPLC-DAD (210 nm) analysis (Zorbax C_8 250 × 9.4 mm, 4.0 mL/min 20 min gradient elution from 90% H_2O/MeCN to 100% MeCN with isocratic 0.01% TFA/MeCN modifier) of the crude *n*-BuOH soluble revealed an extract rich in chemical diversity. Chemical fractionation yielded (–)-ircinianin (**1**), (–)-ircinianin sulfate (**2**), (–)-ircinianin lactam A (**3**) and (–)-oxoircinianin (**5**).

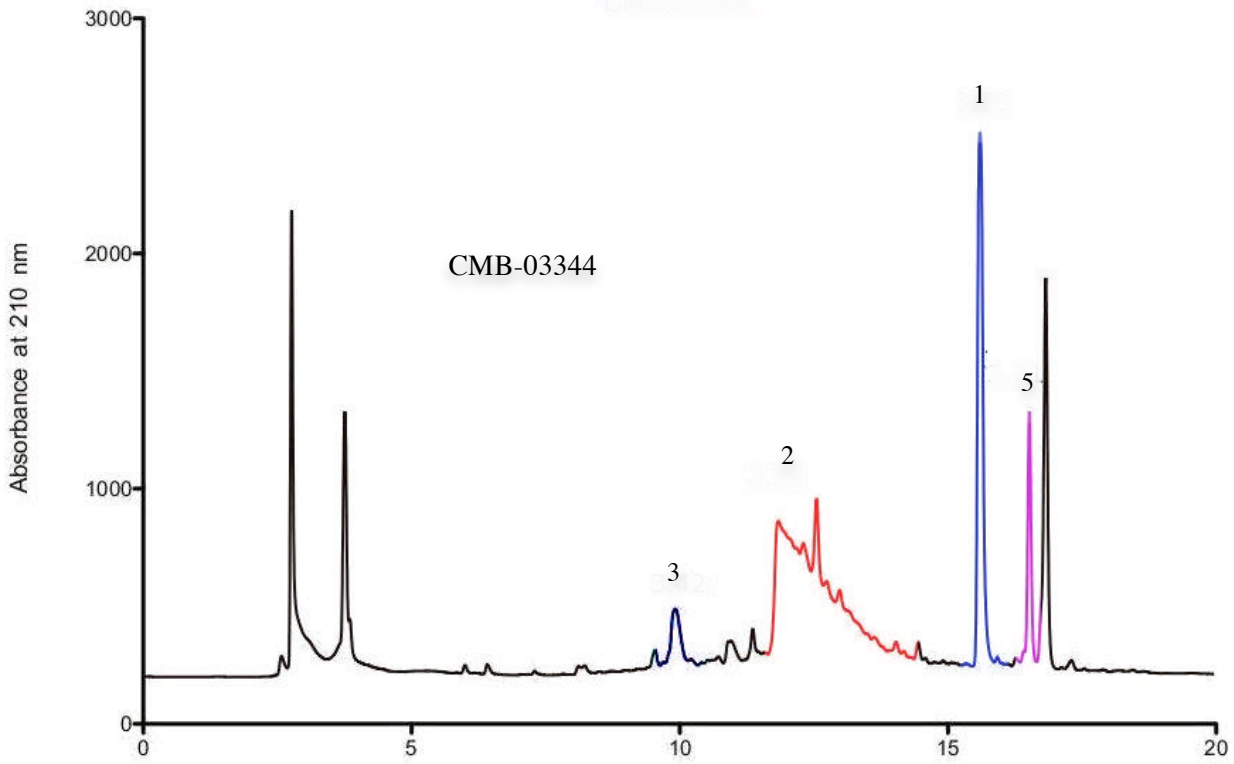

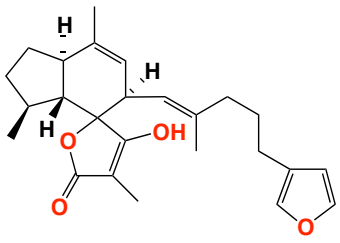

ircinianin (**1**)

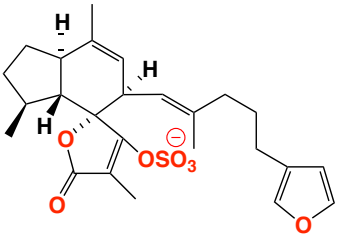

ircinianin sulfate (**2**)

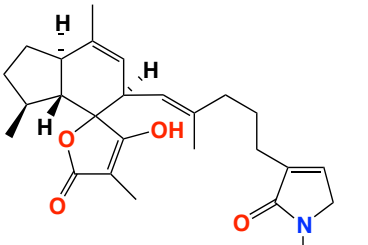

ircinianin lactam (**3**)

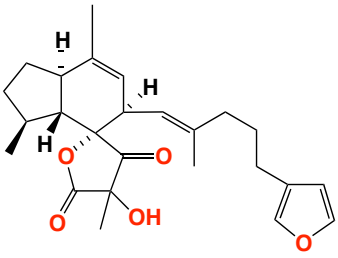

oxo-ircinianin (**5**)

***Psammocinia* sp. (CMB-02858):** An HPLC-DAD (210 nm) analysis (Zorbax C_8 250 × 9.4 mm, 4.0 mL/min 20 min gradient elution from 90% H_2O/MeCN to 100% MeCN with isocratic 0.01% TFA/MeCN modifier) of the crude *n*-BuOH soluble revealed an extract rich in chemical diversity. However, due to a limited material and instability of some metabolites in this specimen, chemical fractionation only yielded (–)-oxoircinianin lactam A (**6**) and (–)-ircinianin lactone A (**7**).

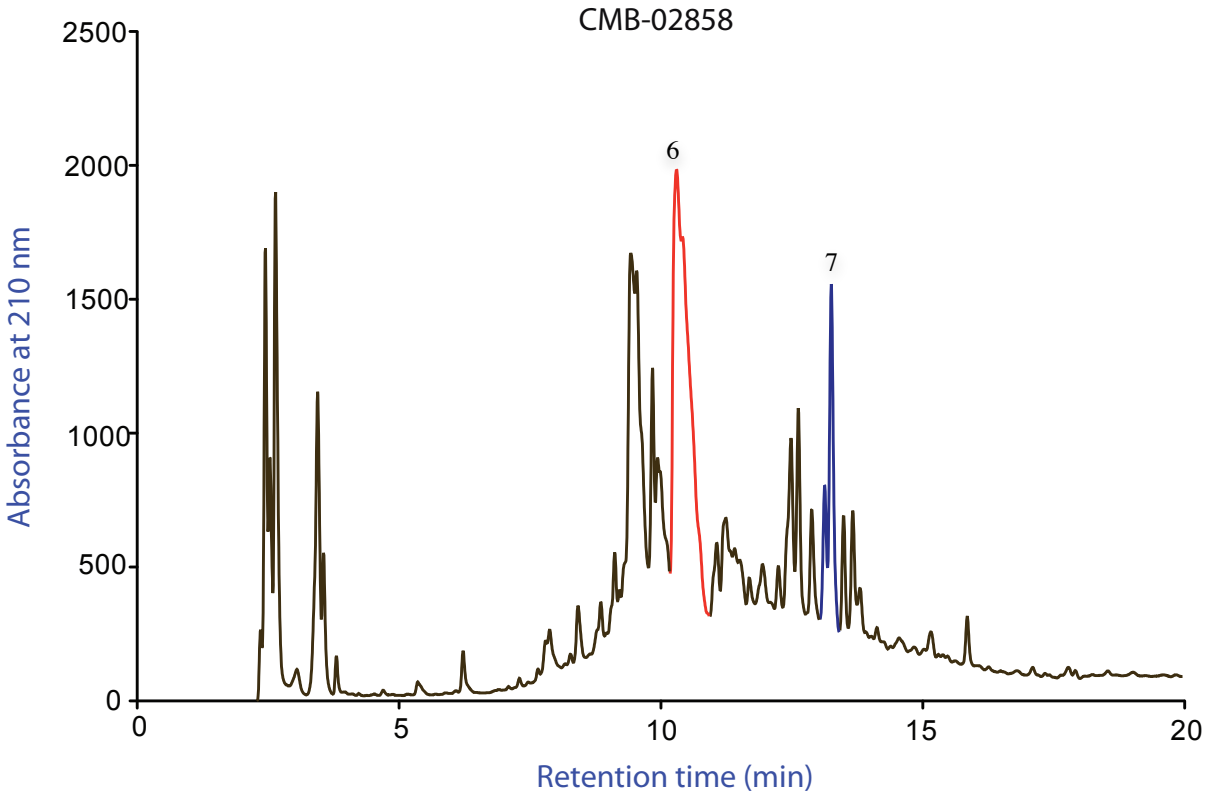

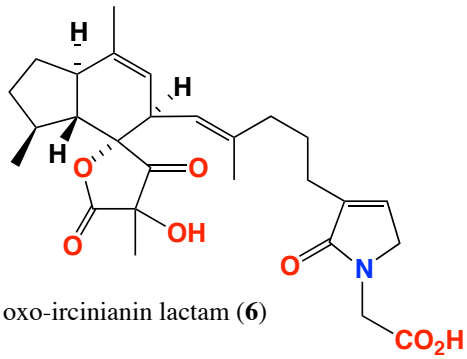

oxo-ircinianin lactam (**6**)

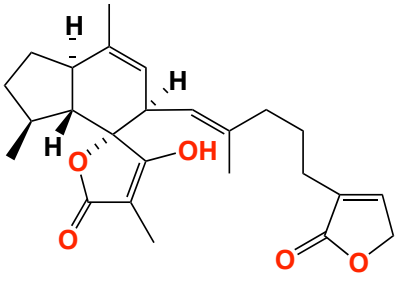

ircinianin lactone (**7**)

HPLC-MS (single ion extraction) Profiling

***Psammocinia* sp. (CMB-01008)** HPLC-DAD-MS (Agilent Zorbax SB-C_8, 5 μm, 150 × 4.6 mm, 15 min gradient elution at 1 mL/min, from 90% H_2O/MeCN to 100% MeCN with isocratic 0.05% formic acid/MeCN modifier] of a 10 μL injection of the *n*-butanol solubles (5 mg/mL in MeOH). (a) HPLC-DAD (254 nm); (b) ESI(+)MS single ion extraction at *m/z* 413, indicating (–)-oxoircinianin (**5**) and (–)-ircinianin lactone A (**7**); (c) ESI(+)MS single ion extraction at *m/z* 397, indicating (–)-ircinianin (**1**); (d) ESI(–)MS single ion extraction at *m/z* 475, indicating (–)-ircinianin sulfate (**2**); (e) ESI(+)MS single ion extraction at *m/z* 486, indicating (–)-oxoircinianin lactam (**6**); (f) ESI(+)MS single ion extraction at *m/z* 470, indicating (–)-ircinianin lactam A (**3**); (g) ESI(–)MS single ion extraction at *m/z* 548, indicating (–)-ircinianin lactam A sulfate (**4**).

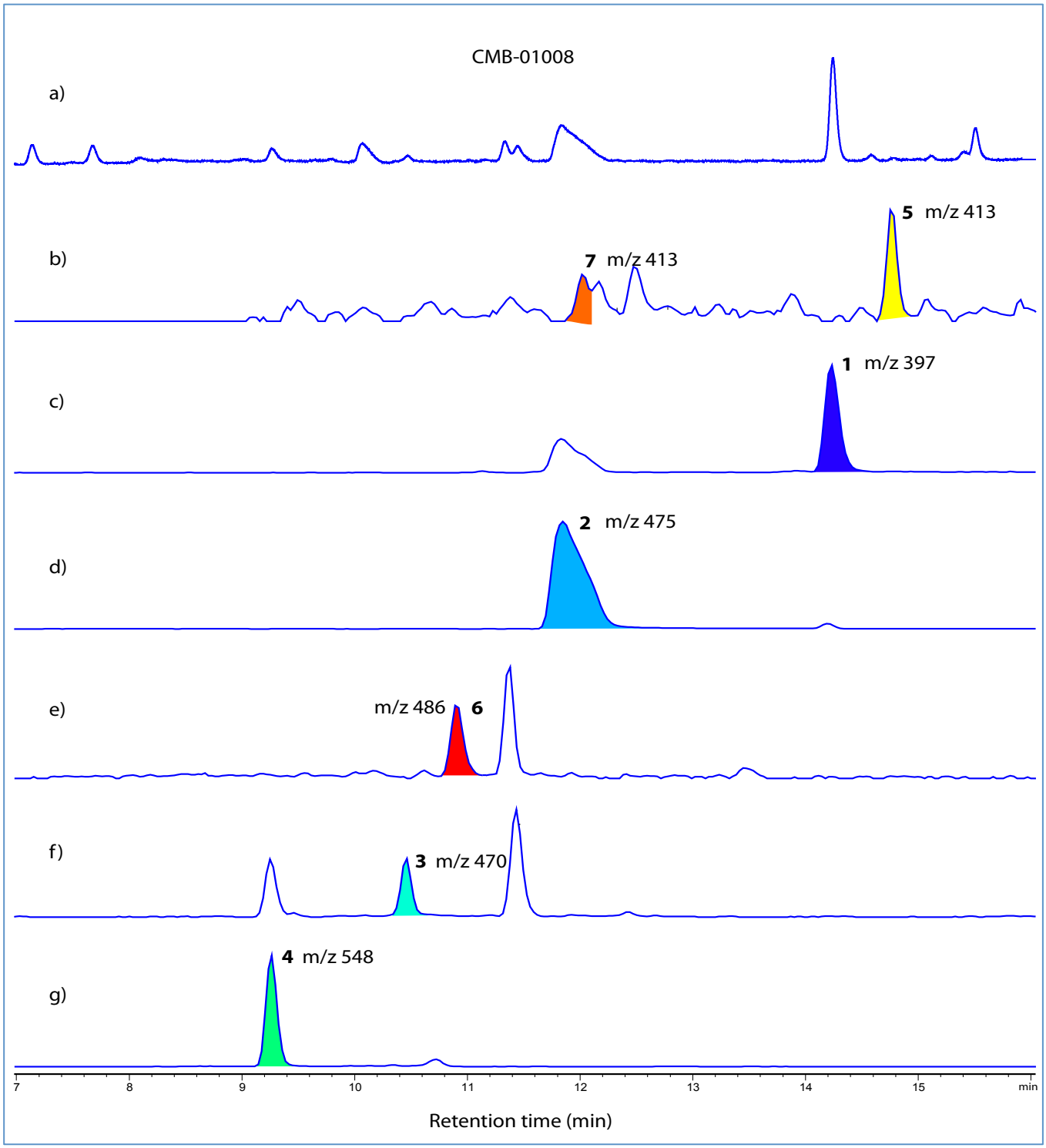

***Psammocinia* sp. (CMB-03344)** HPLC-DAD-MS (Agilent Zorbax SB-C_8, 5 μm, 150 × 4.6 mm, 15 min gradient elution at 1 mL/min, from 90% H_2O/MeCN to 100% MeCN with isocratic 0.05% formic acid/MeCN modifier] of a 10 μL injection of the *n*-butanol solubles (5 mg/mL in MeOH). (a) HPLC-DAD (254 nm); (b) ESI(+)MS single ion extraction at *m/z* 413, indicating (–)-oxoircinianin (**5**) and (–)-ircinianin lactone A (**7**); (c) ESI(+)MS single ion extraction at *m/z* 397, indicating (–)-ircinianin (**1**); (d) ESI(–)MS single ion extraction at *m/z* 475, indicating (–)-ircinianin sulfate (**2**); (e) ESI(+)MS single ion extraction at *m/z* 486, indicating (–)-oxoircinianin lactam (**6**); (f) ESI(+)MS single ion extraction at *m/z* 470, indicating (–)-ircinianin lactam A (**3**); (g) ESI(–)MS single ion extraction at *m/z* 548, indicating (–)-ircinianin lactam A sulfate (**4**).

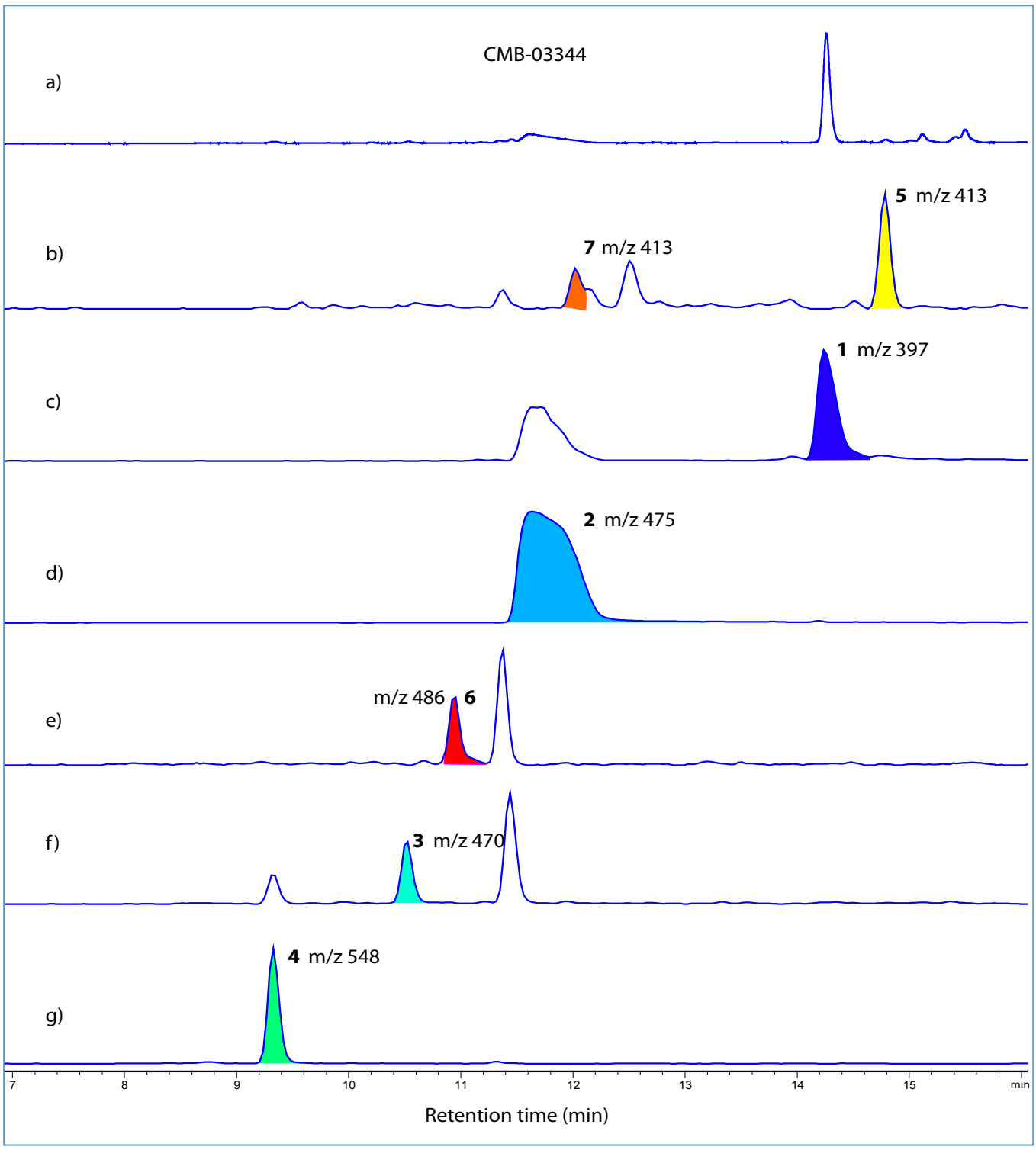

***Psammocinia* sp. (CMB-02858)** HPLC-DAD-MS (Agilent Zorbax SB-C_8, 5 μm, 150 × 4.6, 15 min gradient elution at 1 mL/min, from 90% H_2O/MeCN to 100% MeCN with isocratic 0.05% formic acid/MeCN modifier] of a 10 μL injection of the *n*-butanol solubles (5 mg/mL in MeOH). (a) HPLC-DAD (254 nm); (b) ESI(+)MS single ion extraction at *m/z* 413, indicating (–)-oxoircinianin (**5**) and (–)-ircinianin lactone A (**7**); (c) ESI(+)MS single ion extraction at *m/z* 397, indicating (–)-ircinianin (**1**); (d) ESI(–)MS single ion extraction at *m/z* 475, indicating (–)-ircinianin sulfate (**2**); (e) ESI(+)MS single ion extraction at *m/z* 486, indicating (–)-oxoircinianin lactam (**6**); (f) ESI(+)MS single ion extraction at *m/z* 470, indicating (–)-ircinianin lactam A (**3**); (g) ESI(–)MS single ion extraction at *m/z* 548, indicating (–)-ircinianin lactam A sulfate (**4**).

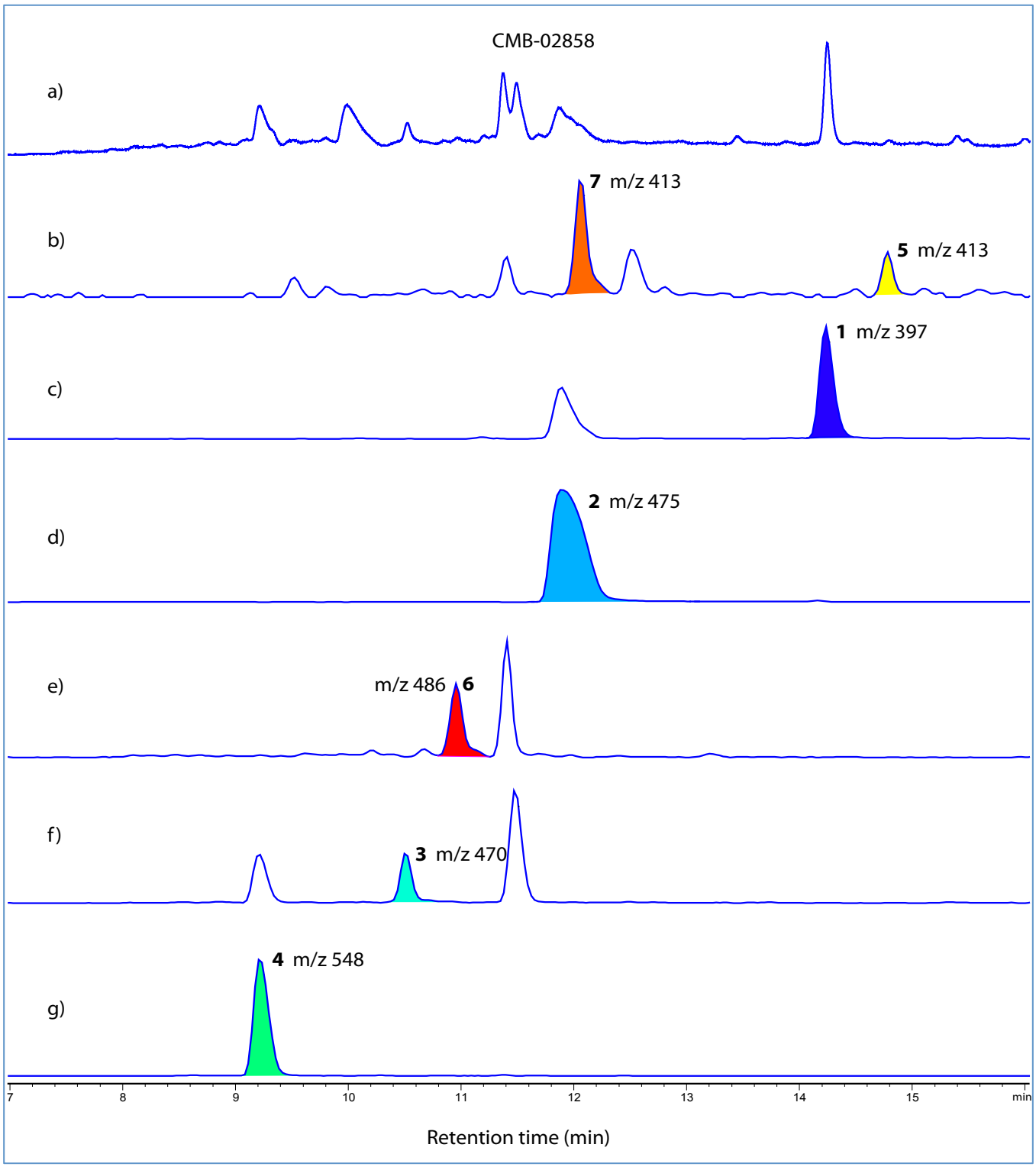

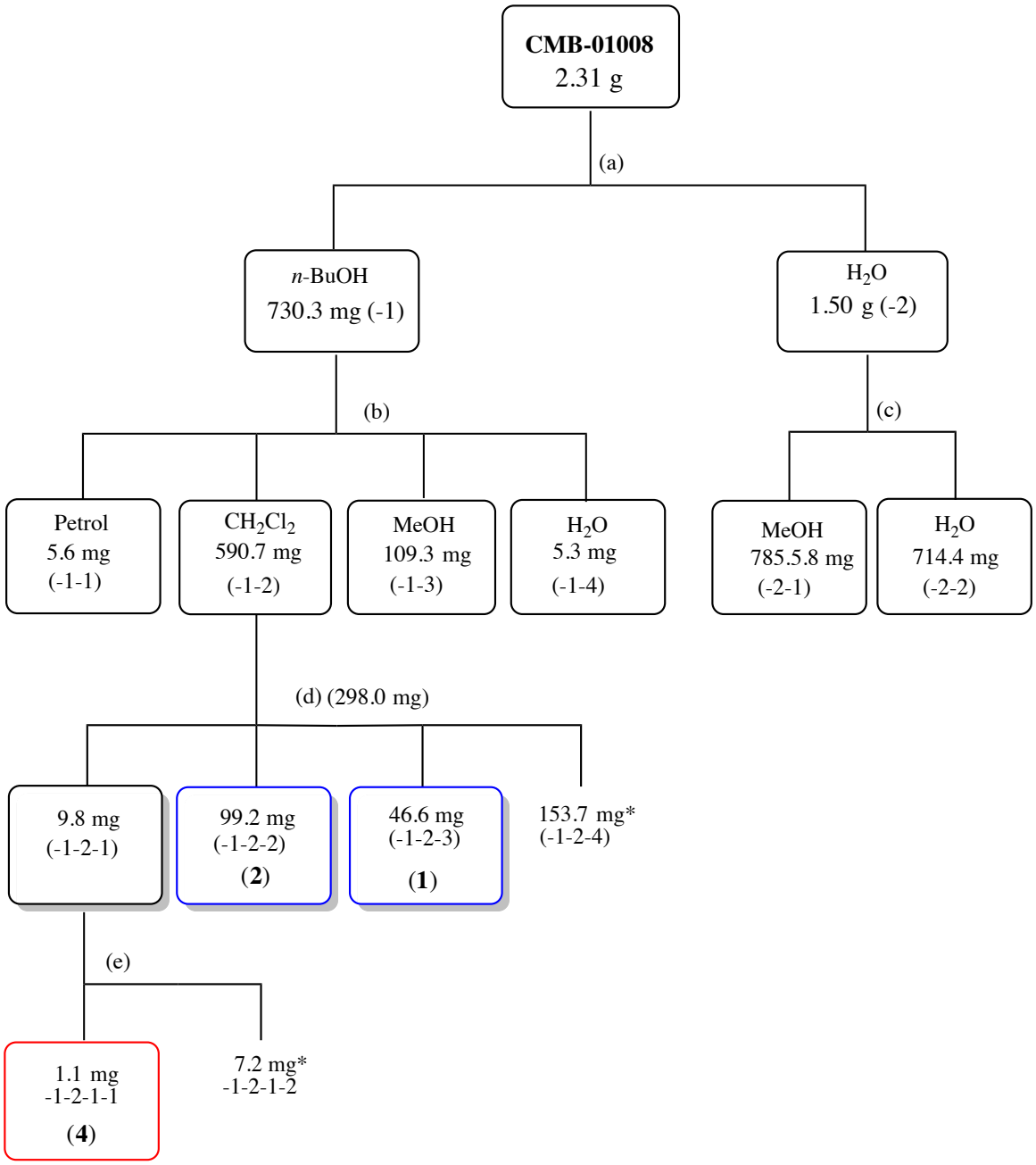

Scheme 4S1. Extraction and purification of *Psammocinia* sp. (CMB-01008)

(a) Solvent partition into *n*-BuOH (-1) and H_2O (-2) solubles.
(b) Sequential trituration of *n*-BuOH solubles into hexanes (-1-1), CH_2Cl_2 (-1-2), MeOH (-1-3) and H_2O (-1-4) solubles.
(c) Sequential trituration of H_2O soluble into MeOH (-2-1) and H_2O (-2-2) solubles.
(d) Semi-preparative fractionation by HPLC (Zorbax C_{18} 5 µm 250 × 9.4 mm, 25 min gradient elution at 4.0 mL/min from 90% H_2O/MeCN to 100% MeCN with isocratic 0.01% TFA/MeCN modifier).
(e) Analytical fractionation by HPLC (Zorbax C_8 5 µm, 150 × 4.6 mm, 25 min gradient elution at 1.0 mL/min from 90% H_2O/MeCN to 100% MeCN with isocratic 0.01% TFA/MeCN modifier).

Blue and red indicate known and new compounds respectively while * were not investigated.
Note – % yields for **1, 2** and **4** are estimated against the total *n*-BuOH solubles.

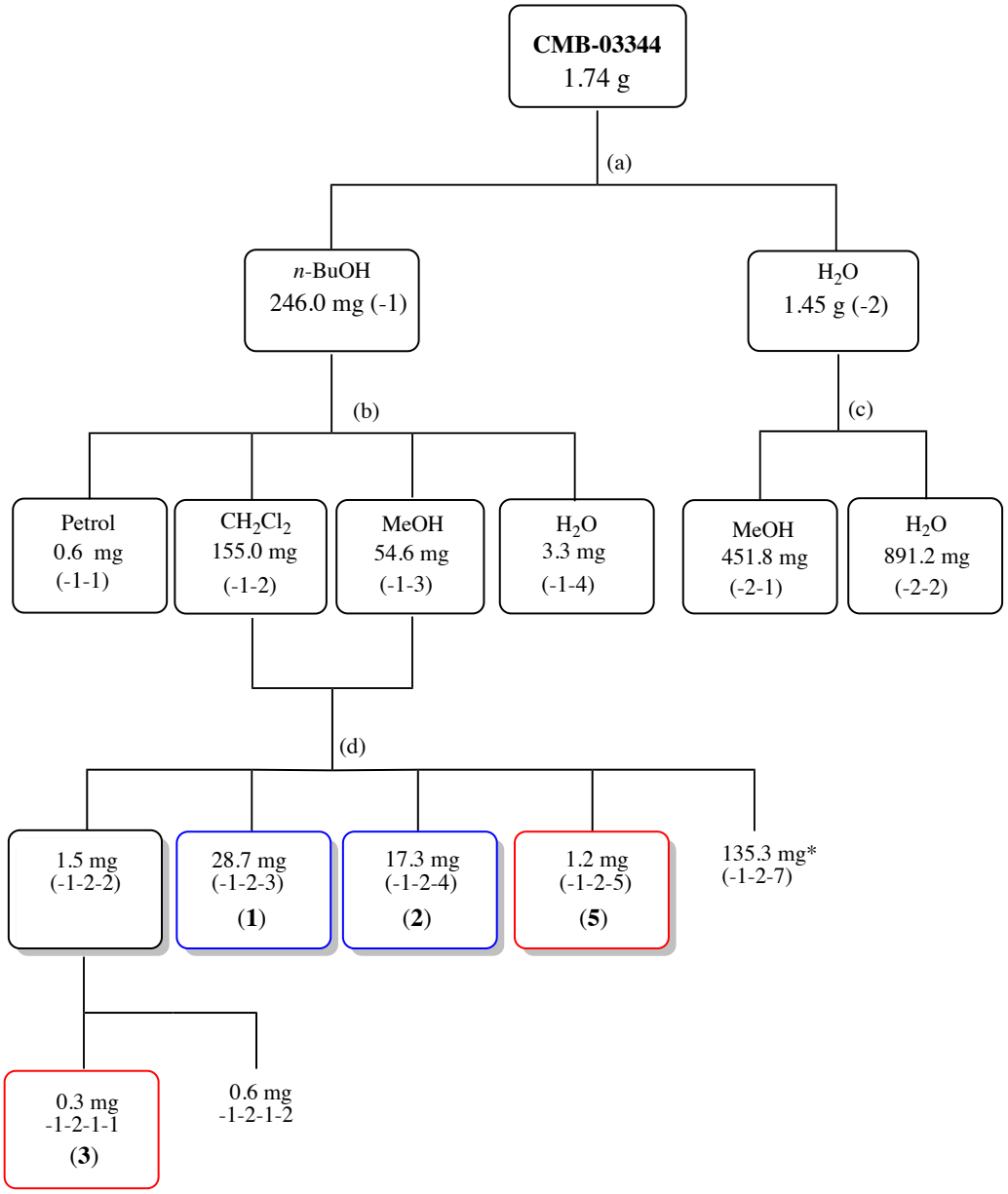

Scheme 4S2. Extraction and purification of *Psammocinia* sp. (CMB-03344)

(a) Solvent partition into *n*-BuOH (-1) and H_2O (-2) solubles.
(b) Trituration of *n*-BuOH into hexanes (-1-1), CH_2Cl_2 (-1-2), MeOH (-1-3) and H_2O (-1-4) solubles.
(c) Sequential trituration of H_2O soluble into MeOH (-2-1) and H_2O (-2-2) solubles.
(d) Semi-preparative fractionation by HPLC (Zorbax C_8 5 µm, 250 × 9.4 mm, 25 min gradient elution at 4.0 mL/min from 90% H_2O/MeCN to 100% MeCN with isocratic 0.01% TFA/MeCN modifier).
(e) Analytical fractionation by HPLC (Zorbax C_8 5 µm, 150 × 4.6 mm, 25 min gradient elution at 1.0 mL/min from 90% H_2O/MeCN to 100% MeCN with isocratic 0.01% TFA/MeCN modifier).
(f) Analytical fractionation by HPLC (Zorbax C_8 5 µm, 150 × 4.6 mm, 15 min gradient elution at 1.0 mL/min from 50% H_2O/MeCN to 100% MeCN with isocratic 0.01% TFA/MeCN modifier).
Blue and red indicate known and new compounds respectively while * means uninvestigated.
Note – % yields for **1**–**3** and **5** are estimated against the total *n*-BuOH solubles.

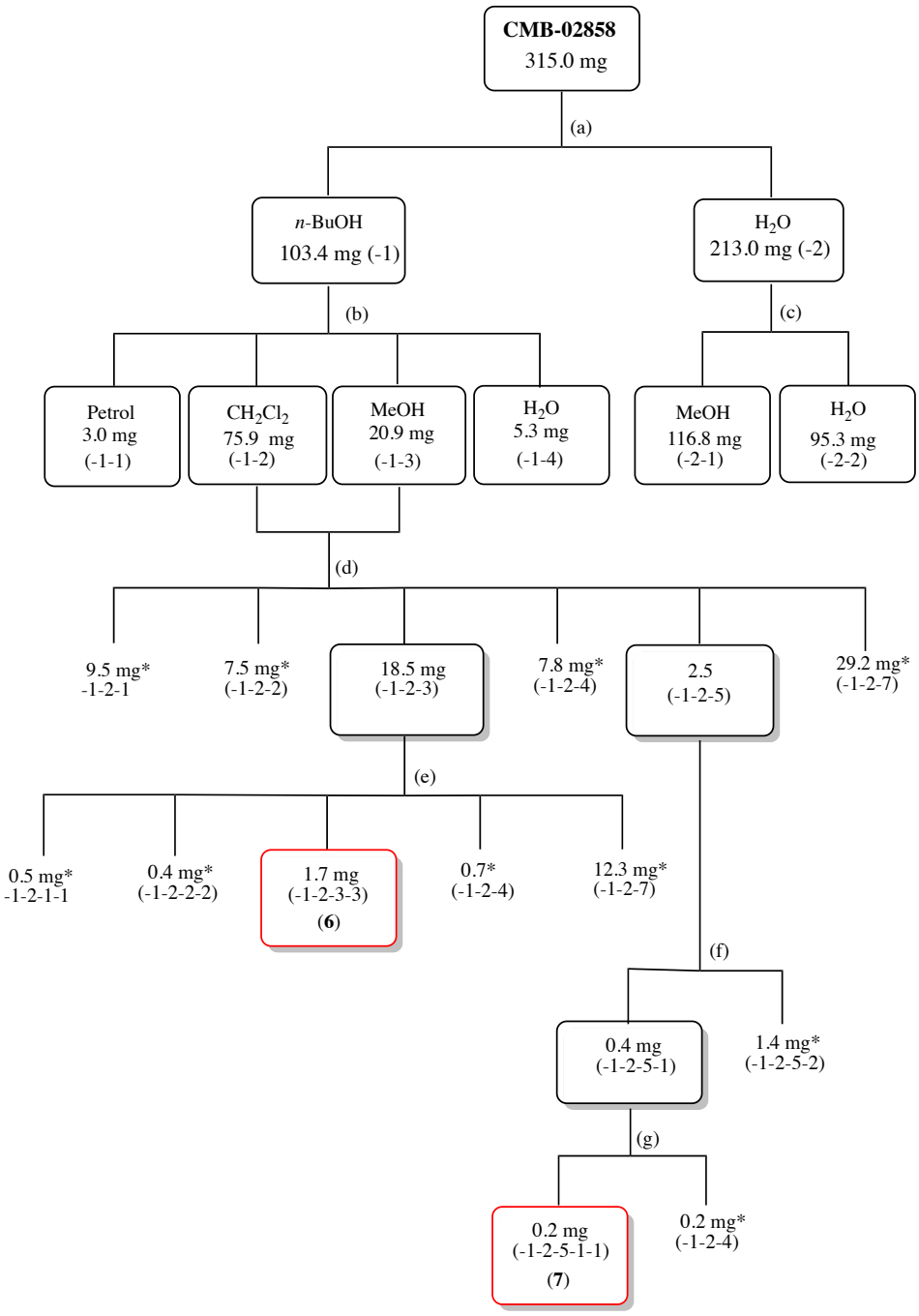

Scheme 4S3. Extraction and purification of *Psammocinia* sp. (CMB-02858)

(a) Solvent partition into *n*-BuOH (-1) and H_2O (-2) solubles.
(b) Trituration of *n*-BuOH into hexanes (-1-1), CH_2Cl_2 (-1-2), MeOH (-1-3) and H_2O (-1-4) solubles.
(c) Sequential trituration of H_2O soluble into MeOH (-2-1) and H_2O (-2-2) solubles.
(d) Semi-preparative fractionation by HPLC (Zorbax C_8 5 mm, 250 × 9.4 mm, 25 min gradient elution at 4.0 mL/min from 90% H_2O/MeCN to 100% MeCN with isocratic 0.01% TFA/MeCN modifier.)
(e) Semi-preparative fractionation by HPLC (Zorbax C_8 5 mm, 250 × 9.4 mm, 25 min gradient elution at 4.0 mL/min from 90% H_2O/MeCN to 100% MeCN with isocratic 0.01% TFA/MeCN modifier).
(f) Analytical fractionation by HPLC (Zorbax C_8 5 mm, 150 × 4.6 mm, 25 min gradient elution at 1.0 mL/min from 90% H_2O/MeCN to 100% MeCN with isocratic 0.01% TFA/MeCN modifier.)
(g) Analytical fractionation by HPLC (Zorbax C_8 5 mm, 150 × 4.6 mm, 15 min gradient elution at 1.0 mL/min from 50% H_2O/MeCN to 100% MeCN with isocratic 0.01% TFA/MeCN modifier).
Blue and red indicate known and new compounds respectively while * means not investigated.

Table 4S1: NMR (600 MHz, CD_3OD) data for (–)-ircinianin (**1**)

#	δ_H (mult., *J* (Hz))	δ_C [A]	COSY	HMBC (^1H-^{13}C)
1	7.38 (dd, 1.7, 1.7)	144.0	2, 4	2, 3, 4
2	6.30 (m)	112.1	1	1, 3, 4
3		126.5		
4	7.26 (m)	140.3	1, 5	1, 2, 3
5	2.41[B] (br t, 7.6)	25.3	4, 6	2, 3, 4, 6, 7
6	1.68 (m)	29.5	5, 7	3, 5, 7, 8
7	2.04 (m)	40.5	6, 10	5, 6, 8, 9, 10
8		136.5		
9	1.57 (d, 1.3)	16.3	10	7, 8, 10
10	5.12 (dm, 10.3)	125.1	7, 9, 11	7, 9, 11
11	3.07 (m)	48.7	10, 12, 14	12, 13, 21
12	5.03 (m)	123.6	11, 14, 15	11, 14, 15, 21
13		137.1		
14	1.71 (dd, 2.8, 1.4)	20.8	11, 12	12, 13, 15
15	2.42[B] (m)	46.2	12, 16a, 16b, 20	
16	a 1.89 (m)	27.3	15, 16b, 17a	17, 18, 20
	b 1.34 (m)		15, 16a, 17b	18
17	a 2.00 (m)	33.6	16a, 17b	
	b 1.30 (m)		16b, 17a, 18	15, 16, 19
18	1.65 (m)	33.2	17b, 19, 20	15, 18, 19
19	0.92 (d, 6.3)	20.7	18	17, 18, 20
20	1.60 (dd, 11.1, 10.5)	52.0	15, 18	18, 21, 24
21		86.9		
22		179.5[C]		
23		97.2		
24		177.7[C]		
25	1.64 (s)	6.1		22, 23, 24

[A] Assignments supported by HSQC and HMBC; [B] Overlapping signals; [C] Assignments interchangeable

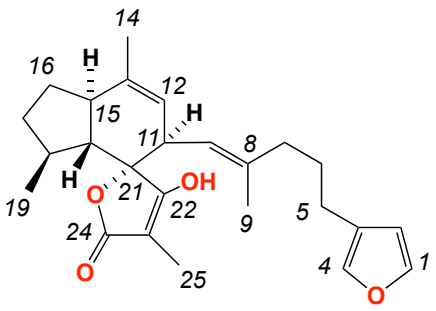

Table 4S2. NMR (600 MHz, CD_3OD) data for (–)-ircinianin sulfate (**2**)

#	δ_H (mult., *J* (Hz))	δ_C [A]	COSY	HMBC (^1H-^{13}C)
1	7.35 (dd, 1.6, 1.6)	143.8	2, 4	2, 3, 4
2	6.32 (br s)	112.3	1	1, 3, 4
3		126.8		
4	7.26 (br s)	140.2	1, 5	1, 2, 3
5	2.37[B] (m)	25.7	4, 6	2, 3, 4, 6, 7
6	1.73 (m)	29.2	5, 7	3, 5, 7, 8
7	2.08 (br t, 7.6)	40.7	6, 10	5, 6, 8, 9, 10
8		137.1		
9	1.57 (br s)	16.5	10	7, 8, 10
10	5.10 (br d, 10.4)	124.3	7, 9, 11	7, 8, 9, 11
11	3.09 (m)	49.0	10, 12, 14	12, 13, 21
12	5.02 (m)	124.1	11, 14, 15	11, 14, 15, 21
13		137.2		
14	1.71 (br s)	20.5	11, 12	12, 13, 15
15	2.39[B] (m)	46.5	12, 16a, 16b, 20	20
16	a 1.88 (m)	27.3	15, 16b, 17a	15, 18, 20
	b 1.38 (m)		15, 16a, 17a, 17b	15, 17
17	a 1.99[C] (m)	33.8	16a, 16b, 17b	16, 20
	b 1.31 (m)		16b, 17a, 18	15, 16, 18, 19
18	1.68 (m)	33.4	17b, 19, 20	16, 17, 20, 21
19	1.00 (d, 6.4)	21.0	18	17, 18, 20
20	1.62 (dd, 10.8, 10.8)	52.3	15, 18	18, 21, 24
21		87.5		
22		177.7[D]		
23		102.6		
24		171.1[D]		
25	2.00[C] (s)	9.4		22, 23, 24

[A] Assignments supported by HSQC and HMBC; [B,C] Overlapping signals; [D] Assignments interchangeable

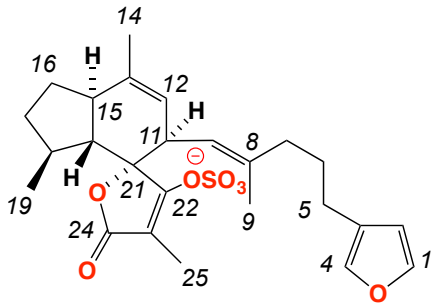

Table 4S3. NMR (600 MHz, CD_3OD) data for ircinianin lactam A (**3**)

#	δ_H (mult., *J* (Hz))	δ_C [A]	COSY	HMBC (^1H-^{13}C)
1	4.07[D] (br s)	53.0	2, 5	2
2	6.89 (br s)	138.0	1, 5	1, 4
3		139.0		
4		173.2		
5	2.26 (m)	25.8	6	
6	1.71[B] (m)	26.9	5, 7	3, 5, 7, 8
7	2.08 (br t, 7.3)	40.4	6	6, 8, 9, 10
8		135.1		
9	1.58 (d, 1.4)	16.2	10	7, 8, 10
10	5.14 (dm, 10.4)	125.5	9, 11	
11	3.07 (m)	48.6	10, 12, 14	
12	5.03 (m)	123.5	11, 14	
13		137.2		
14	1.71[B] (dd, 2.9, 1.4)	20.74[E]	11, 12	12, 13, 15
15	2.42 (m)	46.2	16a, 20	
16	a 1.91 (m)	27.3	17a, 17b	
	b 1.34[C] (m)		15	
17	a 1.98 (m)	33.6	17b	
	b 1.31 (m)		17a, 18	
18	1.67 (m)	33.2	19	
19	0.92 (d, 6.3)	20.66[E]	18	17, 18, 20
20	1.61 (dd, 11.1, 10.4)	51.9	15	
21		ND		
22		179.5		
23		97.4		
24		ND		
25	1.64 (s)	6.1		22, 23
1′	4.07[D] (br s)	47.1		
2′		ND		

[A] Assignments supported by HSQC and HMBC; [B–D] Overlapping signals; [E] Assignments interchangeable
[ND] not detected

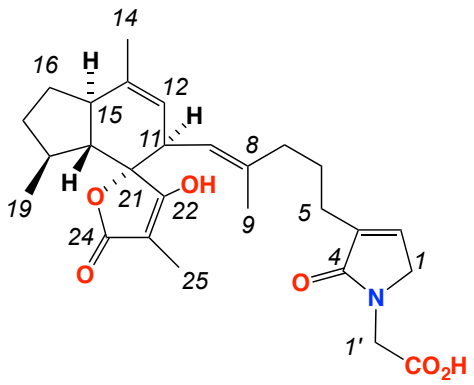

Table 4S4. NMR (600 MHz, CD_3OD) data for (–)-ircinianin lactam A sulfate (**4**)

#	δ_H (mult., *J* (Hz))	δ_C[A]	COSY	HMBC (^1H-^{13}C)
1	4.05 (s)	54.4	2, 5	2
2	6.92 (s)	137.8	1, 5	1
3		139.3		
4		173.4		
5	2.23 (m)	26.6	2, 6	3, 7
6	1.80 (m)	26.8	5, 7	7
7	2.13 (t, 7.5)	40.5	6, 9	8, 9, 10
8		137.1		
9	1.59 (s)	16.4	7	7, 8, 10
10	5.12 (d, 7.2)	124.2	7, 9, 11	
11	3.08 (m)	49.3	10, 12, 14	8, 10
12	5.02 (br s)	123.8	11, 14, 15	7, 9
13		137.1		
14	1.71 (s)	20.4	11, 15, 20	12, 13, 15
15	2.41 (m)	46.4	16, 20	12, 14
16	1.90 (m)	27.0	15, 17	20
17	1.30 (m)	33.6	16, 18	15, 16
18	1.75[B] (m)	33.0	17, 19, 20	15, 16
19	1.01 (d, 6.6)	21.0	18	18, 20
20	1.74[B] (m)	52.0	15, 19	18
21		87.5		
22		177.7		
23		102.7		
24		171.0		
25	2.01 (s)	9.7		22, 23, 24
1′	4.03 (s)	46.8		1
2′		173.0		

[A] Assignments supported by HSQC and HMBC. [B] Overlapping signals.

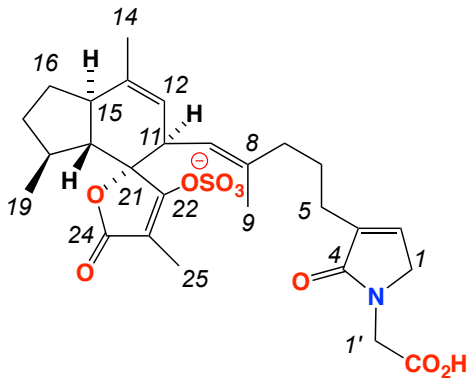

Table 4S5. NMR (600 MHz, CD_3OD) data for (–)-oxoircinianin (**5**)

#	δ_H (mult., *J* (Hz))	δ_C[A]	COSY	HMBC (^1H-^{13}C)
1	7.38 (dd, 1.6, 1.6)	144.0	2, 4	2, 3, 4
2	6.32 (m)	112.1	1	1, 3, 4
3		126.6		
4	7.29 (m)	140.4	1, 5	1, 2, 3
5	2.42[B] (br t, 7.4)	25.0	4, 6	2, 3, 4, 6, 7
6	1.67[C] (m)	29.3	5, 7	
7	2.01 (br t, 7.4)	40.3	6	5, 6, 8, 9, 10
8		137.9		
9	1.57 (d, 1.3)	16.5	10	7, 8, 10
10	4.98 (dm, 10.2)	121.6	9, 11	7, 9
11	3.34 (m)	48.2	10, 12, 14	
12	5.03 (m)	123.9	11, 14	15
13		137.2		
14	1.73[C] (dd, 2.7, 1.4)	21.3	11, 12	12, 13, 15
15	2.42[B] (m)	45.7	16a, 16b, 20	
16	a 1.92 (m)	26.9	15, 16b, 17a	18, 20
	b 1.36 (m)		15, 16b, 17b	
17	a 2.05 (m)	34.1	16a, 17b	16
	b 1.33 (m)		16b, 17a, 18	
18	1.73[C] (m)	33.0	17b, 19	
19	0.84 (d, 6.3)	20.8	18	17, 18, 20
20	1.70[C] (m)	52.0	15	18
21		[ND]		
22		208.1		
23		70.2		
24		175.8		
25	1.39 (s)	19.8		22, 23, 24

[A] Assignments supported by HSQC and HMBC; [B,C] Overlapping signals; [ND] Signals not detected

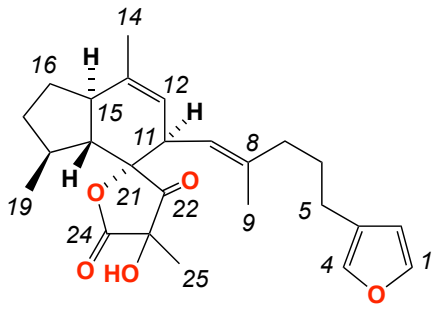

Table 4S6. NMR (600 MHz, CD_3OD) data for (–)-oxoircinianin lactam A (**6**)

#	δ_H (mult., *J* (Hz))	δ_C[A]	COSY	HMBC (^1H-^{13}C)
1	4.07 (td, 1.7, 1.7)	53.1	2, 5	2, 4
2	6.96 (tt, 1.7, 1.7)	139.0	1, 5	1, 4
3		140.1		
4		174.5		
5	2.26 (br t, 7.7)	26.3	1, 2, 6	2, 3, 4, 6, 7
6	1.67 (m)	26.9[D]	5, 7	3, 5, 7, 8
7	2.04 (br t, 7.3)	40.4	6	6, 8, 9, 10
8		137.8		
9	1.58 (d, 1.3)	16.5	10	7, 8, 10
10	5.02 (dm, 10.3)	124.1	9, 11	7, 9
11	3.34 (m)	48.2	10, 12, 14	21
12	5.03 (m)	121.6	11, 14	11
13		137.2		
14	1.73[B] (dd, 2.8, 1.4)	21.3	11, 12	12, 13, 15
15	2.42 (m)	45.6	16a, 16b, 20	
16	a 1.92 (m)	26.8[D]	15, 16b, 17a	18, 20
	b 1.33[C] (m)		15, 16a, 17b	15
17	a 2.05 (m)	34.1	16a, 17b	
	b 1.35[C] (m)		16b, 17a, 18	
18	1.73[B] (m)	33.0	19	
19	0.83 (d, 6.2)	20.8	18	17, 18, 20
20	1.71[B]	52.0	15	18
21		92.9		
22		208.1		
23		70.2		
24		175.7		
25	1.38 (s)	19.8		22, 23, 24
1′	4.23 (s)	44.5		1, 4, 2'
2′		172.5		

[A] Assignments supported by HSQC and HMBC; [B,C] Overlapping signals; [D] Assignments interchangeable.

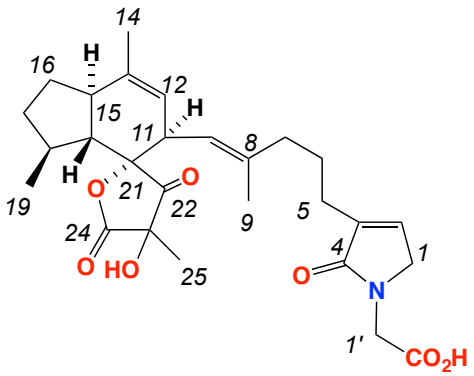

Table 4S7. NMR (600 MHz, CD_3OD) data for (–)-ircinianin lactone A (**7**)

#	δ_H (mult., *J* (Hz))	δ_C[A]	COSY	HMBC (^1H-^{13}C)
1	4.83 (td, 1.8, 1.6)	72.2	2, 5	2, 3, 4
2	7.37 (tt, 1.6, 1.6)	148.0	1, 4	1, 4
3		134.6		
4		177.2		
5	2.26 (m)	25.8	1, 2, 6	2, 3, 4, 6, 7
6	1.71[B] (m)	26.9	5, 7	3, 5, 7
7	2.08 (br t, 7.3)	40.4	6	5, 6, 8, 9, 10
8		136.1		
9	1.58 (d, 1.4)	16.2	10	7, 8, 10
10	5.14 (dm, 10.4)	125.5	9, 11	7, 9
11	3.07 (m)	48.6	10, 12, 14	
12	5.03 (m)	123.5	11, 14	15
13		137.2		
14	1.71[B] (dd, 2.9, 1.4)	20.74[C]	11, 12	12, 13, 15
15	2.42 (m)	46.2	16a, 16b, 20	
16	a 1.91 (m)	27.3	15, 16b, 17a	18, 20
	b 1.34 (m)		15, 16a, 17a, 17b	
17	a 2.01 (m)	33.6	16a, 16b, 17b	16
	b 1.31 (m)		16b, 17a, 18	
18	1.67 (m)	33.2	17b, 19	
19	0.92 (d, 6.3)	20.66[C]	18	17, 18, 20
20	1.61 (dd, 11.1, 10.4)	51.9	15	15, 18
21		86.9		
22		179.5[D]		
23		97.4		
24		177.7[D]		
25	1.64 (s)	6.1		22, 23, 24

[A] Assignments supported by HSQC and HMBC; [B] Overlapping signals; [C,D] Assignments interchangeable

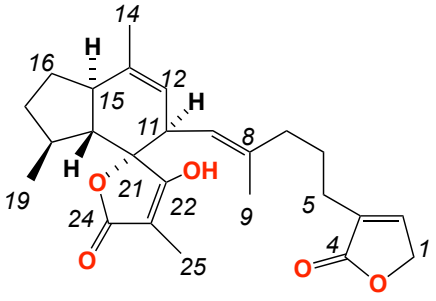

Table 4S8. NMR (600 MHz, CD_3OD) data for (–)-ircinianin acetate (**8**)

#	δ_H (mult., *J* (Hz))	δ_C[A]	COSY	HMBC (^1H-^{13}C)
1	7.39 (dd, 1.6, 1.6)	144.2	2, 4	3, 4
2	6.30 (m)	112.1	1	1, 3, 4
3		126.3		
4	7.26 (m)	140.3	1	1, 2, 3
5	2.38[B] (m)	25.3	6	2, 3, 4, 6, 7
6	1.65[C] (m)	29.4	5, 7	3, 5, 7, 8
7	2.01[D] (m)	40.8	6	5, 6, 8, 9, 10
8		137.6		
9	1.54 (d, 1.2)	16.1	10	7, 8, 10
10	5.02 (br d, 10.5)	124.1	9, 11	7, 9
11	3.09 (m)	48.7	10, 12, 14	
12	4.98 (m)	123.0	11, 14	
13		137.2		
14	1.72 (dd, 2.9, 1.5)	20.6	11, 12	12, 13, 15
15	2.41[B] (m)	46.5	16a, 16b, 20	
16	a 1.93 (m)	27.4	15, 16b, 17a	20
	b 1.37 (m)		15, 16a, 17a, 17b	
17	a 2.03[D] (m)	33.5	16a, 16b, 17b	
	b 1.34 (m)		16b, 17a, 18	
18	1.63[C] (m)	33.0	17b, 19, 20	
19	0.95 (d, 6.5)	20.7	18	17, 18, 20
20	1.68 (dd, 11.1, 10.5)	51.7	15, 18	18
21		[ND]		
22		174.3[E]		
23		114.7		
24		169.1[E]		
25	1.65[C] (s)	9.3		22, 23, 24
$\underline{C}H_3CO$	2.17 (s)	21.0		$CH_3\underline{C}O$
$CH_3\underline{C}O$		165.5		

[A] ^{13}C NMR assignments supported by HSQC experiment; [B–D] Overlapping signals within the column;
[E] Interchangeable signals within the column; [ND] Signals not detected

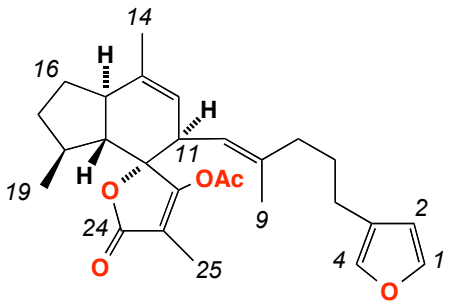

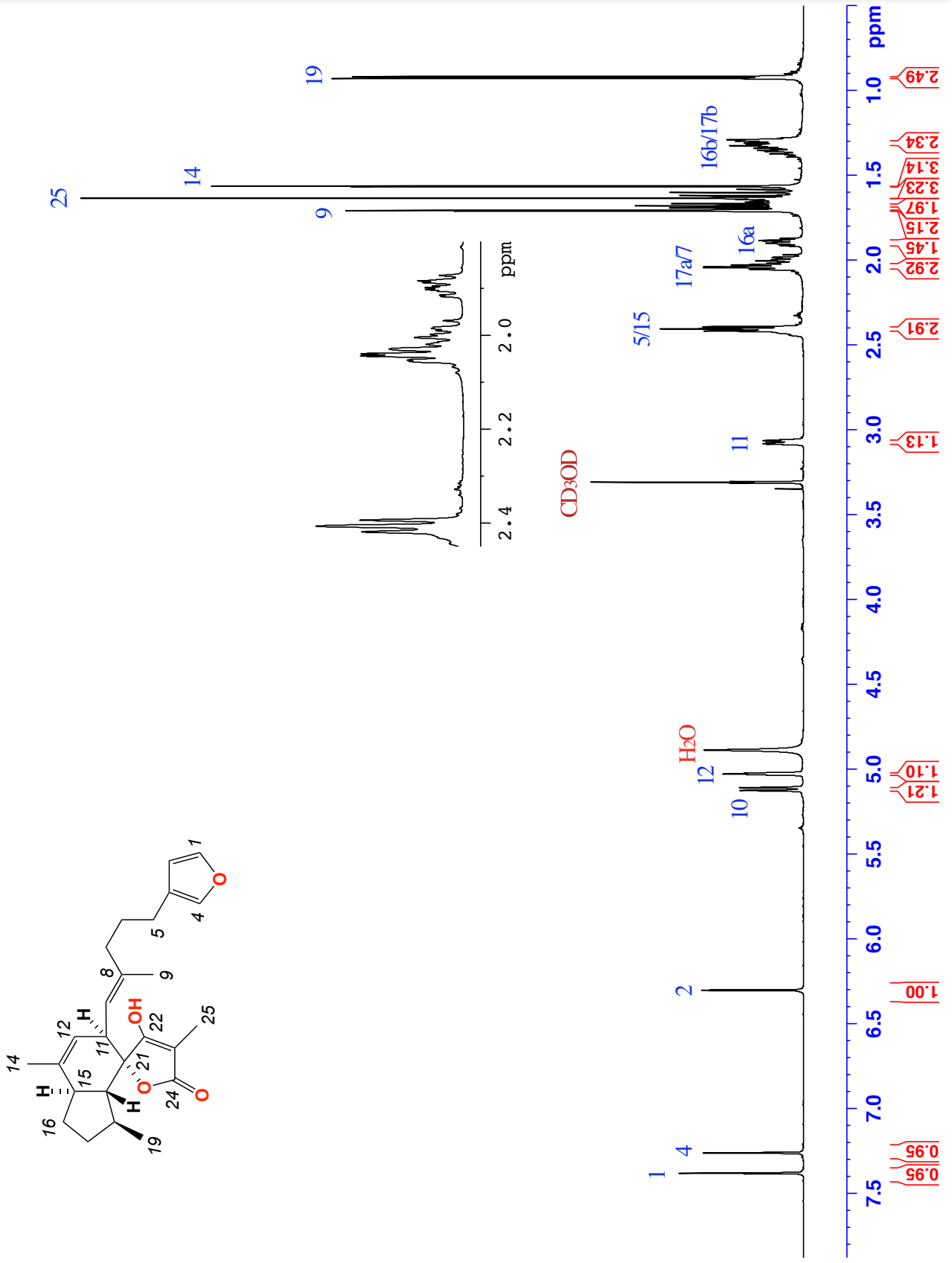

Figure 4S1: ^{1}H NMR (600 MHz, CD_3OD) spectrum of (–)-ircinianin (**1**)

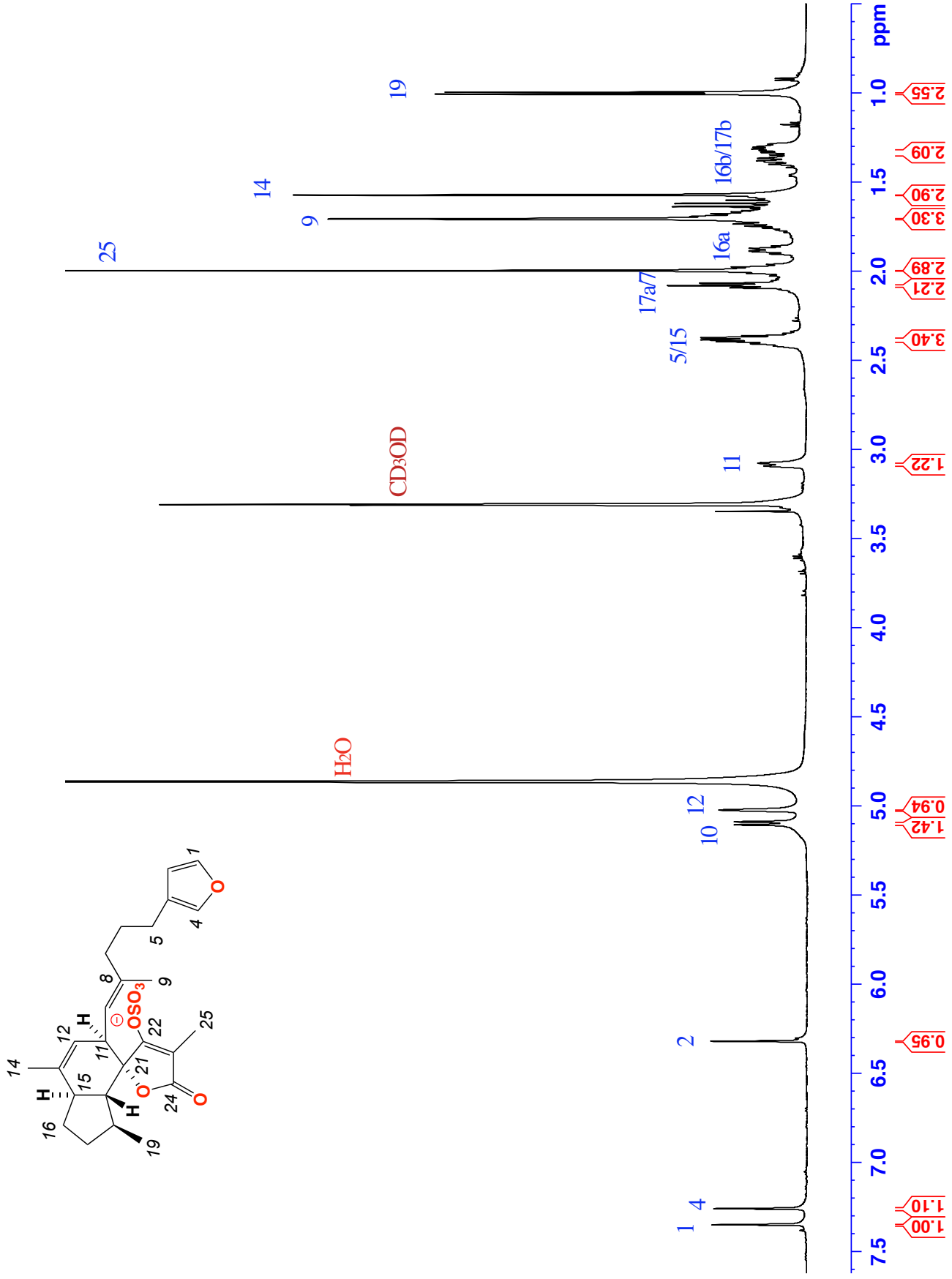

Figure 4S2. ^{1}H NMR (600 MHz, CD_3OD) spectrum of (–)-ircinianin sulfate (**2**)

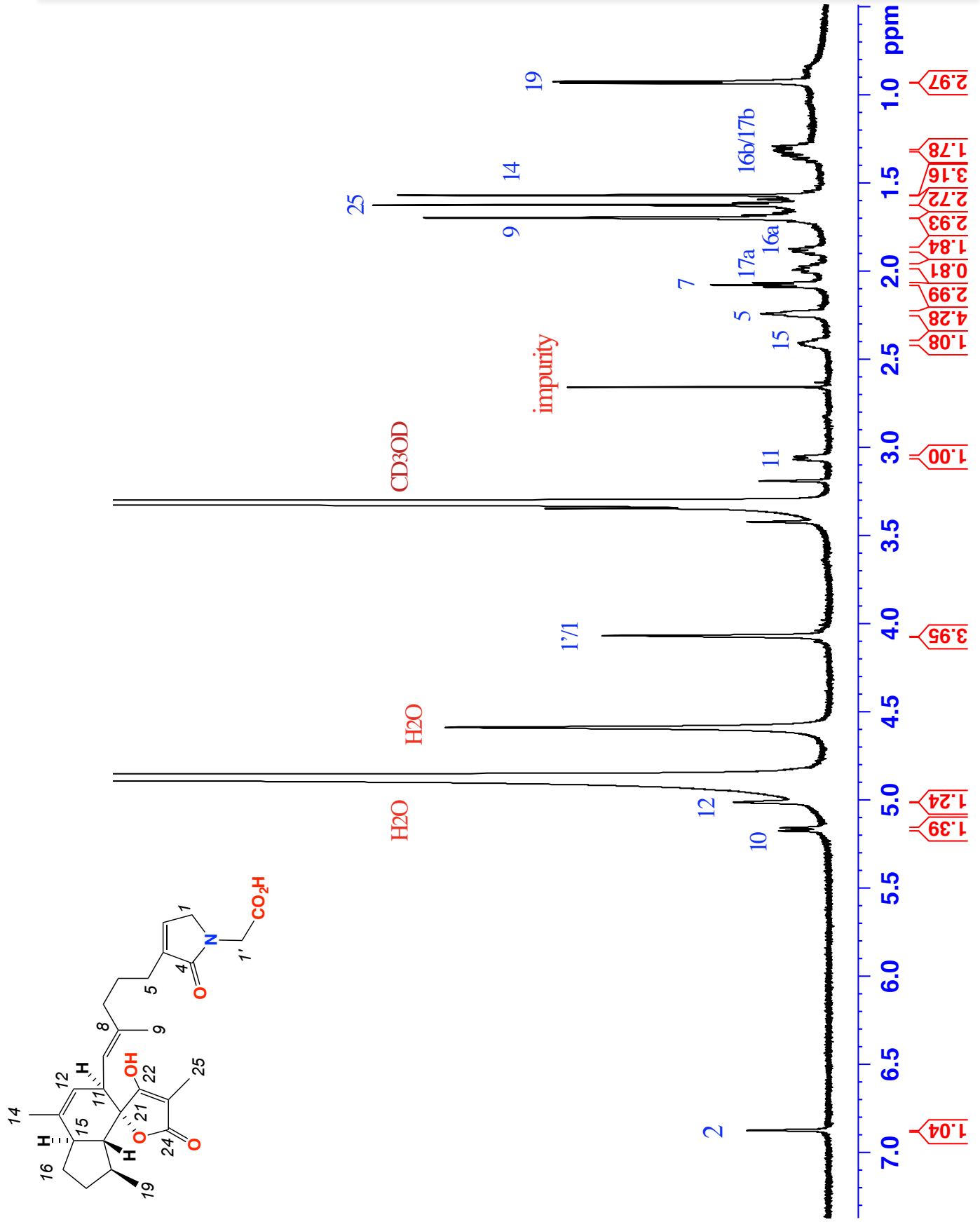

Figure 4S3. ^{1}H NMR (600 MHz, CD_3OD) spectrum of (–)-ircinianin lactam A (**3**)

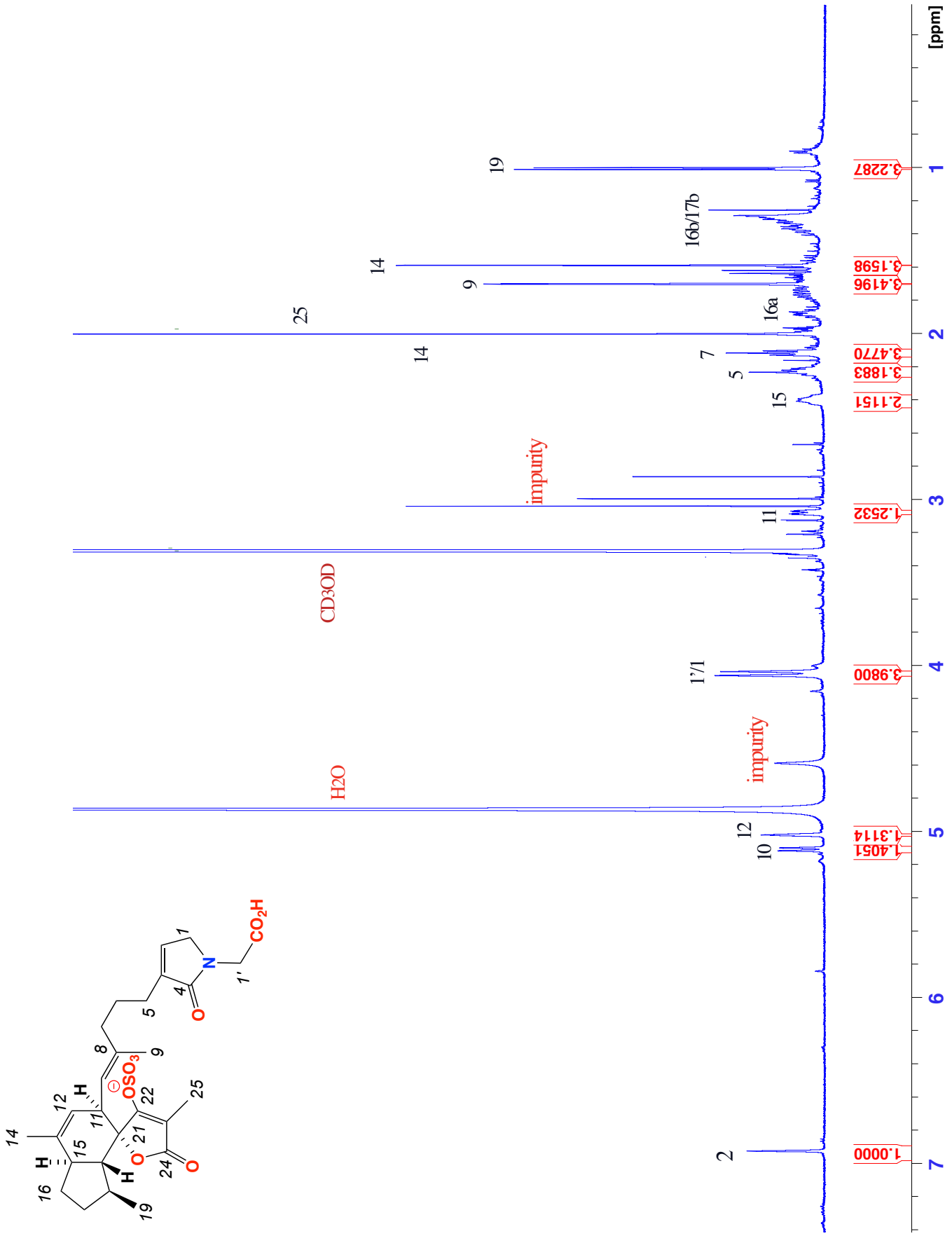

Figure 4S4. ^{1}H NMR (600 MHz, methanol-d_4) spectrum of (–)-ircinianin lactam A sulfate (**4**)

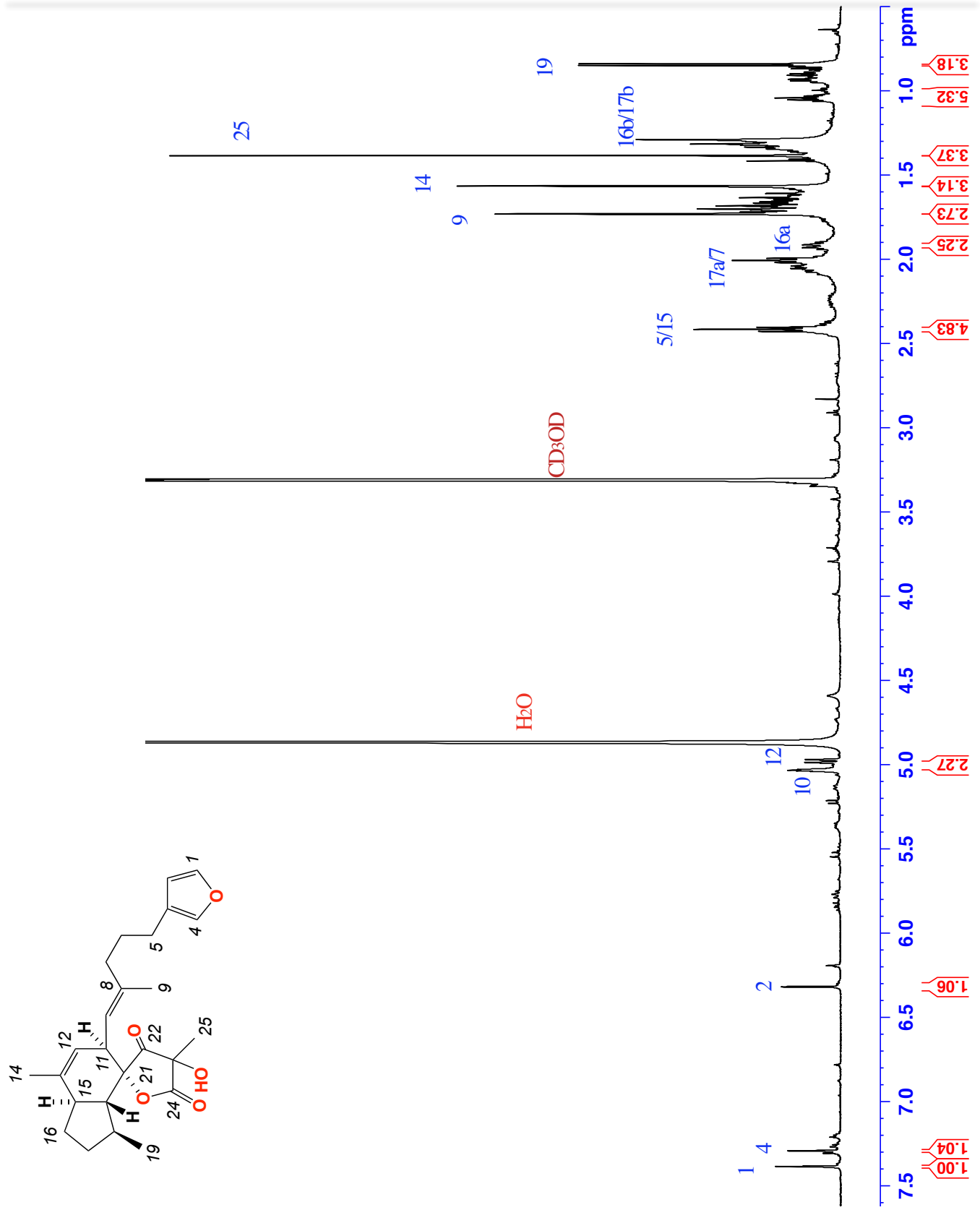

Figure 4S5. ^{1}H NMR (600 MHz, CD_3OD) spectrum of (–)-oxoircinianin (**5**)

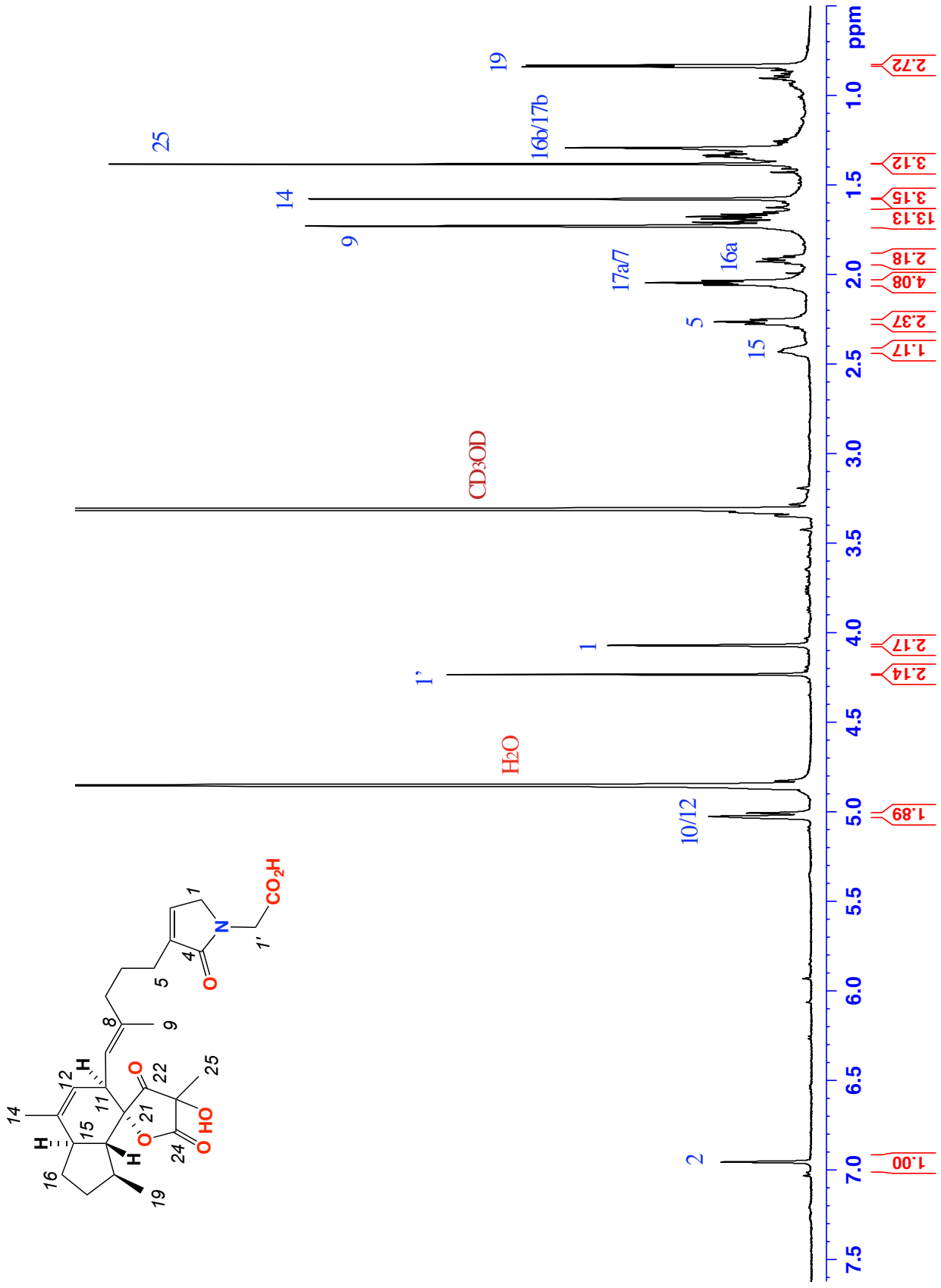

Figure 4S6. ^{1}H NMR (600 MHz, CD_3OD) spectrum of (–)-oxoircinianin lactam A (**6**)

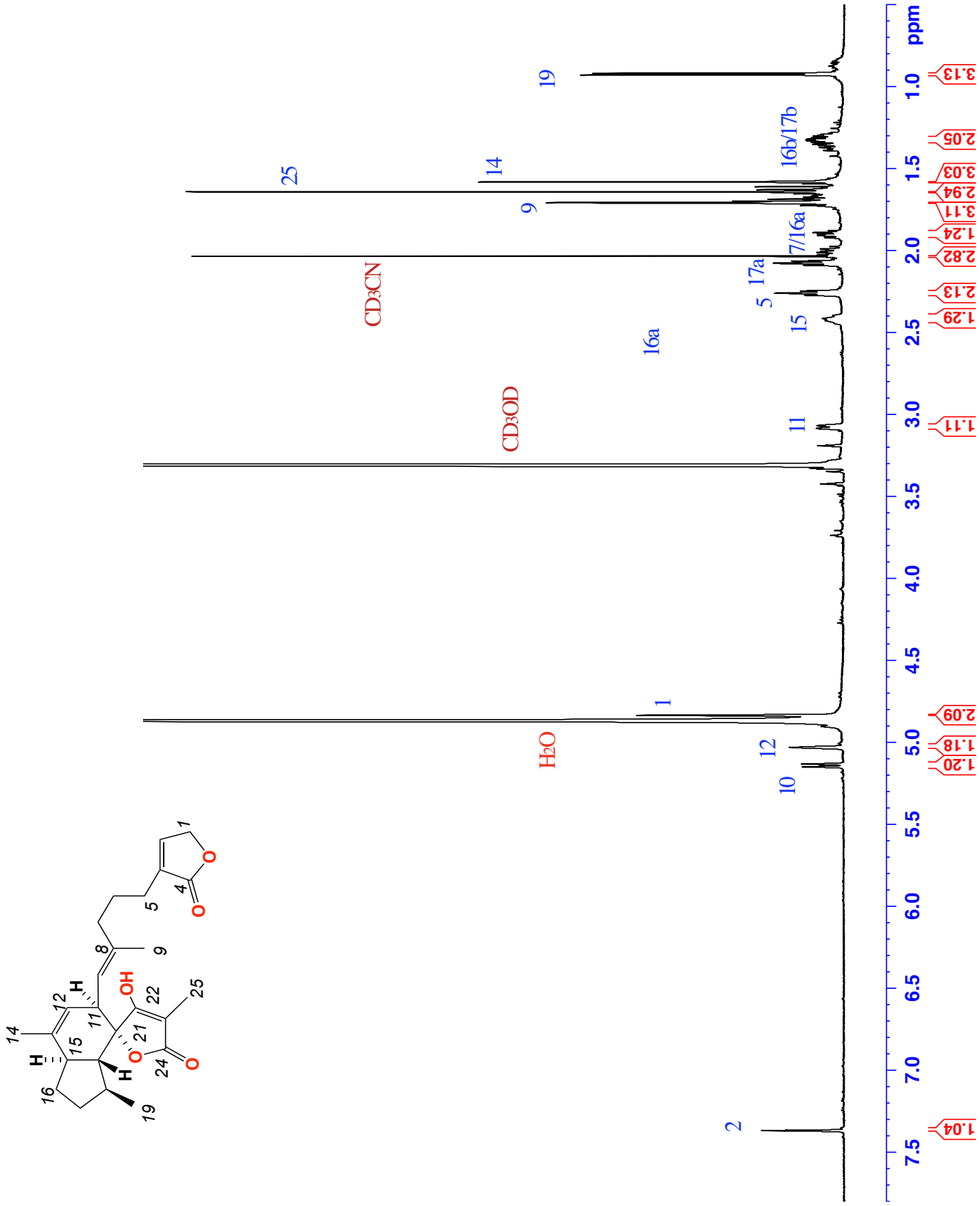

Figure 4S7. ^{1}H NMR (600 MHz, CD_3OD) spectrum of (–)-ircinianin lactone A (**7**)

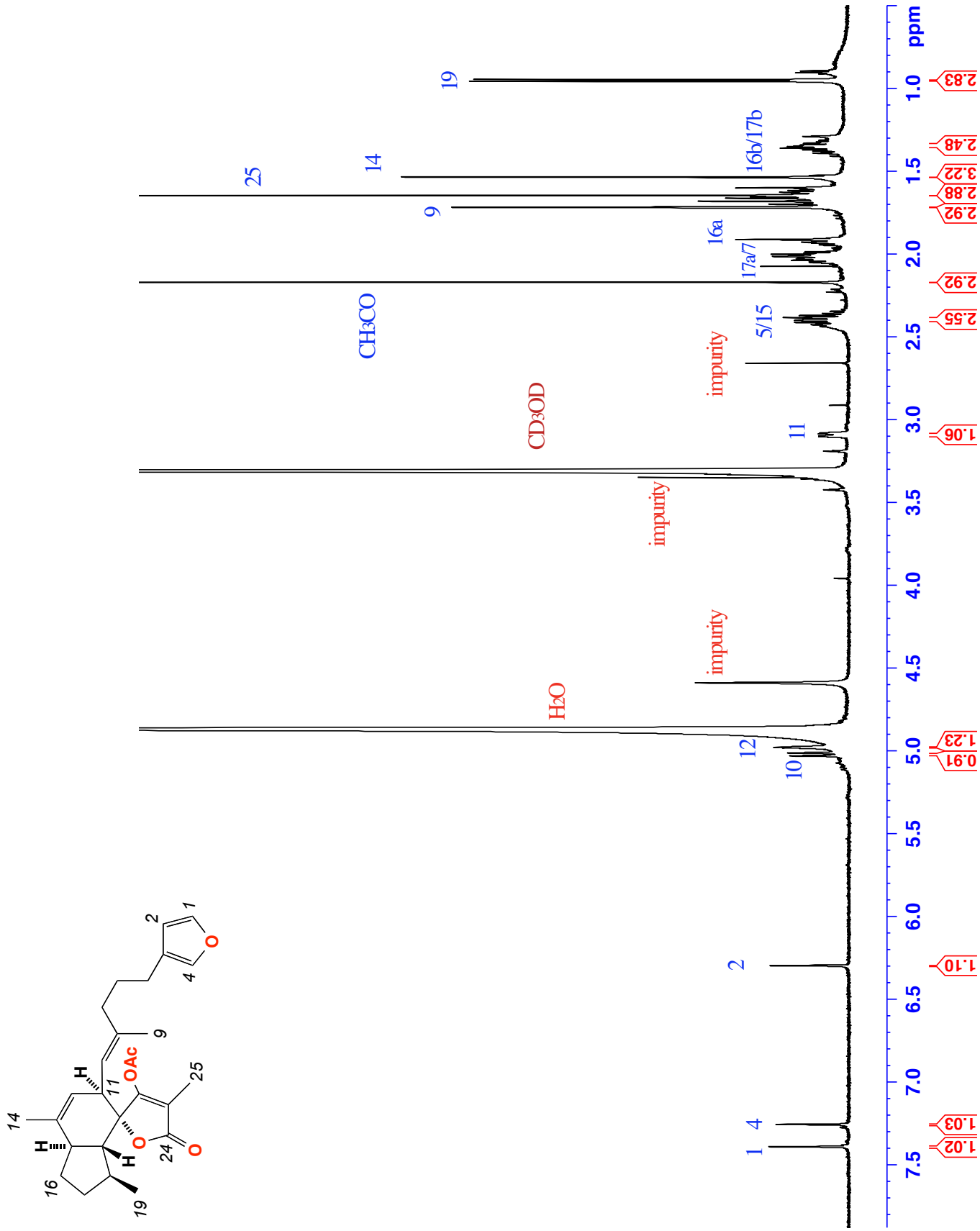

Figure 4S8. ^{1}H NMR (600 MHz, CD_3OD) spectrum of (–)-ircinianin acetate A (**8**)

Pharmacology

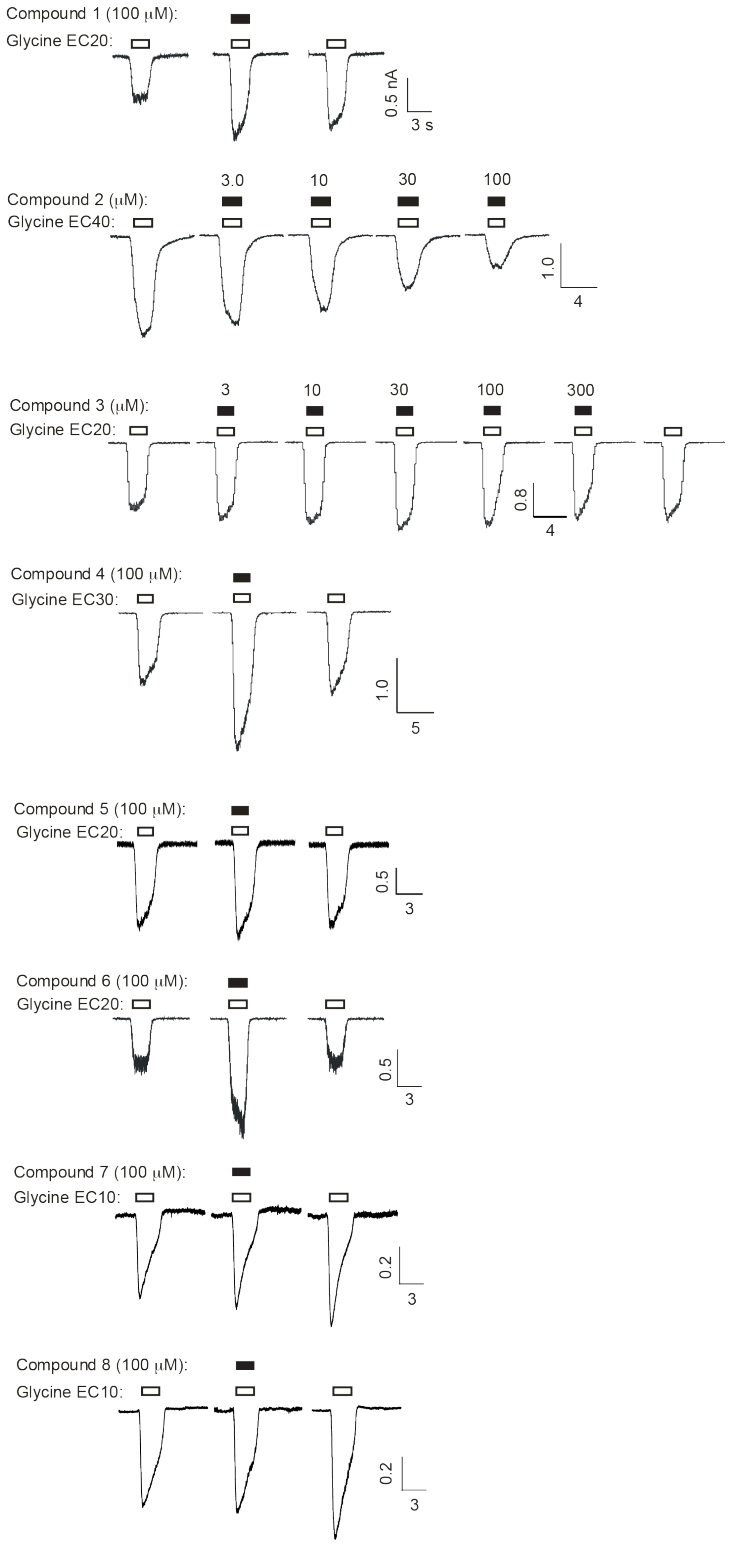

Figure 4S9. The effects of **1**–**8** on α1 GlyRs using whole-cell electrophysiological recording. All traces on a given line were recorded from the same cell with the periods of glycine and drug application indicated by unfilled and filled bars, respectively. The drug concentrations and glycine EC values are also indicated. Scale bars represent current in nA (vertical line) and time in sec (horizontal line). The averaged maximum effects of each compound are summarized in Table S9.

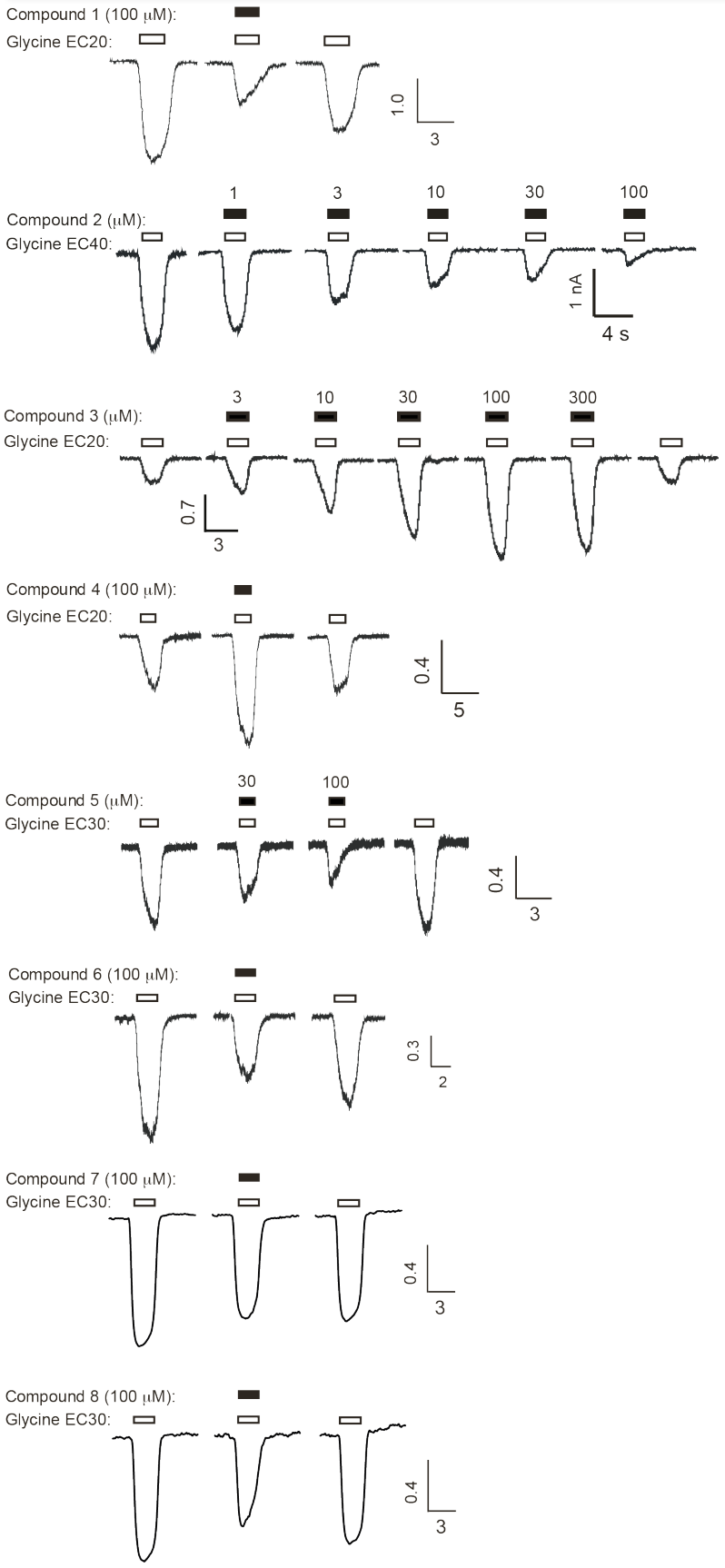

Figure 4S10. The effects of **1**–**8** on α3 GlyRs using whole-cell electrophysiological recording. All traces on a given line were recorded from the same cell with the periods of glycine and drug application indicated by unfilled and filled bars, respectively. The drug concentrations and glycine EC values are also indicated. Scale bars represent current in nA (vertical line) and time in sec (horizontal line). The averaged maximum effects of each compound are summarized in Table S9.

Table 4S9. Averaged maximum effects of **1–8** on α1 and α3 GlyRs. All effects were quantitated via whole-cell patch clamp. The mean percentage change in control glycine-gated current was determined at a concentration of 100 μM of each compound. All results were averaged from 4–6 cells, with the exception of **3** which was averaged from 10 cells at both receptors.

Compound	α1 GlyR		α3 GlyR	
	I/Imax (%)	SEM	I/Imax (%)	SEM
1	175	10	41	3
2	34	5	17	2
3	123	9	367	15
4	190	6	190	5
5	115	3	48	4
6	211	6	57	2
7	118	5	84	8
8	121	7	74	3

CHAPTER 5

IANTHELLALACTAMS & APLYSINOPSINS

5.1. Declaration

Ianthellalactams and aplysinopsins were discovered from one of the priority extracts, Australian *Ianthella cf. flabelliformis*. Chemical profiling revealed the presence of two different structure classes, sesquiterpene and indole alkaloids in the metabolites of the specimen. The terpenoids featured several unreported molecular weights which upon ^{1}H NMR and HRESIMS and suggested the presence of new metabolites (Table 2.2). Although similar investigation indicated the alkaloids as known molecules (Table 2.2), biological profiling showed them as the active component of the Australian *I. flabelliformis*, capable of modulating GlyRα1 at low sub micromolar concentration. Together, these results inspired further investigations leading to the discovery of two new sesquiterepenes, a moderate antagonist of and a potent potentiator of GlyRα1. A paper describing this discovery was recently published in **Bioorganic & Medicinal Chemistry**[139]. This is the third paper published from research collaboration on **GlyR Modulators from Australian Marine Resource** between the Capon Group of Institute for Molecular Bioscience (IMB) and the Lynch Group of Queensland Brain (QBI) of The University of Queensland Australia.

The two-research groups contributed equally to the publication of the paper. As in the first two papers, I was responsible for chemical investigation (isolation, purification and structure elucidation) of all metabolites discovered from the Australian *Ianthella cf. flabelliformis* (CMB-03322). During my lab work at the IMB, I received technical assistance (lab work and data analysis) from Dr. Hua Zhang, Dr. Xiao Xue and Dr. Andrew M. Piggott and was supervised by Professor Robert J. Capon as the head of chemistry lab. Similarly, other co-authors have contributed to this work. Dr. Robiul Islam performed bioassays (Yellow Fluorescence Protein and Patch Clamp assays) at the QBI. He received technical assistance from Dr. Daniel F. Gilbert, Dr. Frank Fontaine and Dr. Timothy I. Webb and was under the supervision of Professor Joseph W. Lynch as the head of pharmacology lab. The contributions of all co-authors to the publication of the paper were listed in the table below.

Balansa, W.; Islam, R.; Fontaine, F.; Piggott, A. M.; Xiao, X.; Zhang, H.; Gilbert, D.F.; Lynch, J. W.; Capon, R. J. Australian Marine Sponge Alkaloids as a New Class of Glycine Gated Chloride Channel Receptor (GlyR) Modulator. *Bioorg. Med. Chem.* **2013**, *21*, 4420-4425.

Contributor	Statement of contribution
Balansa, Walter	Responsible for chemistry (100% working)
Islam, Robiul	Responsible for bioassay (100% working)
Fontaine, Frank	Assisted with lab work and data analysis
Zhang, Hua	Assisted with lab work and data analysis
Piggott, Andrew M.	Assisted with lab work and data analysis
Webb, Timothy, I.	Assisted with lab work and data analysis
Gilbert, Daniel F.	Assisted with lab work and data analysis
Lynch, Joseph W.	Head of pharmacology lab.
Capon, Robert J.	Head of chemistry lab.

5.2. Introduction

The class of marine natural products indole alkaloids known as the aplysinopsins, including both mono and dimeric forms, have been the subject of much attention since first discovered almost four decades ago. From several marine taxa such as sponge[140-143], scleractinian coral[144-147], anemone[148] and mollusc[149], dozen monomeric aplysinopsins have been reported featuring a diverse pattern of bromination and methylation as well as different levels of oxidation and geometry (*E* vs. *Z*)[146,149]. Monomeric aplysinopsins are known to exert a range of biological activities particularly as anticancer and antidepressant agents[150-152], inspiring numerous total syntheses[153-156]. More recently, the discovery of asymmetric and symmetric dimers has generated renewed interest in this structure class. Asymmetric dimers were originally thought to be derived from Diels Alder cycloaddition[146,147] of two monomers but the most recent discovery of symmetric aplysinopsins[157] prompted consideration of an alternate biosynthetic hypothesis, a cyclobutane rearrangement. In addition to their cryptic biogenetic origin and intriguing structures, almost nothing is known about biological activity of the dimeric aplysinopsins.

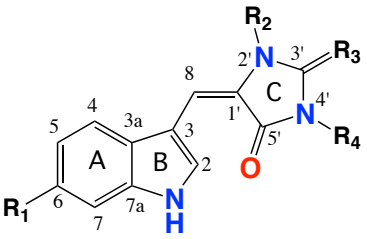

Figure 5.1. Aplysinopsin Structure

5.2.1 Monomeric Aplysinopsins

Aplysinopsin features three distinctive moieties (indole, 8-1′ olefin and 2-aminoimidazole units, Figure 5.1) whose variations particularly at 8-1′ olefin and ring C allow the classification of monomeric aplysinopsin into three main groups. In 1977, Wells *et al* first reported *E*/*Z*-aplysinopsin (**5.1**, **5.2**) and *E*/*Z*-3′-deimino-3′-oxoaplysinopsin (**5.3**, **5.4**) from eight Australian *Thorecta* spp[158]. Aplysinopsin and oxo-aplysinopsin differ only in ring C, featuring iminoimidazolidinone for the previous and imidazolidinedione for the latter.

Following the original report, aplysinopsins were reported from taxonomically unrelated marine invertebrates, with a consistent preference for the *E* over *Z* configuration. Examples include aplysinopsin reported by Hollenbeak and Schmit in 1977 from a Florida Keys *Verongia spengelii*[141], and by Djura and Faulkner from a Belize *Decritus* sp. in 1980[142]. The latter report also described 2′-deimino-methylaplysinopsin (**5.5**) and 6-bromo-2′-deimino-methylaplysinopsin (**5.6**). In 1982, Taylor *at al* reported methylaplysinopsin (**5.7**), which underwent a rapid equilibrium in solution to (*Z*)-methyl aplysinopsin (**5.8**), from an Australian *Aplysinopsis reticulata*[152], while Scheuer *et al* discovered (*E*)-aplysinopsin (**5.1**) along with dihydroaplysinopsin (**5.9)** from a Hawaiian scleractinian coral *Tubastraea cocinea*[159]. The NMR data for dihydroaplysinopsin were not reported until recently by Crews *at al* who also reported a series of other new dihydroaplysinopsins (**5.11-5.13**) from a Papua New Guinean *Thorectandra* and *Smenospongia* sp[160]. In 1985, (*E*)-aplysinopsin was reisolated by Fattorusso *et al* from a Naples Bay anthozoan *Astroides calaycularis*[161] together with 6-bromo-aplysinopsin (**5.14**) and *N*-propionyl derivatives (**5.15**-**5.16**)[161].

In the late 1980s, Guella *et al* reported a series of *E/Z* geometrical of oxo-aplysinopsins from Mediterranean and Pilipino scleractinian corals[144,145]. In 1988, these same authors discovered 3′-deimino-3′-oxoaplysinopsin (**5.17**, **5.18**) and 6-bromo-3′-deimino-3′-oxoaplysinopsin (**5.19**, **5.20**) existing as 5:2 mixture *E:Z* conformational isomers from a Philippine *Tubastrea* sp., and 3′-deimino-2′-4′-bis(demethyl)-3′-oxoaplysinopsin (**5.21**, **5.22**)[145] and 6-bromo-3′-deimino-2′-4′-bis(demethyl)-3′-oxoaplysinopsin (**5.23**, **5.24**) as 2:3 and 1:1 mixtures respectively of *E:Z* conformational isomers from a Mediterranean *Leptopsammia pruvoti*[144]. A year later, the same research group also discovered similar geometrical isomers (**5.25**-**5.28**) from a Philippine *Dendrophyllia* sp[145]. In both reports, Guella *et al* assigned the configuration about 8-1′ olefin based on long range heteronuclear ^{13}C-^{1}H coupling constants ($^{3}J_{C\text{-}H}$) using 2D HMBC correlation technique. This technique differentiated the magnitude of coupling constant ($^{3}J_{C\text{-}H}$) for *E* and *Z* configuration around 8-1′ of aplysinopsins with the previous being smaller (2-6 Hz) than the latter (8-12 Hz). Of interest, the two reports featured typical chemical shifts of H-2 and C-8 being more downfield in *E* than in *Z* isomers, a characteristic used by the same authors in assigning the *E* vs. *Z* configurations to oxo-aplysinopsin[145]. A similar technique was also used by Selic *et al* in resolving geometrical configuration for synthetic aplysinopsins in 2000[162] and by Kobayashi *et al* in assigning natural product aplysinopsins isolated from an Okinawan *Hyrtios erecta* in 2001[151].

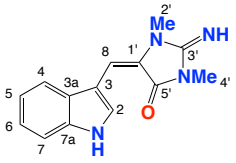

E-aplysinopsin (**5.1**)

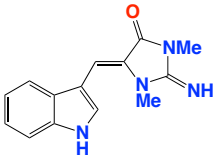

Z-aplysinopsin (**5.2**)

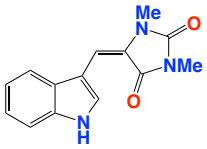

E-3'-deimino-3'-oxo aplysinopsin (**5.3**)

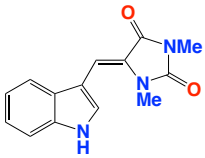

Z-3'-deimino-3'-oxo aplysinopsin (**5.4**)

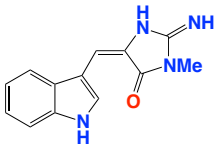

2'-demethyl aplysinopsin (**5.5**)

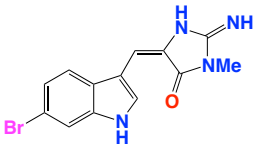

6 bromo-2'-demethyl aplysinopsin (**5.6**)

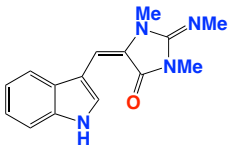

E-methylaplysinopsin (**5.7**)

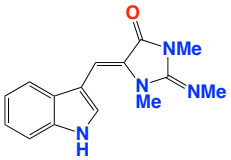

Z-methylaplysinopsin (**5.8**)

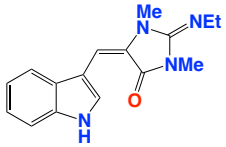

ethyl aplysinopsin (**5.9**)

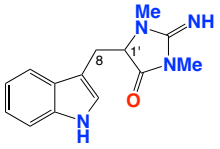

8,1'-dihydro aplysinopsin (**5.10**

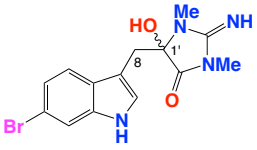

8,1'-hydroxy-6-bromo dihydroaplysinopsin (**5.11**)

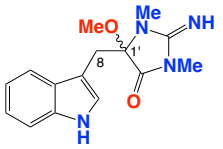

8,1'-methoxy-dihydroaplysinopsin (**5.12**)

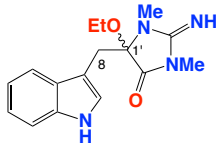

8,1'-ethoxy dihydroaplysinopsin (**5.13**)

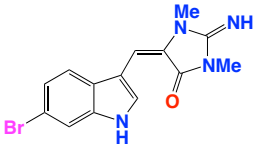

6 bromo-aplysinopsin (**5.14**)

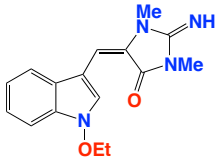

N-isopropionyl aplysinopsin (**5.15**)

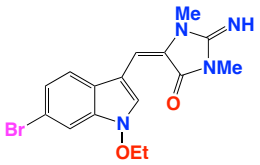

6-bromo-*N*-isopropionyl aplysinopsin (**5.16**)

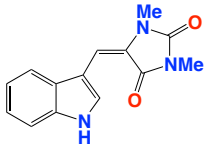

E-3'-deimino-3'-oxoaplysinopsin (**5.17**)

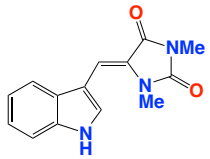

Z-3'-deimino-3'-oxoaplysinopsin (**5.18**)

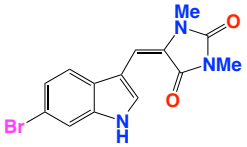

E-6 bromo-3'-deimino-3'-oxoaplysinopsin (**5.19**)

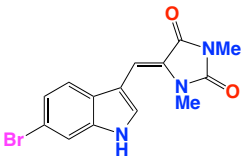

Z-6 bromo-3'-deimino-3'-oxoaplysinopsin (**5.20**)

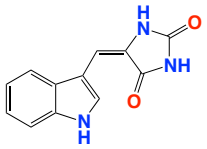

E-3'-deimino -2'-4'-bis(demethyl) oxoaplysinopsin (**5.21**)

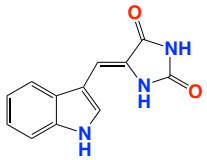

*Z*3'-deimino -2'-4'-bis(demethyl) oxoaplysinopsin (**5.22**)

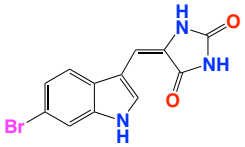

E-6-bromo-3'-deimino -2'-4'-bis(demethyl) oxoaplysinopsin (**5.23**)

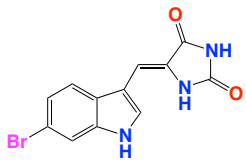

Z-6-bromo-3'-deimino -2'-4'-bis(demethyl) oxoaplysinopsin (**5.24**)

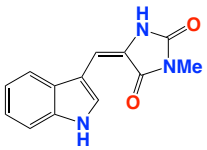

3'-deimino -2'-demethyl-oxoaplysinopsin (**5.25**)

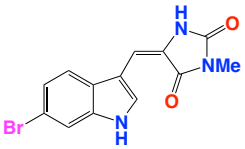

E-6 bromo-3'-deimino -2'-demethyl oxoaplysinopsin (**5.26**)

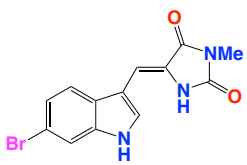

Z-6 bromo-3'-deimino -2'-demethyl oxoaplysinopsin (**5.27**)

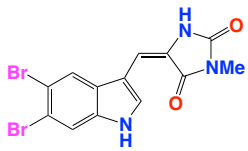

5,6-dirbomo-3'-deimino-2'-demethyl-oxoaplysinopsin (**5.28**)

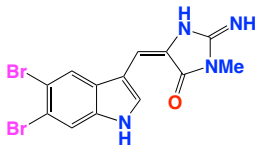

E-5,6 dibromo -3'-deimino-2'-demethyl aplysinopsin (**5.29**)

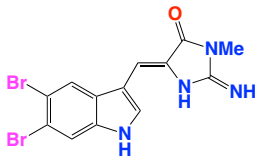

Z-5,6-dibromo -3'-deimino-2'-demethyl aplysinopsin (**5.30**)

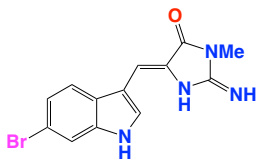

6 bromo-3'-deimino -2'-demethyl aplysinopsin (**5.31**)

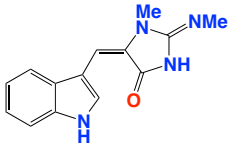

isoplysin (**5.32**)

Apart from geometric isomers, monomeric aplysinopsin derivatives also arise from different patterns of bromination and methylation. Aplysinopsins are typically brominated at C-6, although C-5 bromination is also known such as compounds **5.28**-**5.30**. Methylation in monomeric aplysinopsins has been reported to occur on the indole (i.e. **5.15**-**.5.16**) and iminoimidazole moieties (i.e. **5.1-5.14**, **5.17-5.20** and **5.25-5.32**) with the latter varying from mono methyl (**5.5**-**5.6**, **5.25-5.31**), dimethyl (**5.1-5.4**, **5.10**-**5.11**, **5.14**-**5.20**, **5.32**) and tri-methyls (**5.7**-**5.9**). Aplysinopsins methylated at *N*-2′ exist predominantly as *E* isomer[144,145]. The isomer configuration and methylation pattern were also reported to play an important role in bioactivity, particularly in serotonin receptor modulation (described more detail in bioactivity section, page 129)[149,150].

5.2.2 Dimeric Aplysinopsin

Perhaps the most unusual members of aplysinopsins are the dimeric aplysinopsins initially foreshadowed but not documented by NMR in a 2000 report by Koh and Sweatman[163]. It took another three years before the first aplysinopsin dimer was unambiguously documented. In 2003, Iwaga *et al* reported asymmetric dimeric aplysinopsins tubastrindoles A-C (**5.33-5.35**) from a Japanese scleractinian coral *Tubastraea* sp[147]. The co-occurrence of and structural resemblance between aplysinopsin and tubastrindoles prompted the authors to propose that tubastrindoles were Diels Alder cycloaddition adduct of aplysinopsins[147].

The same year, Mancini *et al* reported on cycloaplysinopsins A-B (**5.36-5.37**) from a Philippine Dendrophyliidae scleractinian coral. Cycloaplysinopsins A-B feature bisspiroiminoimidazolidione suggestive of Diels Alder adducts of oxoaplysinopsin[146]. Interestingly, the authors showed that tubastrindoles and cycloaplysinopsins exist as diastereomers and as such proposed the formation of tubastrindole B and cycloaplysinopsins A and B via a Diels Alder cycloaddition proceeded with oxidation[146] (discussed in more detail in the synthetic achievement part, page 136).

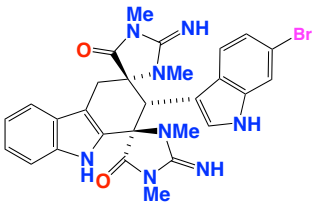

tubastriondole A (**5.33**)

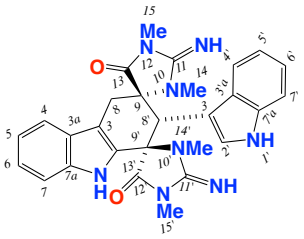

tubastriondole B (**5.34**)

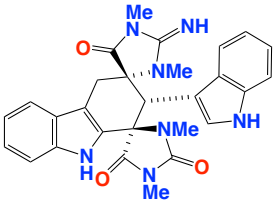

tubastriondole C (**5.35**)

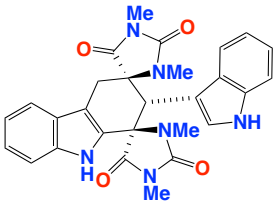

cycloaplysinopsin A (**5.36**)

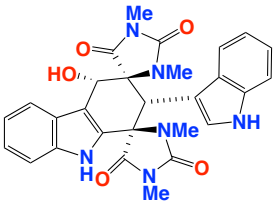

cycloaplysinopsin B (**5.37**)

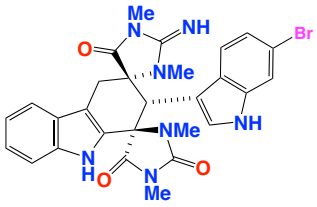

tubastriondole D (**5.38**)

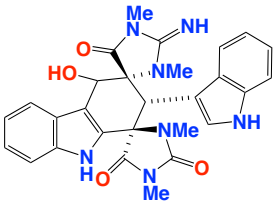

tubastriondole E (**5.39**)

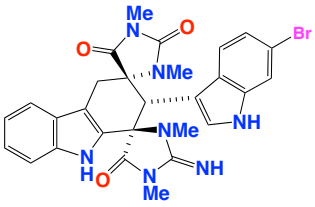

tubastriondole F (**5.40**)

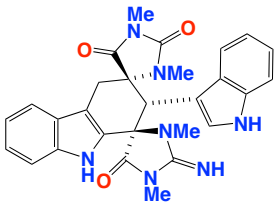

tubastriondole G (**5.41**)

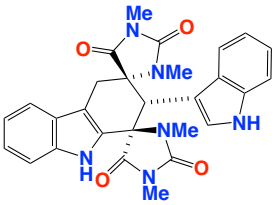

tubastriondole H (**5.42**)

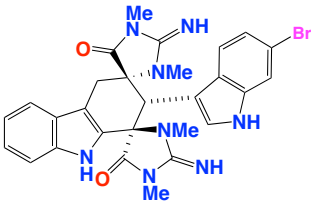

dictazoline A (**5.43**)

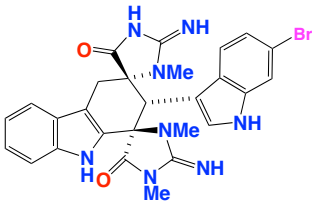

dictazoline B (**5.44**)

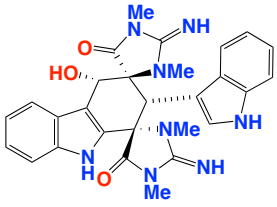

cycloaplysinopsin C (**5.45**)

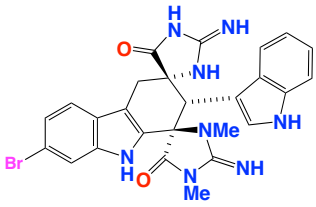

dictazoline C (**5.46**)

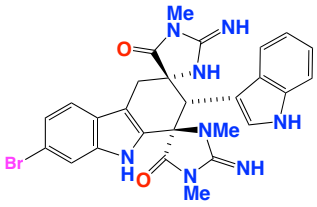

dictazoline D (**5.47**)

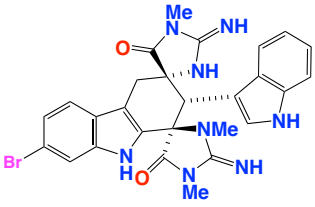

dictazoline E (**5.48**)

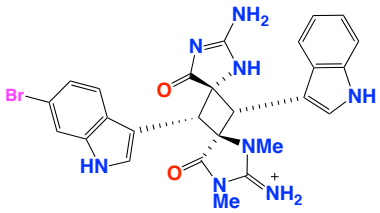

dictazole A (**5.49**)

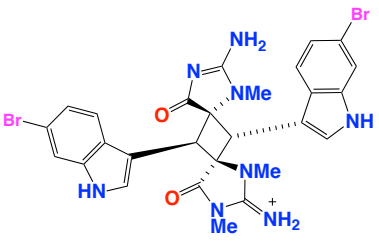

dictazole B (**5.50**)

In 2008, two research groups isolated new asymmetric dimers from a scleractinian coral of the genus *Tubastraea*. Iwagawa *et al* isolated tubastrindoles D-H (**5.38**-**5.42**) from a Japanese scleractinian coral *Tubastraea* sp[164] while William *et al* reported tubastrindole B and C together dictazolines A and B (**5.43**-**5.44**) from a Panamanian *Smenospongia cerebriformis*[165]. In early 2009, Meyer *et al* re-isolated aplysinopsin along with cycloaplysinopsin C (**5.45**), a new aplysinopsin from a Comoro Island *Tubastraea* sp[166]. The latter authors reported cycloaplysinopsin as having a very similar structure with cycloaplysinopsin B (**5.37**) but with different configuration at the spiro cyclohexyl configuration suggesting a new diastereomer[166].

In early 2010, William *et al* re-examined in detail and discovered dictazolines C-E (**5.46**-**5.48**) along with dictazole A (**5.49**) and B (**5.50**)[157]. Compounds **5.49** and **5.50** featured a cyclobutyl instead of a cyclohexyl structure, representing the first symmetric dimeric aplysinopsin. The discovery of dictazoles A and B have given a dimension to the aplysinopsin structure class as the authors proposed a new biosynthetic pathway for the formation of dimeric aplysinopsin, cyclobutane rearrangement (discussed in detail in the synthetic achievement for dimeric aplysinopsin, page 136)[157].

Interestingly, both asymmetric and symmetric aplysinopsin dimers are capable of isomerisation with their stereochemistry mainly assigned on the basis of NOE analysis. To date, three diastereoisomers have been reported in the literature for asymmetric dimers proposed as cycloaddition of two aplysinopsin monomers one acting as diene and the other as dienophile such as in two *E* monomers in cycloaplysinopsin A (**5.36**), *Z* and *E* monomers in tubastrindole B (**5.33**)[146] and *E* and *Z* monomers in cycloaplysinopsin C (**5.45**)[166] (see Scheme 5.1, page 135). Similarly, two epimers for the symmetric aplysinopsins are known today including dictazole A (**5.49**) and dictazole B (**5.50**). These epimers are distinguishable both from their optical rotation values (positive vs. negative for dictazole A and B respectively) and NOE correlations[157] (the presence vs. absence of NOE coupling between two methines in the cyclobutane rings for dictazole A and B respectively)[157,165].

5.2.3 Biological Activity

Despite their intriguing structural features, little is known about biological activity of dimeric aplysinopsins other than the fact that cycloaplysinopsin C (**5.45**) and dictazole A (**5.49**) exerted antiplasmodial[166] and BACE (β-secretase inhibitor screening) modulating[157] activities respectively. In contrast, many biological activities have been reported for the monomeric aplysinopsin including antibacterial, antiplasmodial, anticancer and antidepressant agents with anticancer and antidepressant being the most interesting feature. Apart from bromination, methylation also plays a key role in dictating the bioactivity of the monomeric aplysinopsins[149-151] (see Table 5.1 for detail).

5.2.3.1 Monomer Aplysinopsins

Aplysinopsins have been evaluated against antidepressant targets such as monoamine oxidase (MAO), nitric oxidase synthase (NOS) and the uptake of serotonin receptors. Several serotonin receptors reside in nerve and other cells mediating the effect of serotonin, endogenous ligands and many pharmaceuticals. In particular, 5-TH_2 type receptor (specifically 5-TH_{2A} and 5-TH_{2C}) are drug targets for antidepressant and antiobesity therapeutics[149]. Excessive production of nitric oxide (NO) has been associated with various diseases including post ischemic stroke damage, development of colitis, schizophrenia, tissue damage and pathological inflammation with specific inhibitors of NO production deemed an efficient approach to treat the above-mentioned diseases[151]. MAO inhibitor has a long story of use as an effective treatment for Parkinson's disease, as well as several other diseases including depression. Some aplysinopsins that are active against the above biological targets include **5.5**-**5.7**, **5.9-5.14**, **5.29**-**5.32** and **5.51** (Figure 5.1).

The pharmacological potential of methylaplysinopsin (**5.7**) in inhibiting monoamine oxidase (MAO) has been intensively studied with an *in vitro* study reporting inhibition of MAO from mouse brain homogenate at 0.1-100 μM[167]. Following an oral administration in mice and rats, **5.7** exhibited relatively short-term and reversible inhibition against MAO. In pharmacokinetic studies on rats, it was shown that after intravenous administration, the concentration of methylaplysinopsin in plasma declined rapidly over 4.8 h, reaching the level of below 1 ng/mL 8 h after treatment[167].

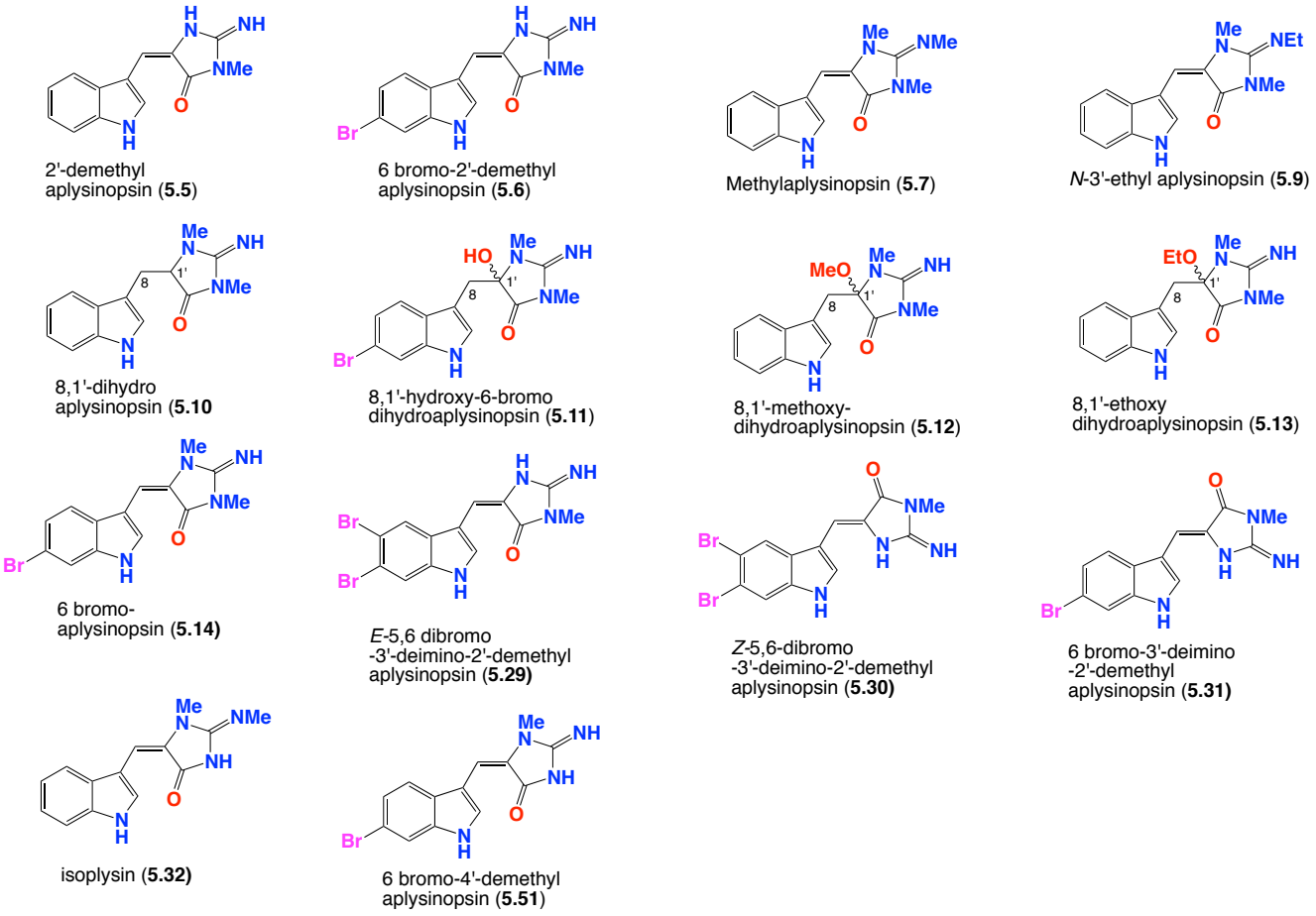

Figure 5.2. Examples of active monomeric aplysinopsins as antimicrobial, anticancer and neuromodulator agents.

Three geometric isomers of aplysinopsins were evaluated as inhibitors of NOS, in particular neuronal and inducible isozymes of nitric oxide synthase, nNOS and iNOS respectively. Examples include the geometrical isomers *E*/*Z*-5,6-dibromo-8Z,2′-demethyl aplysinopsins (**5.29-5.30**) reported by Kobayashi and co-workers from an Okinawan *Hirtois aurecta*[168]. These aplysinopsins showed specific inhibitory activity against nNOS, an activity that was absent from known NOS inhibitor such as N-monomethyl-L-arginine (L-NMMA)[168].

Hamman and co-workers reported several aplysinopsins from a Jamaican sponge *Smenospongia* sp. and three sponges of the family Thorecta[150]. These metabolites included 2′-demethylaplysinopsin (**5.5**), 6-bromo-2′-demethyl-aplysinopsin (**5.6**), methylaplysinopsin (**5.7**), 6-bromo-aplysinopsin (**5.14**), ethyl aplysinopsin (**5.9**) and isoplysin (**5.32**). These monomeric aplysinopsins were evaluated against *Plasmodium falciparum* and serotonin receptors types 2 (5-H_{T2}) particularly 5-HT_{2A} and 5-HT_{2C}[150].

On evaluation against human serotonin receptor subtype 5-HT_{2A} and 5-HT_{2C}, half of the six monomeric aplysinopsins were active against the receptors including 6-bromo-2′-demethylaplysinopsin (**5.6**), ethylaplysinopsin (**5.9**) and 6-bromo aplysinopsin (**5.14**). Although these three compounds showed high affinity antagonist binding towards 5-HT_{2C} receptor subtype, only **5.9** and **5.14** showed potent activity against receptor 5-HT_{2A} subtype[150]. Of these, **5.14** showed the highest affinity against 5-HT_{2C} receptor subtype resembling the equilibrium affinity constant (K_i) value of the indigenous receptor, K_I = 0.13 μM and 0.33 μM for serotonin and **5.14** respectively. In terms of specificity, however, **5.6** revealed >40 fold selectivity for 5-HT_{2C} over 5-HT_{2A}[150]. The authors argued that these results indicated the important role of alkyl chain at *N*-3′ and bromination position at C-6 in increasing binding property and specificity of aplysinopsin type compounds towards the serotonin 5-HT_2 receptor[150] (Table 5.1).

Upon evaluation for antiplasmodial activity, it was shown *in vitro* that 6-bromo-2′-demethylaplysinopsin (**5.6**), 6-bromo-aplysinopsin (**5.14**) and isoplysin (**5.32**) were active against the D6 clone of *Plasmodium falciparum*[150]. Compound **5.14** revealed strong antimalarial activity at 0.34 μg/mL with a selectivity index of 14 while isoplysin (**5.32**) and 6-bromo-2′-demethylaplysinopsin (**5.6**) exhibited moderate activity at 0.97 and 1.1 μg/mL and with a selectivity index of >4.9 and >43 respectively. It was also proven that compound **5.6** inhibited the antimalarial target plasmepsin II enzyme with IC_{50} values of 53 μM (FRET) and 66 μM (FP)[150].

A series of monomeric aplysinopsins have also been evaluated against various pathogenic microbes many of which were inactive and/or with modest antimicrobial activity. Tymiak and Rinehart reported that a mixture of 6-bromo-aplysinopsin (**5.14**) and 6-bromo-4′-demethylaplysinospin (**5.51**) modestly inhibited *Bacillus subtilis* but were inactive against *Escherichia coli*, *Saccharomyces cerevisiae* and *Penicillium atrovenetum*[169]. When screening aplysinopsin (**5.1**) and 6-bromoaplysinopsin (**5.14**) for antibacterial, antiviral and antifungal activities, Gulati *et al* discovered **5.1** as the active compound modestly inhibiting only the fungus *Trichophyton mentagrophytes*[170]. In addition, Koh and Sweatman discovered aplysinopsin (**5.1**) and 6-bromoaplysinopsin (**5.14**) from an Australian scleractinian *Tubastraea faulkneri* as weak antimicrobial agents against *Staphylococcus aureus*[163] while Seagraves and Crews isolated a series dihydroaplysinopsins (**5.9-5.12**) from Papua New Guinean sponges *Thorectandra* sp. and *Smenospongia* sp. as having modest antibacterial activity against *Staphylococcus epidermis* (MIC = 6.25 to 100 ug/mL)[160].

Finally, monomeric aplysinopsin are also known as anticancer agents. According to Hollenbeak and Schmitz, aplysinopsin (**5.1**) showed cytotoxic activity against P388 lymphocytic leukaemia at 200 mg/kg in mice and appeared to be active against P338, human epidermoid carcinoma KB and murine lymphoma LH-1220 cancer cell lines[141]. Together with methylaplysinopsin (**5.7**), aplysinopsin (**5.1**) was also shown to inhibit LH-1220 (IC_{50} 11.5 mg/mL and KB (31% inhibition at 20 μg/mL) cancer cell lines respectively[171]. Isoplysin discovered from an Okinawan *Aplysina* sp. was reported as a weak cytotoxic agent against murine lymphoma L-1210 (IC_{50} 11.5 μg/mL) and human epidermoid carcinoma KB (30% inhibition at 20 μg/mL) cell lines[171].

5.2.3.2 Dimeric Aplysinopsin

Unlike monomeric aplysinopsin, most of the dimeric aplysinopsins have been repeatedly reported as inactive in many bioassays such as antibacterial, antiviral, cytotoxic and BACE1 inhibitor tests with the exception being the antimalarial activity (inhibitor of *Plasmodium falciparum*, IC_{50} = 1.2 μg/mL) attributed to cycloaplysinopsin C (**5.45**)[166] and inhibitory property against BACE1 (IC_{50} = 50 μg/mL) attributed to dictazole A (**5.49**) (Table 5.1)[157].

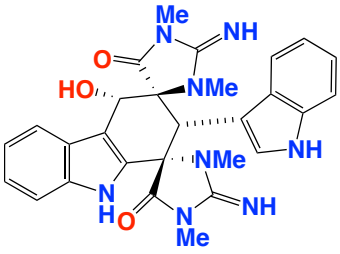

cycloaplysinopsin C (**5.45**)

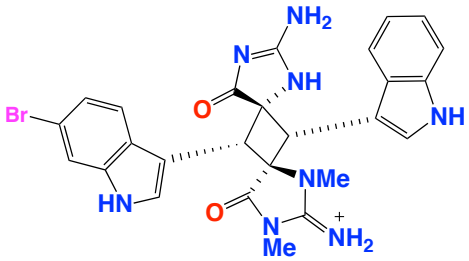

dictazole A (**5.49**)

Table 5.1 Bioactivity of monomeric and dimeric aplysinopsin

No	Compound		Biological Target	Activity /References
5.1	Aplysinopsin/monomer	M	Anticancer Anticancer	Inhibited fungus *Trichophyton mengographytes* Inhibited P388 lymphocytic leukaemia in mice, cytotoxic against P338 human epidemoide carcinoma and LH-1220 cancer cell lines. Cytotoxic against LH-1220 (IC_{50} 2.3 mg/mL).
5.6	6-bromo-2′-demethylaplysinopsin/monomer	M	Antidepressant Antiplasmodial	Stronger displacer of 5-HT_{2A} than 5-HT_{2c} (>100 mM vs. 2.3 μM)[150], weak inhibitor of iNOS (7.5% at 125 mg/mL [168]. Moderate inhibitor of D6 clone (1.1 mg/mL, SI >4.3). Strong inhibitor of antimalarial target plasmepsin II enzyme (IC_{50} 53 μM (FRET) and 6.6 μM (FP)
5.7	Methylaplysinopsin/monomer	M	Antidepressant Anticancer	Tetrabenazine-induced ptosis[158], weak displacer of serotonin but more potent displacer of [3H]-serotonin Cytotoxic against LH-1220 (IC_{50} 3.5 mg/mL)[167].
5.9	Ethylaplysinopsin/monomer	M	Antidepressant	Strong modulator of 5-HT_{2A} and 5-HT_{2C} (1.7 vs. 3.5 μM).
5.10	8-1′-dihydroaplysinopsin/monomer	M	Antibacterial	Weak antibacterial against *Staphylococcus aureus* (mg/mL))[160]
5.10	6-bromo-8-1′-dihydroaplysinopsin /monomer		Antibacterial	Weak antibacterial against *Staphylococcus aureus* (mg/mL))[160]
5.11	8-1′-methoxy-dihydroaplysinopsin/monomer	M	Antibacterial	Weak antibacterial against *Staphylococcus aureus* (mg/mL))[160]
5.12	8-1′-ethoxy dihydroaplysinopsin/monomer	M	Antibacterial	Weak antibacterial against *Staphylococcus aureus* (mg/mL))[160]
5.13	6-bromo-aplysinopsin/monomer	M	Antibacterial Antiplasmodial	Weak antibacterial against *Staphylococcus aureus* (mg/mL))[160] Inhibited D6 clone of *Plasmodium falciparum* (0.34 mg/mL, SI=14 but inactive in vivo studies.
5.29	*E*-5,6-dibromo-2-demethylaplysinoposin/monomer			Strong inhibitor of nNOZ (100% and 32% at 125 and 5 μg/mL respectively[168].
5.30	*Z*-5,6-dibromo-2-demethylaplysinoposin/monomer	M		Stung inhibitor of nNOZ (100% and 22% at 125 and 5 μg/mL respectively[168].
5.31	Isoplysin/monomer	M	Anticancer Antiplasmodial	Inhibited LH-1220 (IC_{50} 11.5 μg/mL) and KB (31% at 20 μg/mL). Moderate inhibitor of D6 clone 0.97 mg/mL and Si >4.9
	6-bromo-4'-demethyl-aplysinopsin/monomer	M		Weak inhibition against *Bacillus subtills* but was inactive against *E. coli*, *S. carevisiae* and *Pencicillium airovenetum*.
5.33	Tubastrindole A/dimer		Antibacterial, antifungal, cytotoxicity, β-secretase	Inactive [147]
5.34	Tubastrindole B/dimer	M	Antibacterial, antifungal, cytotoxicity, β-secretase	Inactive [147]
5.35	Tubastrindole C/dimer	D	Antibacterial, antifungal, cytotoxicity, β-secretase	Inactive [147]
5.36	Cycloaplysinopsin A/dimer	D	NA	NA[146]
5.37	Cycloaplysinopsin B/dimer	D	NA	NA[146]

Note: M = monomer, D = dimer

No	Compound		Biological Target	Activity /References
5.38	Tubastrindole D/dimer	D	Antibacterial, antifungal, cytotoxicity	Inactive [164]
5.39	Tubastrindole E/dimer	D	Antibacterial, antifungal, cytotoxicity	Inactive [164]
5.40	Tubastrindole F/dimer	D	Antibacterial, antifungal, cytotoxicity	Inactive [164]
5.41	Tubastrindole G/dimer	D	Antibacterial, antifungal, cytotoxicity	Inactive [164]
5.42	Tubastrindole H/dimer	D	Antibacterial, antifungal, cytotoxicity	Inactive [164]
5.43	Dictazoline A/dimer	D	BACE assay	Inactive[165]
5.44	Dictazoline B/dimer	D	BACE assay	Inactive [165]
5.45	Cycloaplysinopsin C/dimer	D	Antiplasmodial	Inhibitor of two Plasmodium falciparum strains, a chloroquine-sensitive (F32/Tanzania, IC_{50} 2.7 μM) and chloroquine-resistence (FcB1 Columbia, IC_{50} 1.8 μM)[166]
5.46	Dictazoline C/dimer	D	BACE assay	Inactive [165]
5.47	Dictazoline D/dimer	D	BACE assay	Inactive [165]
5.48	Dictazoline E/dimer	D	BACE assay	Inactive [165]
5.49	Dictazole A/dimer	D	BACE inhibitor (mamapcin 2)	Inhibited BACE1-mediated cleavage of amyloid precursor with an IC_{50} value of 50 μg/mL[157]
5.50	Dictazole B/dimer	D	BACE assay	Inactive

Note: M = monomer, D = dimer

5.2.4 Synthetic Achievement

Despite their intriguing structures, to date there is no synthetic report on dimeric aplysinopsin. Synthetically inaccessible and the absence of bioactivity of dimer aplysinopsin may have been a major factor in impeding the exploration of aplysinopsin biological properties. In contrast, monomeric aplysinopsins have been reported to exert a range of bioactivities in particular antidepressant, anticancer and antilehsmanial inspiring many synthesis efforts.

5.2.4.1 Monomeric Aplysinopsin

One of such synthetic efforts included the incorporation of aplysinopsin into known drug fragment such as antilehsmanial drug pentamidine (**5.53**) to improve potency and efficacy of the known drug. The rationale behind this synthetic effort rested on the dicationic nature of aplysinopsins and pentamidine[154], a pharmachopore responsible for the activity of these alkaloids against plasmepsin II and serotonin receptors[150,154]. This fragment-

based discovery yielded a hit molecule (**5.54**) with IC_{50} value of 18.2 μM, which upon optimisation resulted in **5.55** and **5.56** with IC_{50} values of 6.5 and 2.0 μM for the *Z* and *E* aplysinopsin hybrids respectively[154]. In particular the *E* isomer **5.56** (the most promising compound in this study) showed 10 times stronger than pentamidine in intracellular amastigote assay and 401 times less toxic for human macrophage than the known drug[154].

Another approach was the evaluation and synthesis of monomeric aplysinopsin serotonin receptor particularly type 2-serotonin receptor (5-HT2a and 5HT-2c) due their structural similarity. In 2006, Hamman *et al* reported on aplysinopsin that revealed higher inhibitory selectivity towards 5-HT_{2A} over 5-HT_{2C} encouraged synthesis efforts to discover more selective and potent inhibitors of 5-HT_{2A} over 5-HT_{2C}[150]. Inspired by this discovery, in 2010 Schetz *et al* synthesized more than 20 aplysinopsin derivatives three of which **5.57**-**5.60** exhibited selectivity for 5-HT_{2A} over 5-HT_{2C}[153]. The aplysinopsin analogue **5.60** was approximately 2100-fold more selective at inhibiting the serotonin 5-HT_{2C} receptor subtype: an affinity for 5-HT_{2C} was of 46 μM and no detectable affinity for the 5-HT_{1A} or 5-HT_{2A} receptor subtypes. Also discussed in the paper[153] was structure activity relationship significance of alkylation of the imidazolidinone and bromination of the indole ring[153].

Aplysinopsins have also inspired the discovery of anticancer agents[156]. In 2011, Crooks *et al* synthesized a series of aplysinopsin analogues. These compounds were tested for cytotoxicity against 60 human tumour cell lines including leukaemia, non-small cell lung, colon, CNS, melanoma, ovarian, renal, prostate and brest cancers. Of these, compounds **5.61** inhibited melanoma UACC-257 (GI_{50} = 13.3 μM) and OVCAR-8 (GI_{50} = 19.5 μM) cancer cells. A second analogue **5.62** exhibited cytotoxicity against 60 cancer cell lines (GI_{50} 0.3 to 6.0 μM). Thus, aplysinopsin hybrids **5.61** and **5.62** can be regarded as useful lead compounds for further structural optimization as antitumor agent[156].

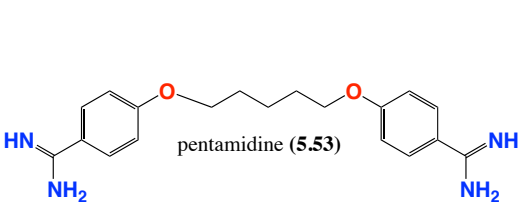

pentamidine **(5.53)**

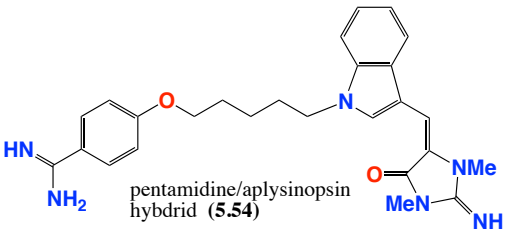

pentamidine/aplysinopsin hybdrid **(5.54)**

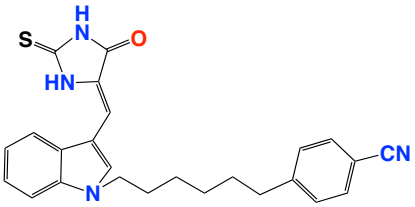

pentamidine/aplysinopsin hybdrid **(5.55)**

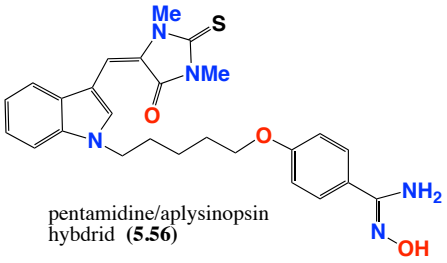

pentamidine/aplysinopsin hybdrid **(5.56)**

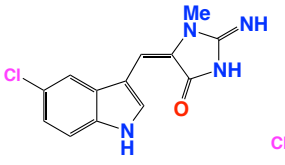

(5.57)

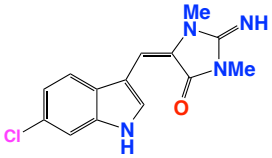

(5.58)

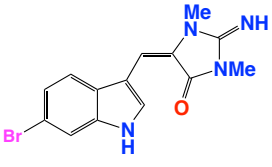

(5.59)

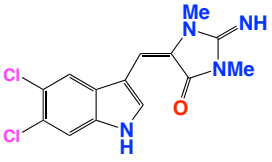

(5.60)

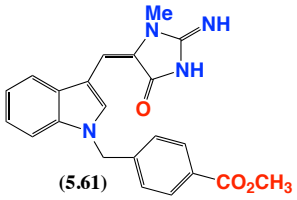

(5.61)

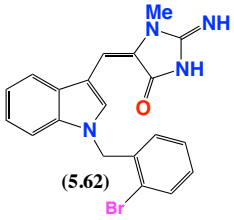

(5.62)

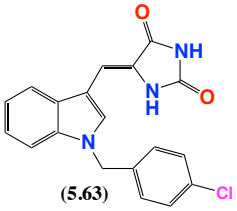

(5.63)

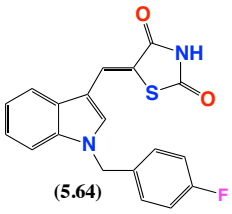

(5.64)

5.2.4.2 Dimeric Aplysinopsins

The co-existence of and striking structural similarities between monomeric and dimeric aplysinopsins have led to the hypothesis that the latter were biosynthetically derived from the former by a Diels Alder cycloaddition process, although the specifics of this mechanism are yet to be agreed (Scheme 5.1)[146].

Although this Diels Alder hypothesis seems creditable, all efforts at synthetically initiating Diels Alder coupling between aplysinopsin monomers have failed. Although the chiral nature of the natural products demands an enzymatic process, the failure to chemically activate a Diels Alder coupling is certainly surprising, and could suggest that the original biosynthetic hypothesis is flawed.

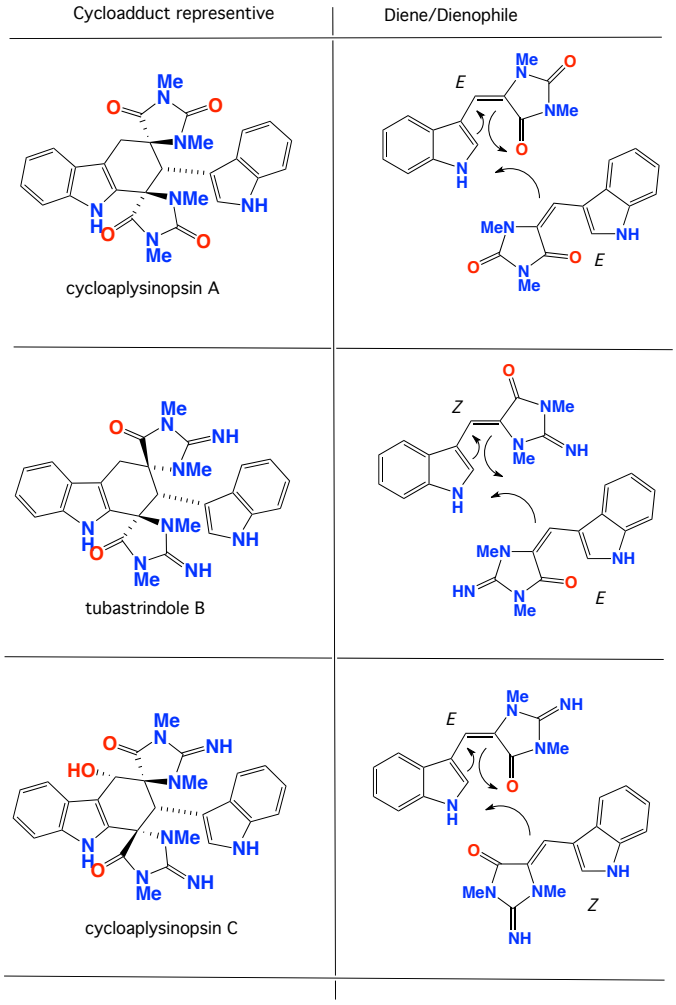

Scheme 5.1. Plausible formation of dimers from monomers adapted from Mancini *et al* 2003[146]

The discovery of dictazoles A-B in early 2010 prompted an alternative biosynthetic hypothesis, one transitioning through a 2+2 cycloaddition leading to the cyclobutyl dictazoles, with concomitant radical ring expansion to deliver the cyclohexyl aplysinopsin dimers[157] (Scheme 5.2 below). It was inspired by an early study on the cyclohexyl moiety in sceptrin (**5.65**)[172] which although initially believed to be derived from a Diels Alder cycloaddition was later determined to be generated by ring expansion in sceptrin (Scheme 5.2). This hypothesis was further supported by the detection of higher levels of the cyclobutyl dictazoles A and B in a Panamanian *Smenospongia* sp[160].

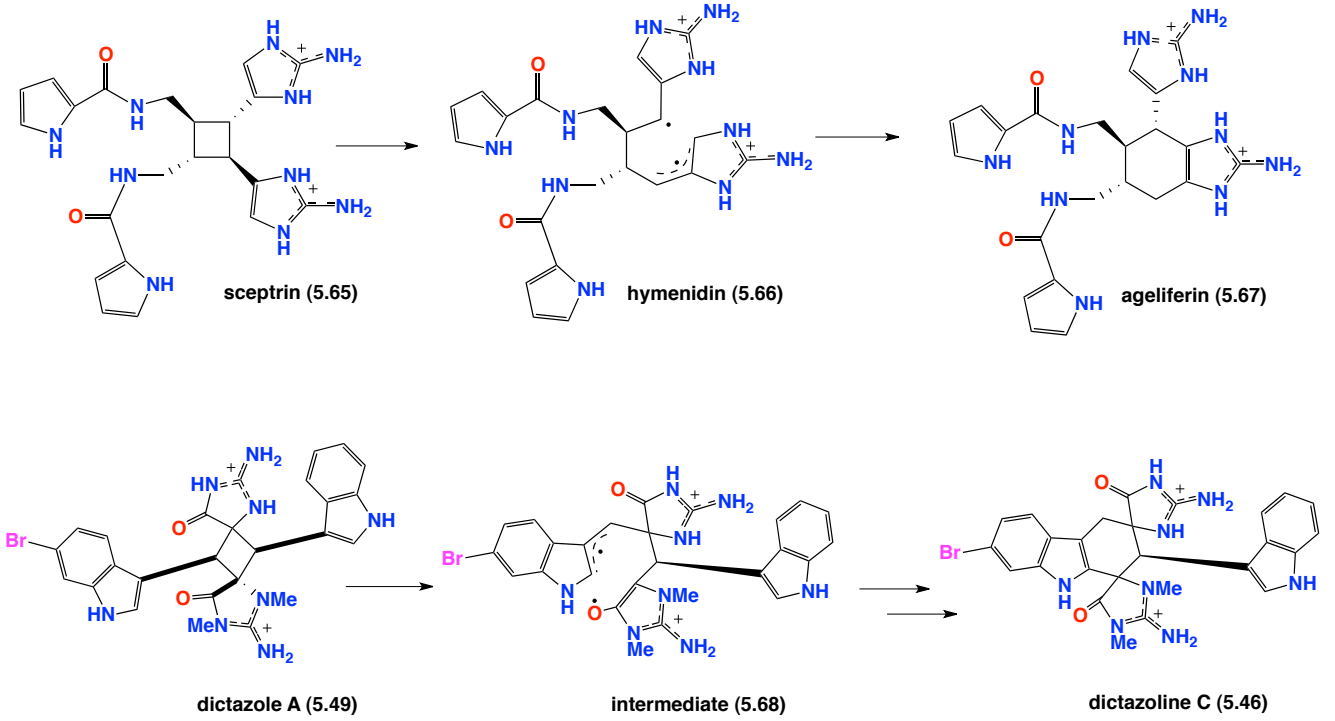

Scheme 5.2. Plausible formation of dictazolines C from dictazole A through a cyclobutane rearrangement (below) inspired by the same reaction in sceptrin[172] (above) adapted from Dai *et al* 2009[157].

This chapter describes the discovery of new, potent and selective modulators of glycine receptors (GlyRs) from an Australian *Ianthella cf flabelliformis*. Chemical profiling (LCMS, ^{1}H NMR and literature studies) showed the presence of two distinct metabolites in the specimen, terpenes and indole alkaloids. Two unreported pseudomolecular ions were detected in the terpenoid containing fractions (t_R = 10.73 and 11.21 min., Table 2.2) while the non-terpenoid fraction revealed pseudomolecular ions correspond to monomeric (t_R = 5.67-9.49 min.) and dimeric aplysinopsins (tR = 5.60 min., Table 2.2). Primary screening revealed indole alkaloid fractions as the active component of the Australian *Ianthella cf. flabelliformis*. In particular, a fraction (t_R = 5.60 and 9.13 min., Table 2.2) corresponding to molecular weights of 508 and 254 (dimeric and monomeric aplysinopsins) showed potent potentiating activity against GlyRα1. These data prompted a more detailed investigation of the metabolites of *Ianthella cf. flabelliformis* as new source of novel, potent and selective GlyR modulators.

The following paper details our discovery of two new nitrogenous sesquiterpenes ianthellalactam A (**5.66**) and B (**5.67**), an artefact ethyldictyondendrilin (**5.68**) and 5 known indole alkaloids aplysinopsin (**5.1**), 8*E*-3′-deimino-3′-oxo-aplysinopsin (**5.3**), 8*Z*-3′-deimino-3′-oxo-aplysinopsin (**5.4**), dihydroaplysinopsin (**5.10**) and tubastrindole B (**5.34**), three of which were novel GlyR modulators (**5.3-5.4** and **5.34**). The activity of these GlyR modulators inspired one-pot synthesis giving rise to four synthetic compounds 8*E*-3′-deimino-2′-4′-bisdemethyl-3′-oxoaplysinopsin (**5.69)**, 8*E*-3′-deimino-4′-bisdemethyl-3′-oxoaplysinopsin **(5.70**), 8*Z*-3′-deimino-4′-bisdemethyl-3′-oxoaplysinopsin (**5.71**), 8*E*-4′-demethylaplysinopsin (**5.72**) and 8*Z*-4′-demethylaplysinopsin (**5.73**), two of which (**5.70-5.71**) showing strong antagonist activity against GlyRα1.

Note: The numbering system for all metabolites of *Ianthella cf. flabelliformis* in this introduction and conclusion of this thesis is different from the ones at the paper and its supporting information.

Bioorganic & Medicinal Chemistry 21 (2013) 4420–4425

Contents lists available at SciVerse ScienceDirect

Bioorganic & Medicinal Chemistry

journal homepage: www.elsevier.com/locate/bmc

Australian marine sponge alkaloids as a new class of glycine-gated chloride channel receptor modulator

Walter Balansa [a,†], Robiul Islam [b,†], Daniel F. Gilbert [b], Frank Fontaine [a], Xue Xiao [a], Hua Zhang [a], Andrew M. Piggott [a], Joseph W. Lynch [b,c,*], Robert J. Capon [a,*]

[a] Institute for Molecular Bioscience, The University of Queensland, St. Lucia, QLD 4072, Australia
[b] Queensland Brain Institute, The University of Queensland, St. Lucia, QLD 4072, Australia
[c] School of Biomedical Sciences, The University of Queensland, St. Lucia, QLD 4072, Australia

ARTICLE INFO

Article history:
Received 25 February 2013
Revised 10 April 2013
Accepted 18 April 2013
Available online 1 May 2013

Keywords:
Glycine-gated chloride channel receptor modulators
Sesterterpene tetronic acid glycinyl lactams
Ianthella cf. *flabelliformis*
Marine natural products chemistry

ABSTRACT

Chemical analysis of a specimen of the sponge *Ianthella* cf. *flabelliformis* returned two new sesquiterpene glycinyl lactams, ianthellalactams A (**1**) and B (**2**), the known sponge sesquiterpene dictyodendrillin (**3**) and its ethanolysis artifact ethyl dictyodendrillin (**4**), and five known sponge indole alkaloids, aplysinopsin (**5**), 8*E*-3′-deimino-3′-oxoaplysinopsin (**6**), 8*Z*-3′-deimino-3′-oxoaplysinopsin (**7**), dihydroaplysinopsin (**8**) and tubastrindole B (**9**). The equilibrated mixture **6**/**7** exhibited glycine-gated chloride channel receptor (GlyR) antagonist activity with a bias towards α3 over α1 GlyR, while tubastrindole B (**9**) exhibited a bias towards α1 over α3 GlyR. At low- to sub-micromolar concentrations, **9** was also a selective potentiator of α1 GlyR, with no effect on α3 GlyR—a pharmacology that could prove useful in the treatment of movement disorders such as spasticity and hyperekplexia. Our investigations into the GlyR modulatory properties of **1**–**9** were further supported by the synthesis of a number of structurally related indole alkaloids.

1. Introduction

Glycine-gated chloride channel receptors (GlyRs) are members of the Cys-loop ion channel receptor family comprising subunits α1–α4 and β. They play a pivotal role in orchestrating inhibitory neurotransmission in the spinal cord, brainstem and retina,[1] with functional GlyRs being formed either as pentameric homomers or as αβ heteromers. GlyR subunits exhibit differential central nervous system distributions that are particularly evident in the superficial dorsal horn of the spinal cord[2] and the retina.[3–6] The physiological consequences of differential distribution patterns are difficult to establish as there are currently few pharmacological probes that can selectively inhibit different GlyR isoforms,[7] and therefore small molecule isoform-selective GlyRs modulators (agonists, antagonists, potentiators) would have significant value as both pharmacological tools and as lead compounds for inflammatory pain,[2,8] opioid-induced breathing disorders,[9] epilepsy[10] and movement disorders.[11] In an attempt to address this need, we recently screened a library of >2500 southern Australian and Antarctic marine invertebrates and algae for metabolites displaying GlyR-modulating properties. This approach successfully identified a number of promising extracts, and in a preliminary report[12] we described sesterterpene tetronic acid glycinyl-lactams from several *Ircinia* spp., as a new class of isoform selective GlyR modulators. This report extends on our earlier findings and details the chemical analysis of a specimen of the GlyR-active sponge *Ianthella* cf. *flabelliformis*.

2. Results and discussion

A portion of the EtOH extract of *Ianthella* cf. *flabelliformis* was decanted, dried in vacuo and subjected to solvent partitioning and trituration. The GlyR-modulatory CH_2Cl_2- and MeOH-soluble materials were further fractionated by reversed phase HPLC to yield two new sesquiterpene lactams ianthellalactams A (**1**) and B (**2**), the known sponge sesquiterpene dictyodendrillin[13] (**3**), its ethanolysis artifact ethyl dictyodendrillin (**4**), and five known sponge indole alkaloids, aplysinopsin[14] (**5**), 8*E*-3′-deimino-3′-oxoaplysinopsin[15] (**6**), 8*Z*-3′-deimino-3′-oxoaplysinopsin[15] (**7**), dihydroaplysinopsin[16] (**8**) and tubastrindole B[17] (**9**) (Fig. 1). The compounds **3**–**9** were characterized by detailed spectroscopic analysis and comparison with literature data (see Supplementary data).

High resolution ESI(+)MS analysis of **1** and **2** revealed quasi-molecular ions $[M+H]^+$ consistent with isomeric molecular formulae ($C_{17}H_{25}NO_3$) incorporating six double bond equivalents

* Corresponding authors. Tel.: +61 7 3346 6375; fax: +61 7 3346 6301 (J.W.L.); tel.: +61 7 3346 2979; fax: +61 7 3346 2090 (R.J.C.).
E-mail addresses: j.lynch@uq.edu.au (J.W. Lynch), r.capon@uq.edu.au (R.J. Capon).
† These authors contributed equally to this work.

0968-0896/$ - see front matter © 2013 Elsevier Ltd. All rights reserved.
http://dx.doi.org/10.1016/j.bmc.2013.04.061

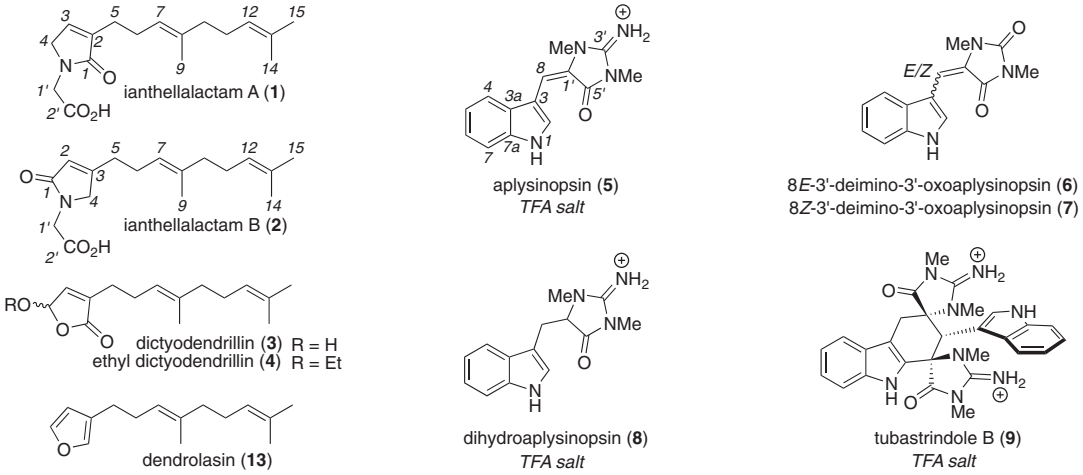

Figure 1. *Ianthella* cf. *flabelliformis* metabolites **1**–**9**, and dendrolasin (**13**).

(DBE). Analysis of the 1D and 2D NMR (methanol-d_4) data for **1** and **2** (Table 1 and Fig. 2) revealed resonances and correlations consistent with common geranyl and glycinyl residues, and differing trisubstituted α,β-unsaturated esters/lactones. These observations account for five DBE and require that both **1** and **2** be monocyclic. Diagnostic deshielded C-9 resonances supported assignment of *E* $\Delta^{7,8}$ configurations for **1** (δ_C 16.3) and **2** (δ_C 16.3), further confirmed by comparison to authentic samples of the closely related dictyodendrillin (**3**) and dendrolasin (**13**). HMBC correlations and significant deshielding of H-3 in **1** (δ_H 6.88) compared to H-2 in **2** (δ_H 5.85) confirmed the presence of regioisomeric glycinyl lactam moieties. Thus the complete structures for ianthellalactams A (**1**) and B (**2**) were assigned as shown.

Although **1** and **2** possess a rare glycinyl lactam moiety in common with the ircinialactams[12] (marine sponge metabolites previously reported by us as potent GlyR modulators), neither **1** nor **2** exhibited any effect against either α1 or α3 GlyRs. Indeed, following a comprehensive testing of all metabolites the GlyR modulatory activity detected in the crude *Ianthella* cf. *flabelliformis* extract was attributed solely to **6**/**7**, and **9** (Fig. 3 and Table 2). Whereas the (photo-activated) equilibrating mixture of geometric isomers **6**/**7** exhibited weak GlyR antagonist activity with a modest

Table 1
^{1}H (600 MHz) and ^{13}C (150 MHz) NMR data for ianthellalactams A (**1**) and B (**2**) in methanol-d_4

Position	Ianthellalactam A (**1**)		Ianthellalactam B (**2**)	
	δ_H, mult. (*J* in Hz)	δ_C[a]	δ_H, mult. (*J* in Hz)	δ_C[a]
1		174.4		175.0
2		139.7	5.85, tt (1.4, 1.4)	121.5
3	6.88, tt (1.6, 1.6)	138.9		164.6
4	4.05, dt (1.6, 1.6)	53.1	4.11, d (1.4)	56.8
5	2.29[b]	27.1	2.48, td (7.4, 1.4)	30.8
6	2.27[b]	27.2	2.30, br td (7.4, 7.1)	27.4
7	5.16, tq (6.9, 1.3)	124.8	5.16, tq (7.1, 1.3)	124.3
8		137.3		137.9
9	1.60, br s	16.3	1.64, br s	16.3
10	1.99, br t (7.6)	41.0	2.00, br t (7.6)	40.9
11	2.08, br td (7.6, 7.0)	27.9	2.08, br td (7.6, 7.0)	27.8
12	5.09, tqq (7.0, 1.4, 1.4)	125.6	5.08, tqq (7.0, 1.4, 1.4)	125.4
13		132.3		132.4
14	1.60, br s	17.9	1.60, br s	17.9
15	1.67, br s	26.0	1.66, br s	26.0
1′	4.21, s	44.9	4.17, s	44.4
2′		173.0		172.9

[a] ^{13}C NMR assignments supported by HSQC data.
[b] Overlapping resonances.

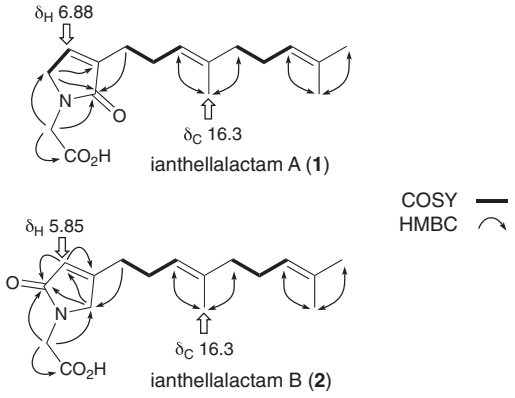

Figure 2. Diagnostic NMR (methanol-d_4) resonances and correlations for **1** and **2**.

bias towards α3 over α1, the dimeric analog tubastrindole B (**9**) proved to be a more potent GlyR antagonist with a bias towards α1 over α3. Of interest, **9** was found to be a selective potentiator of α1 GlyR at low- to sub-μM concentrations (126 ± 5% at 1 μM), while exhibiting no such effect on α3 GlyR—a pharmacology that could prove useful as a treatment for movement disorders such as spasticity and hyperekplexia (pronounced startle response). This unusual difference in activity at lower and high concentrations suggests **9** may have two distinct α1 GlyR binding sites.

To further probe the indole alkaloid GlyR pharmacophore exemplified by **6**/**7** and **9**, we employed aldol condensations to couple indole-3-carboxaldehyde with hydantoin, methyl hydantoin and creatinine, to synthesize the analogs **10**, **11a**/**b** and **12a**/**b** respectively (Fig. 4). Significantly, whereas the unmethylated hydantoin derived alkaloid **10** was prepared as the stable *E* isomer, the methylated analogs **11a** and **11b** derived from methyl hydantoin, and **12a** and **12b** derived from creatinine, existed as photolabile equilibrating mixtures of geometric isomers. These analogs were exposed to UV light for 3 h prior to bioassay to generate ~1:1 mixtures of the *E*/*Z* isomers. Of note, only the mixture **11a**/**b** exhibited significant GlyR modulatory activity, being a more potent GlyR antagonist than either **6**/**7** or **9**, with a bias favoring α1 over α3 (Fig. 3 and Table 2).

A structure–activity relationship analysis inspired by the monomeric alkaloid natural products **5**–**8**, and further informed by the synthetic alkaloid analogs **10**, **11a**/**b** and **12a**/**b**, provides a sense

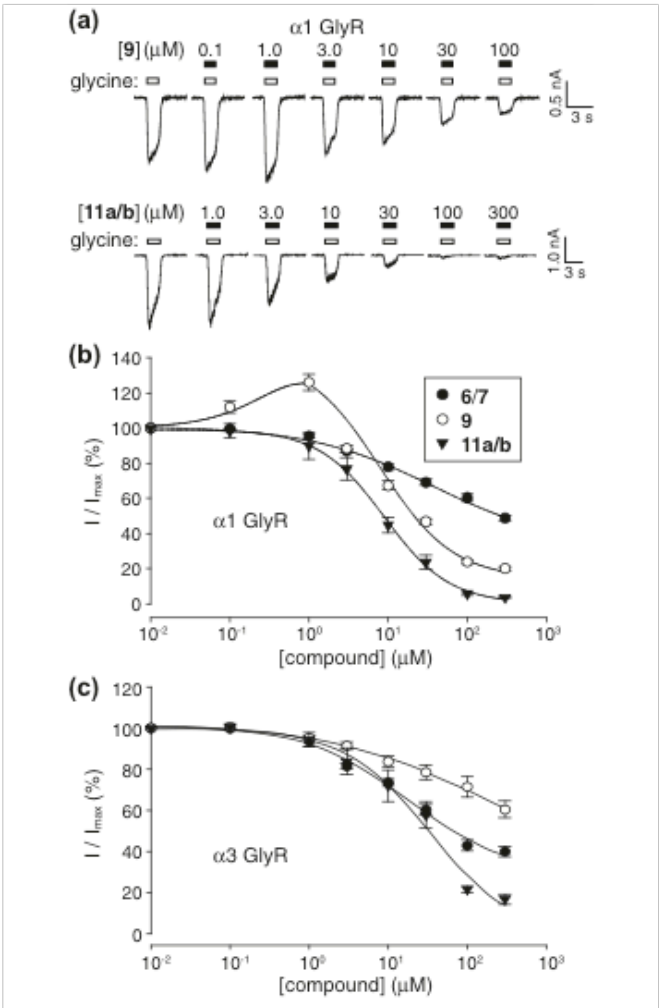

Figure 3. Electrophysiological analysis of **6**/**7**, **9** and **11a**/**b** on α1 and α3 GlyRs. (a) Sample dose–responses of **9** and **11a**/**b** on currents activated by EC_{50} glycine at α1 GlyR. (b) Averaged dose–responses of the 3 compounds at α1 GlyR and (c) α3 GlyR. Mean parameters of best fit to individual inhibitory dose–response relationships are presented in Table 1. Curve fits represent Hill equation fits to averaged data only and these parameters were not used for analysis. An exception is the biphasic curve fit to the **11a**/**b** data at the α1 GlyR, which was fit by the sum of two Hill equations.

Table 2
Automated electrophysiology (concentration dependence) of **6**/**7**, **9** and **11a**/**b** on stably expressed α1 and α3 GlyRs

Compound	α1 GlyR IC_{50} (μM)	α3 GlyR IC_{50} (μM)
6/**7**	>200	67 ± 16[a]
9	25.9 ± 5.3*[,b]	>300
11a/**b**	8.8 ± 0.5*[,c]	33.9 ± 7.0*[,d]

All results averaged from 4–10 cells.
* $p < 0.01$.
[a] $n_H = 0.5 \pm 0.1$.
[b] $n_H = 0.8 \pm 0.1$.
[c] $n_H = 1.0 \pm 0.1$.
[d] $n_H = 0.8 \pm 0.1$.

of the molecular characteristics needed for GlyR potency and isoform selectivity. For example, conversion of the 3′-imino to a 3′-oxo moiety (**5** to **6**/**7**, and **12a**/**b** to **11a**/**b**) leads to a dramatic increase in potency. Likewise, the level of N-methylation plays a critical role in both potency and isoform selectivity with the unmethylated **10** being inactive, the 2′-*N*-methylated **11a**/**b** being

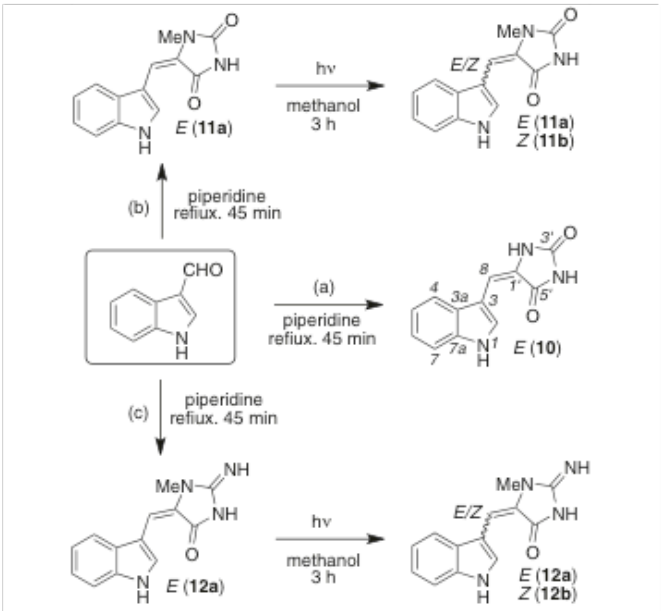

Figure 4. Synthesis of indole alkaloid analogs. (a) Hydantoin; (b) methylhydantoin; (c) creatinine.

selectively potent against α1 GlyRs, and the 2′,4′-*N*,*N*-dimethylated **6**/**7** being selectivity potent against α3 GlyRs. Interestingly, reduction of $\Delta^{8,1'}$(**8**) abolished all activity against both α1 and α3 GlyRs.

3. Conclusion

In summary, our investigations confirm that marine biodiscovery offers a valuable approach to discover new classes of GlyR modulators. Following the screening of a library of marine extracts, we identified a southern Australian marine sponge, *Ianthella* cf. *flabelliformis* as a priority extract for the discovery of small molecule GlyR modulators. Bioassay-guided fractionation yielded the structurally diverse sesquiterpenes **1**–**4** and indole alkaloids **5**–**9**, with the GlyR modulatory activity detected in *Ianthella* cf. *flabelliformis* being attributed to the alkaloids **6**/**7** and **9**. That these sponge alkaloids inhibited GlyR with apparently 'tunable' selectivity for either α1 or α3 GlyRs, prompted the one-pot synthesis of alkaloids **10**, **11a**/**b** and **12a**/**b**, leading to the discovery of the readily accessible and more potent α1 selective GlyR antagonists.

4. Experimental

4.1. General experimental details

Optical rotations were measured on a JASCO P-1010 polarimeter. UV–vis spectra were obtained on a Cary 50 UV–visible spectrophotometer. NMR experiments were performed on a Bruker Avance DRX600. Chemical shifts were calibrated internally against residual solvent signals (DMSO-d_6: $\delta_H = 2.50$, $\delta_C = 39.5$; $CDCl_3$: $\delta_H = 7.26$, $\delta_C = 77.0$; CD_3OD: $\delta_H = 3.30$, $\delta_C = 49.2$). ESIMS were recorded using an Agilent 1100 Series separations module equipped with an Agilent 1100 Series LC/MSD mass detector in both positive and negative ion modes. HRESIMS measurements were obtained on a Bruker micrOTOF mass spectrometer by direct infusion in MeCN at 3 μL/min flow using sodium formate clusters as an internal calibrant. HPLC was performed using an Agilent 1100 series HPLC controlled using ChemStation Rev.B.02.01. All chemicals were purchased from Merck, Sigma–Aldrich or Fluka. Solvents used for general purposes were of at least analytical grade, and solvents used for HPLC were of HPLC grade. Agilent Zorbax C_3 and C_8

250 × 9.4 mm columns were used for HPLC analyses and separations.

4.2. Marine extracts library

A library of >2500 marine invertebrate and alga samples, collected from intertidal, coastal and deep sea locations across southern Australia and Antarctica, were processed to generate an extract library suitably formatted for medium to high throughput bioassay. A portion (7 mL) of the archived EtOH extract of each marine sample was decanted, concentrated in vacuo, weighed and partitioned into *n*-BuOH (2 mL) and H_2O (2 mL). This pre-processing achieves a >10-fold concentration of 'drug-like' small molecules, while simultaneously desalting and simplifying the solubility characteristics of, the *n*-BuOH solubles. Aliquots (1 mL) of both *n*-BuOH and H_2O phases were transferred to deep 96-well plates, to generate a set of extract library plates. These plates were subsequently used to prepare 10- and 100-fold dilution plates.

4.3. Sponge collection and taxonomy

Sponge specimen CMB-03322 was collected by SCUBA from Lonsdale Wall, The Rip, Port Phillip Heads, Victoria (38° 17′ 55″ S, 144° 37′.46″ E). A description of the specimen is as follows: Growth form massive-thickly flabelliform; colour in EtOH likely to be an aerophobic colour change to dark purple; texture barely compressible, harsh, fibrous; oscules scattered, sunken; surface opaque, glossy, conulose; spicules none; ectosome thick collagen with fibres tangential or protruding the surface; choanosome a reticulation of fibres strongly laminated and pith visible. Large primary fibres cored by single column of sand grains, smaller fibres clear of detritus. The sponge was identified as *Ianthella* cf. *flabelliformis* (Order Verongida, Family Ianthellidae) and a type specimen registered with Museum Victoria (Registry No. MVF166222).

4.4. Extraction and fractionation

A portion (350 mL) of the aqueous EtOH extract of the *Ianthella* cf. *flabelliformis* was decanted and concentrated in vacuo to return a black solid (1.74 g), which was subsequently partitioned between *n*-BuOH (3 × 50 mL) and H_2O (50.0 mL). GlyR bioassays (see below) established that all activity was concentrated in the *n*-BuOH solubles (519.7 mg), which were sequentially triturated with 2 × 15 mL aliquots of hexane, CH_2Cl_2 and MeOH, and concentrated in vacuo to return 9.0, 283.0 and 74.6 mg yields respectively. A portion of the CH_2Cl_2 soluble fraction (130 mg) was subjected to HPLC fractionation (Zorbax C_8 5 μm 250 × 9.4 mm column, 4 mL/min, gradient elution of 10–100% MeCN/H_2O over 25 min, with an isocratic 0.01% TFA/H_2O modifier) to yield ianthellalactam A (**1**) (t_R = 12.9 min; 2.6 mg, 0.056%), ianthellalactam B (**2**) (t_R = 13.3 min; 1.7 mg, 0.032%), dictyodendrillin (**3**) (t_R = 13.9 min; 0.2 mg, 0.003%), aplysinopsin (**5**) (t_R = 7.0 min; 2.4 mg, 0.041%), 8*E*-3′-deimino-3′-oxoaplysinopin (**6**) (t_R = 10.1 min; 2.7 mg, 0.051%), 8*Z*-3′-deimino-3′-oxoaplysinopin (**7**) (t_R = 10.6 min; 3.5 mg, 0.067%), dihydroaplysinopsin (**8**) (t_R = 6.4 min; 1.8 mg, 0.034%) and tubastrindole B (**9**) (t_R = 5.8 min; 1.7 mg, 0.029%). Since the MeOH soluble fraction exhibited a similar HPLC-DAD and ^{1}H NMR profile to the CH_2Cl_2 soluble fraction, the remaining CH_2Cl_2 (153.0 mg) and MeOH solubles (74.6 mg) were combined and fractionated using the method outlined above, to yield **1**–**3** and **5**–**9** together with a new minor metabolite/artifact, ethyl dictyodendrillin (**4**) (t_R = 14.2 min; 1.7 mg, 0.029%). Although the geometric isomers 8*E*-3′-deimino-3′-oxoaplysinopsin (**6**) and 8*Z*-3′-deimino-3′-oxoaplysinopsin (**7**) were well resolved by HPLC, the isomers rapidly isomerized during handling (and on exposure to light). Isolation in a darkened laboratory, followed by rapid data acquisition, did permit independent characterization of these photolabile isomers. Note—yields for all isolated compounds were calculated as a weight-to-weight estimate against the crude *n*-BuOH solubles

4.5. Characterization of natural products

4.5.1. Ianthellalactam A (1)

Pale yellow oil. UV–vis (MeOH) λ_{max} (log ε) 203 nm (4.33); NMR (600 MHz, methanol-d_4) see Table 1 and Supplementary Figures S1a and b and Table S1; HRESI(+)MS *m*/*z* 314.1721 (calcd for $C_{17}H_{25}NO_3$ Na 314.1727).

4.5.2. Ianthellalactam B (2)

Pale yellow oil. UV–vis (MeOH) λ_{max} (log ε) 202 nm (4.40); NMR (600 MHz, methanol-d_4) see Table 1 and Supplementary Figures S2a and b and Table S2; HRESI(+)MS *m*/*z* 314.1725 (calcd for $C_{17}H_{25}NO_3$Na 314.1727).

4.5.3. Dictyodendrillin[13] (3)

Colorless oil. ^{1}H NMR (600 MHz, $CDCl_3$) see Supplementary Figures S3a and b. ESI(+)MS *m*/*z* 251 $[M+H]^+$, ESI(−)MS *m*/*z* 249 $[M-H]^-$. Identical with an authentic sample of dictyodendrillin.[13]

4.5.4. Ethyl dictyodendrillin (4)

Colorless oil. UV–vis (MeOH) λ_{max} (log ε) 204.9 (4.27), 201 (4.27); NMR (600 MHz, $CDCl_3$) see Supplementary Figures S4a and b and Table S4.

4.5.5. Aplysinopsin[14] (5)

Yellow solid. UV–vis (MeOH) λ_{max} (log ε) 217 (4.0), 279 (3.49), 391 (3.67); NMR (600 MHz, DMSO-d_6) see Supplementary Figures S5a and b and Table S5; HRESI(+)MS *m*/*z* 255.1247 (calcd for $C_{14}H_{15}N_4O$ 255.1240). Identical with an authentic sample of aplysinopsin.[14]

4.5.6. 8*E*-3′-Deimino-3′-oxoaplysinopsin[15] (6)

Yellow solid. UV–vis (MeOH) λ_{max} (log ε) 203 (4.01), 278 (3.49), 367 (3.83) nm; NMR (600 MHz, DMSO-d_6) see Supplementary Figures S6a and b and Table S6; HRESIMS *m*/*z* 278.0909 (calcd for $C_{14}H_{13}N_3O_2$Na 278.0900).

4.5.7. 8*Z*-3′-Deimino-3′-oxoaplysinopsin[15] (7)

Yellow solid. UV–vis (MeOH) λ_{max} (log ε) 203 (4.01), 218 (4.23), 278 (3.49), 367 (3.83) nm; NMR (600 MHz, DMSO-d_6) see Supplementary Figures S6a and b and Table S7; HRESIMS *m*/*z* 278.0909 (calcd for $C_{14}H_{13}N_3O_2$Na 278.0900).

4.5.8. Dihydroaplysinopsin[16] (8)

Yellow solid. $[\alpha]_D^{23}$ −86 (*c* 0.05 MeOH); UV–vis (MeOH) λ_{max} (log ε) 202 (3.98), 218 (3.93), 280 (3.12) nm; NMR (600 MHz, DMSO-d_6) see Supplementary Figures S8a and b and Table S8; HRESI(+)MS *m*/*z* 257.1393 (calcd for $C_{14}H_{17}N_4O$ 257.1397).

4.5.9. Tubastrindole B[17] (9)

Yellow solid. $[\alpha]_D^{23}$ −44 (*c* 0.1 MeOH); UV–vis (MeOH) λ_{max} (log ε) 202 (4.21), 217 (4.27), 205 (4.24), 268 (3.55) nm; NMR (600 MHz, DMSO-d_6) see Supplementary Figures S9a and b and Table S9; HRESI(+)MS *m*/*z* 509.2415 (calcd for $C_{28}H_{29}N_8O_2$ 509.2408).

4.6. Synthesis of analogs

4.6.1. General synthetic procedures

Solutions of indole-3-carboxaldehyde (1.0 g, 6.9 mmol) and either hydantoin, methyl hydantoin or creatinine (17 mmol, 2.5 equiv) in piperidine (5 mL) were refluxed for 45 min under argon. The solutions were then cooled to room temperature and di-

luted with acetone (10 mL). The resulting yellow precipitates were filtered and washed with cold acetone (10 mL) to yield the essentially pure 8*E* isomers (**10**, **11a** and **12a**). Suspensions of **11a** and **12a** in methanol were exposed to UV light for 3 h, yielding ~1:1 mixtures of the 8*E* and 8*Z* (**11b** and **12b**) isomers.

4.6.2. 8*E*-3′-Deimino-2′,4′-bisdemethyl-3′-oxoaplysinopsin[18] (10)

Yellow solid (0.90 g, 57%). UV–vis (MeOH) λ_{max} (log ε) 227.1 (4.03), 277.9 (3.55), 364 (4.09) nm; NMR (600 MHz, methanol-d_4) see Supplementary Figures S10a and b and Table S10; HRESIMS *m*/*z* 250.0593 (calcd for $C_{12}H_9N_3O_2Na$ 250.0587).

4.6.3. 8*E*-3′-Deimino-4′-demethyl-3′-oxoaplysinopsin[19] (11a)

Yellow solid (0.76 g, 46%). UV–vis (MeOH) λ_{max} (log ε) 228.9 (4.01), 276 (3.49) 336.9 (3.83) nm; NMR (600 MHz, methanol-d_4) see Supplementary Figure S11a and Table S11a; HRESIMS *m*/*z* 264.0746 (calcd for $C_{13}H_{11}N_3O_2Na$ 264.0743).

4.6.4. 8*Z*-3′-Deimino-4′-demethyl-3′-oxoaplysinopsin[19] (11b)

Yellow solid. UV–vis (MeOH) λ_{max} (log ε) 228.9 (4.01), 276 (3.49) 336.9 (3.83) nm; NMR (600 MHz, methanol-d_4) see Supplementary Figure S11b and Table S11b; HRESIMS *m*/*z* 264.0746 (calcd for $C_{13}H_{11}N_3O_2Na$ 264.0743).

4.6.5. 8*E*-4′-Demethylaplysinopsin[20] (12a)

Yellow solid. (0.70 g, 42%). UV–vis (MeOH) λ_{max} (log ε) 228.9 (3.93), 277.9 (3.49), 387 (3.90) nm; NMR (600 MHz, DMSO-d_6) see Supplementary Figure 12a and Table S12a; HRESIMS *m*/*z* 241.1085 (calcd for $C_{13}H_{13}N_3O$ 241.1084).

4.6.6. 8*Z*-4′-Demethylaplysinopsin[20] (12b)

Yellow solid. UV–vis (MeOH) λ_{max} (log ε) 228.9 (3.93), 277.9 (3.49), 387 (3.90) nm; NMR (600 MHz, DMSO-d_6) see Supplementary Figure 12b and Table S12b; HRESIMS *m*/*z* 241.1085 (calcd for $C_{13}H_{13}N_4O$ 241.1084).

4.7. Bioassays

4.7.1. Primary GlyR screening of marine extracts

The initial screen of >2500 marine extracts against recombinantly expressed α1 and α3 GlyRs was performed using a yellow fluorescent protein-based anion flux assay as previously described.[12,21] In this bioassay, 90 μL of each 100-fold diluted *n*-BuOH partition was transferred into one well of a 384-well plate, and was dried under nitrogen. The plates containing dried *n*-BuOH partitions were protected from light and stored at −30 °C until required. On the day of the experiment an aliquot (30 μL) of extracellular solution [NaCl (140 mM), KCl (5 mM), $CaCl_2$ (2 mM), $MgCl_2$ (1 mM), HEPES (10 mM), and glucose (10 mM) (pH 7.4 using NaOH)] was added to each well and mixed/dissolved using a multi-channel pipette. Subsequently, an aliquot (10 μL) of this solution was transferred into the corresponding well of a 384-well plate containing approx. 5000 cells and 15 μL of extracellular solution per well, and incubated at room temperature for 30 min. The 384-well plates were then placed onto the motorized stage of an in-house imaging system[21] and cells were imaged twice: once in 25 μL of extracellular solution containing the *n*-BuOH partition and once 10 s after the injection of 50 μL NaI solution supplemented with 500 μM glycine. The NaI solution was similar in composition to NaCl control solution except the NaCl was replaced by equimolar NaI. Images of fluorescent cells were segmented and quantitatively analyzed using a modified version of DetecTIFF software.[22] In brief, images were segmented using an iterative size and intensity-based thresholding algorithm and the fluorescence signal of identified cells was calculated as the mean of all pixel values within the area of a cell. GlyR activation response was used as a measure of extract potency and was defined as $(F_{init} - F_{final}) \times 100/F_{init}$, where F_{init} and F_{final} were the initial and final values of fluorescence, respectively. All experiments were performed twice in neighboring wells. Hits were selected by visual inspection of color maps generated by analysis software. For hit confirmation, 24 μL of the corresponding 10-fold diluted *n*-BuOH partition was transferred into a well of a 384-well plate, and was dried and stored as described above. On the day of the experiment the dried 10-fold diluted *n*-BuOH partitions were resuspended in 80 μL extracellular solution as described above and two aliquots each of 17 and 10 μL respectively were then transferred in neighboring wells containing ~5000 cells and 15 μL extracellular solution per well. Imaging and image analysis were conducted as described above. The concentration dependence of the drug effects was used as measure for extract potency and level of prioritization. From these experiments we identified *Ianthella* cf. *flabelliformis* (CMB-03322) as an extract with antagonist activity on α1 and α3 GlyRs.

4.7.2. Automated electrophysiology

Electrophysiological screening was performed using an automated planar patch-clamp device (Patchliner, Nanion Technologies GmbH, Munich, Germany). Stable α1 and α3 GlyR expressing HEK293 cell lines, produced as previously described,[12,22] were maintained in Minimal Essential medium. After 2–3 days in culture, cells were trypsinized and suspended in extracellular solution [NaCl (140 mM), KCl (4 mM), $CaCl_2$ (2 mM), $MgCl_2$ (1 mM), HEPES/NaOH (10 mM) and glucose (5 mM) (pH 7.4 adjusted with NaOH)] at a density of 1×10^6 cells/mL before injecting into the Patchliner chip. This standard extracellular solution was employed in all Patchliner experiments. The internal solution contained KCl (50 mM), NaCl (10 mM), KF (60 mM), $MgCl_2$ (2 mM), EGTA (20 mM), HEPES/KOH (10 mM) (pH 7.2). All experiments were performed at room temperature. 1 M glycine (Ajax Finechem, Seven Hills, NSW, Australia) stocks were prepared in water and stored at −20 °C. All test compounds (marine natural products and synthetics) were dissolved in DMSO (Sigma–Aldrich) and stored at −20 °C. From these stocks, solutions for experiments were prepared on the day of recording.

4.7.3. Data analysis

Results are expressed as mean ± standard error of the mean of three or more independent experiments. The Hill equation was used to calculate the half inhibitory concentration (IC_{50}) and Hill coefficient (n_H) values of individual concentration–response relationships. All curves were fitted using a nonlinear least squares algorithm (Sigmaplot 11.0; Jandel Scientific, San Rafael, CA, USA). Statistical significance was determined by unpaired Student's *t*-test, with $p < 0.05$ representing significance.

Acknowledgments

We thank L. Goudie for taxonomic identification of marine sponges and acknowledge the generous support of an Australian Development Scholarship (W.B.) and a University of Queensland Scholarship (R.I.). This research was funded in part by the Institute for Molecular Bioscience, the Queensland Brain Institute, The University of Queensland, the National Health and Medical Research Council (project grant #613448) and the Australian Research Council (LP120100088).

Supplementary data

Supplementary data associated with this article can be found, in the online version, at http://dx.doi.org/10.1016/j.bmc.2013.04.061.

References and notes

1. Lynch, J. W. *Physiol. Rev.* **2004**, *84*, 1051.
2. Harvey, R. J.; Depner, U. B.; Wassle, H.; Ahmadi, S.; Heindl, C.; Reinold, H.; Smart, T. G.; Harvey, K.; Schutz, B.; Abo-Salem, O. M.; Zimmer, A.; Poisbeau, P.; Welzl, H.; Wolfer, D. P.; Betz, H.; Zeilhofer, H. U.; Muller, U. *Science* **2004**, *304*, 884.
3. Haverkamp, S.; Muller, U.; Harvey, K.; Harvey, R. J.; Betz, H.; Wassle, H. *J. Comp. Neurol.* **2003**, *465*, 524.
4. Haverkamp, S.; Muller, U.; Zeilhofer, H. U.; Harvey, R. J.; Wassle, H. *J. Comp. Neurol.* **2004**, *477*, 399.
5. Heinze, L.; Harvey, R. J.; Haverkamp, S.; Wassle, H. *J. Comp. Neurol.* **2007**, *500*, 693.
6. Weltzien, F.; Puller, C.; O'Sullivan, G. A.; Paarmann, I.; Betz, H. *J. Comp. Neurol.* **2012**, *520*, 3962.
7. Webb, T. I.; Lynch, J. W. *Curr. Pharm. Des.* **2007**, *13*, 2350.
8. Xiong, W.; Cui, T.; Cheng, K.; Yang, F.; Chen, S. R.; Willenbring, D.; Guan, Y.; Pan, H. L.; Ren, K.; Xu, Y.; Zhang, L. *J. Exp. Med.* **2012**, *209*, 1121.
9. Manzke, T.; Niebert, M.; Koch, U. R.; Caley, A.; Vogelgesang, S.; Hulsmann, S.; Ponimaskin, E.; Muller, U.; Smart, T. G.; Harvey, R. J.; Richter, D. W. *J. Clin. Invest.* **2010**, *120*, 4118.
10. Eichler, S. A.; Kirischuk, S.; Juttner, R.; Schaefermeier, P. K.; Legendre, P.; Lehmann, T. N.; Gloveli, T.; Grantyn, R.; Meier, J. C. *J. Cell. Mol. Med.* **2008**, *12*, 2848.
11. Chung, S. K.; Vanbellinghen, J. F.; Mullins, J. G.; Robinson, A.; Hantke, J.; Hammond, C. L.; Gilbert, D. F.; Freilinger, M.; Ryan, M.; Kruer, M. C.; Masri, A.; Gurses, C.; Ferrie, C.; Harvey, K.; Shiang, R.; Christodoulou, J.; Andermann, F.; Andermann, E.; Thomas, R. H.; Harvey, R. J.; Lynch, J. W.; Rees, M. I. *J. Neurosci.* **2010**, *30*, 9612.
12. Balansa, W.; Islam, R.; Fontaine, F.; Piggott, A. M.; Zhang, H.; Webb, T. I.; Gilbert, D. F.; Lynch, J. W.; Capon, R. J. *Bioorg. Med. Chem.* **2010**, *18*, 2912.
13. Tran, N. H.; Hooper, J. N. A.; Capon, R. J. *Aust. J. Chem.* **1995**, *48*, 1757.
14. Kazlauskas, R.; Murphy, P. T.; Quinn, R. J.; Wells, R. J. *Tetrahedron Lett.* **1977**, *18*, 61.
15. Guella, G.; Mancini, I.; Zibrowius, H.; Pietra, F. *Helv. Chim. Acta* **1988**, *71*, 773.
16. Okuda, R. K.; Klein, D.; Kinnel, R. B.; Li, M.; Scheuer, P. J. *Pure Appl. Chem.* **1982**, *54*, 1907.
17. Iwagawa, T.; Miyazaki, M.; Okamura, H.; Nakatani, M.; Doe, M.; Takemura, K. *Tetrahedron Lett.* **2003**, *44*, 2533.
18. Rashid, M. A.; Gustafson, K. R.; Cardellina, J. H., II; Boyd, M. R. *J. Nat. Prod.* **1995**, *58*, 1120.
19. Jakse, R.; Recnik, S.; Svete, J.; Golobic, A.; Golic, L.; Stanovnik, B. *Tetrahedron* **2001**, *57*, 8395.
20. Djura, P.; Faulkner, D. J. *J. Org. Chem.* **1980**, *45*, 735.
21. Kruger, W.; Gilbert, D.; Hawthorne, R.; Hryciw, D. H.; Frings, S.; Poronnik, P.; Lynch, J. W. *Neurosci. Lett.* **2005**, *380*, 340.
22. Gilbert, D. F.; Meinhof, T.; Pepperkok, R.; Runz, H. *J. Biomol. Screen.* **2009**, *14*, 944.

SUPPORTING INFORMATION

Australian Marine Sponge Alkaloids as A New Class of Glycine-Gated Chloride Channel Receptor Modulator

Walter Balansa,[a§] Robiul Islam,[b§] Daniel F. Gilbert,[b] Frank Fontaine,[a] Xue Xiao,[a] Hua Zhang,[a] Andrew M. Piggott,[a] Joseph W. Lynch,[b,c*] Robert J. Capon,[a1]

[a] *Institute for Molecular Bioscience, The University of Queensland, St. Lucia, QLD, 4072, Australia*
[b] *Queensland Brain Institute, The University of Queensland, St. Lucia, QLD, 4072, Australia*
[c] *School of Biomedical Sciences, The University of Queensland, St. Lucia, QLD, 4072, Australia*

Table of Contents

[1] Authors to whom correspondence should be addressed.
JWL – Ph: +61-7-3346-6375; Fax: +61-7-3346-6301; Email: j.lynch@uq.edu.au
RJC – Ph: +61-7-3346-2979; Fax: +61-7-3346-2090; Email: r.capon@uq.edu.au
[§] These authors contributed equally to this work

Chemical Profiling

An HPLC analysis (Zorbax C_8 250 × 9.4 mm, 4.0 mL/min, gradient elution from 10–100% MeCN/H_2O over 25 min, with an isocratic 0.01% TFA/H_2O modifier) of the crude *n*-BuOH solubles from sponge CMB-03322 revealed an extract rich in chemical diversity.

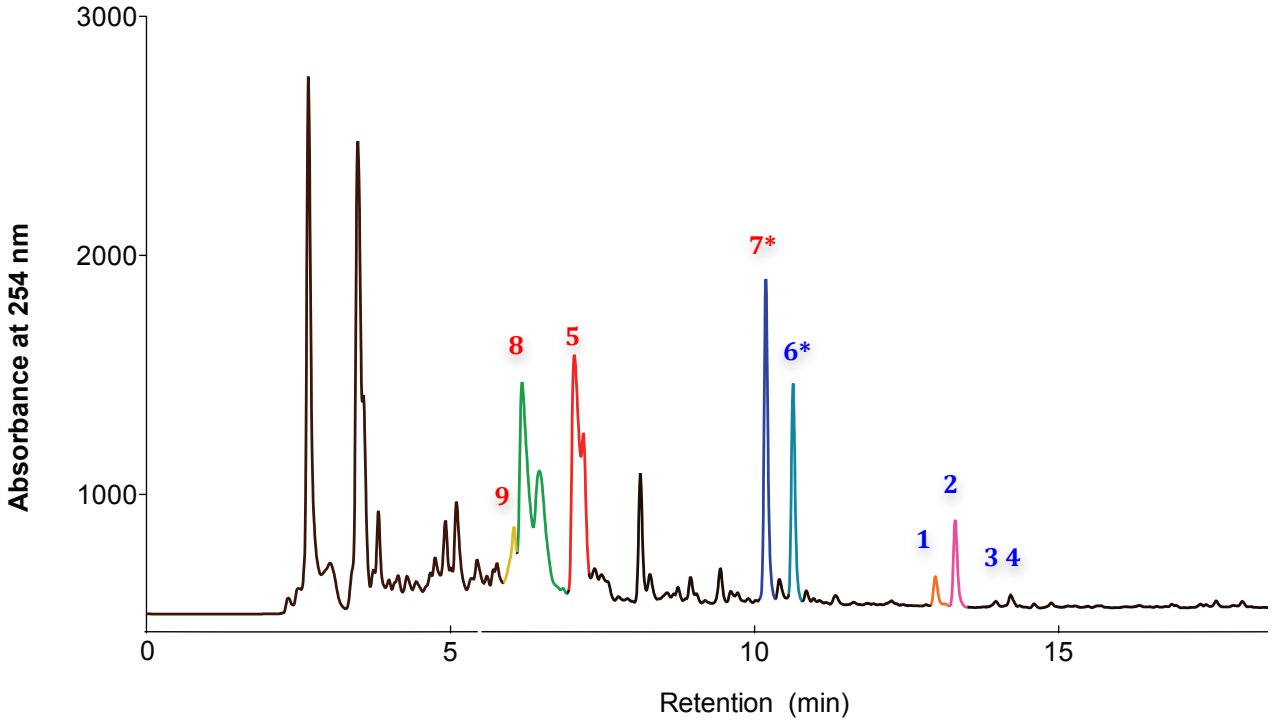

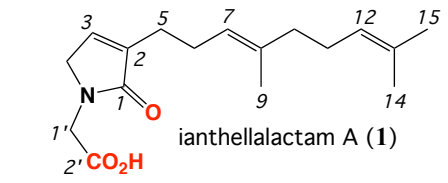
ianthellalactam A (**1**)

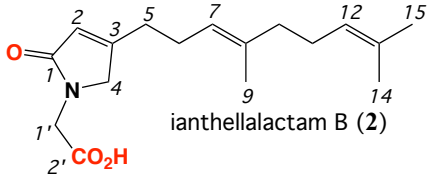
ianthellalactam B (**2**)

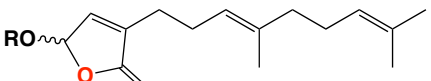
dictyodendrillin (**3**) R = H
ethyl dictyodendrillin (**4**) R = Et

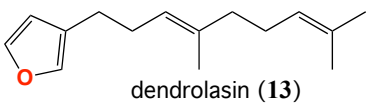
dendrolasin (**13**)

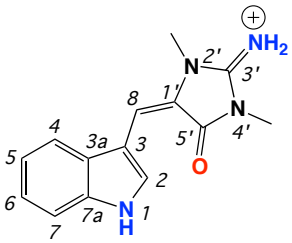
aplysinopsin (**5**)
TFA salt

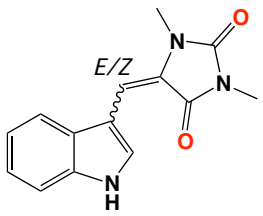
8*E*-3'-deimino-3'-oxoaplysinopsin (**6**)
8*Z*-3'-deimino-3'-oxoaplysinopsin (**7**)

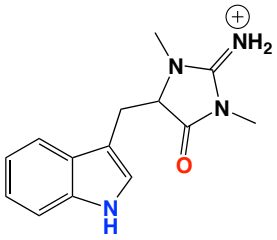
dihydroaplysinopsin (**8**)
TFA salt

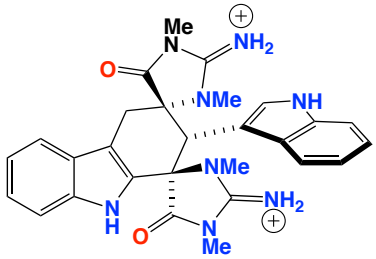
tubastrindole B (**9**)
TFA salt

Isolation Scheme

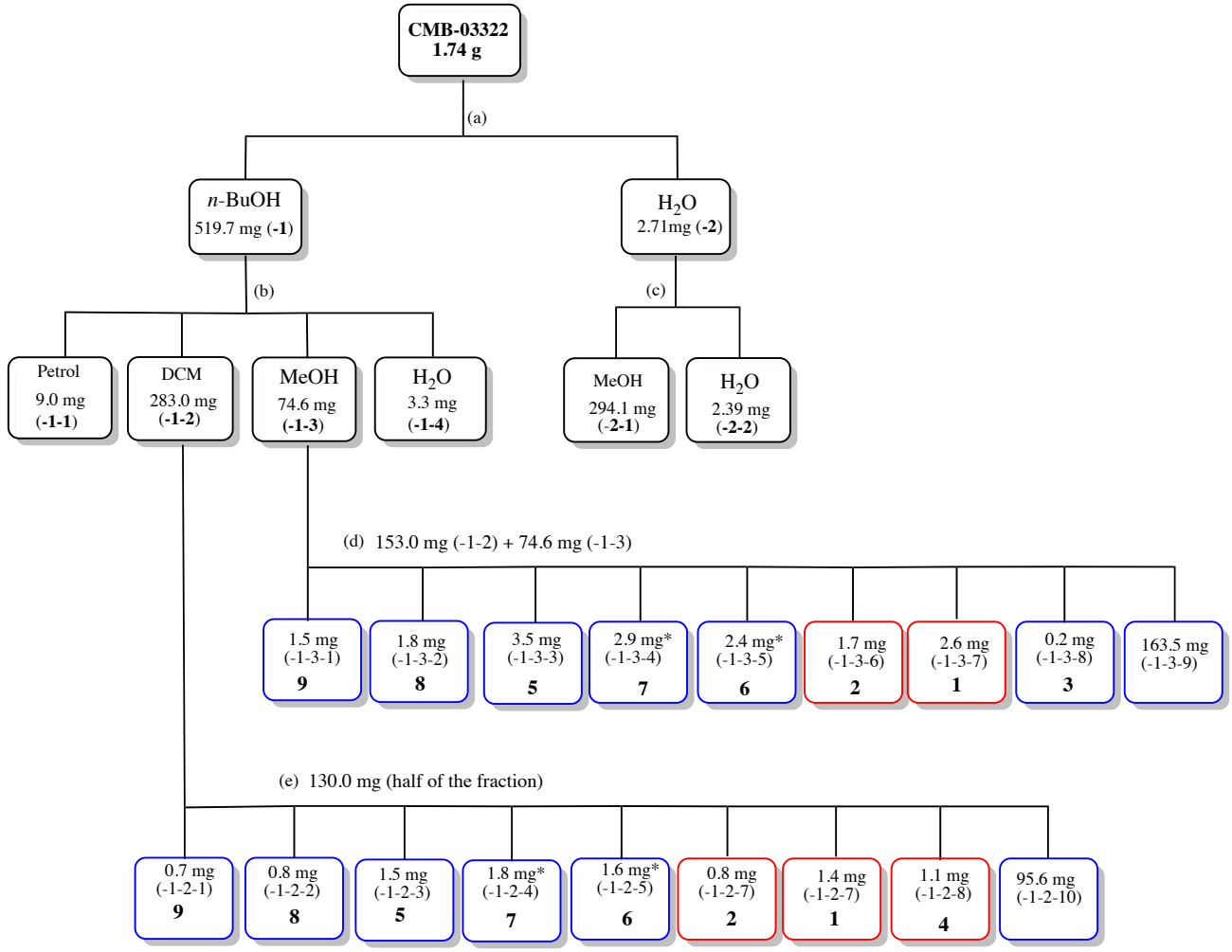

Scheme 5.1. Extraction and purification of CMB-03322

(a) Partition into *n*-BuOH (-1) and H_2O (-2) solubles
(b) Sequentially triturate *n*-BuOH solubles into hexane (-1-1), CH_2Cl_2 (-1-2), MeOH (-1-3) and H_2O (-1-4)
(c) Sequentially triturate water solubles into MeOH (-2-1) and H_2O (-2-2)
(d) HPLC [Zorbax C_8 (250 × 9.4 mm), 4.0 mL/min, gradient 10-100% MeCN/H_2O over 25 min, with isocratic 0.01% TFA modifier]
(e) HPLC [Zorbax C_8 (250 × 9.4 mm), 4.0 mL/min, gradient 10-100% MeCN/H_2O over 25 min, with isocratic 0.01% TFA modifier]
(f) Blue and red indicate known vs. new compounds respectively, while * indicates equilibrating isomers.

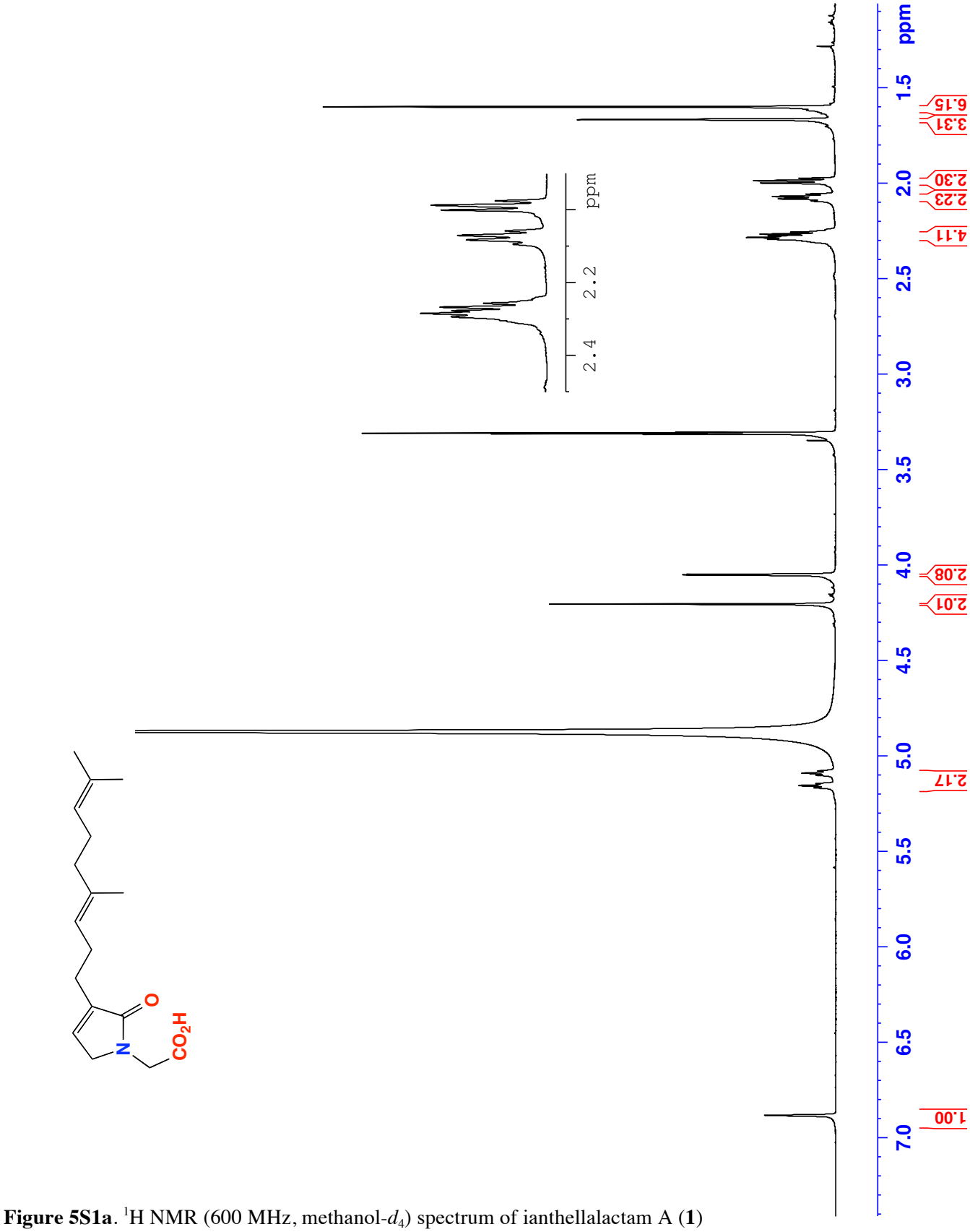

Figure 5S1a. ^{1}H NMR (600 MHz, methanol-d_4) spectrum of ianthellalactam A (**1**)

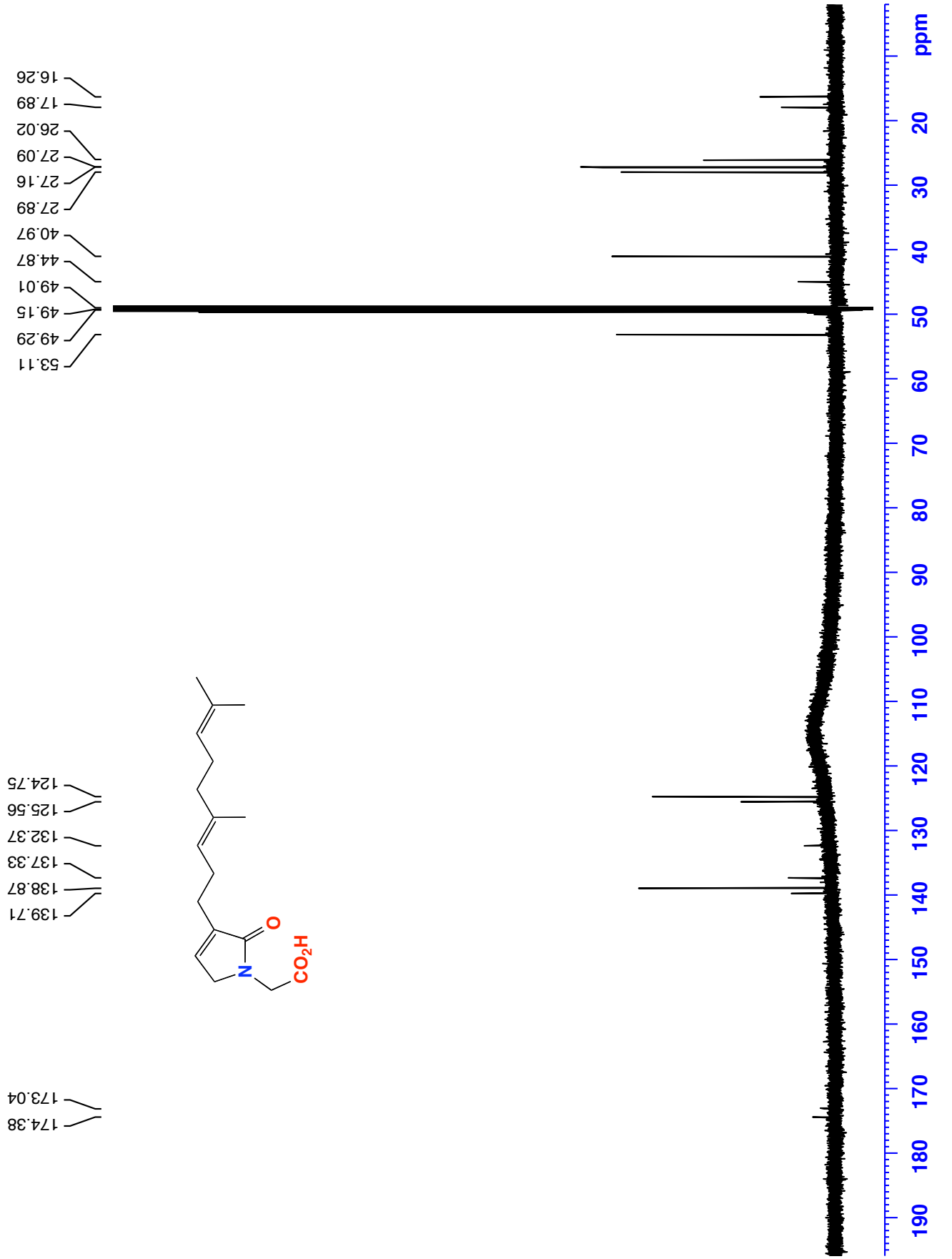

Figure 5S1b ^{13}C NMR (150 MHz, methanol-d_4) spectrum of ianthellalactam A (**1**)

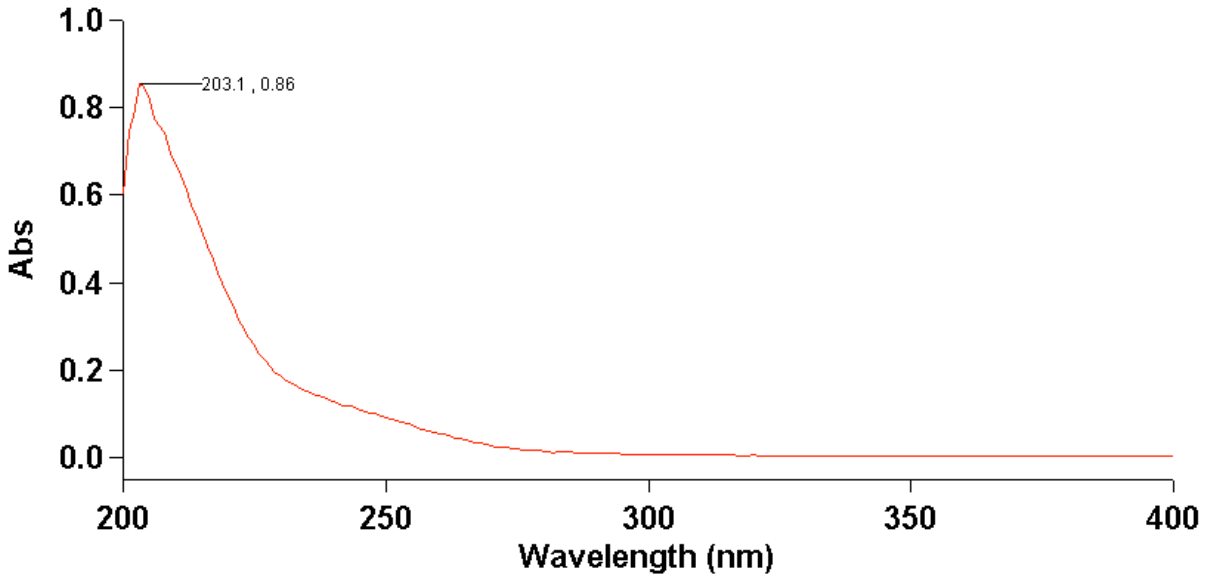

Figure 5S1c. UV-vis (MeOH) spectrum of ianthellalactam A (**1**)

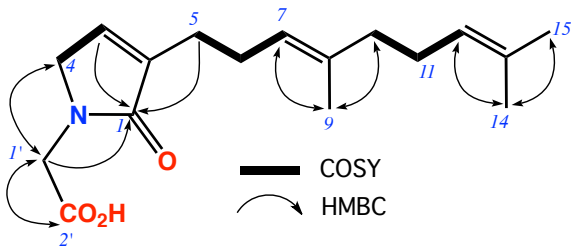

Figure 5S1d: Selected 2D NMR correlations for ianthellalactam A (**1**)

Table 5S1: NMR (600 MHz, CD_3OD) data for ianthellalactam A (**1**)

No.	δ_H (mult., *J* (Hz))	δ_C [A]	COSY	HMBC (^{1}H to ^{13}C)
1		174.4		
2		139.7		
3	6.88 (tt, 1.6, 1.6)	138.9	4, 5	1, 2, 4, 5
4	4.05 (dt, 1.6, 1.6)	53.1	3, 5	1, 2, 3
5	2.29[B]	27.1	3, 4, 6	1, 2, 3, 6, 7
6	2.27[B]	27.2	5, 7, 9	2, 5, 7, 8
7	5.16 (tq, 6.9, 1.3)	124.8	6, 9	5, 6, 9, 10
8		137.3		
9	1.60 (br s)	16.3	6, 7	7, 8, 10
10	1.99 (br t, 7.6)	41.0	11	7, 8, 9, 11
11	2.08 (br td, 7.6, 7.0)	27.9	10, 12, 14, 15	8, 10, 12, 13
12	5.09 (tqq, 7.0, 1.4, 1.4)	125.6	11, 14, 15	14, 15
13		132.3		
14	1.60 (br s)	17.9	11, 12	12, 13, 15
15	1.67 (br s)	26.0	11, 12	12, 13, 14
1′	4.21 (s)	44.9		1, 2′, 4
2′		173.0		

[A] ^{13}C NMR assignments supported by HSQC data. [B] Overlapping signals.

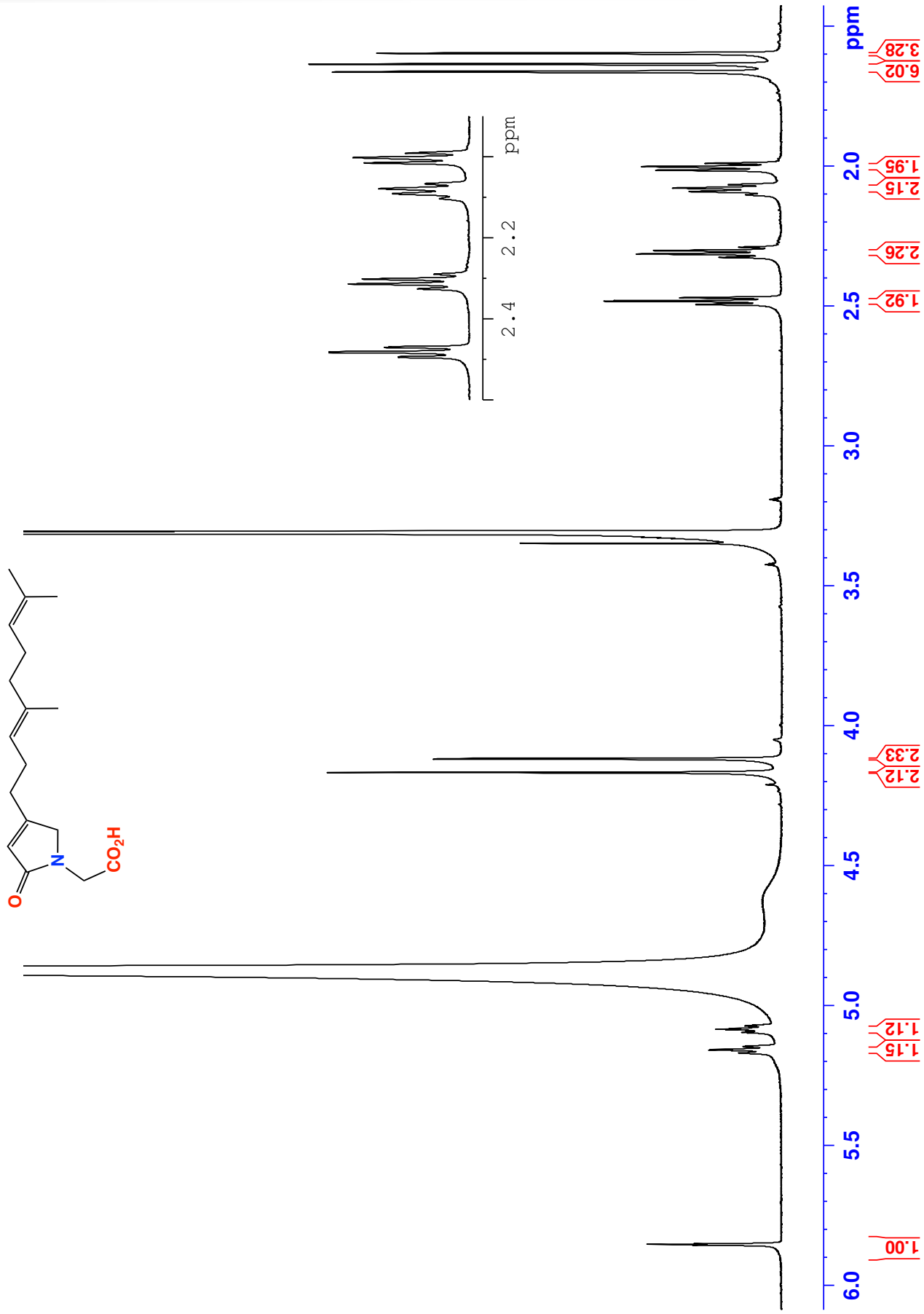

Figure 5S2a. ^{1}H NMR (600 MHz, methanol-d_4) spectrum of ianthellalactam B (**2**)

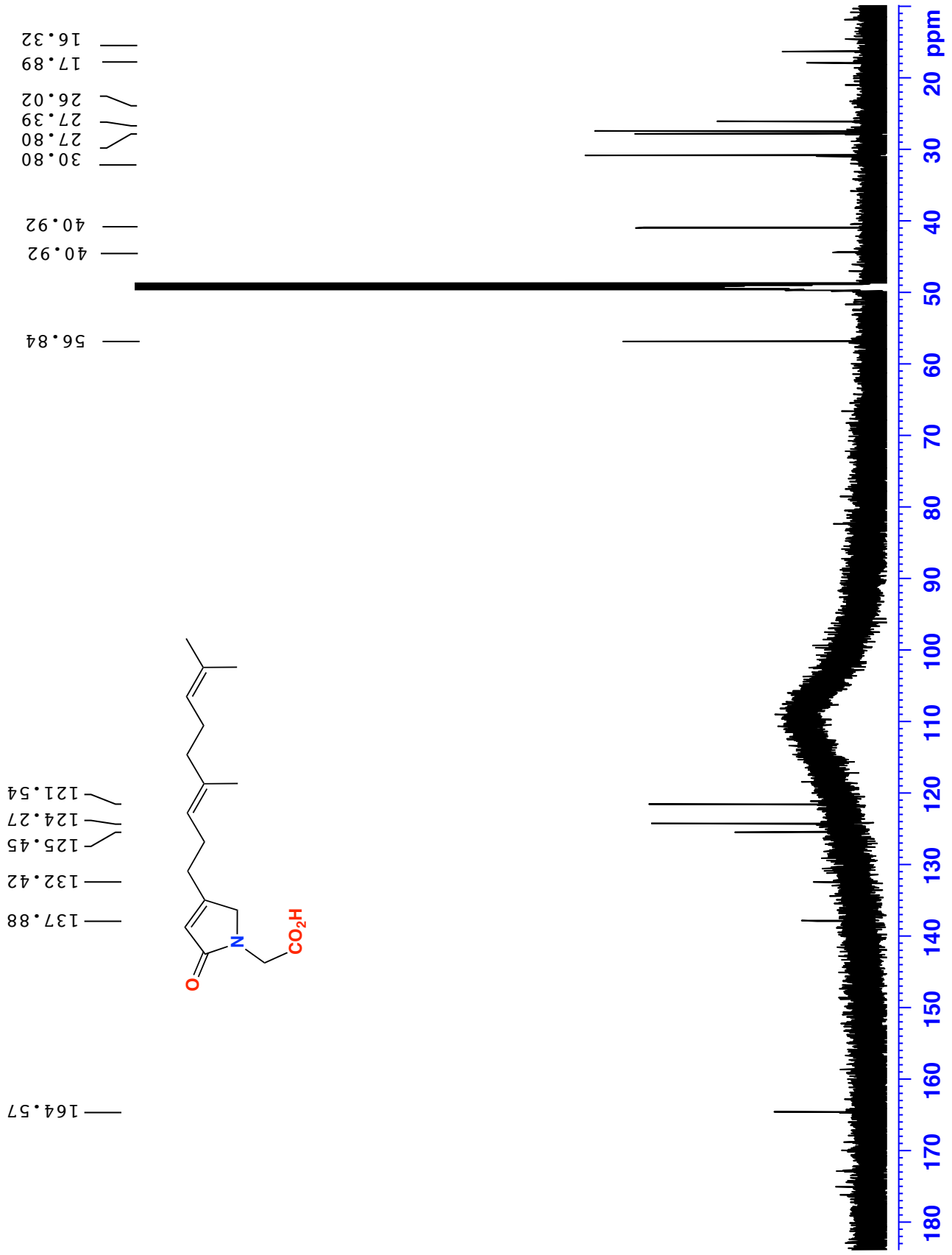

Figure 5S2b. ^{13}C NMR (150 MHz, methanol-d_4) spectrum of ianthellalactam B (**2**)

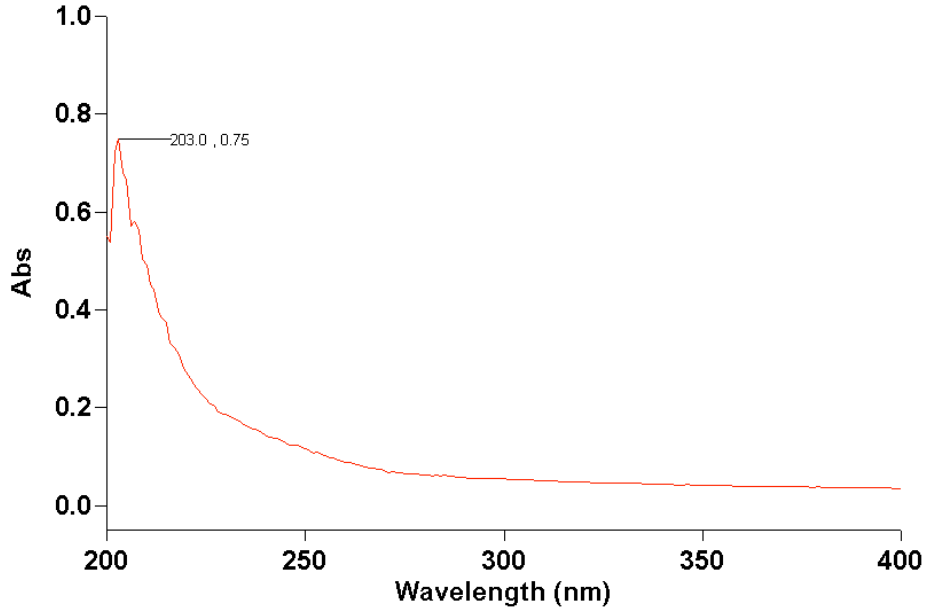

Figure 5S2c. UV-vis (MeOH) spectrum of ianthellalactam B (**2**)

Figure 5S2d: Selected 2D NMR correlations for ianthellalactam B (**2**)

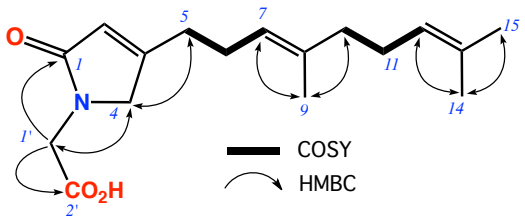

Table 5S2: NMR (600 MHz, CD_3OD) data for ianthellalactam B (**2**)

No.	δ_H (mult., *J* (Hz))	δ_C [A]	COSY	HMBC (^1H to ^{13}C)
1		175.0		
2	5.85 (tt, 1.4, 1.4)	121.5	4, 5	1, 3, 4, 5
3		164.6		
4	4.11 (d, 1.4)	56.8	2	1, 2, 3
5	2.48 (td, 7.4, 1.4)	30.8	2, 6	2, 3, 4, 6, 7
6	2.30 (br td, 7.4, 7.1)	27.4	5, 7, 9	3, 5, 7, 8
7	5.16 (tq, 7.1, 1.3)	124.3	6, 9	5, 6, 9, 10
8		137.9		
9	1.64 (br s)	16.3	6, 7	7, 8, 10
10	2.00 (br t, 7.6)	40.9	11	7, 8, 9, 11, 12
11	2.08 (br td, 7.6, 7.0)	27.8	10, 12, 14, 15	8, 10, 12, 13
12	5.08 (tqq, 7.0, 1.4, 1.4)	125.4	11, 14, 15	14, 15
13		132.4		
14	1.60 (br s)	17.9	11, 12	12, 13, 15
15	1.66 (br s)	26.0	11, 12	12, 13, 14
1′	4.17 (s)	44.4		1, 4, 2′
2′		172.9		

[A] ^{13}C NMR assignments supported by HSQC data.

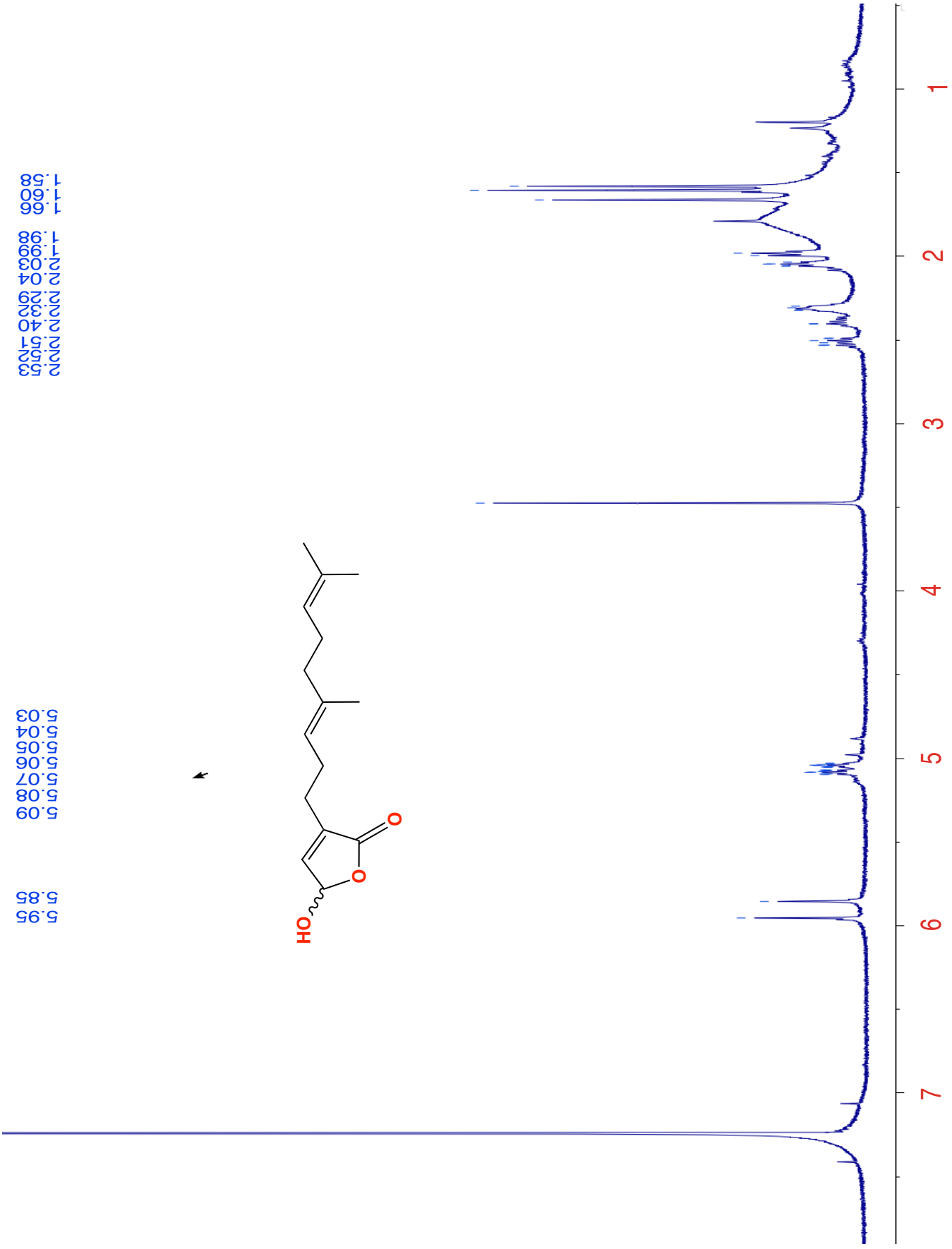

Figure 5S3a. ^{1}H NMR (600 MHz, $CDCl_3$) spectrum for dictyodendrillin (**3**)

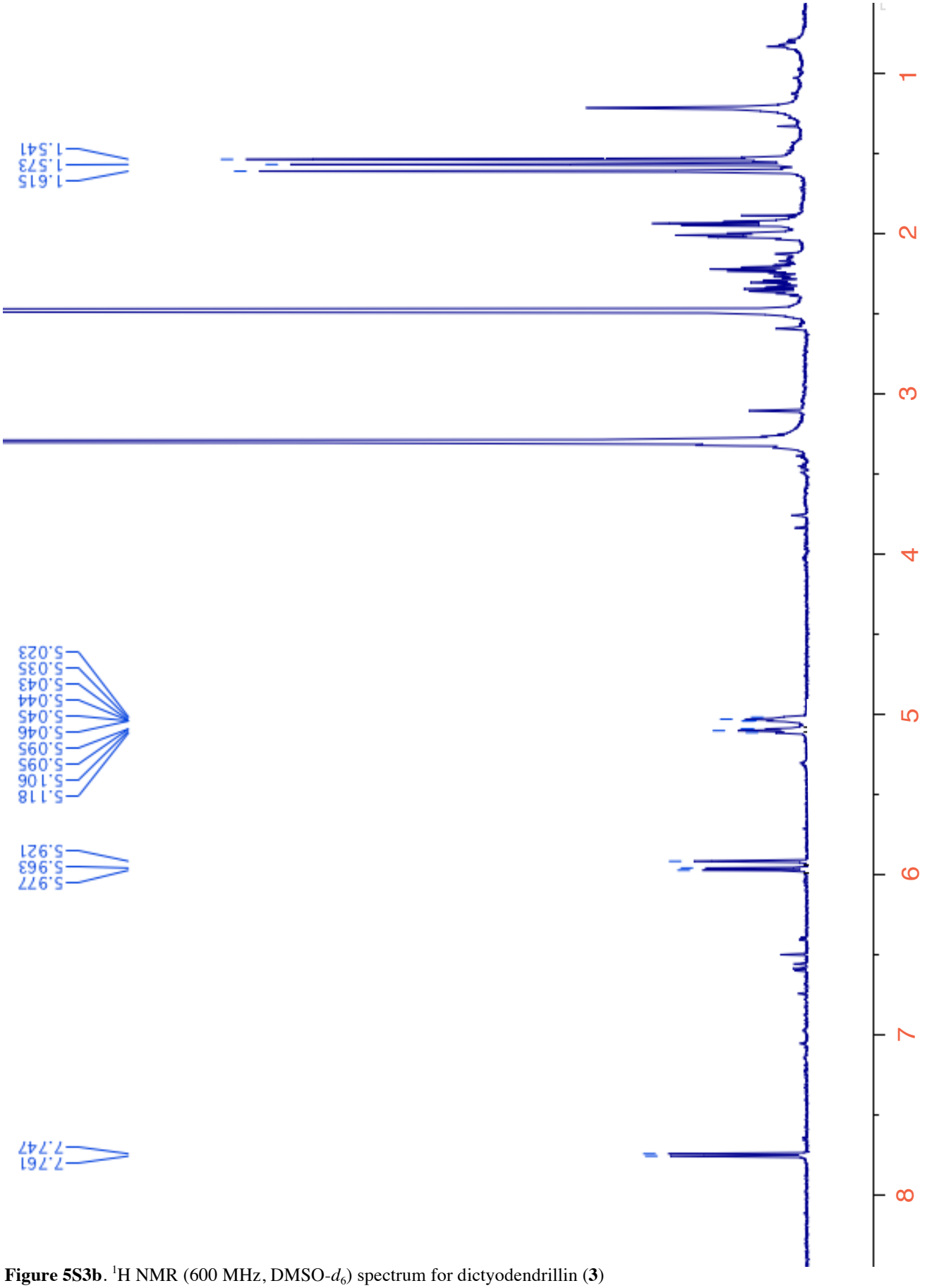

Figure 5S3b. ^{1}H NMR (600 MHz, DMSO-d_6) spectrum for dictyodendrillin (**3**)

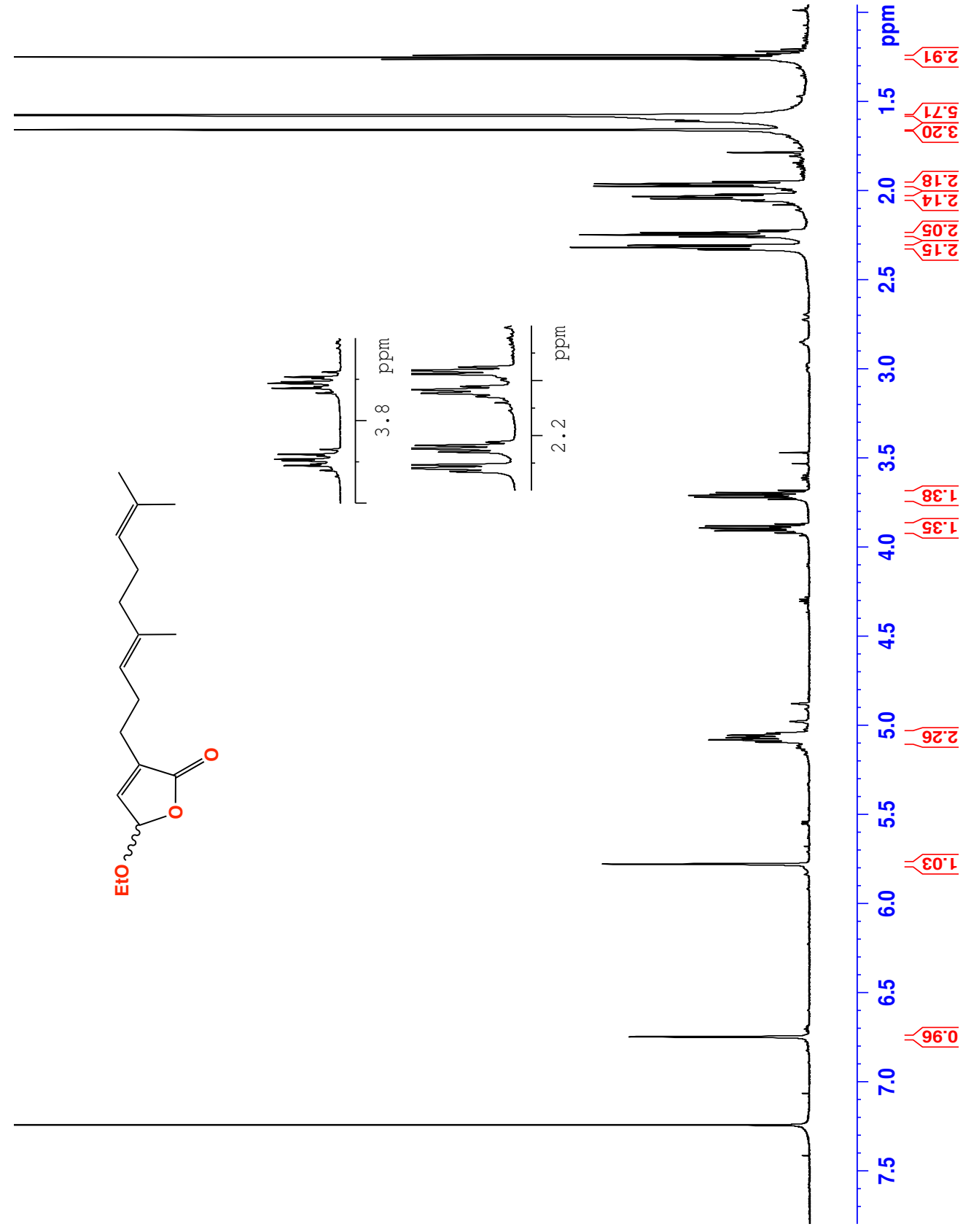

Figure 5S4a. ^{1}H NMR (600 MHz, $CDCl_3$) spectrum for ethyl dictyodendrillin (**4**)

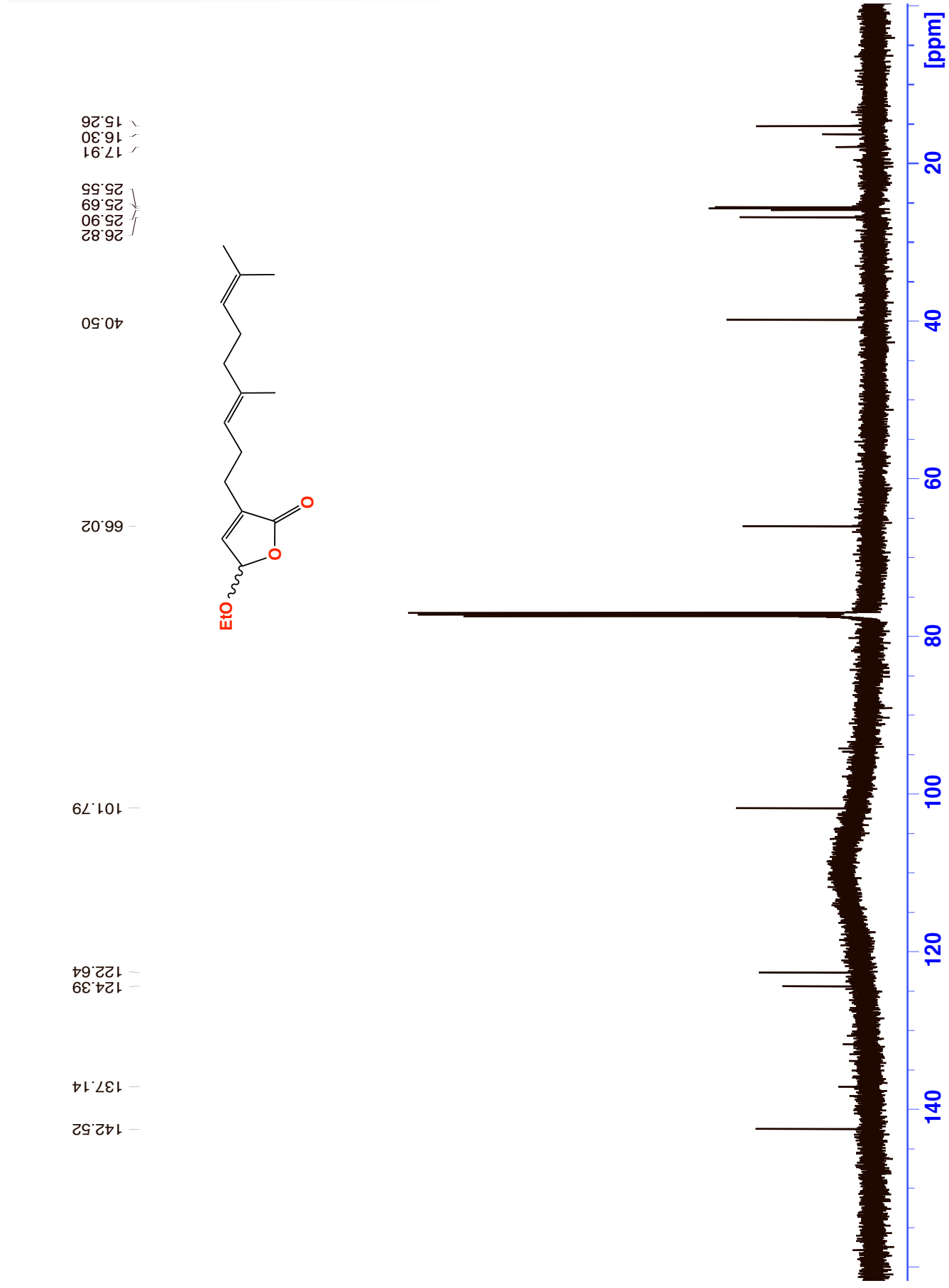

Figure 5S4b. ^{13}C NMR (150 MHz, $CDCl_3$) spectrum for ethyl dictyodendrillin (**4**)

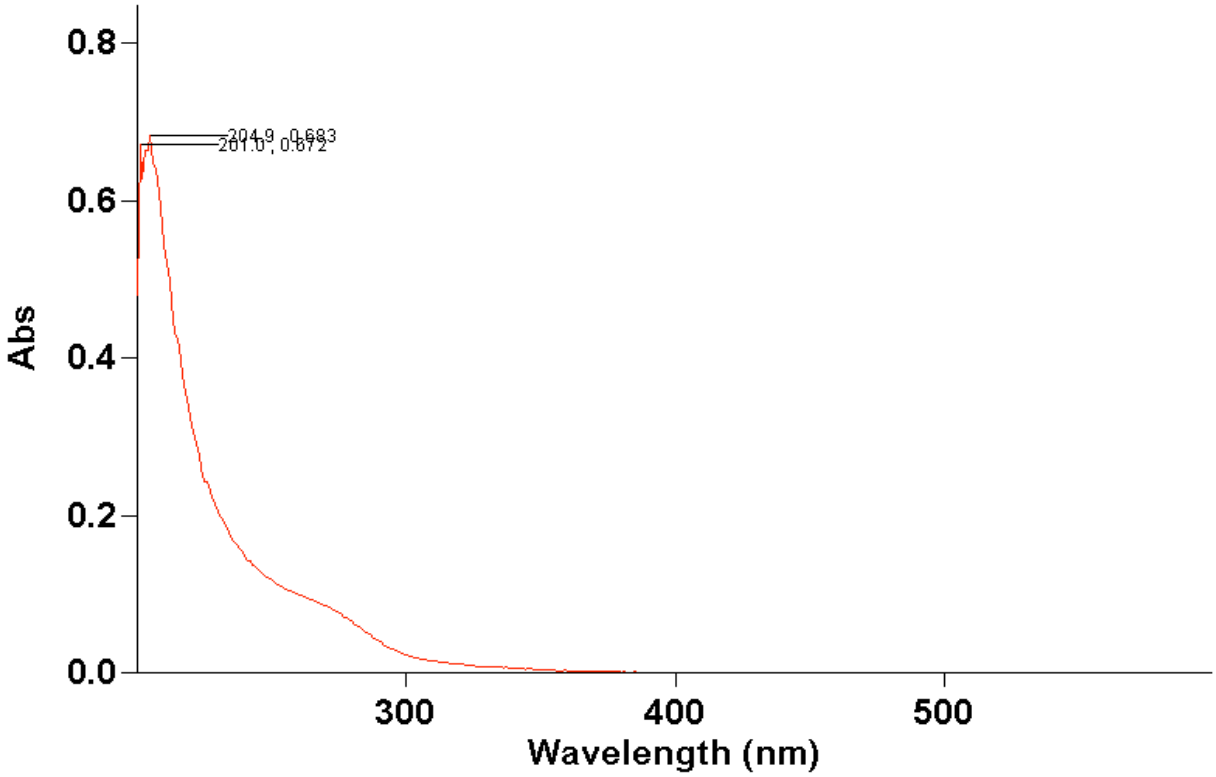

Figure 5S4c. UV-vis (MeOH) spectrum for ethyl dictyodendrillin (**4**)

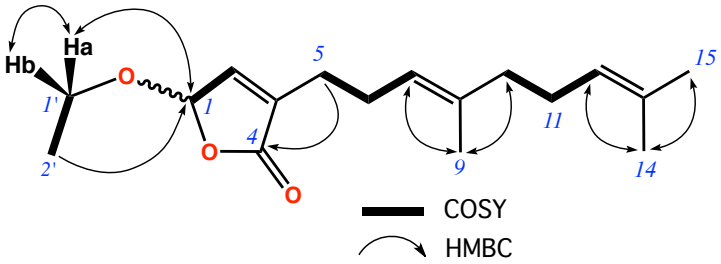

Figure 5S4d: Selected 2D NMR correlations for ethyl dictyodendrillin (**4**)

Table 5S4. NMR (600 MHz, $CDCl_3$) data for ethyl dictyodendrillin (**4**)

No.	δ_H (mult., *J* (Hz))	δ_C[A]	COSY	HMBC (^{1}H to ^{13}C)
1	5.78 (br s)	101.2	2, 5	1′, 3, 4
2	6.75 (d, 1.3)	142.0	4, 5	1, 3, 4, 5
3		138.2		
4		172.2		
5	2.32 (t, 7.4)	25.1	2, 6	2, 3, 4, 6, 7
6	2.25 (dt, 7.1, 7.3)	26.1	5, 7	3, 5, 7
7	5.07 (t, 7.4, 7.6)	121.9	6, 9	5, 9, 10
8		137.2		
9	1.57 (br s)	16.8	7	7, 8, 10
10	1.96 (t, 7.6)	40.5	11	8, 9, 11, 12
11	2.04 (dt, 7.1, 7.6)	27.3	10, 12	8, 10, 12, 13
12	5.05 (t, 7.1)	124.0	11, 14, 15	14, 15
13		132.4		
14	1.57 (br s)	16.5	12	13, 15
15	1.65 (br s)	26.0	12	12, 13, 14
1′a	3.89 (m)	65.0	2′, 1′b	1
1′b	3.70 (m)		2′, 1′a	
2′	1.25 (t, 7.3)	15.2	1′	1

[A] ^{13}C NMR assignments supported by HSQC data

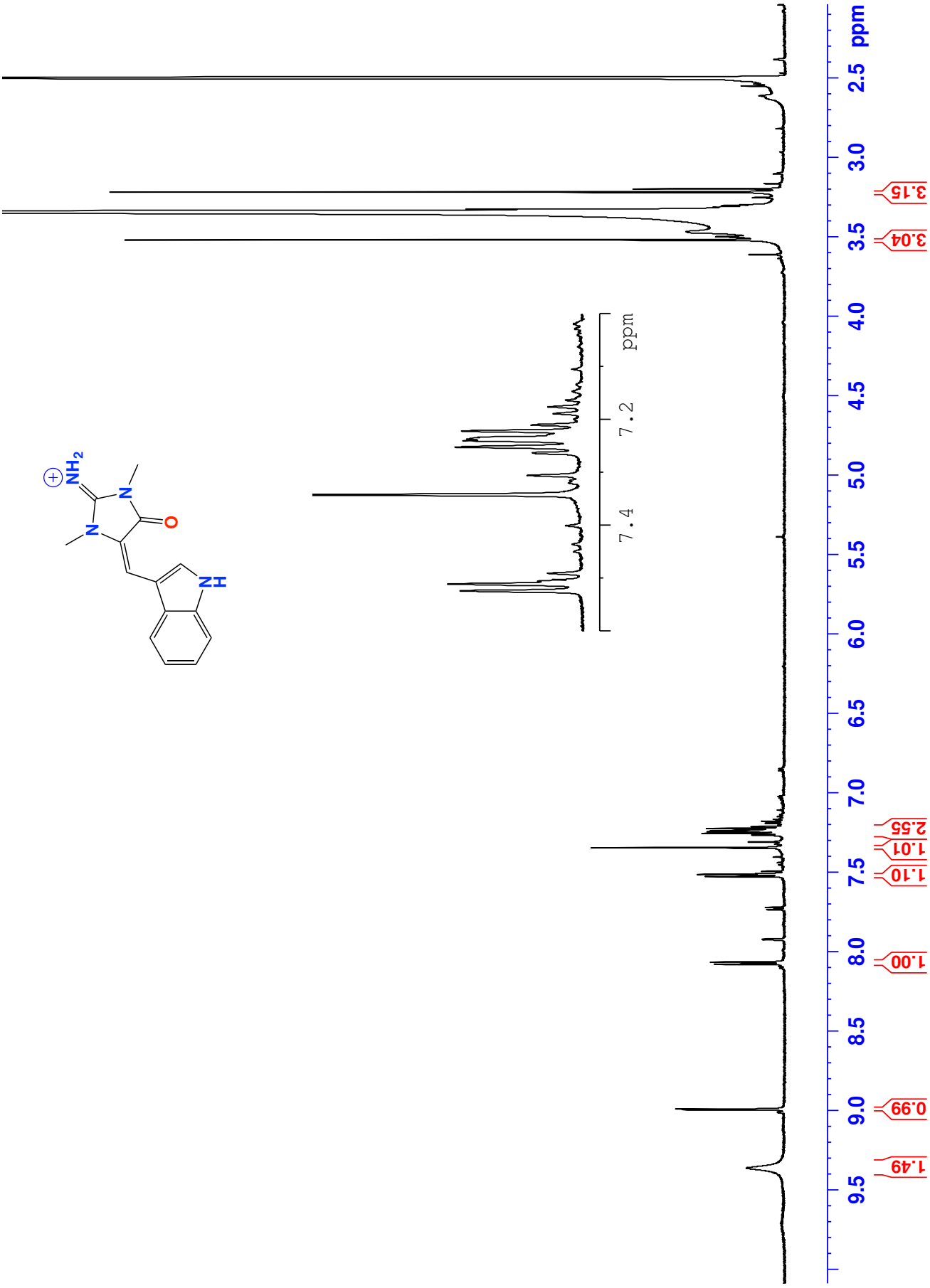

Figure 5S5a. ^{1}H NMR (600 MHz, DMSO-d_6) spectrum of aplysinopsin TFA salt (**5**)

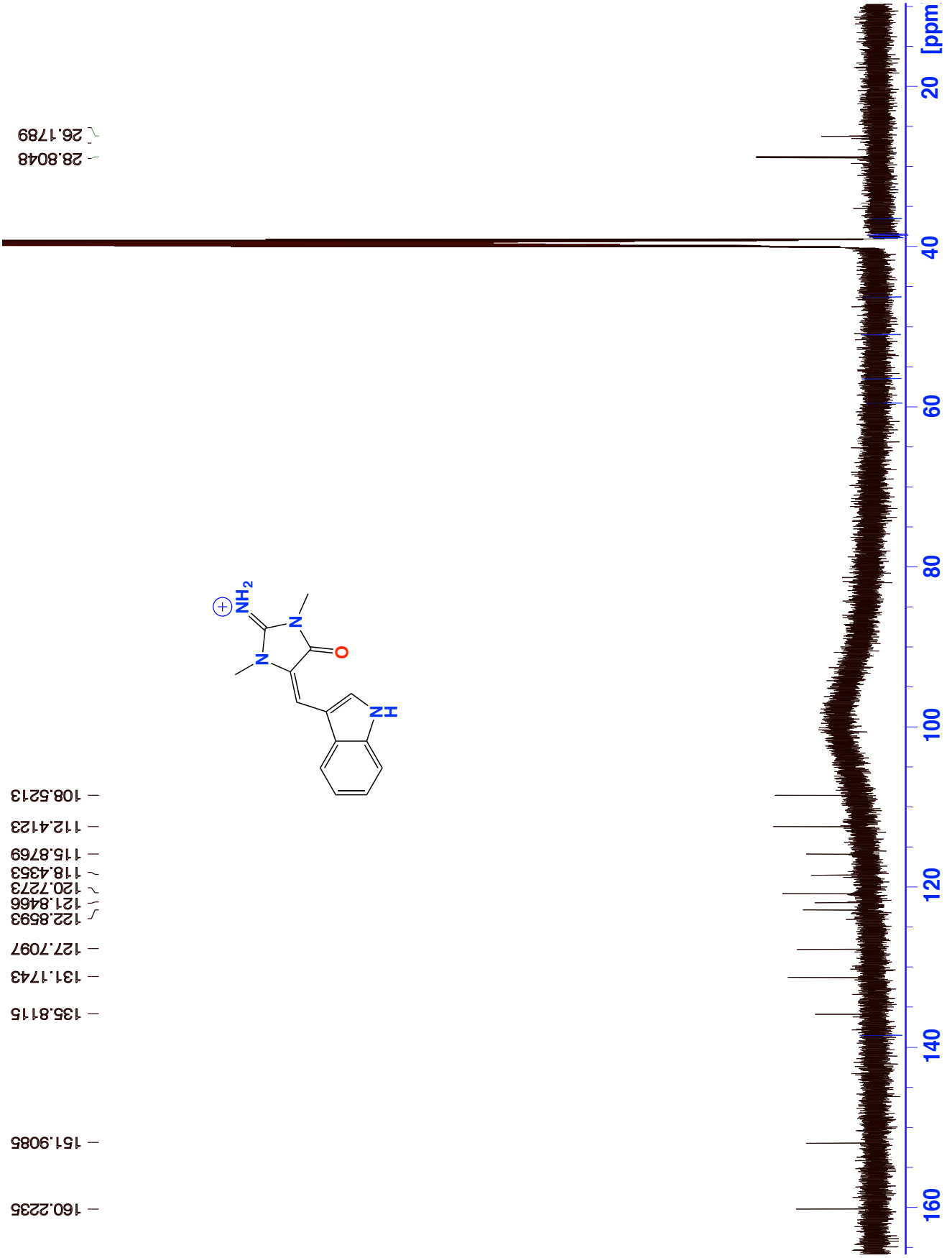

Figure 5S5b ^{13}C NMR (150 MHz, DMSO-d_6) spectrum of aplysinopsin TFA salt (**5**)

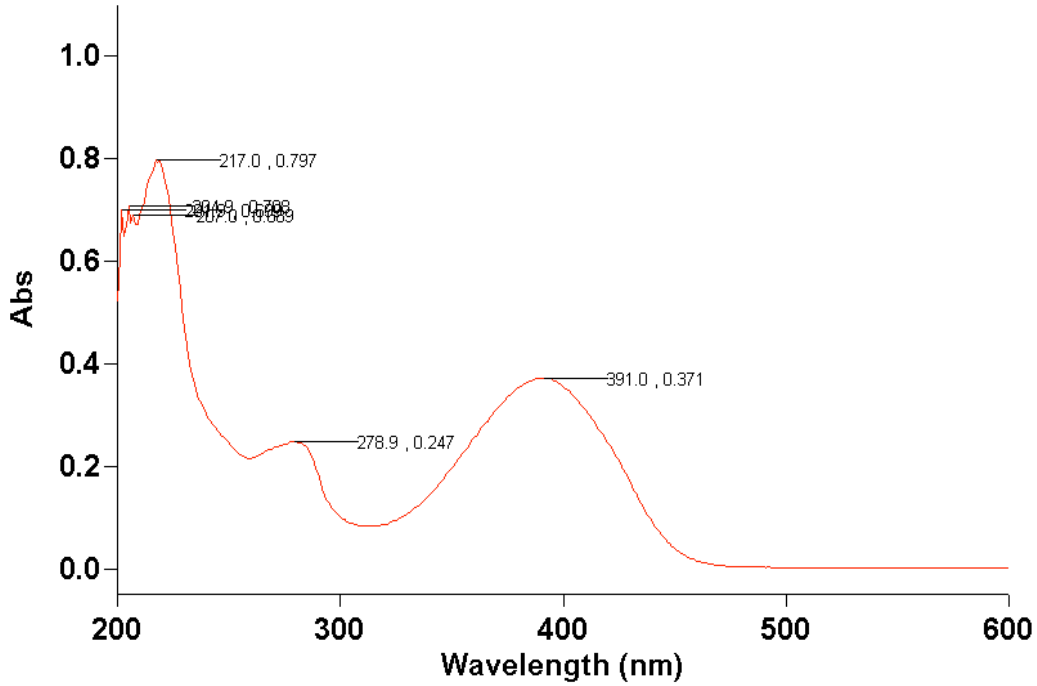

Figure 5S5c. UV-vis (MeOH) spectrum of aplysinopsin TFA salt (**5**)

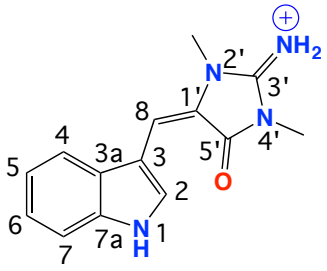

Table 5S5: NMR (600 MHz, DMSO-d_6) data for aplysinopsin TFA salt (**5**)

No.	δ_H (mult., *J* (Hz))	δ_C[A]	COSY	HMBC (^{1}H to ^{13}C)
2	8.99 (d, 3.0)	131.2		3, 3a, 7a
3		108.5		
3a		127.7		
4	8.06 (br d, 7.6)	118.5	5	6, 7a
5	7.22 (br dd, 7.6, 7.1)	120.8	4, 6	3a, 7
6	7.25 (br dd, 7.8, 7.1)	122.8	5, 7	4, 7a
7	7.52 (br d, 7.8)	112.4	6	3a, 5
7a		135.8		
8	7.34 (s)	115.8		2, 3, 3a, 1′, 5′
1′		121.9		
2′-*N*Me	3.52 (s)	28.8		1′, 3′
3′		152.0		
4′-*N*Me	3.22 (s)	26.2		3′, 5′
5′		161.2		
1-NH	9.36 (br s)			

[A] ^{13}C NMR assignments supported by HSQC data

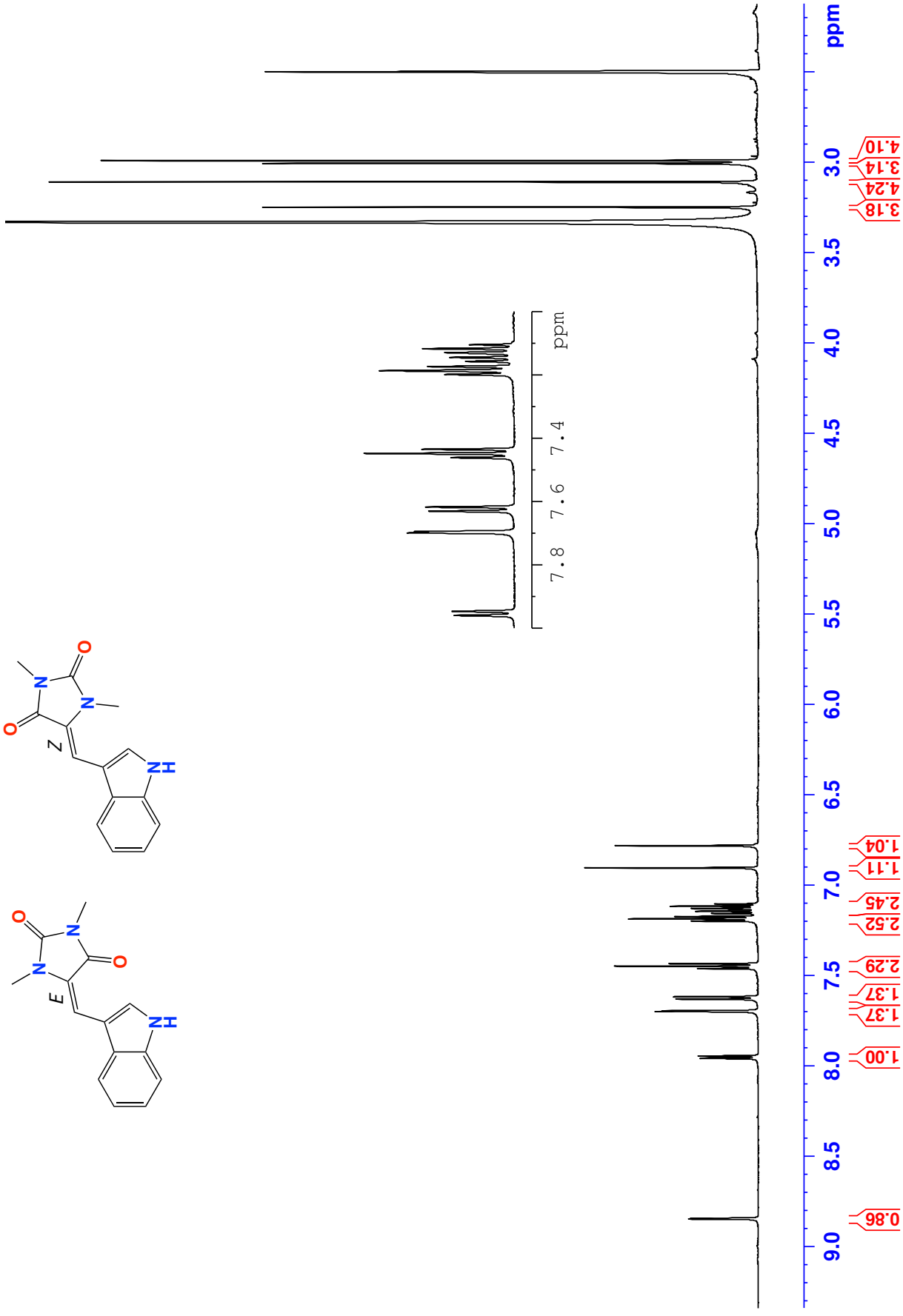

Figure 5S6a. ^{1}H NMR (600 MHz, DMSO-d_6) spectrum of a mixture of 8*E*/*Z*-3′-deimino-3′-oxoaplysinopsins (**6**/**7**).

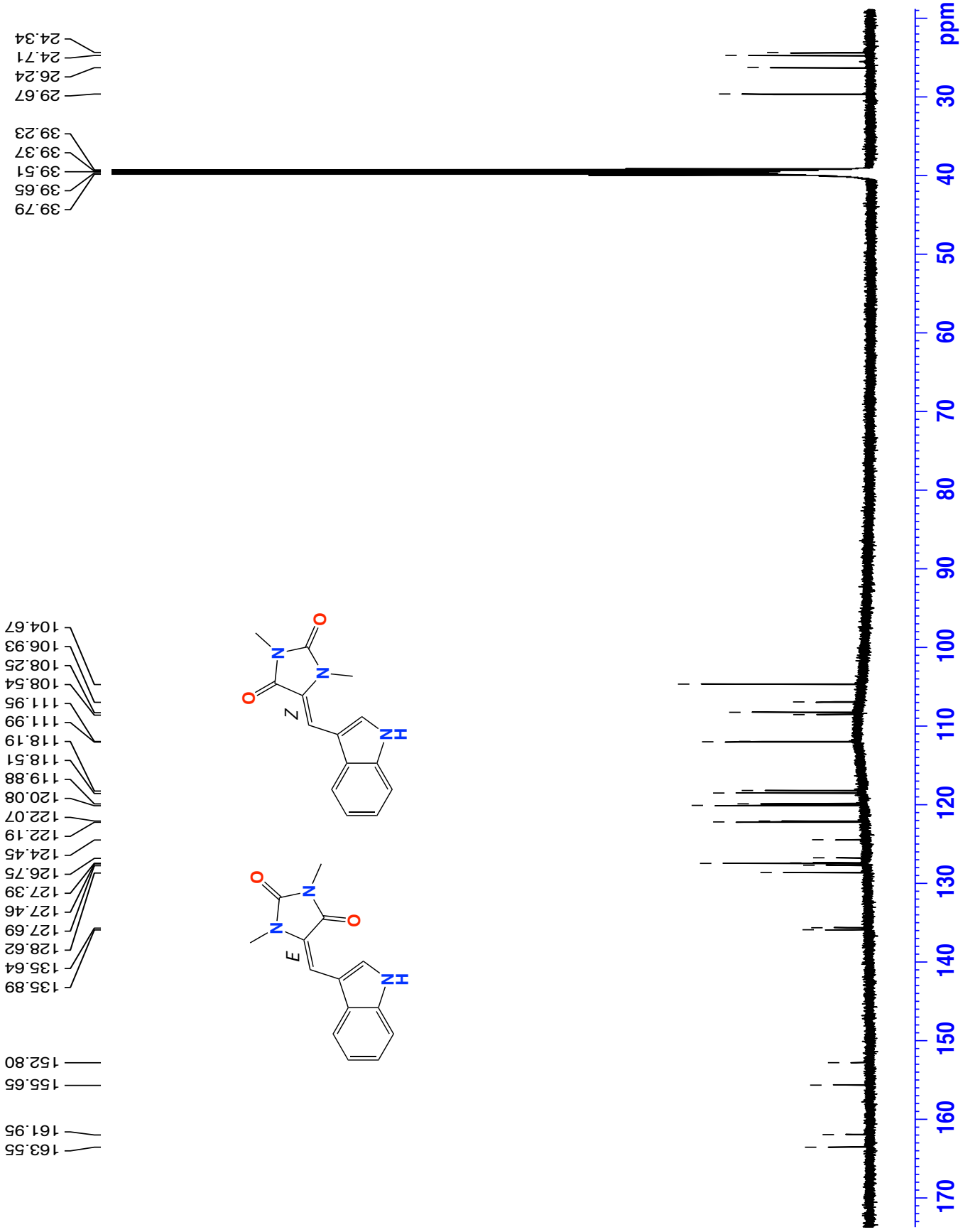

Figure 5S6b. ^{13}C NMR (150 MHz, DMSO-d_6) spectrum of a mixture of 8*E*/*Z*-3′-deimino-3′-oxoaplysinopsins (**6**/**7**).

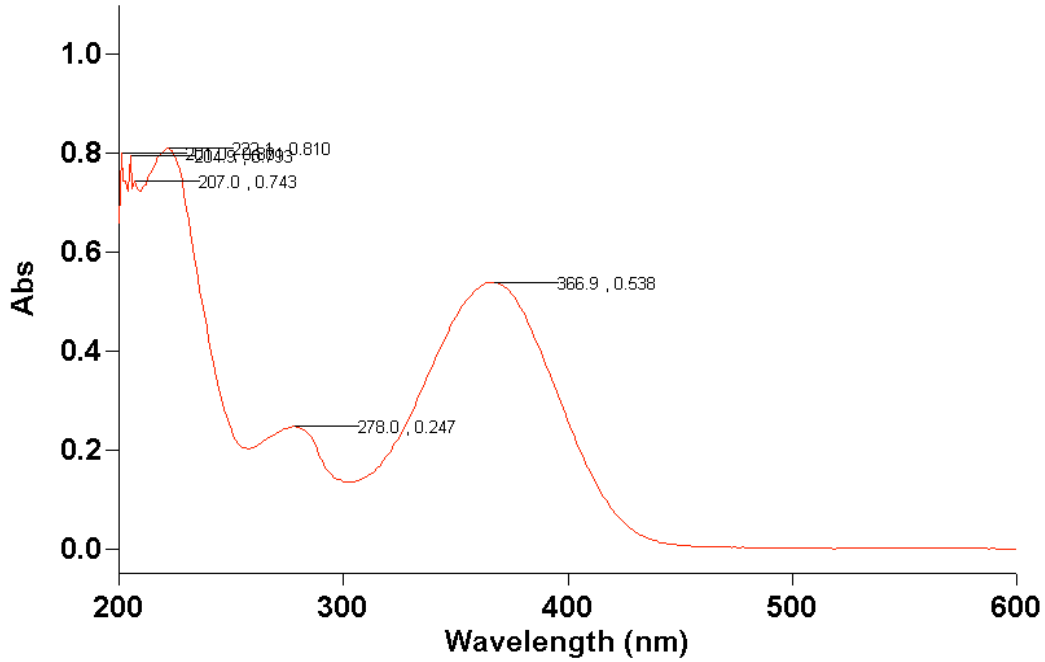

Figure 5S6c. UV-vis (MeOH) spectrum of a mixture of 8*E*/*Z*-3′-deimino-3′-oxoaplysinopsins (**6**/**7**).

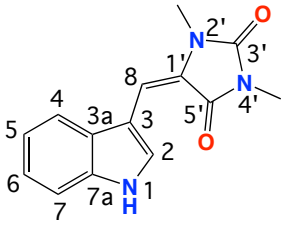

Table 5S6. NMR (600 MHz, DMSO-d_6) data for 8*E*-3′-deimino-3′-oxoaplysinopsin (**6**)

No.	**δ_H (mult., *J* (Hz))**	**δ_C[A]**	**COSY**	**HMBC (^{1}H to ^{13}C)**
2	8.85 (d, 2.7)	128.6		3, 3a, 7a
3		108.5		
3a		127.7		
4	7.95 (br d, 7.8)	118.2	5	3, 3a, 6, 7, 7a
5	7.14 (br dd, 7.8, 7.4)	119.9	4, 6	3a, 4, 6, 7
6	7.19 (br dd, 7.9, 7.4)	122.1	5, 7	4, 7, 7a
7	7.46 (br d, 7.9)	111.9	6	3a, 4, 5
7a		135.6		
8	6.78 (s)	108.3		2, 3, 3a, 1′, 5′
1′		124.5		
2′-Me	3.01 (s)	24.3		1′, 3′
3′		152.8		
4′-Me	3.25 (s)	26.2		3′, 5′
5′		161.9		

[A] ^{13}C NMR assignments supported by HSQC data

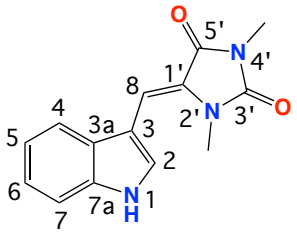

Table 5S7. NMR (600 MHz, DMSO-d_6) data for 8*Z*-3′-deimino-3′-oxoaplysinopsin (**7**)

No.	δ_H (mult., *J* (Hz))	δ_C[A]	COSY	HMBC (^{1}H to ^{13}C)
2	7.70 (d, 2.6)	127.5		3, 3a, 7a, 8
3		106.9		
3a		127.4		
4	7.62 (br d, 7.9)	118.5	5	3, 3a, 6, 7, 7a
5	7.12 (br dd, 7.9, 7.2)	120.1	4, 6	3a, 4, 6, 7
6	7.19 (br dd, 8.0, 7.2)	122.2	5, 7	4, 7, 7a
7	7.44 (br d, 8.0)	112.0	6	3a, 4, 5
7a		135.9		
8	6.90 (s)	104.7		2, 3, 1′, 5′
1′		126.7		
2′-Me	3.11 (s)	29.6		1′, 3′
3′		155.7		
4′-Me	2.99 (s)	24.7		3′, 5′
5′		163.6		

[A] ^{13}C NMR assignments supported by HSQC data

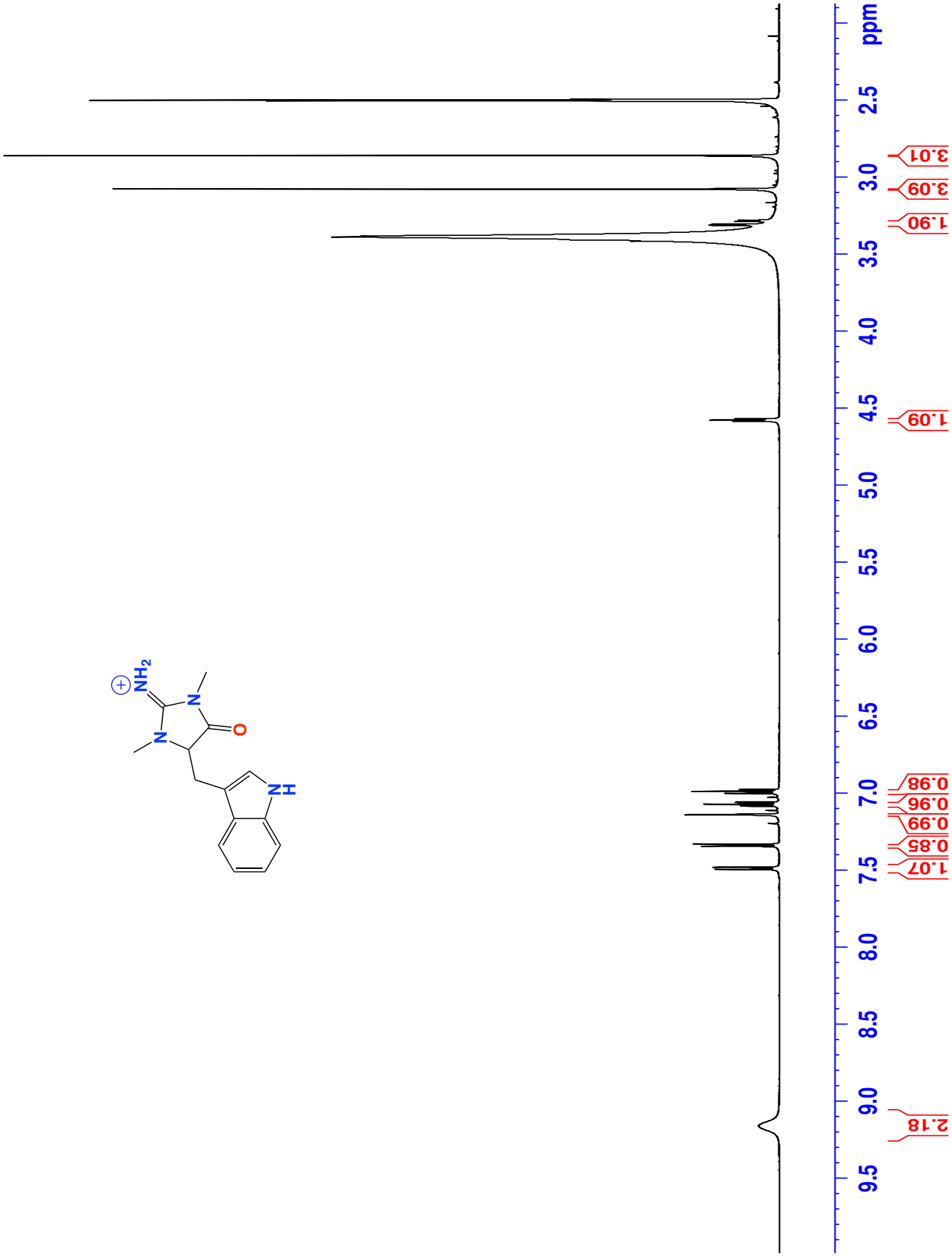

Figure 5S8a. ^{1}H NMR (600 MHz, DMSO-d_6) spectrum for dihydroaplysinopsins TFA salt (**8**).

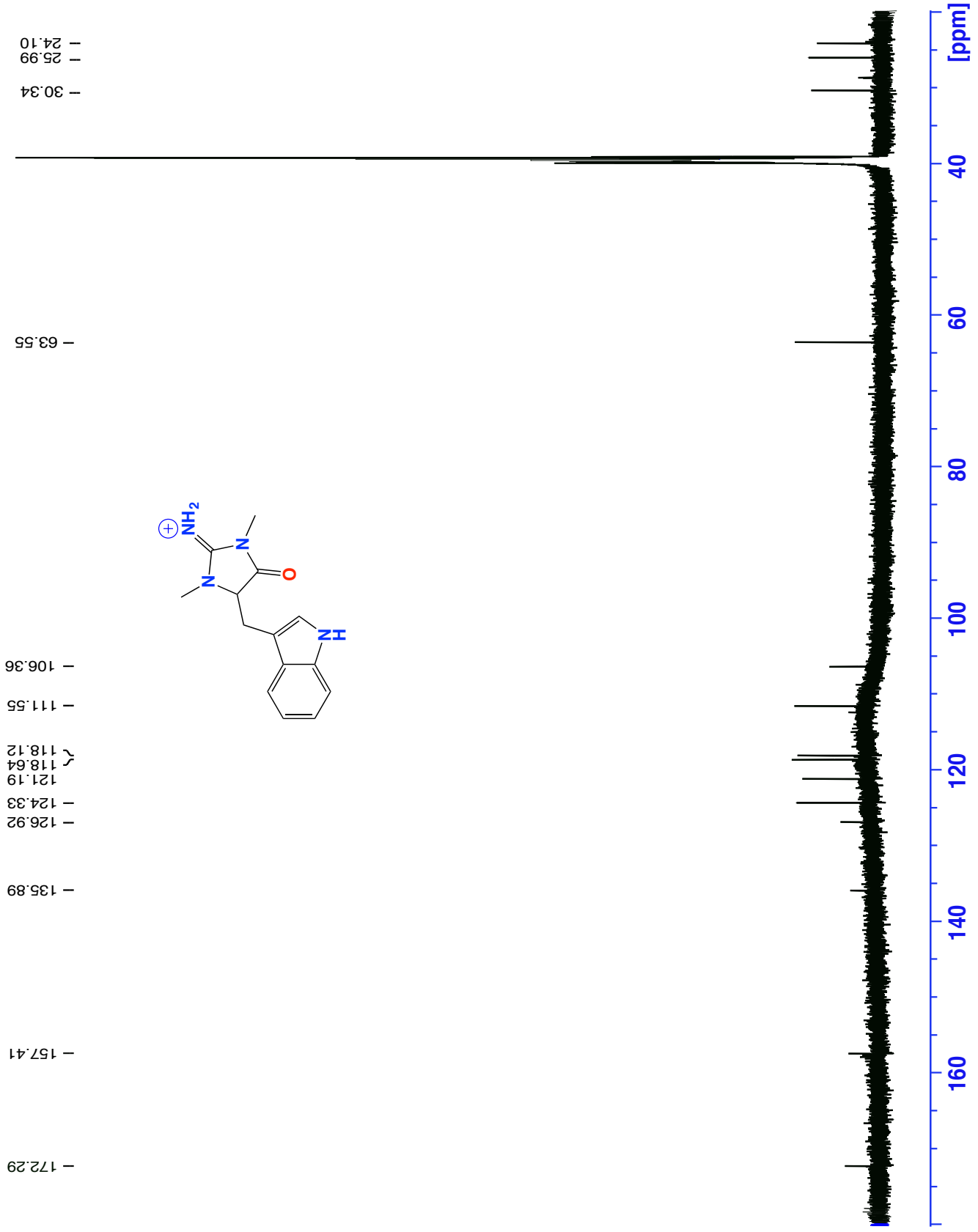

Figure 5S8b. ^{13}C NMR (150 MHz, DMSO-d_6) spectrum for dihydroaplysinopsins TFA salt (**8**).

Figure 5S8C. UV-vis (MEOH) spectrum for dihydroaplysinopsin TFA salt (**8**)

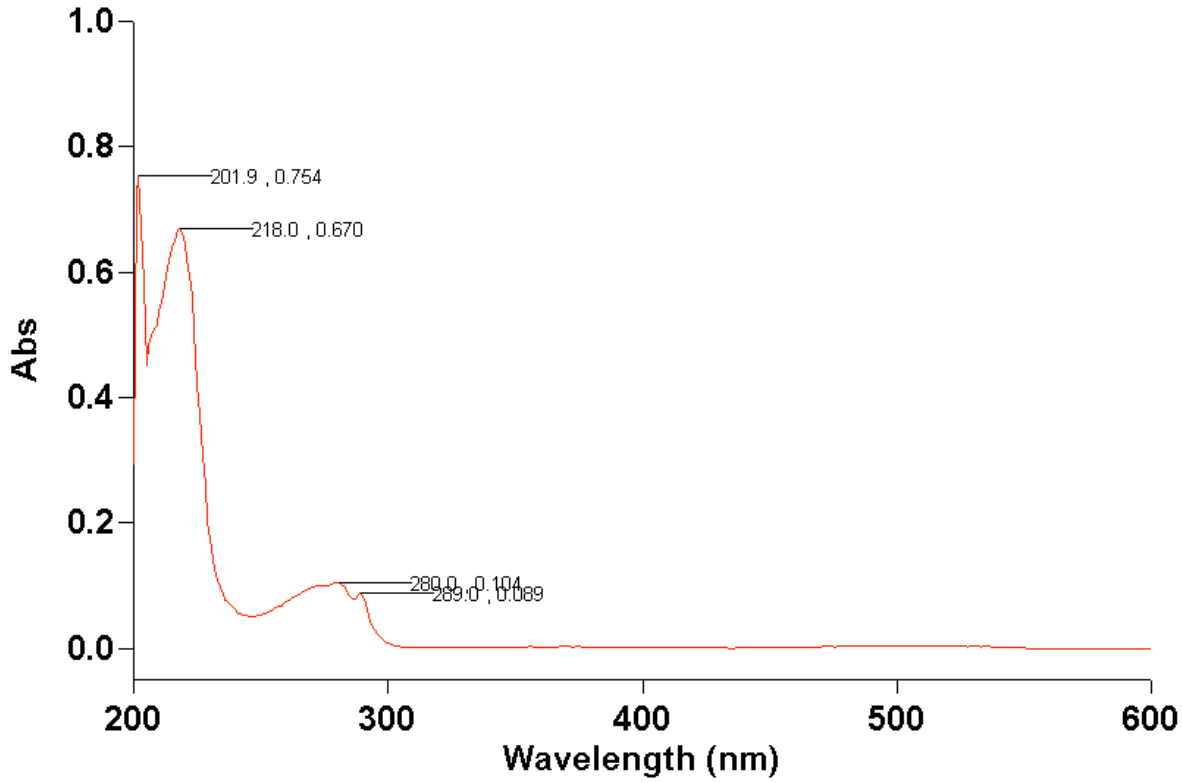

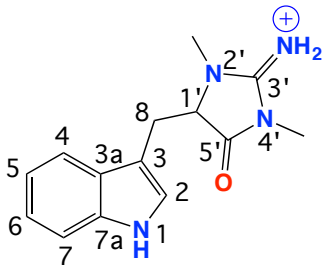

Table 5S8. NMR (600 MHz, DMSO-d_6) data for dihydroaplysinopsin TFA salt (**8**)

No.	δ_H (mult., *J* (Hz))	δ_C [A]	COSY	HMBC (^{1}H to ^{13}C)
2	7.14 (d, 2.4)	124.3		3, 3a, 7a
3		106.4		
3a		126.9		
4	7.49 (br d, 8.0)	118.1	5	3, 3a, 6, 7a
5	6.99 (ddd, 8.0, 8.0, 1.0)	118.7	4, 6	3a, 7
6	7.07 (ddd, 8.0, 8.0, 1.0)	121.2	5, 7	4, 7a
7	7.34 (ddd, 8.0, 1.0, 0.8)	111.6	6	3a, 5
7a		135.9		
8α	3.40[B]	24.1	1′, 8β	2, 3, 3a, 1′, 5′
8β	3.29 (dd, 15.5, 4.2)		1′, 8α	2, 3, 1′
1′	4.58 (dd, 5.2, 4.2)	63.6	8α/β	3, 3′, 5′, 8
2′-Me	3.08 (s)	30.3		1′, 3′
3′		157.5		
4′-Me	2.86 (s)	26.0		3′, 5′
5′		172.3		
3′-NH_2	9.17 (br s)			

[A] ^{13}C NMR assignments supported by HSQC data; [B] obscured by H_2O signal

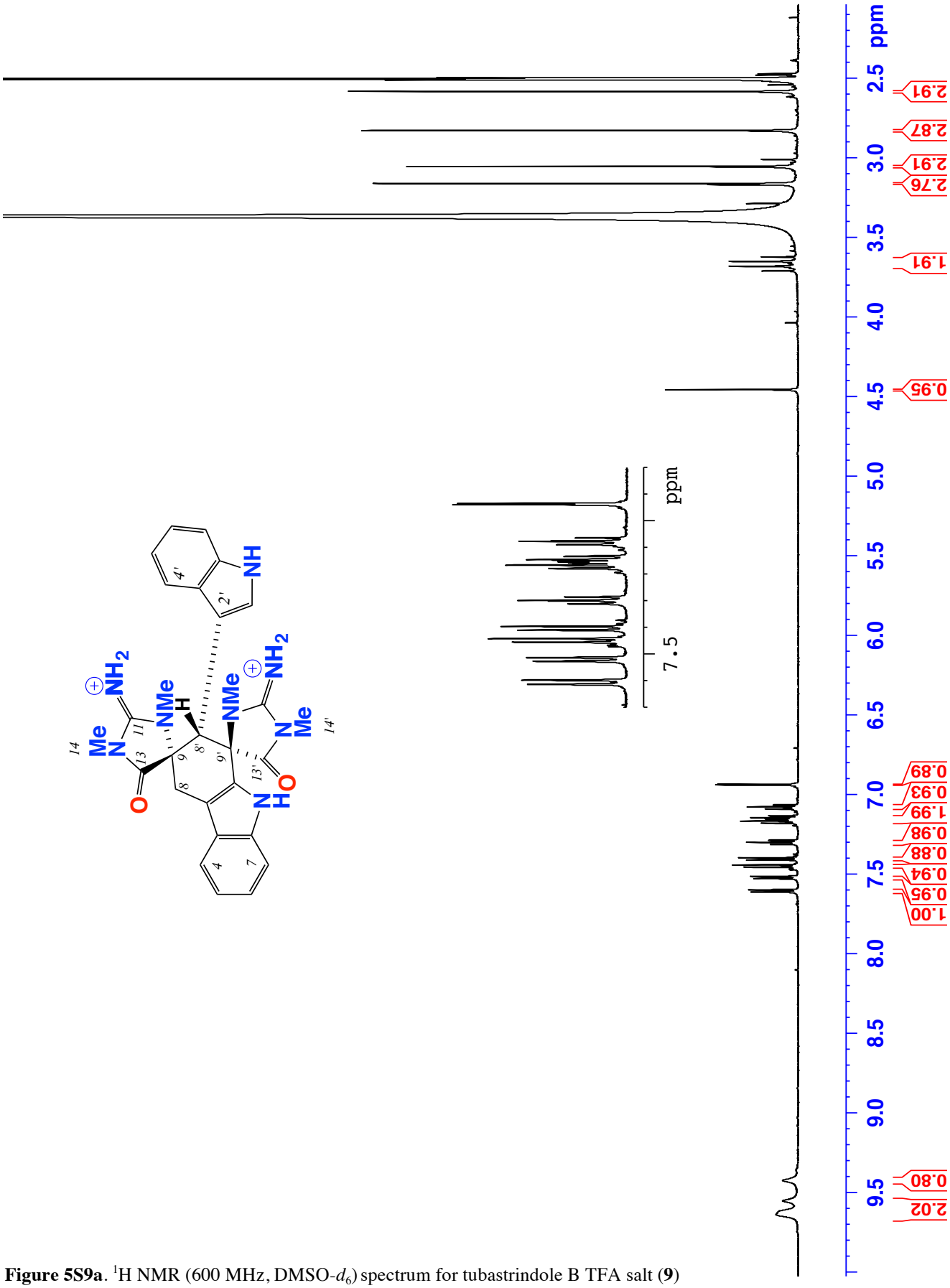

Figure 5S9a. ^{1}H NMR (600 MHz, DMSO-d_6) spectrum for tubastrindole B TFA salt (**9**)

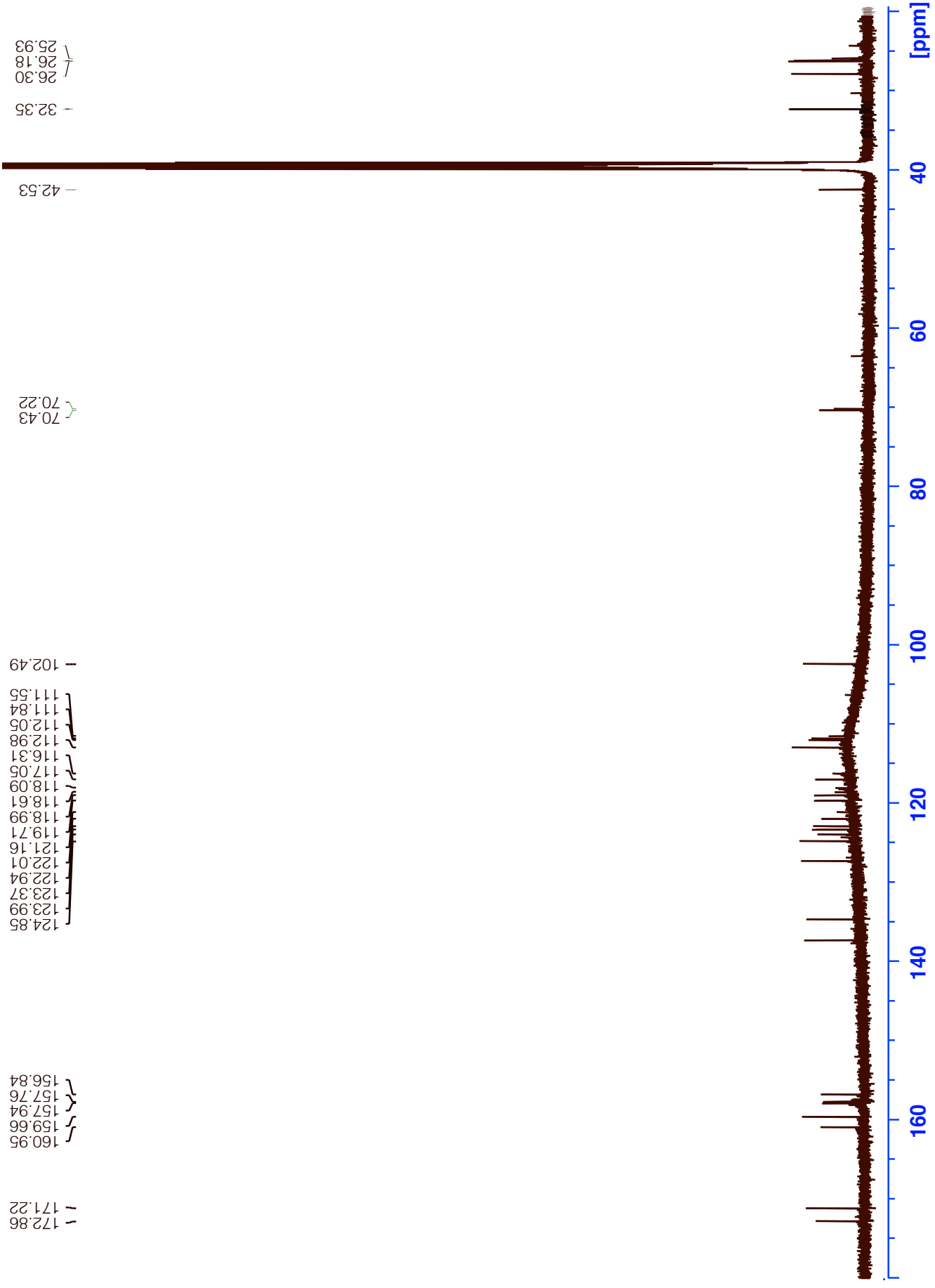

Figure 5S9b. ^{13}C NMR (150 MHz, DMSO-d_6) spectrum for tubastrindole B TFA salt (**9**)

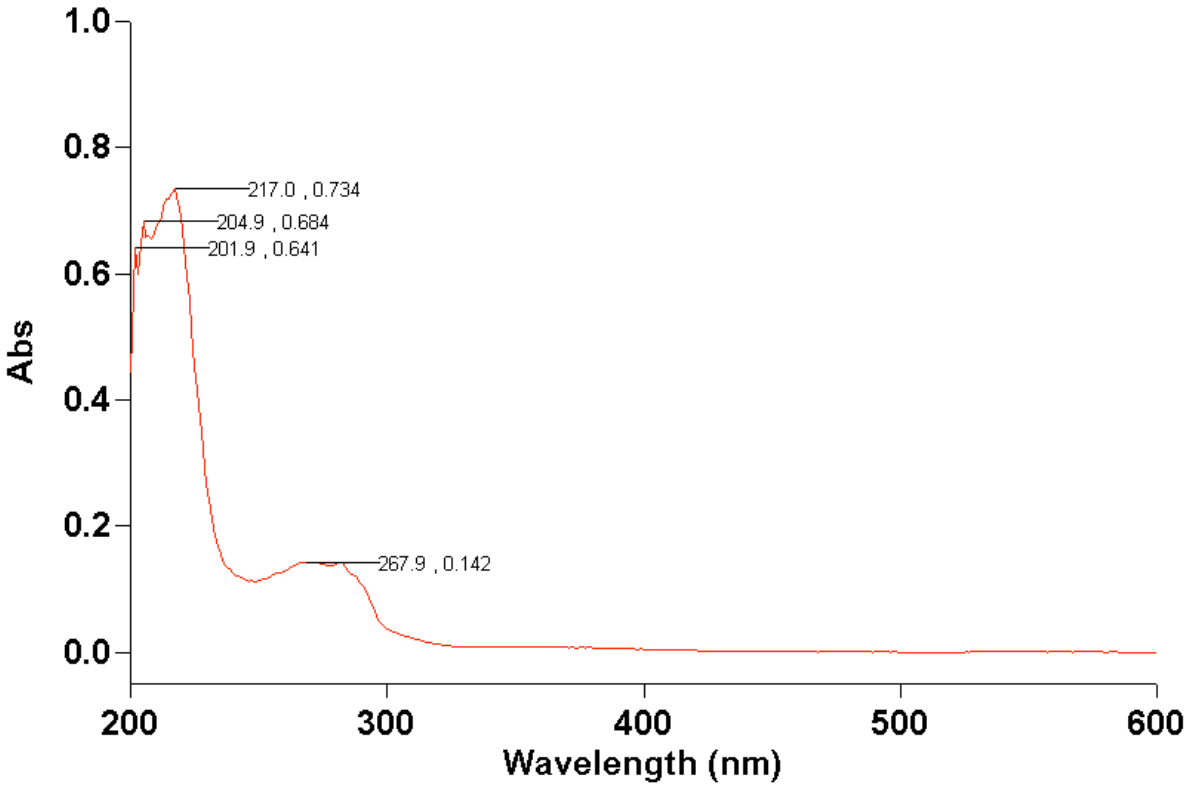

Figure 5S9c. UV-vis (MEOH) spectrum for tubastrindole B TFA salt (**9**)

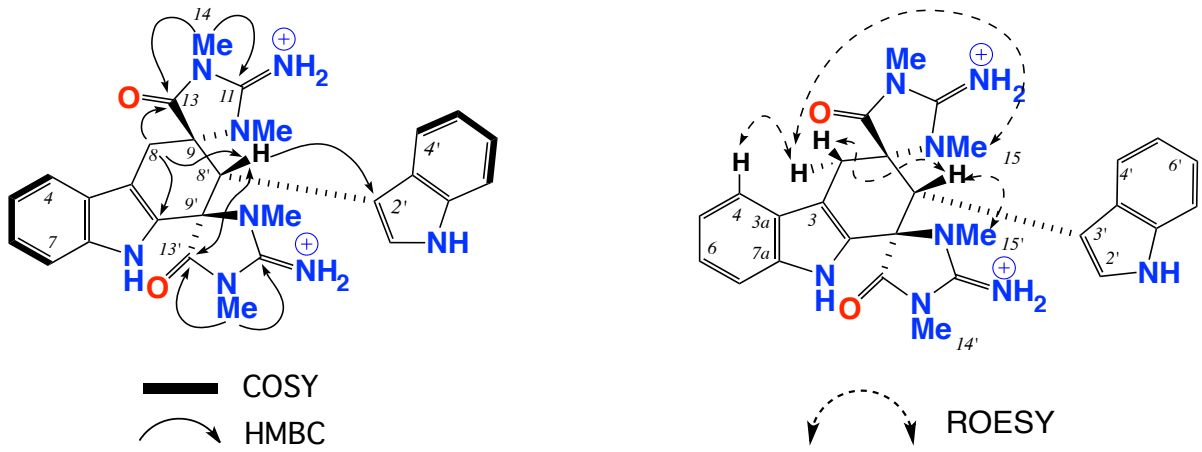

Figure 5S9d. Selccted 2D NMR correlations for tubastrindole B TFA salt (**9**)

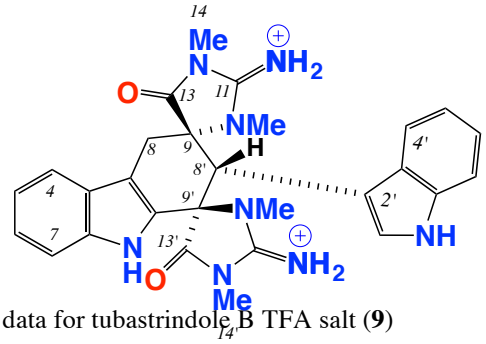

Table 5S9. NMR (600 MHz, DMSO-d_6) data for tubastrindole B TFA salt (**9**)

No.	δ_H (mult., *J* (Hz))	δ_C [A]	COSY	HMBC (^{1}H to ^{13}C)	ROESY
2		123.4			
3		117.0			
3a		127.3			
4	7.60 (d, 8.0)	118.7	5	3a, 6, 7a	8α
5	7.17 (dd, 8.0, 1.0)	119.4	4, 6	3a, 7	
6	7.29 (dd, 8.3, 1.0)	123.6	5, 7	5, 7, 7a	
7	7.44 (dd, 8.3, 1.0)	111.7	6	3a, 6	
7a		137.4			
8α	3.69 (d, 17.2)	25.8	8β	2, 3, 8′, 9	4, 14
8β	3.63 (d, 17.0)		8α	3, 9, 13	4, 8′, 15′
9		70.2			
11		161.0			
13		172.8			
14	3.16 (s)	32.1		9, 11	2′
15	2.58 (s)	26.0		11, 13	
1-*N*H	9.65 (br s)				
2′	6.9 (d, 2.7)	123.4	3′	3′, 3′a, 7′a	14′, 15′
3′		102.4			
3′a		127.3			
4′	7.52 (d, 8.0)	116.6	5′	3′, 6′, 7′a	8′, 14′
5′	7.13 (dd, 8.1, 1.0)	121.6	4′, 6′	3′a, 4′, 7′	
6′	7.15 (dd, 8.1, 1.0)	119.4	5, 6′	7′a, 3a	
7′	7.40 (dd, 9.0, 1.0)	111.6	6′	3′a, 6′	
7′a		134.7			
8′	4.45 (s)	42.2		2′, 3′, 3′a, 9′, 13′	4′, 8β, 14′
9′		70.3			
11′		159.7			
13′		171.2			
14′	3.05 (s)	27.5		9, 11′	4′
15′	2.83 (s)	26.3		11′, 13′	
1′-*N*H	9.50 (d, 0.6)				

[A] ^{13}C NMR assignments supported by HSQC data.

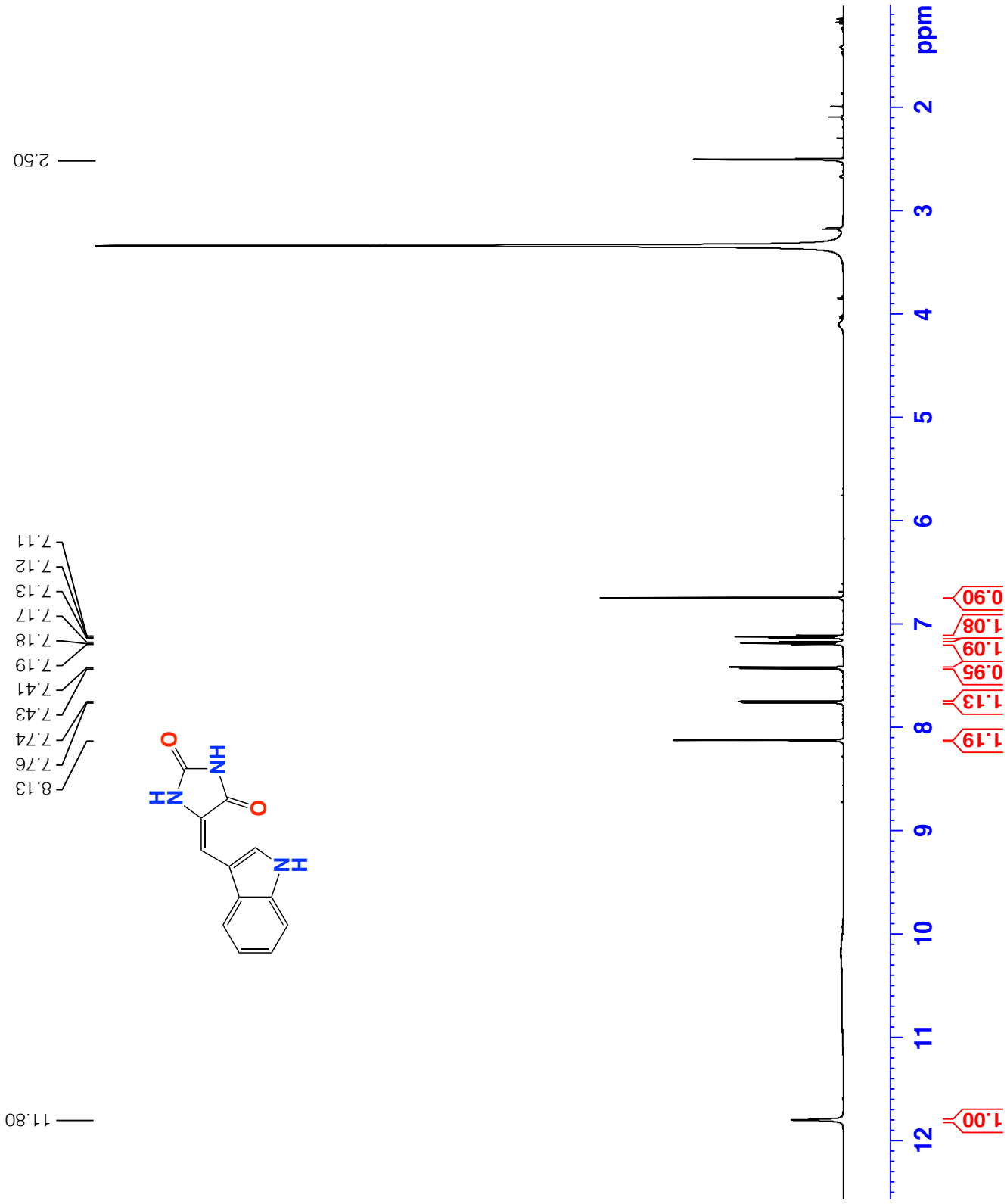

Figure 5S10a. ^{1}H NMR (600 MHz, DMSO-d_6) spectrum for 8*E*-3′-deimino-2′-4′-bisdemethyl-3′-oxoaplysinopsin (**10**)

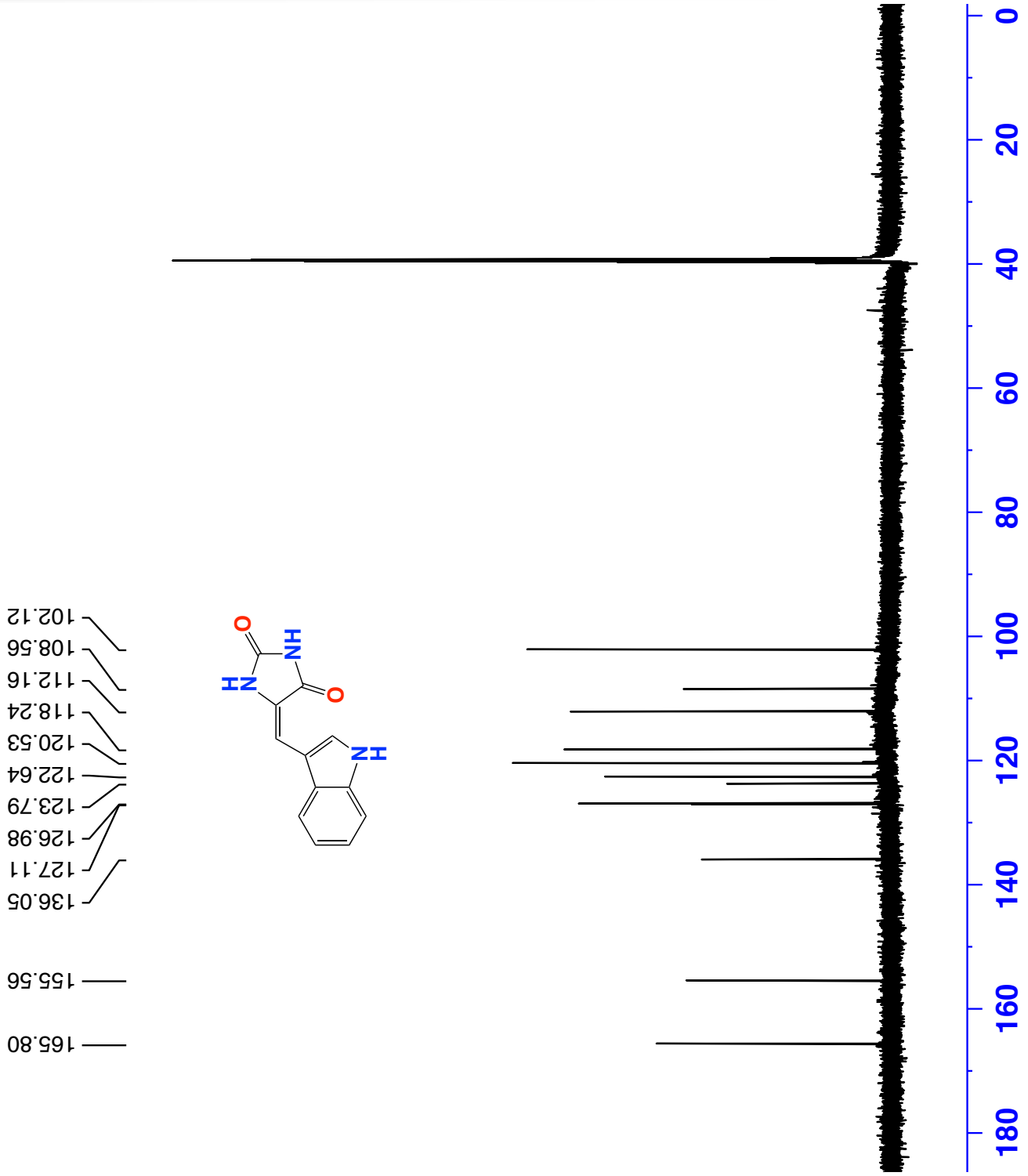

Figure 5S10b. ^{13}C NMR (150 MHz, DMSO-d_6) spectrum for 8*E*-3′-deimino-2′,4′-bisdemethyl-3′-oxoaplysinopsin (**10**)

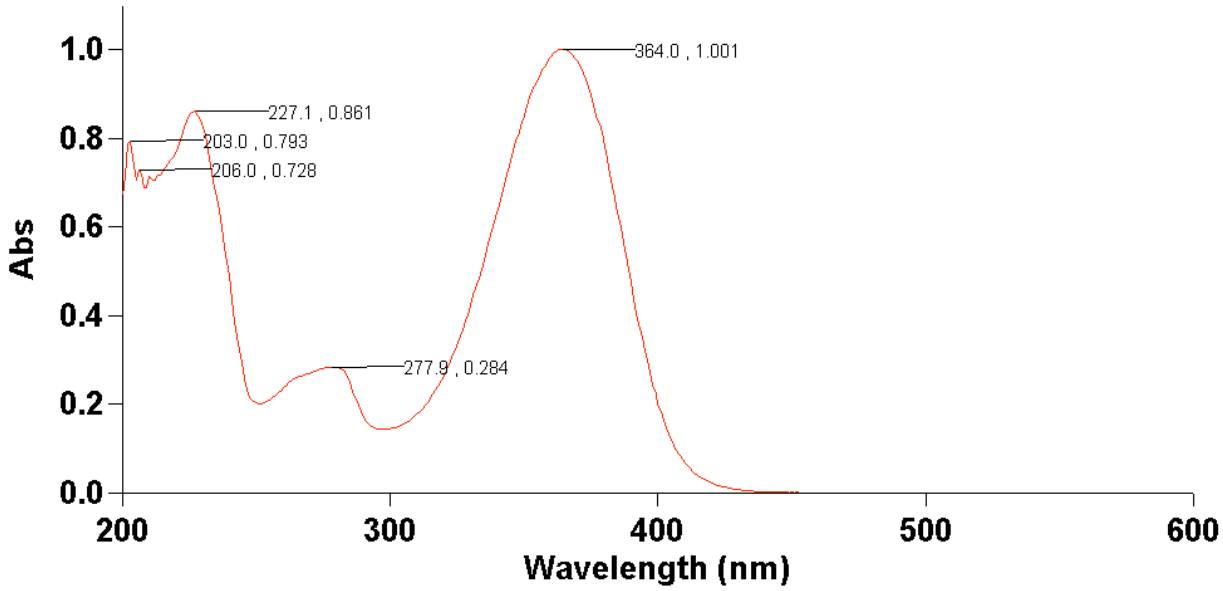

Figure 5S10c. UV-vis (MeOH) spectrum for 8*E*-3′-deimino-2′,4′-bisdemethyl-3′-oxoaplysinopsin (**10**)

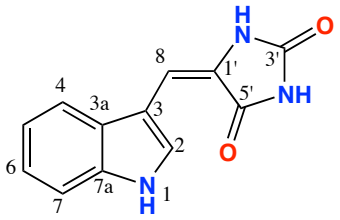

Table 5S10: NMR (600 MHz, DMSO-d_6) data for 8*E*-3′-deimino-2′,4′-bisdemethyl-3′-oxoaplysinopsin (**10**)

No.	δ_H (mult., *J* (Hz))	δ_C [A]	COSY	HMBC (^{1}H to ^{13}C)
2	8.14 (d, 2.4)	128.0		3, 3a, 7a
3		108.0		
3a		127.0		
4	7.75 (br d, 8.0)	118.1	5	3, 3a, 6, 7a
5	6.99 (ddd, 8.0, 8.0, 1.0)	120.1	4, 6	3a, 7
6	7.15 (ddd, 8.0, 8.0, 1.0)	123.0	5, 7	4, 7a
7	7.41 (ddd, 8.0, 1.0, 0.8)	112.0	6	3a, 5
7a		136.0		
8	6.76 (s)	102.0		2, 3, 3a, 1′, 5′
1′		127.0		
3′		165.0		
5′		165.0		
1-*N*H	11.8 (br s)			3, 3a, 7a

[A] ^{13}C NMR assignments supported by HSQC data.

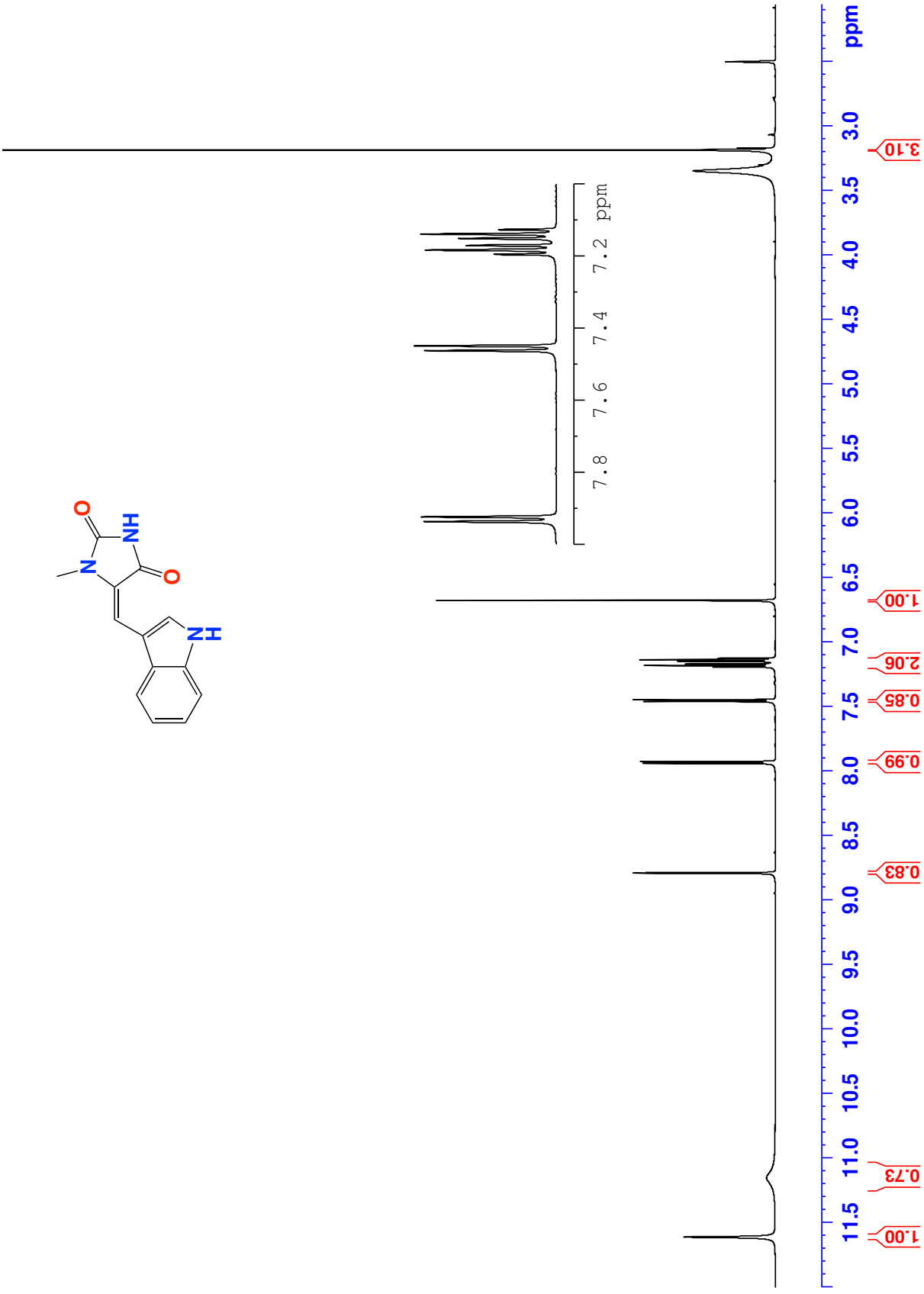

Figure 5S11a. ^{1}H NMR (600 MHz, DMSO-d_6) spectrum for 8*E*-3′-deimino-4′-demethyl-3′-oxoaplysinopsin (**11a**)

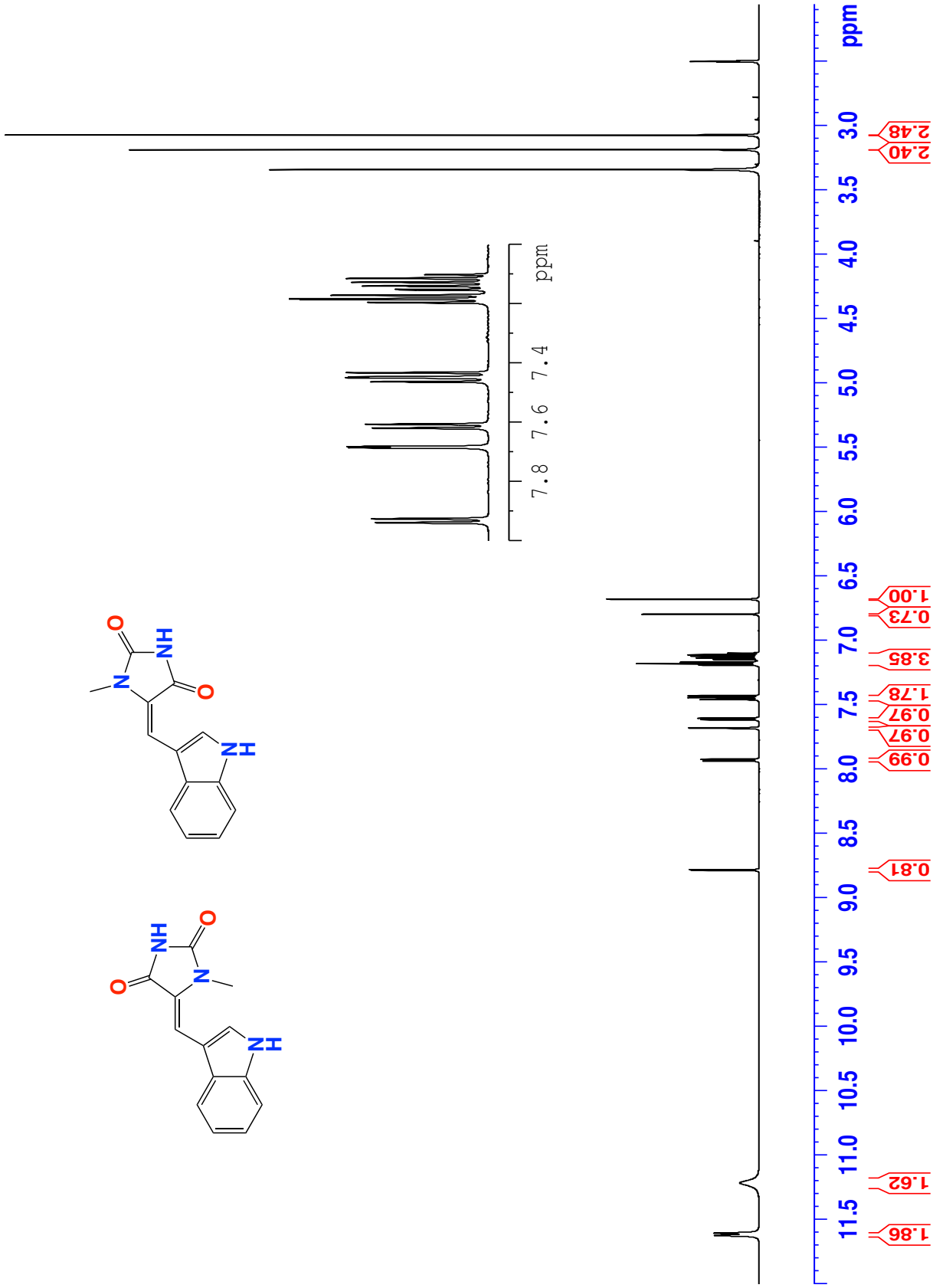

Figure 5S11b. ^{1}H NMR (600 MHz, DMSO-d_6) spectrum for a mixture of 8*E*/Z-3′-deimino-4′-demethyl-3′ oxoaplysinopsins (**11a/b**)

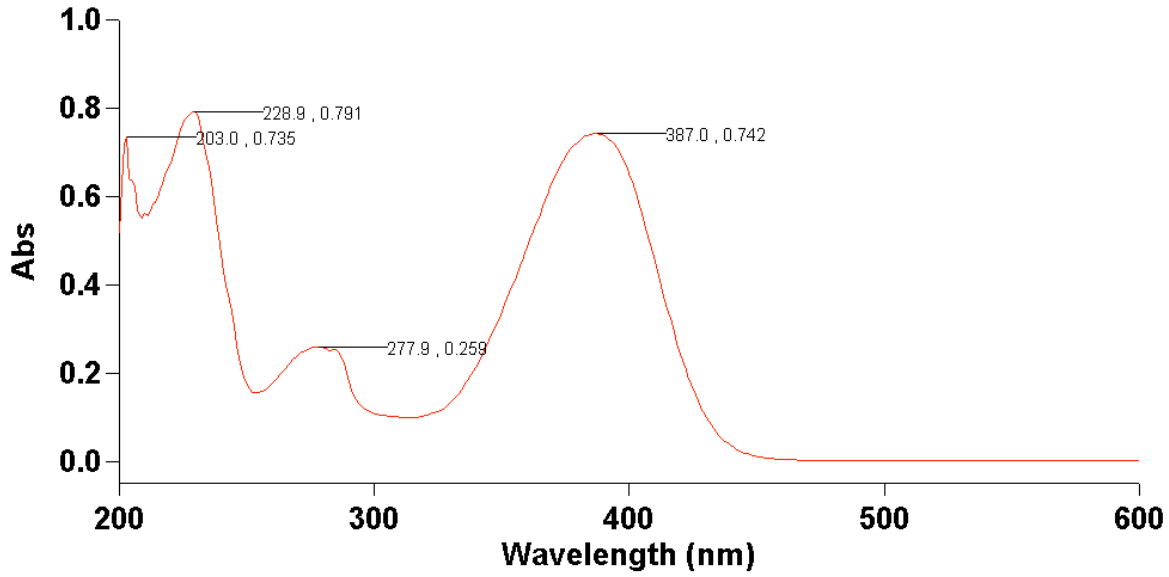

Figure 5S11c. UV-vis (MeOH) spectrum for a mixture of 8*E*/*Z*-3′-deimino-4′-demethyl-3′-oxoaplysinopsins (**11a/b**)

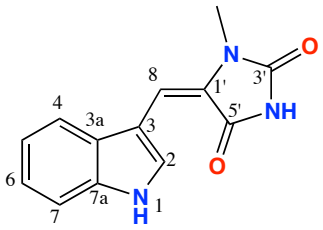

Table 5S11a. NMR (600 MHz DMSO-d_6) data for 8*E*-3′-deimino-4′-demethyl-3′-oxoaplysinopsin (**11a**)

No.	**δ_H (mult., *J* (Hz))**	**δ_C[A]**	**COSY**	**HMBC (^{1}H to ^{13}C)**
2	8.78 (d, 2.2)	128.6		3, 3a, 7a
3		108.8		
3a		126.0		
4	7.93 (d, 7.98)	117.9	5	3, 3a, 7a
5	7.18 (ddd, 8.1, 8.0, 1.0)	119.8	4, 6	3a, 7
6	7.13 (ddd, 8.0, 7.9, 1.0)	122.0	5, 7	4, 7a
7	7.48 (d, 7.98)	111.8	6	3a, 5
7a		135.4		
8	6.68 (s)	107.6		1′, 2, 3, 5′
9		125.9		
2′-Me	3.19 (s)	27.6		1′, 3′
3′		153.3		
4′-*N*H	11.61 (br s)			3, 3a, 7a
5′		163.5		

[A] ^{13}C NMR assignments supported by HSQC data.

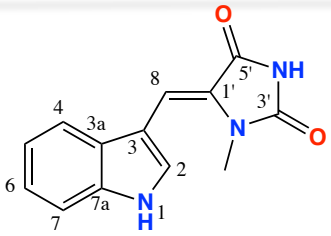

Table 5S11b. NMR (600 MHz, DMSO-d_6) data for 8*Z*-3′-deimino-4′-demethyl-3′-oxoaplysinopsin (**11b**)

No.	**δ_H (mult., *J* (Hz))**	**δ_C [A]**	**COSY**	**HMBC (^{1}H to ^{13}C)**
2	7.68 (br s)	128.5		3, 3a, 7a
3		108.8		
3a		127.6		
4	7.61 (d, 7.86)	117.6	5	3, 3a, 7a
5	7.18 (ddd, 8.0, 8.0, 1.0)	119.5	4, 6	3a, 7
6	7.13 (dd, 8.1, 8.0, 1.0)	121.0	5, 7	4, 7a
7	7.44 (dd, 8.1, 1.0)	111.5	6	3a, 5
7a		135.4		
8	6.68 (s)	102.1		
1′		130.0		3, 3′, 5′, 8
2′-Me	3.07 (s)	27.5		1′, 3′
3′		165.0		
4′-*N*H				3′, 5′
5′		177.0		
1-*N*H	11.51 (br s)			

[A] ^{13}C NMR assignments supported by HSQC data.

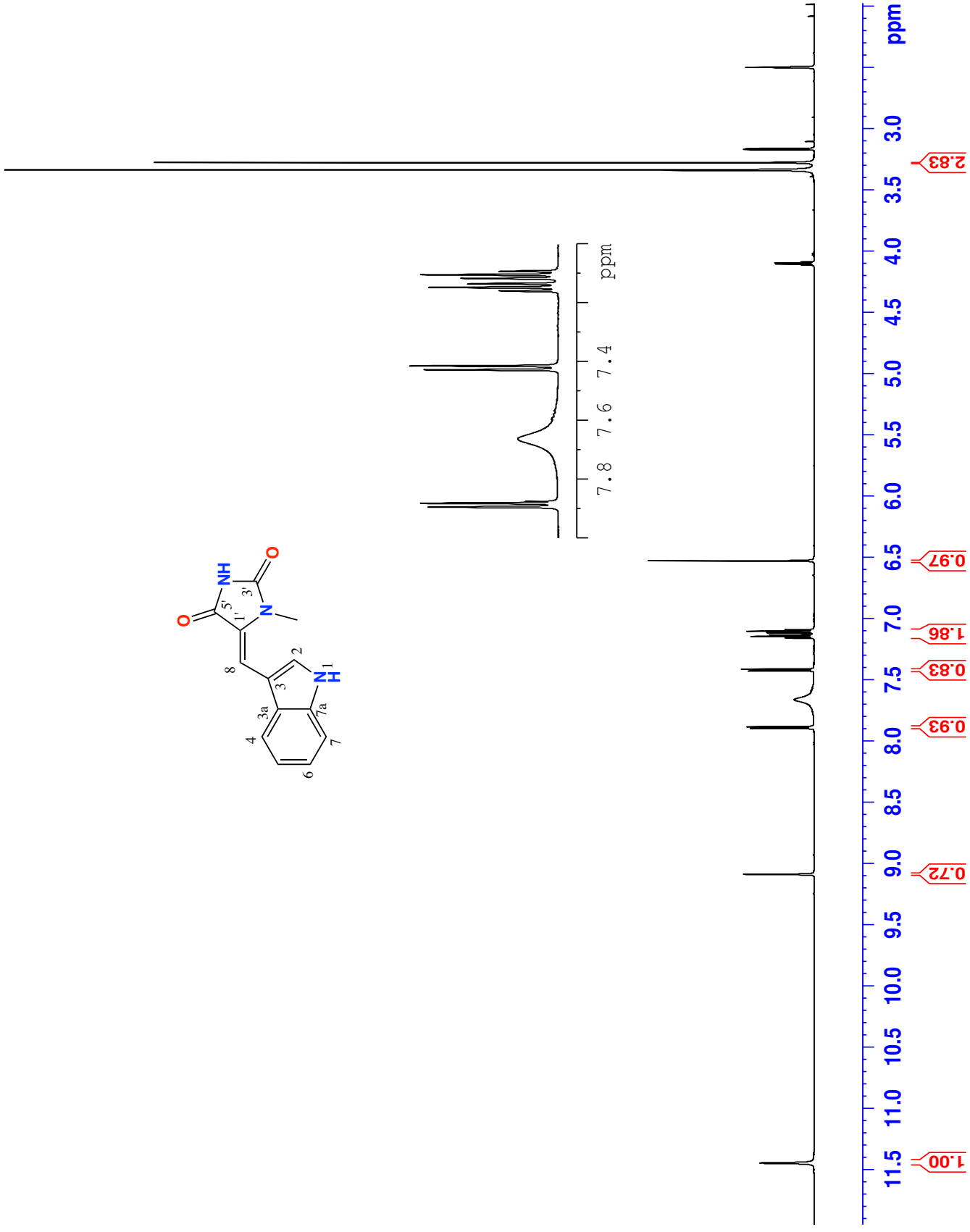

Figure 5S12a. ^{1}H NMR (600 MHz, DMSO-d_6) spectrum for 8*E*-4′-demethylaplysinopsin (**12a**)

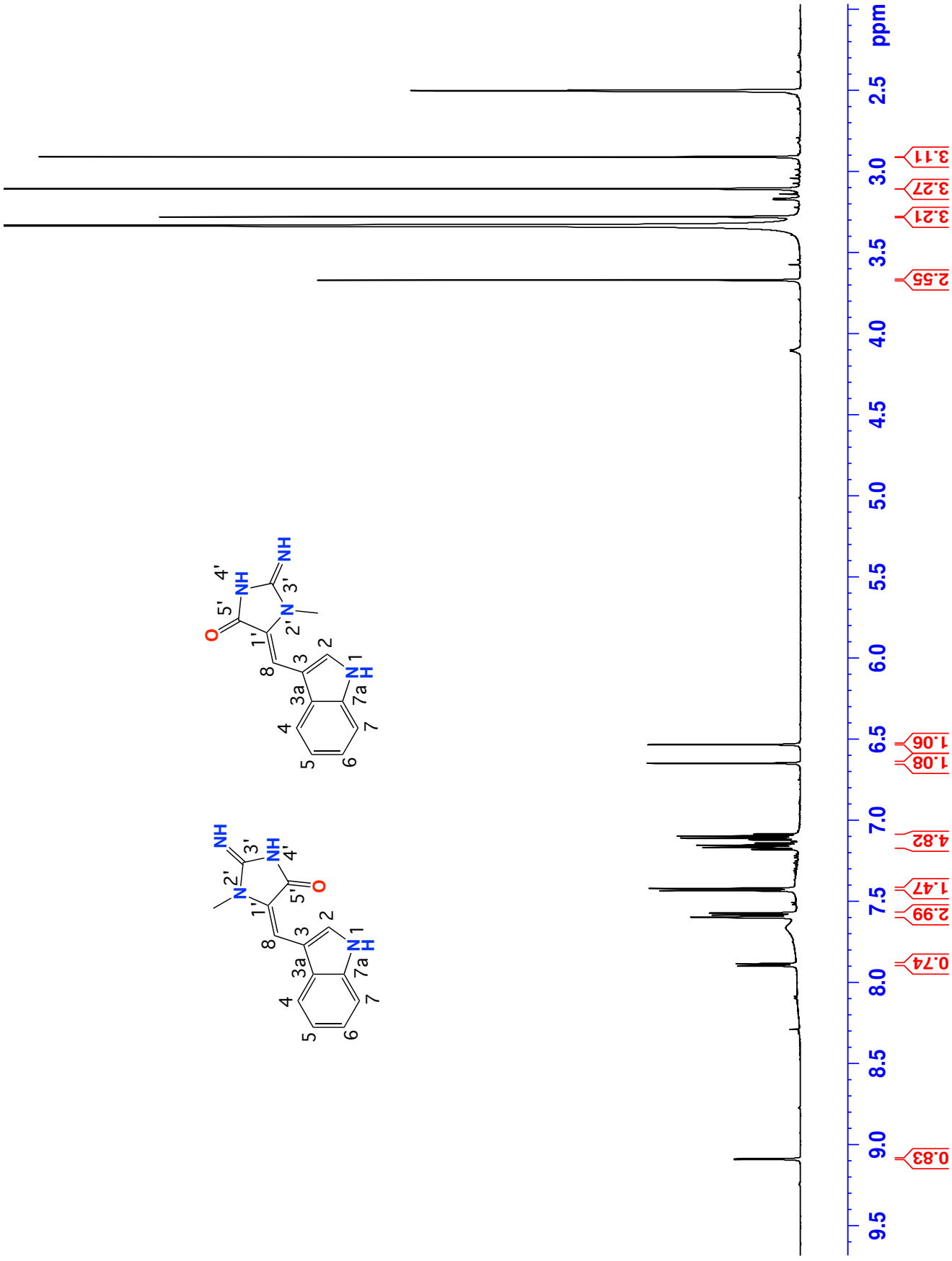

Figure 5S12a. ^{1}H NMR (600 MHz, DMSO-d_6) spectrum for mixture of 8*E*-4′-demethylaplysinopsin (**12a**) and 8*Z*-4′-demethylaplysinopsin (**12b**)

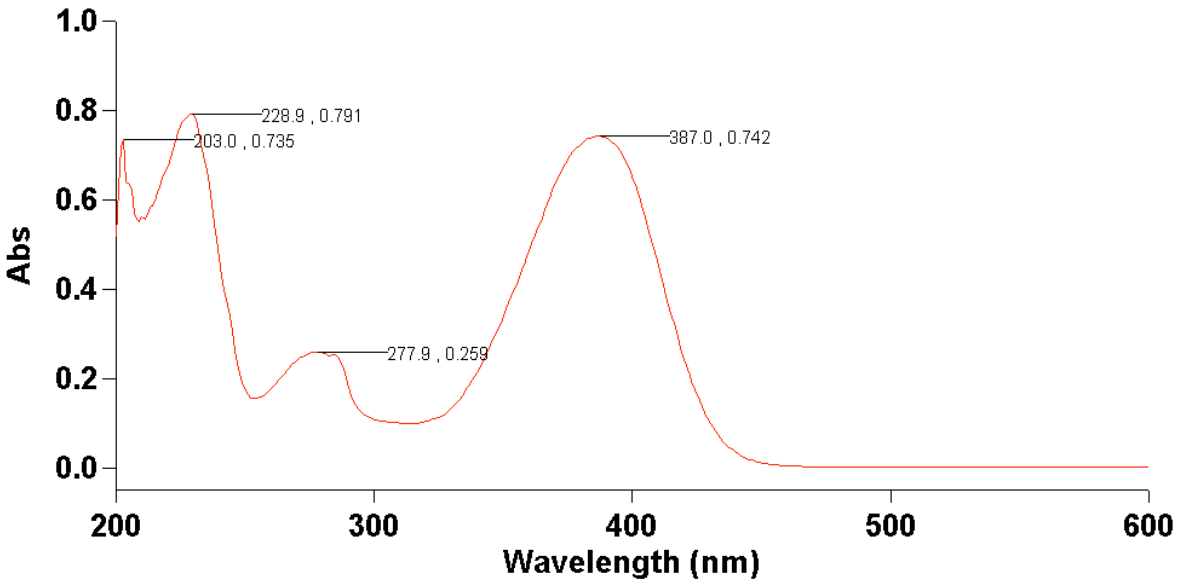

Figure 5S12c. UV-vis (MeOH) spectrum of a mixture of 8*E*-4′-demethylaplysinopsin (**12a**) and 8*Z*-4′-demethylaplysinopsin (**12b**)

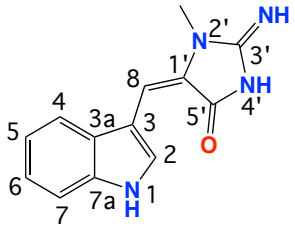

Table 5S12a. NMR (600 MHz, DMSO-d_6) data for 8*E*-4′-demethylaplysinopsin (**12a**)

No.	**δ_H (mult., *J* (Hz))**	**δ_C[A]**	**COSY**	**HMBC (^{1}H to ^{13}C)**
2	8.78 (d, 2.2)	128.6		3, 3a, 7a
3		108.8		
3a		126.0		
4	7.93 (d, 8.0)	117.9	5	3, 3a, 7a
5	7.18 (ddd, 8.1, 8.0, 1.0)	119.8	4, 6	3a, 7
6	7.13 (ddd, 8.0, 7.9, 1.0)	122.0	5, 7	4, 7a
7	7.48 (d, 8.0)	111.8	6	3a, 5
7a		135.4		
8	6.68 (s)	107.6		1′, 2, 3, 5′
1′		125.9		
2′-Me	3.19 (s)	27.6		1′, 3′
3′		153.3		
4′-*N*H	11.61 (br s)			3, 3a, 7a
5′		163.5		

[A] ^{13}C NMR assignments supported by HSQC data.

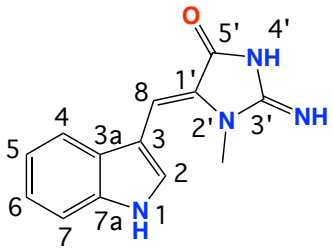

Table 5S12b. NMR (600 MHz, DMSO-d_6) data for 8*Z*-4′-demethylaplysinopsin (**12b**)

No.	**δ_H (mult., *J* (Hz))**	**δ_C[A]**	**COSY**	**HMBC (^{1}H to ^{13}C)**
2	7.59 (d, 1.74)	126.5		3, 3a, 7a
3		108.8		
3a		127.4		
4	7.57 (d, 7.92)	118.4	5	3, 3a, 7a
5	7.10 (ddd, 8.0, 8.0, 1.0)	119.0	4, 6	3a, 7
6	7.11 (ddd, 7.56, 8.0, 1.0)	121.5	5, 7	4, 7a
7	7.42 (d, 8.94, 0.9)	111.5	6	3a, 5
7a		136.0		
8	6.64 (d, 0.96)	102.4		1′, 2, 3, 5
1′		132.5		
2′-Me	3.10 (s)	31.2		1′, 3′
3′		169.5		
4′-NH				
5′		177.5		
1-NH	11.51 (brs)			3, 3a, 7a

[A] ^{13}C NMR assignments supported by HSQC data.

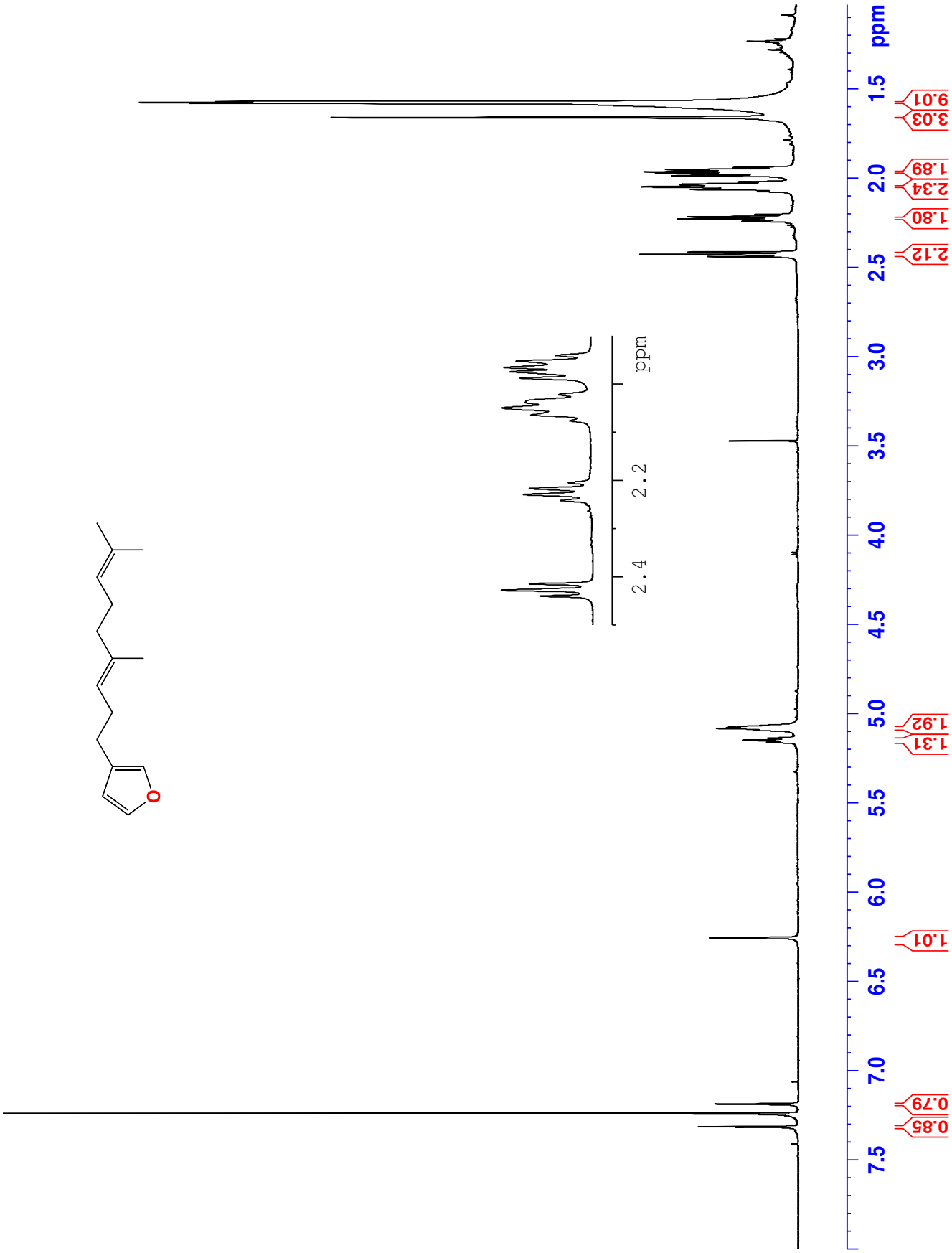

Figure 5S13. ^{1}H NMR (600 MHz, $CDCl_3$) spectrum for dendrolasin (**13**)

CHAPTER 6

CONCLUSION & OUTLOOK

6.1. Conclusion

In summary, chemical and biological investigations successfully challenged a library of more than 2,500 marine extracts to focus our attention on extracts of 7 southern Australian sponges including 3 members of Ircinidae family (CMB-03363, CMB-01064 and CMB-03231), 3 members of *Psammocinia* genus (CMB-01008, CMB-02858 and CMB-03344) and 1 member of genus *Ianthella* (CB-03322). Bioassay guided fractionations using YFP assay on the 7-priority specimens yielded 24 compounds, 13 of which were new metabolites. They included ircinialactam A (**3.45**), 8-hydroxyircinialactam A (**3.46**), 8-hydroxyircinialactam B (**3.47**), ircinialactam C (**3.48**), *ent*-ircinialactam C (**3.49**) and ircinialactam D (**3.50**), (–)-ircinianinlactam A (**4.11**), (–)-ircinianinlactam A sulfate (**4.12**), (–)-oxo-ircinianin (**4.13**), (–)-oxo-ircinianin lactam (**4.14**), (–)-ircinianin lactone (**4.15**), ianthellalactam A (**5.1**) and ianthellalactam B (**5.2**) (Table 6.1). Two of these new metabolites (**4.13**-**4.14**) featured an unprecedented moiety, a modified tetronic acid hitherto unknown in natural products, and eleven of them (**3.45**-**3.50**, **4.11**-**4.12, 4.14, 5.1**-**5.2**) contained the rare glycinyl lactam functionality. Curiously, all priority specimens produced at least one compound with glycinyl lactam moiety (Table 6.1), a functional group that mimics glycine and *N*-arachidonyl glycine (NAGly), which are known to exert anti-inflammatory activity with glycine acting as an anti-inflammatory micronutrient[174,] and NAGly as an inhibitor of anandamide[173,174] (see page 207 for NAGly).

To confirm the activity observed in the primary screening using YFP, we screened 24 MNPs against α1 and α3 GlyRs with an automated patch clamp electrophysiology. This gold standard method in screening ion channel modulators confirmed the presence of 14 GlyR modulators further grouped into 7 potentiators (**3.45**-**3.47**, **3.53**, **4.1**, **4.14** & **5.34**) and 2 antagonists (**4.2** & **5.34**) of GlyRα1, 2 potentiators (**4.11** & **4.12**) and 7 antagonists (**3.45**, **3.48**-**3.50**, **3.53**, **4.2**, **5.3** & **5.4**) of GlyRα3 (Table 6.1). The level of activity against GlyRs varied among the modulators and was classified as weak GlyRs modulators such as **4.1**, **4.2**, **5.3**, and **5.4**, modest GlyR modulators including **3. 45**-**3.50** and strong GlyR modulators such as **3.46, 3.47**, **3.53**, **4.11, 4.14** and **5.34**. One pot synthesis inspired by the activity of **4.2**, **4.3** and **5.34** gave two potent GlyRα1 antagonists (**5.70** & **5.71**) (Figure 6.1a)

Table 6.1. Natural products discovered from seven priority samples and their synthetic derivatives

No	Compound/Source	Molecular weight/Molecular Formula	Status	Activity against GlyRs	
				GlyRα1	GlyRα3
3.45	ircinialactam A/ CMB-01064 and CMB-03363	471/$C_{27}H_{37}NO_6$	New/MNPs	MP (140% at 100 μM)	MA (IC_{50} = ≥30)
3.46	8-hydroxyircinilactam A/ CMB-01064 and CMB-03363	489/$C_{27}H_{39}NO_7$	New/MNPs	SP (sub to low micromolar range)[101]	–
3.47	8-hydroxyircinialactam B/ CMB-01064	489/$C_{27}H_{39}NO_7$	New/MNPs	SP (EC_{50} = 0.5 μM)[101]	–
3.48	ircinialactam C/ CMB-01064 and CMB-03363	405/$C_{23}H_{35}NO_5$	New/MNPs	–	MA (IC_{50} = ≥30 μM)[101]
3.49	*ent*-ircinialactam C/ CMB-03231	405/$C_{23}H_{35}NO_5$	New/MNPs	–	MA (IC_{50} = ≥30 μM)[101]
3.50	ircinialactam D/ CMB-03363	551/$C_{29}H_{45}NO_9$	New/MNPs	–	MA (IC_{50} = ≥30 μM)[101]
3.51	7*E*,12*E*,20*Z*,18S-variabilin/ CMB-01064 and CMB-03363	398/$C_{25}H_{34}O_4$	Known/MNPs	–	–
3.52	7E,12*Z*,20*Z*,18S-variabilin/ CMB-01064 and CMB-03363	398/$C_{25}H_{34}O_4$	Known/MNPs	–	–
3.53	12*E*,20*Z*,18*S*-hydroxyvariabilin/ CMB-01064 and CMB-03363	416/$C_{25}H_{36}O_5$	Known/MNPs	–	–
4.1	(–)-ircinianin/ CMB-01064 and CMB-03363	396/$C_{25}H_{32}O_4$	Known /MNPs	WP (~80% at 100 μM)[133]	–
4.2	(–)-ircinianin sulfate/ CMB-01064 and CMB-03363	475/$C_{25}H_{31}O_7S^-$	Known /MNPs	MA (IC_{50} = 38.4 μM)	SA ((IC_{50} = 3.2 μM)[133]
4.11	(–)-ircinianinlactam A/ CMB-01064 and CMB-03363	469/$C_{27}H_{35}NO_6$	New /MNPs	–	SP (EC_{50} = 8.5 μM)[133]
4.12	(–)-ircinianinlactam A sulfate/ CMB-01008	548/$C_{27}H_{34}NO_9S^-$	New/MNPs	–	WP (~70% at 100 μM)[133]
4.13	(–)-oxoircinianin/CMB-03344	412/$C_{25}H_{32}O_5$	New/MNPs	–	–
4.14	(–)-oxoircinianin lactam A/ CMB-02858	485/$C_{27}H_{35}NO_7$	New/MNPs	MP (~110% at 100 μM)[133]	–
4.15	(–)-ircinianin lactone/ CMB-02858	412/$C_{25}H_{32}O_5$	New/MNPs	–	–
4.16	(–)-ircinianin acetate	438/$C_{27}H_{34}O_5$	New/synthetic	–	–
5.1	aplysinopsin/CMB-03322	254/$C_{14}H_{15}N_4O$	Known/MNPs	–	
5.3	8*E*-3'-deimino-3'-oxoaplysinopsin/ CMB-03322	255/$C_{14}H_{13}N_3O_2$	Known /MNPs	–	WA (IC_{50} = 67 μM)[139]
5.4	8*Z*-3'-deimino-3'-oxoaplysinopsin /CMB-03322	255/$C_{14}H_{13}N_3O_2$	Known /MNPs	–	WA (IC_{50} = 67 μM)[139]
5.10	dihydroaplysinopsin TFA salt /CMB-03322	256/$C_{14}H_{17}N_4O$	Known /MNPs	–	–
5.34	tubastrindole B/CMB-03322	508/$C_{28}H_{29}N_8O_2$	Known /MNPs	SP (≤ 1.0 μM), MA (IC_{50} = 25.9	

				μM)[139],	–
5.66	ianthellalactam A/CMB-03322	291/$C_{17}H_{25}NO_3$	New/MNPs	–	–
5.67	ianthellalactam B/CMB-03322	291/$C_{17}H_{25}NO_3$	New/MNPs	–	–
5.68	ethyldictyondendrilin/ CMB-03322	278/	New/artefact	–	–
5.69	8*E*-3′-deimino-2′-4′-bisdemethyl-3′-oxoaplysinopsin	250/$C_{12}H_9N_3O_2$	Known/Synthetic	–	–
5.70	8*E*-3′-deimino-4′-demethyl-3′-oxoaplysinopsin	250/$C_{13}H_{13}N_3O_2$	Known/Synthetic	SA (IC_{50} = 8.8 μM)	–
5.71	8*Z*-3′-deimino-4′-demethyl-3′-oxoaplysinopsin	250/$C_{13}H_{13}N_3O_2$	Known/Synthetic	SA (IC_{50} = 8.8 μM)	–
5.72	8*E*-4′-demethyl-3′-oxoaplysinopsin	241/$C_{13}H_{13}N_4O$	Known/Synthetic	–	–
5.73	8*E*-4′-demethyl-3′-oxoaplysinopsin	241/$C_{13}H_{13}N_4O$	Known/Synthetic	–	–

Note : WA, MA and SA = weak, modest and strong antagonists respectively. WP, MP and SP = weak, moderate and strong potentiators respectively

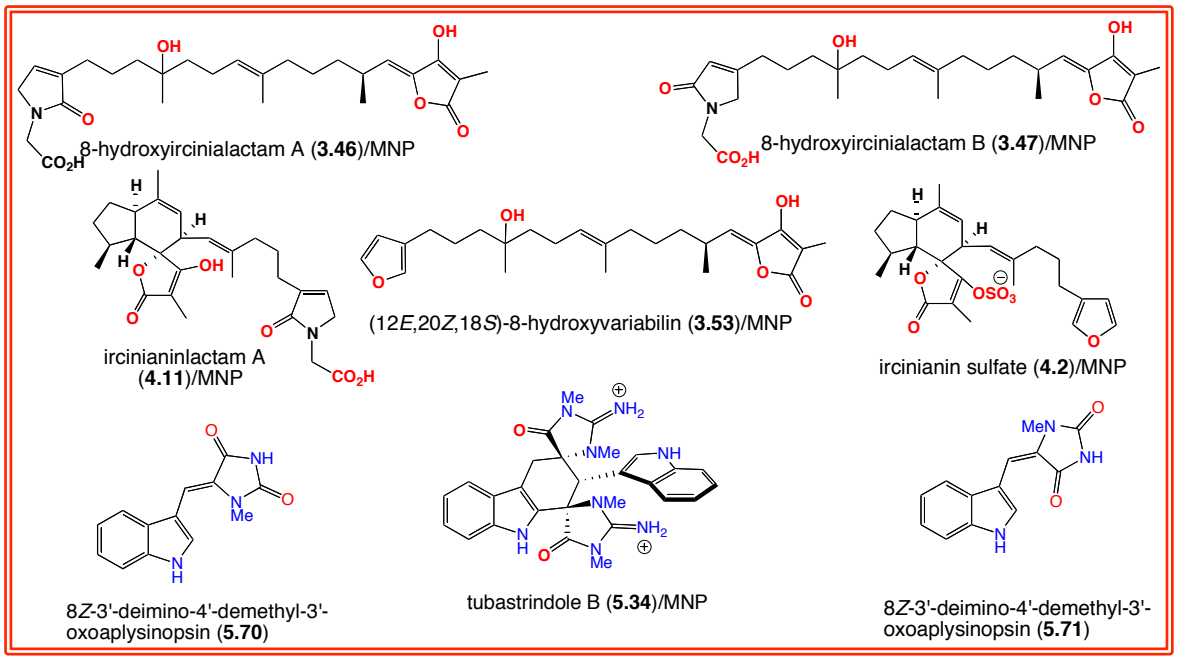

Figure 6.1a. Strong modulators of GlyRs

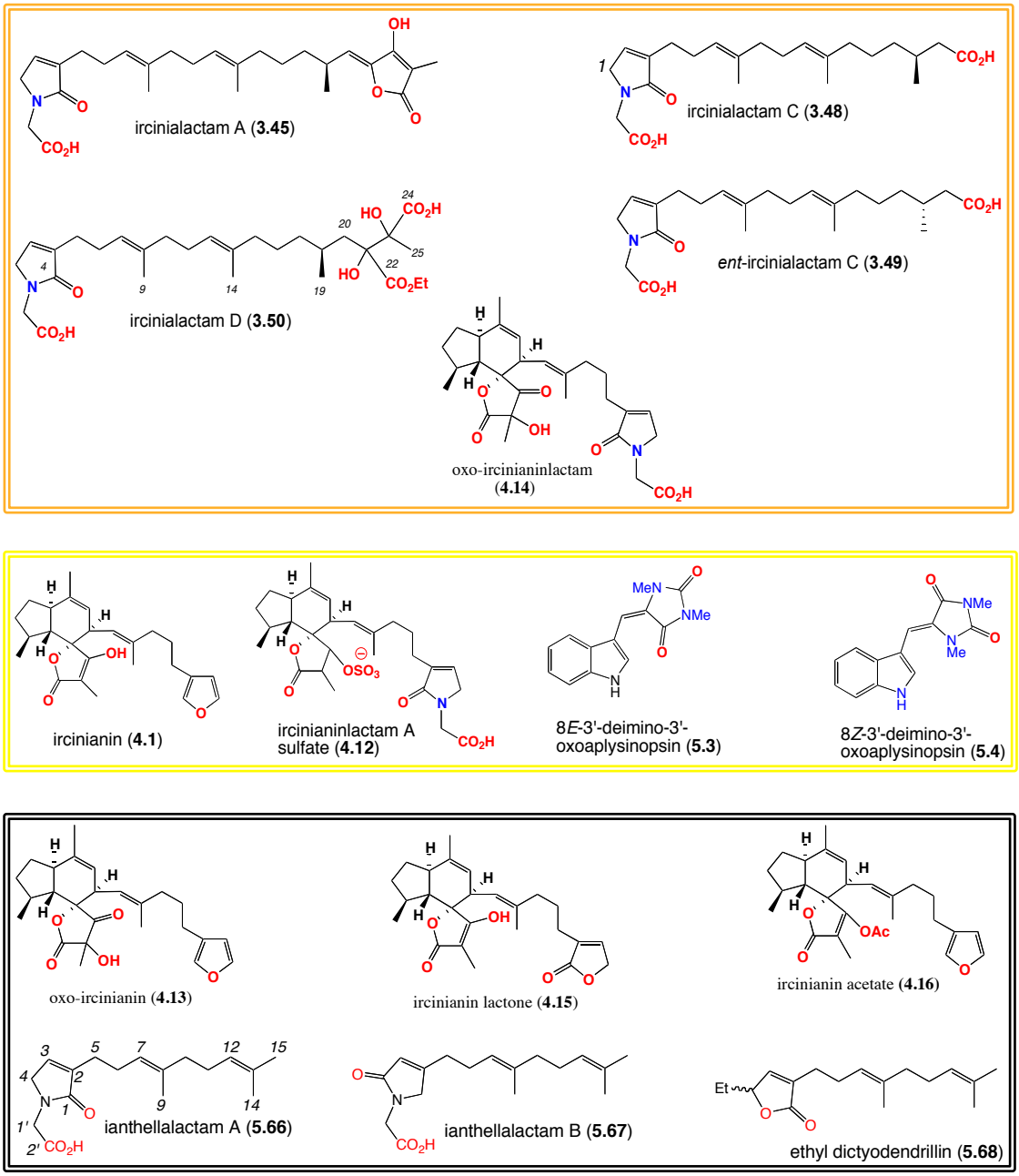

Figure 6.1b. Moderate (orange box) and weak (yellow bow) GlyR modulators as well as inactive molecules (black box) against GlyRs.

Many of the above GlyR modulators may inspire the development of new pharmacological tools capable of probing the distribution and function of GlyR isoforms, potentially advancing the development of GlyR targeting therapeutics to treat epilepsy, spasticity, hyperekplexia and chronic inflammatory pain. For example, at low concentration 12*E*,20*Z*,18*S*-hydroxyvariabilin (**3.53)** and tubastrindole B (**5.34)** strongly potentiated GlyRα1 with IC_{50} value of 1.2 μM for the sesterterpene tetronic acid and 120% glycine enhancement at 1.0 μM for the indole alkaloid. At higher concentration, they also showed antagonist activity but against different GlyR subunits with the former acting as a strong GlyRα1 antagonist (IC_{50} = 7.0 μM) while the latter as a modest GlyRα3 inhibitor (25.9 μM) (Table 6.1). This bifunctional activity particularly for **5.34** indicates that the dimeric aplysinopsin may have two different GlyRα1 binding sites. As pointed out in general introduction (page 11 and the ircinialactam paper), potent antagonist of **3.53** against GlyRα3 may be useful in identifying the function of GlyRα3 signaling in the spinal cord and/or treatment of temporal lobe epilepsy[101]. Similarly, in addition to being crucial in uncovering pharmacological functions of GlyRα1, potent and/or selective GlyRα1 potentiators attributed to **3.46**, **3.47** and **4.14** (Table 6.1) may play a key role in the development of therapeutics for movement disorders such as hyperekplexia, spasticity and chronic anti-inflammatory pain[101,133,139] although as a target for pain treatment GlyRα1 is less favorable than GlyRα3 due to the risk of side effects attributed to GlyRα1[1]. Hence, a potent and specific activity of (–)-ircinianinlactam A (**4.11**) (IC_{50} = 8.5 μM) against GlyRα3, the emerging pain target, renders **4.11** as the most interesting lead for the development of novel chronic anti-inflammatory pain drug(s)[1,19,21,44].

Together, the medical potentials of the above GlyR modulators, the absence of specific and potent GlyR modulator particularly GlyRα3[1,44] and the availability of synthetic methods for variabilin[129], glycinyl lactam[126] and ircinianin[136] type compounds offer an excellent opportunity for the development of GlyR pharmacological probes and/or novel, potent and specific drugs for treating hyperekplexia, spasticity, epilepsy and particularly chronic anti-inflammatory pain. The latter target attributes to the potent and/or specific modulating activity of 8-hydroxyircinialactam A (**3.46**) and B (**3.47**), (–)-oxo-ircinianinlactam A (**4.14**) against GlyRα1 and importantly of potent and selective activity of (–)-ircinianinlactam A (**4.11**) GlyRα3. The potential of these lead molecules to inspire the discovery of novel, specific and potent anti-inflammatory drug(s) is worth further research attention and is the subject of the following viewpoint.

6.2. Outlook

Over the years, drug discovery including anti inflammatory pain and marine derived drugs (MDDs) has always been challenging[45,66]. Conspicuously, material supply, structural complexity of the present GlyR modulators and lack of support from pharmaceutical companies remain the major hurdles faced by academia and industry in developing MDDs[67,69,87] leading to low rate of drug discovery from marine resource[66]. The same issues are posing a serious challenge to the development of current GlyR modulators discovered from Australian marine sponges. However, it is worth noting that most marine derived bioactive molecules in the pipeline (clinical trials) have their origin in academia research[87] with salinosporamide A (**1.38**) being the fastest MDDs to enter the pipeline due to its strategic research development[87]. In addition, widespread use of analgesics such as strong opioids, NSAIDs and COX inhibitors has been the subject for many debates presenting a challenge as well as providing an opportunity for the development of analgesic with new mode of actions[45]. The following section is a description of the possibility of bringing the novel, potent and specific GlyRα1 potentiators (**3.46**, **3.47** and **4.14**) and particularly the novel, potent and selective GlyRα3 potentiator, (–)-ircinianinlactam A (**4.11**), to the pipeline by considering a number of drug development aspects through a SWOT (strength weakness opportunity and threat) analysis.

6.2.1. Strength Weakness Opportunity and Threat (SWOT) Analysis

Although mainly applied in business ventures, SWOT analysis is also applicable for analyzing a product, place, industry or person[175]. It provides a systematic approach for identifying factors affecting the internal strength and weakness as well as external opportunity and threat allowing the internal factors to effectively meet the external ones[176]. Identification of SWOT is crucial in that it allows one to determine the benefit of the process or the necessity to enhance different aspects prior to detailed economic evaluation[177]. With this regards, SWOT analysis is undertaken to identify internal strength and weakness as well as external opportunity and threat regarding the possibility of bringing GlyR modulators discovered from Australian marine sponges in particular (–)-ircinianinlactam A (**4.11**) to the pipeline.

Strength. GlyR is an emerging target for pain treatment[5,21] safer than opioid receptors due to its discrete distribution at the nociceptive neurons in the spinal cord of the dorsal horn, the pain terminal[1]. Interestingly, recent study has shown cannabinoid-GlyRs interaction as playing a crucial role in cannabis-induced analgesia underscoring the importance of GlyR in particular GlyRα3 as a promising target for pain treatment. Also, unlike the known GlyR modulators, all GlyR modulators discovered in this study were novel (Table 6.1 and Figure 6.1). Of interest, the rare molecule (–)-ircinialactam A (**4.11**) has emerged as the most interesting lead compound for the discovery of novel, potent and specific GlyR modulators due to its potent and specific modulating activity against the GlyRα3. Apart from being rare, ircinialactam A and other glycinyl lactams are synthetically accessible which are of great interest to the drug discovery.

Weakness: Several weaknesses in developing current GlyR modulators include material supply, structural complexity, the absence of *in vivo* study and the lack of industrial support. For example, all GlyR modulators existed as minor components with purification of 12E,18*S*-8-hydroxyvariabilin A and 8-hydroxyvariabilin B requiring the use of LC-SPE-NMR. In addition, synthetically inaccessible GlyR modulator such as tubastrindole B is hampering the development of this promising GlyRα1 potentiator. Moreover, apart from the absence of *in vivo* study, the specificity of all GlyR modulators for particular subunit of the chloride channel receptors has not been confirmed, as they have not been evaluated against other receptor members of cys-loop LGIC superfamily. Importantly, marine drug discovery is still academia-based research that lacks in industrial support. Furthermore, although several anticancer in clinical pipeline have their origin in academia, the lack of support from pharmaceutical company remains one of the major hurdles in the development of marine based drugs.

Opportunities: The current analgesics give patients only 25% of pain relief with many of these pain relief drugs having adverse side effects including addiction[45]. Based on the U$50 billion global value for pain market in 2009, it was predicted the market would continue to grow in the future due to an increasing number of ageing population[45]. In addition, despite the widespread use of known analgesics, the unmet medical condition for pain treatments was predicted to potentially fill specific market for pain treatment. Moreover, as the understanding of pain mechanism grows, more specific pain targets are now available (Figure 6.2)[45]. Importantly, the most recent studies have shown that several tetrahydrocannabinoids (THCs) exerted anti-inflammatory activity by activating GlyRα3 instead of CB_1 receptor[21].

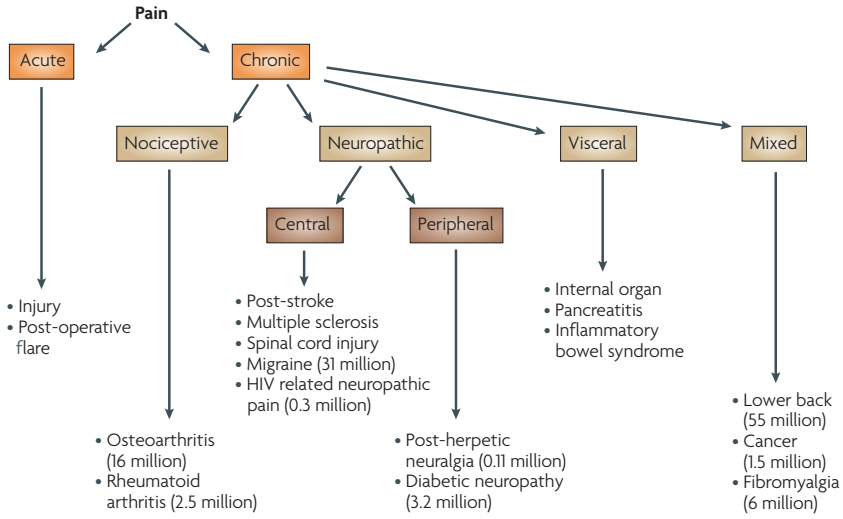

Figure 6.2. Pain classification and representative indications modified from Melnikova 2010[45]

Threat: Two major threats to developing of new analgesic are upcoming regulations and the current trend in developing analgesics[45]. It was predicted that the safety issue of current analgesics in the market would result in future stricter regulations and give only narrow window of opportunity for analgesics with new mode of action. In contrast, pain drug development is still in favor of the known analgesics such as the modulators of cannabinoid receptors whose market sharing remains the highest among today's approved analgesics. Also, recent pain market analysis strongly indicated that pharmaceutical companies are opting to reformulating the old analgesics (e.g. OxyContin and morphine/naltrexone combination) than discovering new drugs. Indeed, a 2010 figure showed that most of the pain relief marketed drugs derived from the known analgesics with Remoxy and Ofirmev as the only new comers (Figure 6.3)[45].

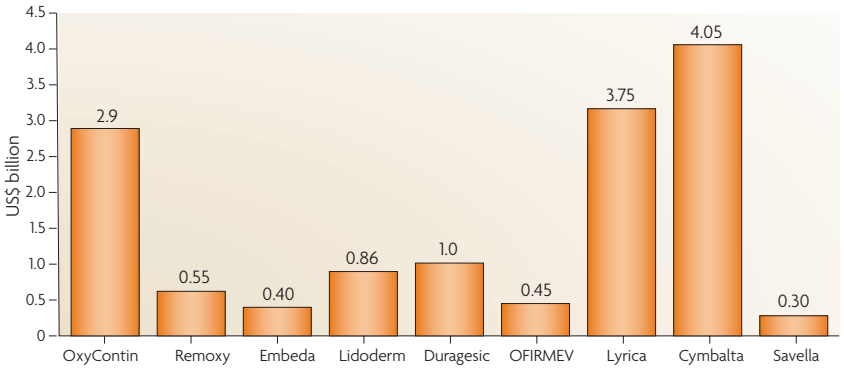

Figure 6.3. Projected annual peak sells of selected pain drugs representative for various pain medications modified from Melnikova 2010[45]

Considering the SWOT, the development of GlyR modulators for pharmacological probes/drug include prioritizing target molecules, tackling supply issue, evaluating current GlyR modulators against other members of cys-loop ligand gated ion channel and/or other receptors as well as conducting *in vivo* assay focusing on specific pain target (i.e. neuropathic pain) and establishing a partnership with a pharmaceutical company.

Prioritization of a target molecule for discovering anti-inflammatory pain from the recent discovery takes into consideration bioactivity, specificity and synthetic accessibility of current GlyR modulators. For example, although aplysinopsin type compounds, both monomers and dimer, strongly antagonized GlyRα1[139], they also inhibited GlyRα3 suggesting their unspecific activity against either GlyRα1 or GlyRα3. Also, as mentioned in the introduction of Chapter 5, dimeric aplysinopsin has not been synthetically accessible and therefore is not considered as lead compound for the development of pain relief drugs at this moment. In contrast, apart from being synthetically accessible[126,136], both linear (8-hydroxyircinialactam A (**3.46**), 8-hydroxyircinialactam B (**3.47**) and cyclic sesterterpene glycinyl lactams (ircinianinlactam (**4.11**) and oxo-ircinianinlactam A (**4.14**) showed potent and specific modulation activity against GlyRα1 (**3.46**-**3.47** and **4.14**) and GlyRa3 (**4.11**)[101,133] rendering them feasible target for the development of pharmacological tools and/or drugs for treating inflammatory pain. The following describes two plausible synthetic strategies in generating novel anti-inflammatory pharmacological tools and/or drugs inspired by both linear and cyclic glycinyl lactams.

6.2.2 Synthetic Strategy

6.2.2.1 First Approach

The first approach incorporates wistarin and ircinianin synthesis[136] followed by the conjugation of the tetra- and pentacyclic sesterterpenes with several amines such as glycine, taurine, ethanolamine and dopamine[126]. Also our preliminary study suggested that the oxo-ircinianin and other ircinianin derivatives could be generated through oxidation of ircinianin under UV in the presence of Rose Bengal suggesting the possibility to generate oxo-ircinianin and other ircinianin derivatives through oxidation. Once ircinianin is obtained, it will be oxidized to yield regioisomers hydroxy-γ-lactones (**6.2** and **6.3**). Conjugation of **6.2** and **6.3** with glycine will produce

hemiaminals (**6.4**-**6.5**) and reduction of **6.4** and **6.5** with $NaBH_3CN$ will give both α and β-substituted γ-lactams, ircinianin lactams (ILMs) (**6.6**-**6.7**). Similarly, conjugations between regioisomer-γ-lactones with ethanolamine, dopamine or taurine are expected to yield both regioisomers of ircinianin-ethanolaminyls (IELs) (**6.10**-**6.11**), ircinianin-taurinyls (ITLs) (**6.14**-**6.15**) and ircinianin-dopaminyls (IDLs) (**6.18**-**6.19**) (Scheme 6.1). The same treatments to oxo-ircinianins and wistarins are predicted to yield oxo-ircinianin lactaminyls (OLLs) (**6.20**-**6.21**), oxoircinianin-ethanolaminyls (OELs) (**6.22**-**6.23**), oxo-ircinianintaurinyls (OTLs) (**6.24**-**6.25**), oxoircinianin-dopaminyls (ODLs) (**6.26**-**6.27**), wistarin-lactaminyls (WLLs) (**6.28**-**6.29**), wistarin-ethanolaminyls (WELs) (**6.30**-**6.31**), wistarin-taurinyls (WTLs) (**6.32**-**6.33**) and wistarin-dopaminyls (WDLs) (**6.34**-**6.35**) (Figure 6.2).

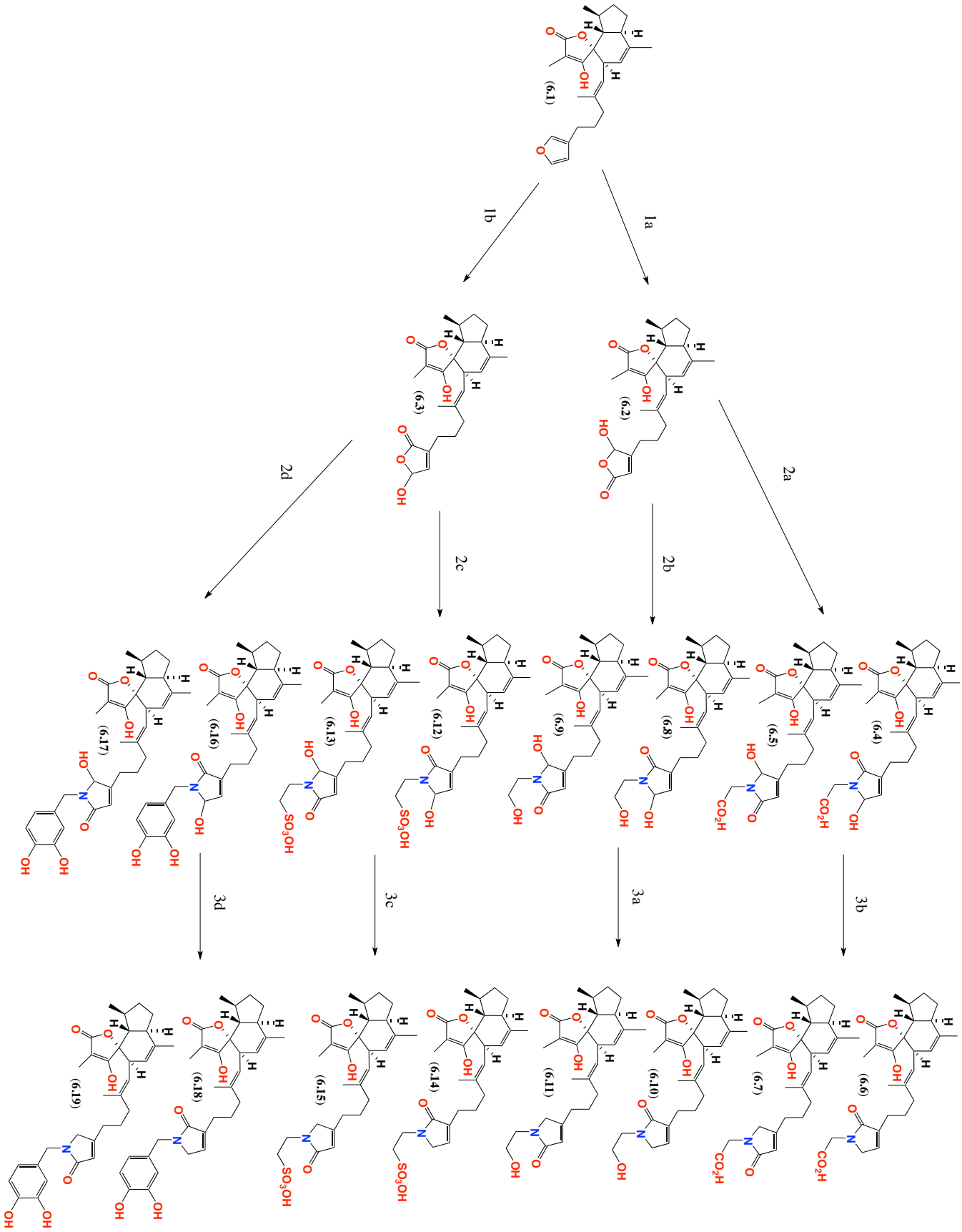

Scheme 6.1. Synthesis of ircinianin lactams and derivatives. MCPBA, NaOAc and AcOH, (2a) glycine, (2b) ethanolamine, (2c) taurine and (2d) dopamine (3a-d) $NaBH_3CN$, HCl, MeOH.

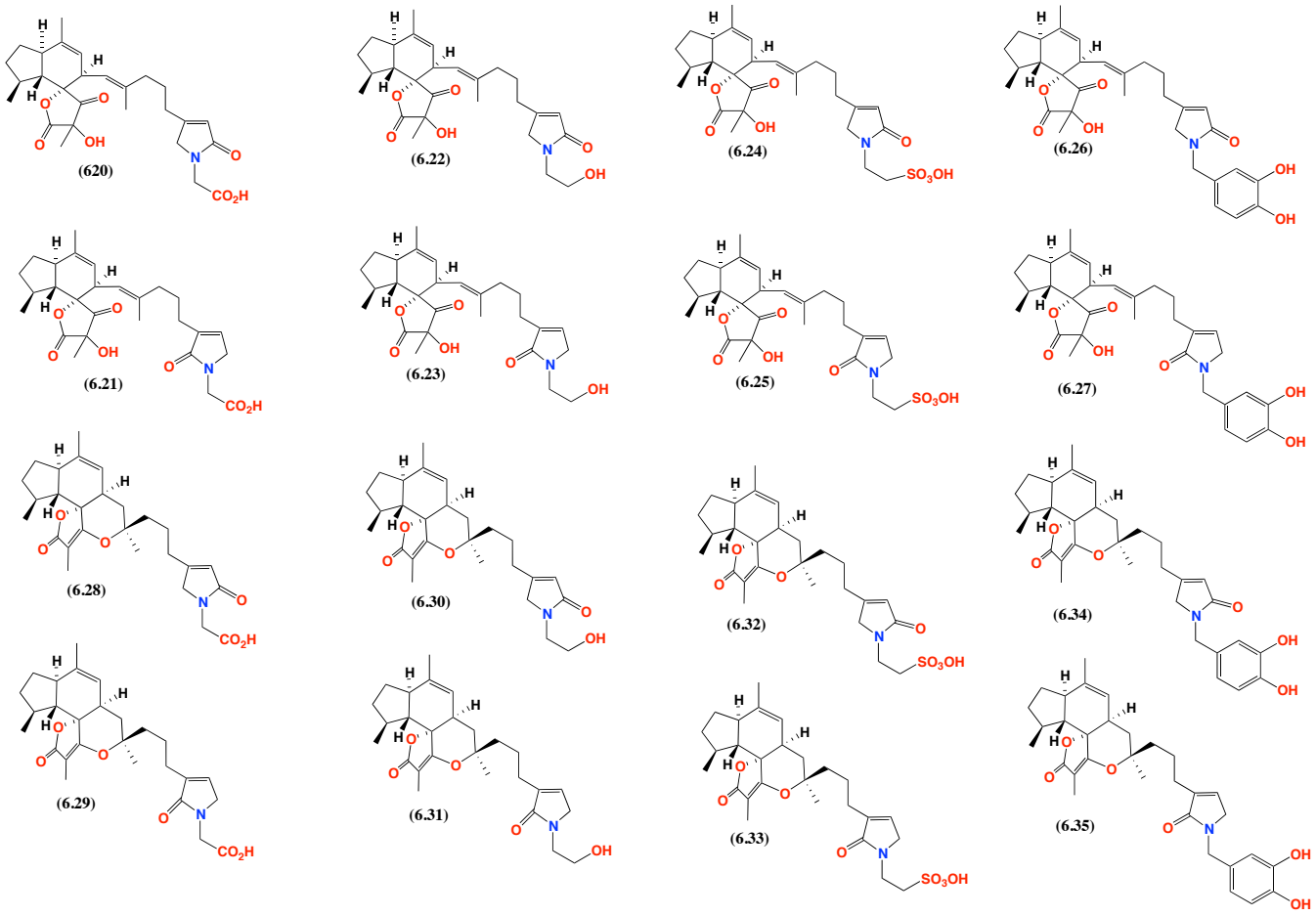

6.2.2.2 Second Approach

Alerted by the inactivity of ircinialactam C, *ent*-ircinialactam C, ircinialactam D (Chapter 3)[101], ianthellalactam A and ianthellalactam B (Chapter 5)[133] and inspired by anti-inflammatory activity of as *N*-arachidonyl glycine (NAGly)[174] and potent activity of sesterterpene glycinyl lactams against GlyRs[101,133], a second approach involves coupling between glycinyl moiety and a range of fatty acids such as arachidonic, linolenic, and lenoleic acids instead of linear terpene units.

The premise is that fatty lipoaminoacid such as *N*-arachidonyl glycine (NAGly) **(6.36)** was abundant in the rat skin and spinal cord, exerting a strong anti-nociceptive effects *in vivo*[21]. The anti-inflammatory activity of NAGly was linked with its ability in inhibiting the hydrolysis of anandamide or *N*-arachidonyl-ethanolamine (AEA)

(**6.37**)—an endogenous ligand for the brain receptors of marijuana's active principle Δ^9-tetrahydrocannabinol, the type-1 cannabinoid receptor (CB_1)[21]—by fatty acid amide hydrolase (FAAH), the regulator of AEA signaling *in vivo*. NAGly was also not recognized by AEA membrane receptor and more importantly was inactive against cannabinoid receptors[178,179] suggesting not only that NAGly's inflammatory activity was independent of CB_1 receptor but also that it was deprived of adverse effects related to CB_1 such as drug abuse and addiction[21]. Interestingly, several tetrahydrocannabinoids were very recently reported to exert their analgesic effect by modulating, not CB_1, but GlyRs in particular GlyRα3 strongly suggesting that cannabis-induced analgesia was correlated with potentiation of GlyRs by cannabinoid, a mechanism currently largely unexplored due to the lack of understanding regarding mechanism and behavioral implication of cannabinoid potentiation of GlyRs[21]. Unfortunately like other fatty acid amides such as arachidonilglycerol (**6.38**), *N*-acyl taurine (**6.39**), *N*-palmitolethanolamine (**6.40**) and oleamide (**6.41**), NAGly was prone to FAAH hydrolysis[174] with its rapid metabolism by the enzyme leading to the low level of AEA which in turn diminished anti-inflam=[matory activity.

Over the years, many studies have addressed this issue by replacing the acylic amide or ester with cyclic substituent with A9-octadeceynoil-a-keto-N4-oxazolopyridine (**6.42**) as a good example exerting K_i value of 140 pM against FAAH[174]. Curiously, our results strongly indicated that glycinyl lactam moiety dictated the activity of both linear and cyclic sesterterpenes towards α1 and α3 GlyRs (Chapter 3 and Chapter 4)[101,133] and that *N*-acyl glycine (**6.43**) can be viewed as the cyclic version of *N*-arachidonic glycine. Therefore, we propose that replacement of the glycine with glycinyl lactam moiety will result in *N*-arachidonic acid lactams (NALs) that are more resistant to FAAH hydrolysis and can maintain high level of AEA in the spinal cord which in turn exert more potent anti-inflammatory activity.

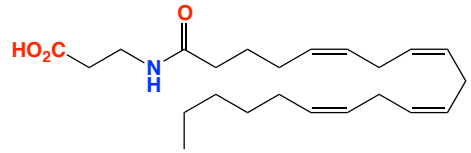

N-arachydonyl glycine (NAGly) **(6.36)**

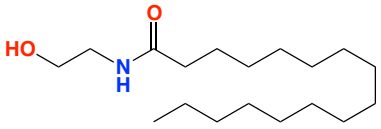

palmitolethanolamine **(6.40)**

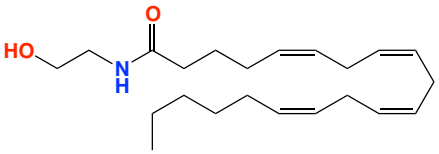

N-arachydonyl ethanolamine (AEA) **(6.37)**

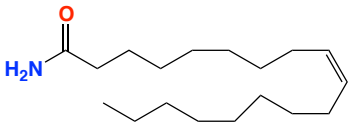

oleamide **(6.41)**

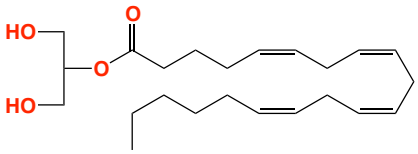

arachydonylglycerol **(6.38)**

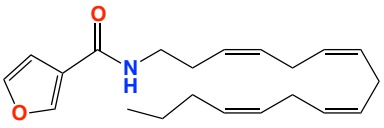

A9-octadeceynoil-a-keto
N4-oxazolopyridine **(6.42)**

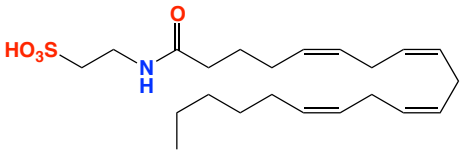

N-acyl taurine **(6.39)**

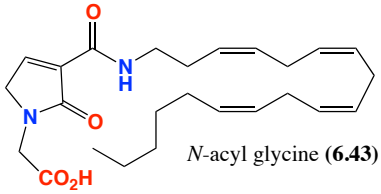

N-acyl glycine **(6.43)**

The preparation of NALs proceeds from alkyl furan analogues through the corresponding Grignard reagent via a coupling with primary alcohols prepared from readily available fatty acids (i.e. arachidonic, linolenic, linoleic and oleic acids) to yield a library of 3-alkylfurans that can be transformed by photo-oxidation and/or NBS to alkylbutenolides (Figure 6. 4A). Treatment of alkylbutenolides with glycine will yield the target *N*-glycinyl lactams (NGLs). With a successful synthetic methodology in place as shown in Figure 6.4A, replacement of glycine with other amines will lead to *N*-glycinyl lactams (NGL), *N*-ethanolaminyl (NEL), *N*-taurinyl (NTL) and *N*-dopaminyl (NDL) structure class (Figure 6.4B). The following steps would be to couple NGL, NEL, NTL and NDL with a range of fatty acids such as arachidonic acid, linolenic acid, linoleic acid and oleic acid (Scheme 6.2a). Treatment of acyl chloride of arachidonic acid with NGL, NEL, NDL and NTL will give *N*-acyl glycinyl lactam (NAGL) (**6.43**), *N*-acyl ethanolaminnyl lactam (NAEL) (**6.44**), *N*-acyl dopaminyl lactam (NADL) (**6.45**) and *N*-acyl taurinyl lactam (NATL) (**6.46**) respectively (Scheme 6.2a). Alternatively, these compounds can be prepared from direct condensation between the arachidonic acid and the corresponding amine or alcohol in the presence of dicyclohexylcarbodiimide (DCC) and catalytic amounts of *N*,*N*-dimethyl-4-4-aminopyridine (DAMP) (Scheme 6.2b). Reacting a series of fatty

acids (linoleic, linolenic and oleic acids) and NGL, NEL, NTL and NDL will generate NAGL (**6.43**), NAEL (**6.44**), NATL (**6.45**) and NADL (**6.46**) (Figure 6.2b).

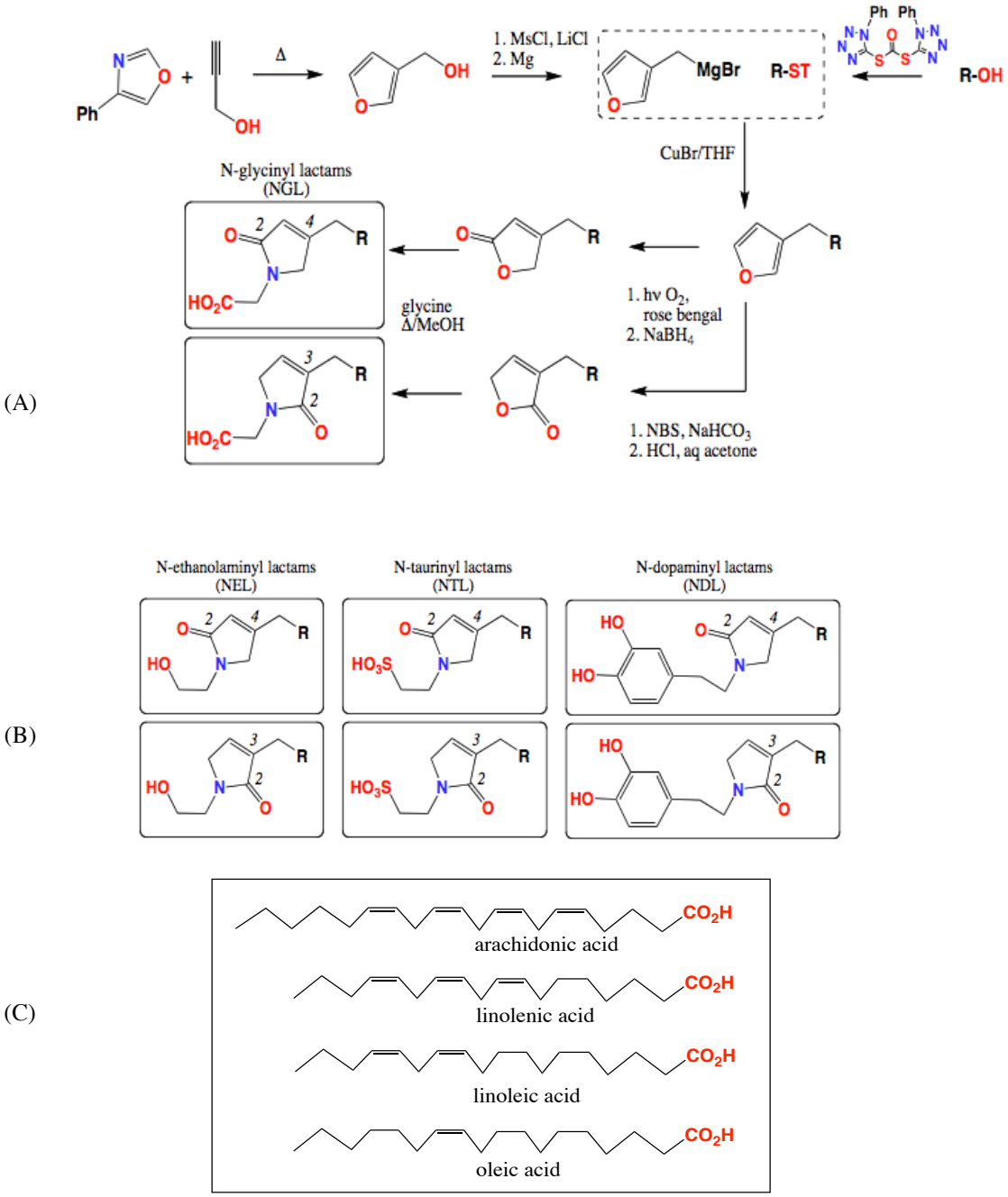

Figure 6.4. Synthesis of glycine moiety from alkyl furan and fatty acids (A), NEL, NTL and NDL (B) and faty acids (C)

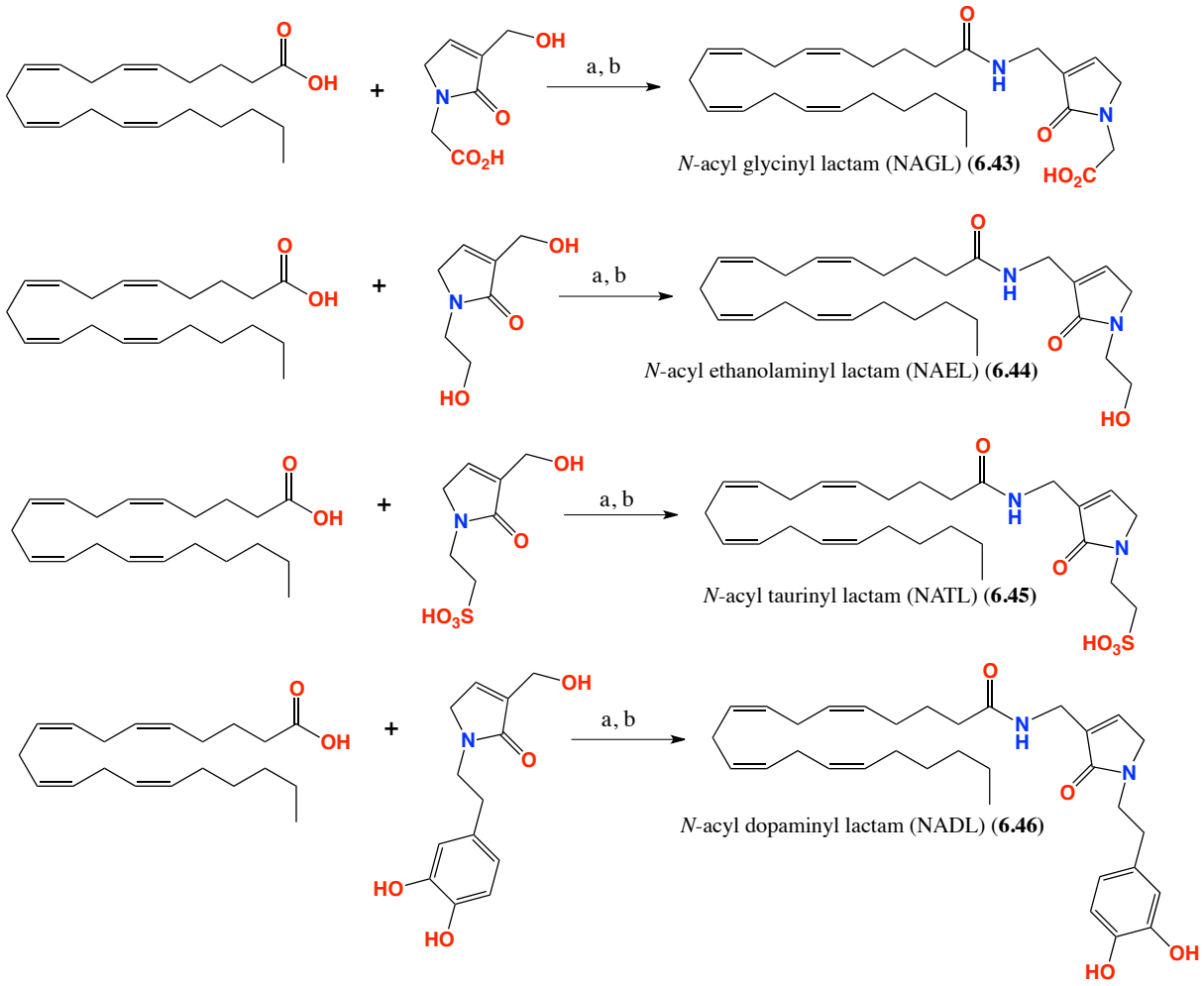

Scheme 6.2. Synthesis of NAGL, NEGL, NDGL and NTGL. (a) oxalyl chloride, DMF CH_2Cl_2, rt (b) DCC, DAMP, CH_2Cl_2, rt.

Once synthetic analogues have been produced, their biological activities need to be evaluated *in vitro* and *in vivo* studies. To determine their specificity towards GlyRα1 and/or GlyRα3, all synthetic compounds obtained from the first and second approaches will be evaluated in SAR studies against all GlyR subunits and/or other members of cys-loop LGIC. Promising candidates will be further evaluated in enzymatic catalytic against FAAH to evaluate their specificity against GlyR. Furthermore, Tail Flick Reflex (TFR) and Hot Plate Test (HPT) should be conducted for promising candidates with the previous aiming at evaluating spinal reflex while the latter assessing supraspinal processing[180]. All these evaluations need to be performed prior to establishing research collaboration with a pharmaceutical company as this approach was shown to be effective in bringing salinosporamide A in to the pipeline, the fastest MDDs to enter the clinical trials[70].

Toward this end, screening of >2,500 southern Australia and Antarctic marine invertebrates against GlyRs using YFP and automated patch clamp electrophysiology successfully identified a series of GlyR modulators from 7 priority specimens, featuring three main pharmacophores such as aplysinopsin, linear and cyclic sesterterpene glycinyl lactams. In particular, the latter two pharmachopores may contribute to the discovery of new GlyR pharmacological tools and/or therapeutics to treat CNS diseases. For example, in addition to having potential in treating hyperekplexia, spasticity and other movement disorders, 8-hydroxyircinialctam A (**3.46**), 8-hydroxyircinialctam B (**3.47**), (–)-oxo-ircinianin lactam (**4.14**) can inspire the development of GlyRα1 pharmacological probes and/or pain relief drug(s) due to their specific and/or potent potentiation activity against GlyRα1. More importantly, (–)-ircinianinlactam A (**4.11**)[133] potently and specifically potentiated GlyRα3, the emerging pain target whose activation by cannabinoid was recently shown to contribute to analgesia[21], rendering **4.11** as the most interesting lead molecule for the development of both GlyR pharmacological probe(s) and/or chronic anti-inflammatory pain drug(s).

Despite their promising anti-inflammatory potential, limited material remains the major challenge for the development of these lead compounds precluding, at the moment, intensive pharmacological studies such as *in vitro* against other receptor members of LGIC superfamily or *in vivo* in animal models[133]. Fortunately, both ircinianin[136] and glycinyl lactam[126] type compounds are now synthetically accessible suggesting the feasibility of developing anti-inflammatory pain drugs by mimicking both linear and cyclic glycinyl lactam pharmacophores. Hence, two synthetic approaches are proposed to achieve this goal including derivatisation of ircinianinlactams and incorporation of glycinyl lactam moiety to fatty acids. Following on the synthetic applications, it is recommended that comprehensive *in vitro* and *in vivo* studies are conducted before establishing partnership with a pharmaceutical company, a successfully applied strategy in rapidly advancing salinosporamide A to the pipeline[70].

Therefore, provided that synthetic plans are well-addressed, high potency and specificity towards GlyRs in particular GlyRα3 are confirmed both *in vitro* and *in vivo* assays and partnership with a pharmaceutical company is established, novel, potent and specific GlyRα1 and GlyRα3 modulators have a fighting chance of advancing to the pipeline and hopefully to the clinic.

REFERENCES:

1. Webb, T. I.; Lynch, J. W. Molecular pharmacology of the glycine receptor chloride channel. *Curr. Pharm. Des.* **2007**; 13: 3250-3258.

2. Lynch, J.W. Molecular structure and function of the glycine receptor chloride channel. *Physiol. Rev.* **2004**; 84: 1051-1095.

3. Collingridge, G.; Olsen, R. W.; Peters, J.; Spedding, M. A Nomenclature for ligand-gated ion channels. *Neuropharmacology* **2008**: 1-4.

4. Overington, J. P.; Al-Lazikani, B.; Hopkns, A. L. How many drug targets are there? *Nat. Rev. Drug Dis.* **2006**; 5: 993-996.

5. Verkman, A. L.; Galietta, J. L. Chloride Channels as Drug Targets. *Nat. Rev. Drug Disc.* **2009**; 8:153-171.

6. Taly, A.; Corringer, P. J.; Guedin, D.; Lestage, P.; Changeux, J. P. Nicotinic receptors: allosteric transitions and therapeutic targets in the nervous system. *Nate Rev. Drug Disc.* **2009**(8): 733-750.

7. Nothdurfter, C.; Tanasic, S.; DiBebedetto, B.; Rammes, G.; Wagner, E. M. Kirmeier, T.; Ganal, V.; Kessier, J. S.; Rein, T.; Holsboer, F.; Rupprecht, R. Impact of lipid raaft integrity on 5-HT3 receptor function and its modulation by antidepressants. *Neuropharmacology*. **2010**; 35: 1510-1519.

8. Barnes, N. M.; Sharp, T. A review of central 5-HT2 receptors and their function. *Neuropharmacology*. **1999**; 38:1083-1152

9. Eisensamer, B.; Rammes, G.; Gimpi, G.; Shapa, M.; Ferrari, U. Antidepressants are functional antagonists at the serotonin type 3 (5-HT3) receptor. *Mol. Psychiatry*. **2003**; 8: 994-1007.

10. Rammes, G.; Eisensamer, B.; Ferrari, U.; Shapa, M.; Gimpi, G.; Gilling, K. Antipsychotic drugs antagonized human serotonin type 3 receptros currents in a noncompetitive manner. *Mol. Psychiatry*. **2004**; 9: 846-858.

11. Beker, C. M. Convulsants acting at the inhibitory glycine receptor. *Handbk. Exp. Pharmacol*. **1992**(102): 539-575.

12. Jacob, T. C.; Moss, S. J.; Jurd, R. . GABA A receptor traffickng and its role in the dynamic modulation of neuronal inhibition. *Nat. Rev. Neuro. Sci*. **2008**; 9: 331-343.

13. Yevenes, G. E.; Zeilhofer, H. U. Allosteric modulation of glycine receptors *Brit. J. Pharm*. **2012**.

14. Caulfield, W. L.; Collie, I. T.; Dickins, R.S.; Epemolu, O.; McGuire, R.; Hill, D. R.; McVey, G.; Morphy, R. The First Potent and Selective Inhibitors of the Glycine Transporter Type 2. *J. Med. Chem*. **2001**; 44: 2679-2682.

15. Karlin, A. Emerging structure of the nicotinic acetylcholine receptors. *Nat. Rev. Neurosci*. **2002**; 3: 102-114.

16. Shiang, R.; Ryan, S. G.; Zhy, Y.Z.; Hahn, A. F.; O'Connell, P.; Wasmuth, J. J. Mutations in the aplha1 subunit of the inhibitory glycine receptor cause the dominant neuologic diorder, hyprekplexia. . *Nat. Genet*. **1993**; 5: 351-358.

17. Boulenguez, P.; Liabeuf, S.; Bos, R.; Bras, H.; Xavier, J. C.; Brocard, C.; Stil, A.; Darbon, P.; Cattaert, D.; Delpire, E.; Marsala, M.; Vinay. L. Down-regulation of the potassium-chloride cotransporter KCC2 contributes to spasticity after spinal cord injury. *Nat. Med. Adv. Onl*. **2009**: 1-7.

18. Eichler, S.A.; Forstera, B.; Smolinky, B.; Jutter R.; Lehman, T.N.; Fahling, M.; Schwarz, G.; Legendre, P.; Meier, J.C. . Splice-specific roles of glycine receptor alpha 3 in the hippocampus. *Eur. J. Neuro. Sci*. **2009**; 30: 1077-1091.

19. Harvey, R. J.; Depner, U. B.; Wassle, H.; Ahmadi, S.; Heindl C.; Renold, H.; Smart, T. G.; Harvey K.; Schutz, B.; Abo-Salem, O. M.; Zimmer, A.; Posbeau, P.; Welzl, H.; Wolfer, D. P.; Betz, H.; Zeilhofer, H. U.; Muller, U. GlyRa3: An essential target for sinal PGE2-mediated inflammatory pain sensitization *Science*. **2004**; 304: 884-887.

20. Betz, H.; Laube, B. Glycine receptors: recent insight into their structural organization and functional diversity *J.*

Neurochem. **2006**; 97: 1600-1610.

21. Xiong, W.; Cheng K. Jun.; Cui, T.; Godlewski, G.; RIse, K. C.; Xu, Y.; Zhang, L. Cannabinoid potentiation of glycine receptors contributes to cannabis-induced analgesia. *Nat*. *Chem*. *Biol*. **2011**; 7: 296-301.

22. Vannier, C.; Triller, A Glycine receptors: Molecular and cell biology. **2009**: 921-927.

23. Malosio, M. L.; Marquess, P, B.; Kuhse, J.; Betz, H. . Widespread expression of glycine receptor subunit mRNAs in the adult and developing rat brain. *EMBO, J*. **1991**; 10:2401-2409.

24. Haverkamp, S.; Muller, U.; Zeilhofer, H. U.; Harvey, R. J, Wassle, H. Diversity of glycine receptors in the mouse reina: localization of the alpha-2 subunit. *J*. *Compar*. *Neurol*. **2004**; 477: 399-411.

25. Harvey, R. J.; Schmieden, V.; von Holst, A>; Laube, B.; Rohrer, H.; Beta, H. Glycine Receptros Containing the alpha 4 subunit in the embrionic symphatetic nervous system, spinal cord and male genetical ridge. *Eur*. *J*. *Neurosci* **2000**; 12: 994-1001.

26. Grudzinska, J.; Schemm, R.; Haeger, S.; Nicke, A.; Schmaizing, G.; Betz, H.; Laube, B. . The beta subunit determines the ligand binding properties of synaptic glycine receptors. *Neuron*. **2005**; 45: 727-739.

27. Kim, E. Y.; Schrader, N.; Smolinsky, B. ; Bedet, C.; Vannier, C.; Schwarz, G.; Schindelin, H. . Deciphering the structural framework of glycine receptor acnhoring by gephyrin. *EMBO, J*. **2006**; 25: 1385-1395.

28. Van den Eynden, J.; Ali S. S.; Horwood, N.; Carmans, S.; Brone, B.; Hellings, N.; Steels, P.; Harvey, R. J.; Rigo, J. M. Glycine and Glycine Receptor Signaliing in Non-Neuronal Cells. *Front*. *Mol*. *Neurosci*. **2009**; 2: 1-9.

29. Kling, C.; Koch, M.; Saul, B.; Becker, C M. The frameshift mutation oscillator (GlyRα1 spd-ot) produces a complete loss of glycine receptor α1-polypeptide in mouse central nervous system *Neuroscience* **1997**; 78: 411-417.

30. Bakker, M.; van Dijk, J. G.; van den Maagdenberg, A. M. J. M.; Tijssen, M. A. J. Startle syndromes. *Neurology thelancet com*. **2006**; 5: 513-524

31. O'Shea, S. M.; Becker, L.; Weiher, H.; Betz, H.; Laube, B. . Propofol restores the function of hyperekplexic mutant glycine receptors in Xenopus Oocyte and mice. *J*. *Neuroscience*. **2004**; 24: 2322-2327.

32. Andermann, F.; Keene, D. L.; Andermann, E.; Quesney, L. F. Startle diseases or hyperekplexia future delineation of the syndrome. *Brain* **1980**; 103: 985-997

33. Floeter, M. K.; Hallet, M. Glycine receptors: a startling connection. *Nat*. *Genet*. **1993**; 5: 319-320.

34. Schofield, P. R. The role of glycine and lgycine receptors in myoclonus and stratle syndromes. *Adv*. *Neurol*. **2002**; 89: 263-274.

35. Lester, H. A.; Dibas, M. I.; Dahan, D. S.; Leite, J. F.; Dougherty, D. A. Cys-loop receptors: new twists and turns. *TRENDS in Neurosciences*. **2004**;27(6):329-336.

36. Ryan, S. G.; Buckwalter, M. S.; Lynch, J. W.; Handord, C. A.; Sagure, L.; Shiang, R.; Wasmuth, J. J.; Campre, S. A.; Schofield, P.; O'Connell, P. . A missense mutation in the gene encoding the alpha 1 subunit of the inhibitory glycine receptor in the spasmodic mouse *Nature* **1994**: 131-135.

37. Saul, B.; Schieden, V.; Kling, C.; Mulhardt, C.; Gass, P.; Kuhse, J.; Backer, C. M. . Point of mutation of glycine receptor alpha1 subunit in the spasmodic mouse affects agonist responses *Fedn*. *Eur*. *Biochem*. *Socs*. *Lett*. **1994**; 350: 71-76.

38. Yang, Z.; Aubrey, K. R.; Alroy, I.; Harvey, R. J.; Vandenberg, R. J.; Lynch, J. W. Subunit-specific modulation of glycine receptors by cannabinoids and *N*-arachidonyl-glycine *Biochem*. *Pharm*. **2008**; 76: 1014-1023

39. Heinze, L.; Harvey, R. J.; Hevekamp, S.; Wassle, H. Diversity of glycine receptors in the mouse retina: localisation of the alpha-4 subunit. *J*. *Compar*. *Neurol*. **2007**; 500: 693-707.

40. Wassle, H.; Henze, ; Ivanova, E.; Majumdar, S.; Weiss, J. Harvey, R. J.; Haverkamp, S. . Glycinergic transmission in

the mammalian retina. *Front. in Mol. Neurosci.* **2009**; 2: 1-12.

41. Young, R.; T. L.; Ivic, L.; Kriegstein, A. R.; Cepko, C. L. Charaterizaton of mice with targeted deletion of glycine receptor alpha 2. *Mol. Cell. Biol.* **2006**; 26: 5728-5734.

42. Becker, C.; Schmieden, V.; Tarroni, P.; Strasser, U.; Betz, H. Isoform-selective deficit of glycine receptors in the mouse mutant spastic. *Neuron.* **1992**; 8: 283-289.

43. Zeilhofer, H. U. The glycinergic control of spinal pain processing. *Cel. Mol. Life Sci.* **2005**; 62: 2027-2035.

44. Lynch, J. W.; Calliseter, R. J. Glycine Receptors: A new therapeutic target in pain pathway *Curr. Op. Invest. Drugs* **2006**: 48-53.

45. Melnikova, I. Pain Market. *Nat. Rev. Drug Disc.* **2010**; 9: 589-590.

46. McGivern, J.G. Targeting N-type and T-type calcium channels for the treatment of pain. *Drug Discov. Today* **2006**; 11: 245–253.

47. Kerr, L. M.; Ysohikami, D. A venom peptide with a novle presynaptic blocking action *Nature* **1984**; 308: 282-284.

48. Maksay, G. Biodirectional allosteric modulation of strychnine-sensitive glycine receptors by tropeins and 5-HT3 serotonin receptor ligands *Neuropharmacology.* **1998**; 37: 1633-1641.

49. Raymond, V.; Sattelle, D. B. Novel animal-health drug targets from ligand-gated chloride channels. *Nat. Rev. Drug Disc.* **2002**; 1: 427-436.

50. Shan, Q.; Haddrill, J. L.; Lynch, J. W. Ivermectin, an uncoventionla agonist of the glycine receptor chloride channel *J. Biol. Chem.* **2001**; 276: 12556-125564.

51. Hawthorne, R.; Lynch, J. W. A Picrotoxin-specific Conformational Change in the Glycine Receptor M2–M3 Loop. *J. Biol. Chem.* **2005**;280:35836-35843.

52. Sedelnikova, A.;Erkkila, B. E.; Harris, H.; Zakharkin, S. O.; Weiss, D. S. . Stoichiometry of a pore mutation that abolishes picrotoxin-mediated antagonism of the GABAA receptor *J. Physiol.* **2006**; 577.2: 569-577.

53. Chesnoy, M. D. Potentiation of chloride responses to glycine by three 5-HT3 antagonists in rat spinal neurones. *Br. J. Pharmacol.* **1996**;118:2115-2125.

54. Macor, E. J.; Gurley, D.; Lanthron, T.; Loch, J.; Mack, R.A.; Mullen, G.; Trani, O.; Wright, N.; Gordon, J. C. The 5-HT3 Antagonist Tropisetron (ICS 205-930) is a Potent and Selective Niotonic Receptor Partial Agonist *Bioorg. Med. Chem.* **2001**; 11: 319-321.

55. Jensen, A. A.; Begum, N.; Vogensen, S. B.; Knapp, K. M.; Gundertofte, K.; Dzyuba, S. V.; Ishii, H.; Nakanishi, K.; Kristiansen, U.; Strømgaard, K. . Probing the Pharmacophore of Ginkgolides as Glycine Receptor Antagonists. *J. Med. Chem.* **2007**;50:1610-1617.

56. Chatterjee, S. S.; Kondratskaya, E. L.; Krishtal, O. A. Structure- activity studies with Ginkgo biloba extract constituents as receptor- gated chloride channel blockers and modulators. *Pharmacopsychiatry.* **2003**;36:1507-1518.

57. Stromgaard, K.; Saito, D. R. Shindou, H.; Ishii, S.; Shimizu, T.; Nakanishi, K. . Gingolide derivatives for photolabeling studies: preparation and pharmacological evaluation. *J. Med. Chem.* **2002**; 42: 4038-4046.

58. Huang, S. H.; Duke, R. K.; Chebib, M.; Sasaki, K.; Wada, K.; Johnston, G. A. R. Ginkgolides, diterpene trilactones of Ginkgo biloba, as antagonists at recombinant GABAA receptors. *Eur. J. Pharmacol.* **2004**;494:131-138.

59. Vogensen, S. B.; Strømgaard, K.; Shindou, H.; Jaracz, S.; Suehiro, M.; Ishii, S.; Shimizu, T.; Nakanishi, K. Preparation of 7-Substituted Ginkgolide Derivatives: Potent Platelet Activating Factor (PAF) Receptor Antagonists. *J. Med. Chem.* **2003**;*46*:601-608.

60. Philippe, G.; Nguyen, L.; Angenot, L.; Fre´de´rich, M.; Moonen, G.; Tits, M.; Rigo, J. M. Study of the interaction of

antiplasmodial strychnine derivatives with the glycine receptor. *Eur. J. Pharm.* **2006**;*530*:15-22.

61. Jensen, A. A.; Gharagozloo, P.; Birdsall, N. J. M.; Zlotos, D. P. Pharmacologial charaterisation of strychnine and brucine analogues at glycine and alpha7 nicotinic acetylcholine receptors. *Eur. J. Pharm.* **2006**; 539:27-33.

62. Kehne, J.H.; Baron, B. M.; , Harrison, B. L.; McCloskey, T. C.; Palfreyman, M .G.; Poirot, P.; Salituro, F. G.; Siegel, W. G.; Slone, A. L.; Van Giersbergen, P. L. M.; White, S MDL 100,458 and MDL 102,288: two potent and selective glycine receptor antagonists with different functional profiles. *Eur. J. Pharm.* . **1995**;284:109-118.

63. Eichler, S.A.; Kirischuk, S.; Jüttner, R.; Schafermeier, P.K.; Legendre, P.; Lehmann, T.N.; Gloveli, T.; Grantyn, R.; Meier, J.C. Glycinergic tonic inhibition of hippocampal neurons with depolarizing GABAergic transmission elicits histopathological signs of temporal lobe epilepsy. *J. Cell. Mol. Med.* **2008**; 12(6B): 2848-2866.

64. Chung, S. K.; Vanbellinghen, J. F.; Mullins, J. G.; Robinson, A.; Hantke, J.; Hammond, C. L.; Gilbert, D. F.; Freilinger, M.; Ryan, M.; Kruer, M. C.; Masri, A.; Gurses, C.; Ferrie, C.; Harvey, K.; Shiang, R.; Christodoulou, J.; Andermann, F.; Keene, D. L.; Andermann, E.; Quesney, L. F, Andermann ET, R. H.; Harvey, R. J.; Lynch, J. W.; Rees, M. I. Pathophysiological mechanisms of dominant and recessive GLRA1 mutations in hyperekplexia. *J. Neurosci.* **2010**; 30(28): 9612-9620.

65. Maksay, G.; Vincze, Z.; Nemes, P. Synthesis of heteroaromatic tropeines and heterogeneous binding to glycine receptors. *Bioor. Med. Chem* **2009**; 17: 6872-6878.

66. Mayer, A.M.S.; Glaser, K. B.; Cuevas, C.; Jacobs, R. S.; Kem, W.; Little, D.; McIntosh, M.; Newman D.; Potts, B. C.; Shuster, D. E. The odyssey of marine pharmaceuticals: a current pipeline perspective *Trends pharm. Sci.* **2010**; 31: 225-265.

67. Molinski, T, F. Drug development from marine natural products *Nat. Rev. Drug. Disc.* **2009**; 8: 69-85.

68. Newman, D. J., Cragg, G. M. Marine natural products and related compounds in clinical and advanced preclinical trials. *J. Nat. Prod.* **2004**; 67: 1261-1238.

69. Koehn, F. E.; Carter, G. T. The evolving role of natural prouducts in drug discovery *Nat. Rev. Drug Disc.* **2005**; 4: 206-220.

70. Glaser, K. B.; Mayer, A. M. S. A renaissance in marine pharmacolgy: from preclinilcal curiosity to clinical reality *Biochem. Pharm.* **2009**; 78: 440-448.

71. Al-Sabi, A.; McArthur, J.; Ostroumov, V.; French, R. J. Marine toxins that target voltage-gated sodium channels. *Marine Drugs.* **2006**; *4*:157-192.

72. Arias, H. R. Marine toxins targeting ion channels. *Marine Drugs.* **2006**; *4*: 37-69

73. Oliver, B. M. w-Conotoxin MVIIA: from marine snail venom to analgesic drug. *In drugs from the sea (Fusetani, N, ed.).* 2000: 75-85.

74. Wright, A. E.; Forleo, D. A.; Gunawardana, G. P.; Gunasekera, S. P,; Koehn, F. E.; McConnel, O. J. Antirumor tetrahydroisoquinoline alkaloids from the colonial ascidian *Ecteinascidia turbinaria. J. Org. Chem.* **1990**; 55:4508-4512.

75. Verweij, J. Soft tissue sacroma trials: one size no longer fits all. *J. Clin. Oncol.* **2009**; 27: 3085-3087.

76. Yap, T. A. Beyond chemotherapy: targeted therapies in ovarian cancer. *Nat. Rev. Cancer.* **2009**; 9: 167-181.

77. Rinehart, K. L. Ecteinascidins 729, 743, 745, 769A, 759B, and 770: potent antitumor agents from the Caribbean tunicate Ecteinascidia turubinaria *J. Org. Chem.* **1990**; 55: 4512-4515.

78. Lippert, J. W. Vascular disrupting agents. *Bioorg. Med. Chem.* **2007**; 15: 605-615.

79. Jackson, K. The Halichondrins and E7389. *Chem. Rev.* **2009**; 109: 3044-3079.

80. Okouneva, T. Inhibition of centromers dynamics by erubilin (E7389) during mitotic metaphase *Mol. Cancer Ther.*

2008; 7: 2003-2011.

81. Hamann, M. T.; Scheuer, P. J. . Kahalide F: A bioactive depsipeptide from the sacoglossan mollusk, Elysia refescens *J. Am. Chem. Soc.* **1993**; 115: 5825-5826.

82. Sashidhara, K.; White, K. N.; Crews, P. A selective account fo effective paradigms and significant outcomes in the discovery of inspirational marine natural products *J. Nat. Prod.* **2009**;72:588-603.

83. Feling, R. H. Salinosporamide A: a highly cytotoxic proteasome inhibitor from a novel microbial source, a marine bacterium of the new genus Salinopora. *Angew. Chem. Int. Ed.* **2003**; 42: 355-357.

84. Talpira, R. Hemiasterlin adn geodiamolide TA: two new cytotoxic peptide from the marine spogne Hemiasterella minor *Tetrahedron Lett.* **1994**; 35: 4453-4456.

85. Nakao, Y.; Fusetani, N. Enzyme inhibitors from marine invertebrates *J. Nat. Prod.* **2007**; 70: 689-710.

86. Newman, D. J. The bryostatins. *In anticancer agents from natural products (Cragg G M et al, eds)*. 2005:137-150.

87. Keith BGMA, M. S. A renaissance in marine pharmacolgy: from preclinilcal curiosity to clinical reality *Biochemical Pharmacology* 2009;78:440-448.

88. Dalisay, D. S.; Rogers, E. W.; Edison, A. S.; Molinski, T. D. . Structure elucidation at the nanomole scale: Triaxozole macrolides thiazole contaiining cyclic peptides from the nudibranch hexabrancus sanguineus *J. Nat. Prod.* **2009**; 72: 732-738.

89. Castro, A.; Moco, S.; Coll, J.; Vervoort, J LC-MS-SPE-NMR for the Isolation and Characterization of neo-Clerodane Diterpenoids from Teucrium luteum subsp. flaWoWirens. *J. Nat. Prod.* 2009.

90. Clarkson, C.; Staerk, D.; Hansen, S. H.; Smith, P, J.; Jaroszewski, J. W. Discovering new natutral products directly from crude extracts by HPLC-SPE-NMR: Chinane diterpenes in Harpagophytum procumbens *J. Nat. Prod.* **2006**; *69*: 527-530.

91. Sorensen, D.; Raditsis, A.; Trimble, L. A.; Blackwell, B. A.; Sumarah, M. W.; Miller, J. D. Isolation and structure elucidation by LC-MS-SPE/NMR: PR toxin- and cuspidatol related eremohilane sesquiterpenes from Penicillium roqueforti *J. Nat. Prod.* **2007**; 70: 121-123.

92. Nerenberg, J. B.; Hung, D. T.; Somers, P. K.; Schreiber, S. L. Total synthesis of the immunosuppressive agent (-)-discodermolide. *J. Am. Chem. Soc.* **1993**;*115*:12621-12622.

93. Dunlop, J.; Bowlby, M.; Peri, R.; Vasilyev, D.; Arias, R. . High-thoughtput electrophysiology: an amerging paradigm for ion-channel screening and physiolgy. *Nat. Rev. Drug. Disc.* **2008**; 7: 358-368.

94. Sabry, O. M.; Andrews, S.; McPhail, K. L.; Goeger, D. E.; Yokochi, A.; LePage, K. T.; Murray, T. F.; Gerwick, W. H. . Neuroxic meroditerpenoids from the tropical marine brown alga Stypopodium flabelliforme. *J. Nat. Prod.* **2005**; 68:1022-1030.

95. Sabry, O.M.; Andrews, S.; McPhail, K.L.; Goeger, D.E.; Yokochi, A.; LePage, K.T.; Murray, T.F.; Gerwick, W.H. Neurotoxic meroditerpenoids from the tropical marine brown alga Stypopodium flabelliforme. *J. Nat. Prod.* **2005**;68:1022-1030.

96. Edwards, D. J.; Marquez, B.; Nogle, L. M.; McPhail, K.; Geoeger, D. E.; Roberts, M. A.; Verwick, W. H. . Structure and biosynthesis of the jamaicamides, new mixed polyketide-peptide neurotoxins from the marine cyanobacterium *Lyngbya majuscula Chem. & Biol.* **2004**; 11: 817-833.

97. Wu, M.; Okino, T.; Nogle, L. M.; Marquez, B. L.; Williamson, R. T.; Sitachitta, N.; Berman, F. W.; Murray, T. F.; McGough, K.; Jacobs, R.; Colsen, K.; Asano, T.; Yokokawa, F.; Shioiri, T.; Gerwick, W. H. Stucture, synthesis and biological properties of kalkitoxin, a novel neurotoxin from the marine cyanobacterium Lyngbya majuscule. *J. Am. Chem. Soc.* **2000**; 200: 1241-1242.

98. Rentas, A. L.; Rosa, R.; Rodriguez, A. D.; De Motta, G. E. Effect of alkaloid toxins from tropical marine sponge on

membrane sodium currents. *Toxicon*. **1995**; 33: 491-497.

99. Bickmeyer, U.; Drechsler, C.; Kock, M.; Assmann, M. Brominated pyrrole alkaloids from marine Agelas sponges reduce depolarization-induced cellular calcium elevation. *Toxin*. **2004**;44:45-51.

100. Kem, W.; Soti, F.; Wildeboer, K.; LeFrancois, S.; MacDougall, K.; Wei, D. Q.; Chou, K.C.; Arias, H. R. . The nermertine toxin anabaseine and its derivative DMXBA (GTS-21): Chemical and pharmacological properties. *Marine Drugs*. 2006; 4: 255-273.

101. Balansa, W.; Islam, R.; Fontaine, F.; Piggott, A. M.; Zhang, H; Webb, T. I.; Gilbert, D. F.; Lynch, J. W.; Capon, R. J. . Ircinialactams: Subunit-selective glycine receptor modulators from Australian sponges of the family *Irciniidae*. *Bioorg. Med. Chem*. **2010**; 18: 2912-2919

102. Kruger, W.; Glibert, D.; Hawthorne, R.; Hryciw, D. H.; Frings, S.; Poronnik, P.; Lynch, J. W. Yellow fluorescent protein-based assay for high-throughput screening of glycine and GABAA receptor chloride channel. *Neurosc. Lett*. **2005**; 380:340-345.

103. Mathes, C.; Friis, S.; Finley, M.; Liu, Y. . QPatch: The missing link between HTS and ion channel drug discovery *Comb. Chem. & HTS*. 2009; 12: 78-95.

104. Cook, S.; Bergquist, P. R. Family Irciniidae Gray, 1867. *Systema Porifera: A Guide to the Classification of Sponges, Edited by John N.A. Hooper and Rob W.M. Van Soest, Kluwer Academic/Plenum Publishers, New York*. **2002**:1022.

105. Barrow, C. J.; Blunt, J. W; Munro, M. H. G; Perry, N. B. Variabilin and related compounds from a sponge of the genus *Sarcotragus J. Nat. Prod*. **1988**; 51(2): 275-281.

106. Barrow, C. J, .; Blunt, J. W; Munro, M. H. G; Perry, N. B. Oxygenated furanosestertepene tetronic acids from a sponge of the genus *Ircinia. J Nat. Prod*. **1988**; *51*:1294-1298.

107. Wang, N.; Song, J.; Jang, K. H.; Lee, H. S.; Li, X.; Oh, K. B.; Shin, J. Sesterterpenoids from the sponge *Sarcotragus* sp. *J. Nat. Prod*. **2008**; *71*(4): 551-557.

108. Choi, K.; Hong, J. K.; Lee, C. O.; Kim, D. K.; Sim, C. J.; Im, K. S.; Jung, J. H. Cytotoxic furanosesterterpenes from a marine sponge *Psammocinia* sp. *J. Nat. Prod*. **2004**; 67(7): 1186-1189.

109. Faulkner, D. J. Variabilin, an antibiotic from sponge, *Ircinia variabilis*. *Tetrahedron Lett*. **1973**; *39*: 3821-3822.

110. Gonzales, G. A.; Redriguez, M. L.; Barrientos, S. M. On the stereochemistry and biogenesis of C21 linear furanoterpenes in *Ircinia* sp. *J. Nat. Prod*. **1983**;46:256-261.

111. Holler, U.; Konig, G. M.; Wright, A. D. The new sesterterpene tetronic acids from the marine sponge *Ircinia oros*. *J. Nat. Prod*. **1997**; *60*(8): 832-835.

112. Martinez, A.; Duque, C.; Sato, N.; Tanaka, R.; Fujimoto, Y. (18R)-variabilin from the sponge *Ircinia felix*. *Nat. Prod. Lett*. **1995**;6(1): 1-6.

113. Capon, R. J.; Dragaville, T. R.; Davis, R. The absolute stereochemistry of variabilin and related sesterterpene tetronic acids. *Nat. Prod. Lett*. **1994**; 4:51-56.

114. Liu, Y. H.; Mansoor, T. A.; Hong, J. K.; Lee, C. O.; Sim, C. J.; Im, K. S.; Kim, N. D.; Jung, J. H. New cytotoxic sesterterpenoids and norsesterterpenoids from two sponges of the genus *Sarcotragus*. *J. Nat. Prod*. **2003**; *66*(11): 1451-1456.

115. Liu, Y. H.; Hong, J. K.; Lee, C. O.; Im, K. S.; Kim, N. D.; Choi, J. S.; Jung, J. H. Cytotoxic pyrrolo- and furanoterpenoids from the sponge *Sarcotragus* species. *J. Nat. Prod*. **2002**; 65(*9*): 1307-1314.

116. Rotherberg, I.; Subiak, P. The structure of some antibiotics from the sponge *Ircinia strobilina*. *Tet. Lett*. **1975**; *10*: 769-772.

117. Davis, R.; Capon, R. J. Two for one-Structure revision of the marine sesterterpene tetronic acid strobilinin to

(8Z,13,20Z0-strobilinin and (8E-13Z,20Z)-stroblinin. *Aust. J. Chem.* **1994**; 47(5): 933-936.

118. McPhail, K.; Coleman, M, T, D.; Coetzee, P. A new furanosesteterpene from the South African nudibranch *Hypselodoris capensis* and a Dictyoceratida sponge *J. Nat. Prod.* **1998**; 61: 961-964.

119. Song, J.; Jeong, W.; Wang, N.; Lee, H. S.; Sim, C. J.; Oh, K. B.; Shin, J. Scalarane sesterterpene from the sponge *Smenospongia sp. J. Nat. Prod.* **2008**; *71*:1866-1871.

120. Shin, J.; Rho, J. R.; Seo, Y.; Lee, H. S.; Cho, K.W.; Sim, C.J. Sarcotragins A and B, new sesterpenoid alkaloids from the sponge *Sarcotragus* sp. *Tet. Lett.* **2001**; 42: 3005-3007.

121. Buttler, M. S.; Capon, R. J. The luffarins (A-Z), novel terpenes from an Australian marine spogne, Luffariella geometrica *Aust. J. Chem.* **1992**; 45: 1705-1743.

122. Mitchell, S. S.; Harper, M. K.; Faulkner, D. J. Spongiabutenolides A-D: minor gama-hydroxybetenolide diterpenenoids from a Phillippines *Spongia* sp. . *Tetrahedon.* **1999**; 55:10887-10892.

123. Barrow, C. J.; Blunt, J. W.; Munro, M. H. G. Autooxidation studies on the marine sesterterpene tetronic acid, variabilin *J. Nat. Prod.* **1989**; *52*: 346-359

124. Faulkner, D. J. Interesting apsects of marine natural products chemistry. *Tetraheron* **1977**; 33:1421-1443.

125. Pham, A. T.; Carney, J. R.; Yoshida, W. Y.; Scheuer, P. J. Humanamide, a Nitrogenous Spongian Derivative from a *Spongia* sp. *Tetrahedron Lett* **1992**; 33:1147-1148.

126. Mori, D.; Kimura, Y.; Kitamura, S.; Sakagami, Y.; Yoshioka, Y.; Sinntani, T.; Okamoto, T.; Ojika, M. . Spongolactams, farnesyl transferase inhibitors from a marine sponge: isolation through an LC/MS guided assay, structure adn semisyntheses *J. Org. Chem.* **2007**; 72: 7190-7198.

127. El Sayed, K. A.; Mayer, A. M. S.; Kelly, M.; Hamann, M. T. . The biocatalytic transformation of furan to amide in the biactive marine natural products palinurin *J. Org. Chem.* **1999**; *64*: 9258-9260.

128. Decker, M.; Nguyen, T. T. H.; Lehman, J. Investigations into the mechanism of lactamization of lactones yielding in a novel route to biologically active tryptamine derivatives. *Tetrahedon.* **2004**; 60: 4567-4578.

129. Takabe, K.; Hiroya, H.; Sugomoto, H.; Nomoto, M.; Yoda, H. First asymmetric synthesis of the marine furanosesterterpene natural products, (18S0-variabilin, employing enzymatic desymmetrization of propanediol derivtives. *Tet. Asym.* **2004**;15:909-912.

130. Pawlik, J. R.; McFall, G.; Zea, S. Does the odor from sponges of the genus *Ircinia* protect them from fish predator. *J. Chem. Ecol.* **2002**;28:1003-1115.

131. Epifanio, R. D. A.; Gabriel, R.; Martins, D. L.; Muricy, G. The sesterterpene variabilin as a fish predation deterent in the Western Atlantic sponge *Ircinia strobilina. J. Chem. Ecol.* **1999**;9:2247-2254.

132. Paloma, L. G.; maria, C. M.; Terracciano, S.; Casapullo, A.; Riccio, R Chemistry and biology of anti-inflammatory marine natural products, phospholipase A2 inhibitors. *Curr. Op. Invest. Drugs.* **2005**;9:2247-2254.

133. Balansa, W.; Islam, R.; Fontaine, F.; Piggott, A. M.; Zhang, H.; Xiao, X.; Webb, T. I.; Gilbert, D. F.; Lynch, J. W.; Capon, R. J. Sesterterpene glycinyl-lactams: a new class of glycine receptor modulator from Australian marine sponges of the genus *Psammocinia. Org. Biomol. Chem.* **2013**; 11: 4695-4701

134. Coll, J. C.; Kearns, P. S.; Ridout, J. A.; Hooper, J. Ircinianin sulfate from the marine sponge *Ircinia* (*Psammocinia)* wistarii. *J. Nat. Prod.* **1997**; *60*: 1178-1179.

135. Hofheinz, W.; Schonholzer, P. Ircinianin, a novel sesterterpene from a marine sponge. *Helv. Chim. Acta.* **1977**;60(4):1367-1370.

136. Uenishi, J.; Kawahama, R.; Yonemitsu, O. Total Synthesis of (-)-Ircinianin and (+)-Wistarin *J. Org. Chem.* **1997**; 62:

1691-1701.

137. Gregson, R. P.; Ouvrier, D. Wistarin, a tetracyclic furanosesterterpene from the marine sponge *Ircinia wistarii*. *J. Nat. Prod*. **1982**;45(4): 412-414.

138. Fontana, A.; Fakhr, I.; Mollo, E.; Cimino, G. (-)-Wistarin from the marine sponge Ircinia sp.: the first case of enantiomeric sesterterpenes. *Tetrahedron Asymmetry*. **1999**; 10(20): 3869-3872.

139. Balansa, W.; Islam, R.; Gilbert, D.F.; Fontaine, F.; Xiao, X.; Zhang, H.; Piggott, A. M.; Lynch, J. W.; Capon, R. J. Australian marine sponge alkaloids as a new class of glycine-gated chloride channel receptor modulator. *Bioorg. Med. Chem*. **2013**; 21: 4420-4425

140. Kazlauskas, R.; Murphy, P.T.; Quinn, R. J.; Wells, R. J. Aplysinopsin, a new tryptophan derivative from a sponge. *Tet. Lett*. **1977**; 1: 61-64.

141. Hollenbeak, K.H.; Schmitz, F. J. Aplysinopsin: Antineoplastic tryptophan derivative from marine sponge Verongia spengelii. *Lloydia*. **1977**; 40: 479-481.

142. Djura, P.; Faulkner, D.J. Metabolites of the marine sponge *Derictus* sp. *J. Org. Chem*. **1980**; 45: 737-738.

143. Djura, P.; Stierle, D.B.; Sullivan, B.; Faulkner, D.J. Some metabolites of the marine sponges *Smenospongia aurea* and *Smenospongia* (*Polyfibrospongia*) *echina*. *J. Org. Chem*. **1980**; 45:1435-1441.

144. Guella, G.; Mancini, I.; Zibrowius, H.; Pietra, F. Novel aplysinopsin type alkaloids from scleractinian corals of the family Dendrophylliidae of the Mediterranean and the Philippines. Configurational assignment criteria, stereospecific synthesis, and photoisomerization. *Helv. Chim. Acta*. **1988**; *71*(4): 773-781.

145. Guella, G.; Mancini, I.; Zibrowius, H.; Pietra, F. . Aplysinopsin-type alkaloids from *Dendrophyllia* sp., a scleractinian coral of the family Dendrophylliidae of the Philippines. Facile photochemical (*Z*/*E*) photoisomerization and thermal reversal. *Helv. Chim. Acta*. **1989**; *72*: 1444-1450.

146. Mancini, I.; Guella, G.; Zibrowius, H.; Pietra, F. . On the origion of quasi-racemic aplysinopsin cycloadducts, (bis)indole alkaloids isolated from scleractinian coral fo the family Dendrophyllidae. Involvement of enatiodefective Diels-Alderases or asymmetric induction in artifact processes involving adventitious catalyist? *Tetrahedon*. **2003**; 59: 8757-8762.

147. Iwagawa, T.; Miyazaki, M.; Okamura, H.; Nakatani, M.; Doe, M.; Takemura, K Three novel bis(indole) alkaloids from a stony coral, *Tubastraea* sp. *Tet. Lett*. **2003**; 44(12): 2533-2535.

148. Murata, M.; Miyagawa-Kohshima, K.; Nakanishi, K.; Naya, Y. Characterization of compounds that induce symbiosis between sea anemone and anemone fish. *Science*. **1986**; 234:585-587.

149. Bialonska, D.; Zjawiony, J. K. Aplysinopsins-marine indole alkaloids: chemistry, bioactivity and ecological significance. *Marine Drugs*. **2009**; 7:166-183

150. Hu, J. F.; Schetz, J. A.; Kelly, M.; Peng, J. N.; Ang, K. K. H.; Flotow, H.; Leong, C. Y.; Ng, S. W.; Buss, A. D.; Wilkin, S. P.; Hamman, M. T. New antiinfective and human 5-HT2 receptor binding natural product and semisynthetic compounds from the Jamaican sponge *Smenospongia aurea*. *J. Nat. Prod*. **2002**; *65*: 476-480.

151. Aoki S, Ye Y, Higuchi K, et al. Novel neuronal nitric oxide synthase (nNOS) selective inhibitor, aplysinopsin-type indole alkaloid, from marine sponge Hyrtios erecta *Chem. Pharm. Bull*. **2001**;49:1372-1374.

152. Taylor, K. M.; Lambert, J. A. B.; Davis, P. A.; Spence, I. Methylaplysinopsin and other marine natural products affecting neurotransmission *Federation Proc*. **1981**; 39: 15-20.

153. Cummings, D. F.; Canseco, D. C.; Sheth, P.; Johnson, J. E.; Schetz, J. A. Synthesis and structure affinity relationships of novel small molecule natural prouduct derivatives capable of discriminating between serononin 5-HT1A, 5-HT2A, 5-HT2C receptor subtypes. *Biorg. Med. Chem. Lett*. **2010**; 18: 4783-4792.

154. Porwal, S.; Chauhan, S. S.; Chauhan, P. M. S.; Shakya, N.; Verma, A.; Gupta, S. Discovery of novel antileshmanial

agents in an attempt to synthesize pentamidine-aplysinopsin hybrid molecule. *J. Med. Chem.* **2009**; 52: 5793-5802.

155. Penthala, N. R.; Yerramreddy, T. R.; Crooks, P. A. Microwave assisted synthesis and in vitro cytotoxicities of substituted (Z)-2-amino-5-(1-benzyl-1H-indole-3-yl)methylene-1-1methyl-1H-imidazole-4(5H)-ones against human tumor cell lines. *Biorg. Med. Chem. Lett.* **2010**; 20: 591-593.

156. Penthala, N. R.; Yerramreddy, T. R.; Crooks, P. A. . Synthesis and in vitro screening of novel N-benzyl aplysinopsin anlagos as potential anticancer agents *Biorg. Med. Chem. Lett.* **2011**; 21: 1411-1413.

157. Dai, J.; Jimenez, J. I.; Kelly, M.; Williams, P. Dictazoles: potential vinyl cyclobutane biosynthetic prcursors to the dictazolines *J. Org. Chem.* **2009**; 75: 2399-2402.

158. Wells, K. M.; Murphy. P. T, Inventor. 5-(-indol-3-ylmethylene)-1,3-dimethyl-2-methylamino-4-imidazolidinone. **1980**.

159. Okuda, R. K.; Klein, D.; Kinnel, R. B.; Li, M.; Scheuer, P. J. Marine natural products: the past twenty years and beyond. *Pure. Appl. Chem.* **1982**; 54: 1907-1914.

160. Seagraves, N. L.; Crews, P. Investigation of brominated tryptophan alkaloids from two Thorectidae sponges: Thorectandra and Semonospngia. *J. Nat. Prod.* **2005**; 68: 1484-1488.

161. Fattorusso, E.; Lanzotti, V.; Magno, S.; Novellino, E. Tryptophan derivtives from a Mediterranean anthozoan, *Astroides calycularis J. Nat. Prod.* **1985**; 48: 924-927.

162. Selic, L.; Stanovnik, B. Dimethylamine substitution in N,N-dimethyl enamines. Synthesis of aplysinopsin analogues adn 3-aminotetrahydrocoumarin dertivatives. *Tetrahedon.* **2001**; *57*: 3159-3164.

163. Koh, E. G. L.; Swetman, H. J. . Chemical warfare among scleractinians: bioactive natural products from Tubastraea faulkneri Wells kill larvae of potential competitors. *J. Exp. Mar. Biol.* **2000**; 251: 141-160.

164. Iwagawa, T.; Miyazaki, M.; Yokogawa, Y.; Okamura, H.; Nakatani, M.; Doe, M.; Morimoto, Y.; Takemura, K. Aplysinopsin dimers from a stony coral, *Tubastraea aurea. Heterocycles.* **2008**; 75:2023-2028.

165. Dai, J.; Jimenez, J. I.; Kelly, M.; Barnes, S.; Lorenzo, P.; Williams, P. Dictazolines A and B, bisspiroimidazolidinones from the marine sponge Semnospongia cerebriformis. *J. Nat. Prod.* **2008**; 71: 1287-1290.

166. Meyer, M.; Delberghe, F.; Liron, F.; Guillaume, M.; Valentin, A.; Guyot, M. . An antiplasmodial new (bis)indole alkaloid from the hard coral Tabstraea sp. . *Nat. Prod. Res.* **2009**;23 178-182.

167. Baird, L. J.; Davis, P. A.; Taylor, K. M. Methylaplysinopsin: a natural product of marine origin with effects on serotonergic neurotransmission. *Clin. Exp. Pharmacol. Physiol.* **1982**; 9(203): 203-212

168. Aoki, S.; Ye, Y.; Higuchi, K.; Takashima, A.; Tanaka. Y.; Kitagawa, I.; Kobayashi, M. Novel neuronal nitric oxide synthase (nNOS) selective inhibitor, aplysinopsin-type indole alkaloid, from marine sponge *Hyrtios erecta. Chem. Pharm. Bull.* **2001**; 49(10):1372-1374

169. Tymiak, A.A.; Rinehart, K.L Constituents of morphologically similar sponges. *Tetrahedron Lett.* **1985**; 41: 1039-1047.

170. Gulati, D.; Chauhan, P. M. S.; Bhakuni, R. P.; Bhakuni, D. S. A new synthesis of aplysinopsin, a marine alkaloid and its analogues and their biological activities. *Indian J. Chem.* **1993**; 33B: 4-9.

171. Kondo, K.; Nishi, J.; Ishibasi, M.; Kobayashi, J. Two new tryptophan-derived alkaloids from the Oknawan marine sponge Aplysina sp. *J. Nat. Prod.* **1994**; 57(7): 1008-1011.

172. Baran, P. S.; O'Malley, D. P.; Zografos, A. L. *Angew. Chem., Int. Ed.* **2004**;43:2674-2677.

173. Wheeler MDI, K.; Enomoto, N.; Stacklewitz, R. F.; Seabra, V.; Zhong, Z.; Yin, M.; Schemmer, P.; Rose, M. L.; Rusyn, I.; Bradford, B.; Thurman, R. G. Glycine: a new anti-inflammatory immunonutrient. *Cell. Mol. Life Sci.*

1999;56:843-856.

174. Rodriquez, M. L. L.; Viso, A.; Gutierrez, S. O.; Fowler, J. C.; Tiger, G.; de Lago, E.; Ruiz, J. F.; Ramos, J. A. . Design, synthesis and biological evaluation of new endocannabionoid transporter inhibitors. *Eur. J. Med. Chem.* **2003**; 38: 403-412.

175. Humphrey, A. SWOT analysis for management counsulting *SRI Alumni Newsletter (SRI International)* **2005**, 2013.

176. Dibb, S.; Russell, Y.; Simkin, L. The EU Marketing Environment: Pharmaceuticals and Japanese Strategy. *Eur. Manag. J.* **1997**; 15:195-205.

177. Ronco, M. P. F.; de Lucas, A.; Rodri´guez, J. F.; Garci´a, M. T.; Gracia, I. New considerations in the economic evaluation of supercritical processes: Separation of bioactive compounds from multicomponent mixtures. *J. Supercrit. Fluids* **2013**; 79:345-355.

178. Burstein, S.H.; Rossetti, R. G.; Yagen, B.; Zurier, R. B. Oxidative metabolism of anandamide. *Prostaglandins Other Lipid Mediat.* **2000**; 61: 29–41

179. Huang, S. M.; Bisogno, T.; Petros, T. J.; Chang, S. Y.; Zavitsanos, P. A.; Zipkin, R. E.; Sivakumar, R.; Coop, A.; Maeda, D. Y.; De Petrocellis, L.; Burstein, S.; Di Marzo, V.; Walker, J. M. Identification of a new class of molecules, the arachidonyl amino acids, and characterization of one member that inhibits pain. *J. Biol. Chem.* **2001**; 276: 42639–42644.

180. Grossman, M.L.; Basbaum, A.I.; Fields, H.L. Afferent and efferent connections of the rat tail flick reflex (a model used to analyze pain control mechanisms). *J. Comp. Neurol.* **1982**; 206: 9–16.